

Electronic Thesis and Dissertation Repository

---

4-14-2020 10:00 AM

## Water Supply Capacity Development in the Context of Global Change

Patrick Breach, *The University of Western Ontario*

Supervisor: Simonovic, Slobodan P., *The University of Western Ontario*

A thesis submitted in partial fulfillment of the requirements for the Doctor of Philosophy degree in Civil and Environmental Engineering

© Patrick Breach 2020

Follow this and additional works at: <https://ir.lib.uwo.ca/etd>



Part of the [Environmental Engineering Commons](#), [Sustainability Commons](#), [Systems Engineering Commons](#), and the [Water Resource Management Commons](#)

---

### Recommended Citation

Breach, Patrick, "Water Supply Capacity Development in the Context of Global Change" (2020). *Electronic Thesis and Dissertation Repository*. 6930.

<https://ir.lib.uwo.ca/etd/6930>

This Dissertation/Thesis is brought to you for free and open access by Scholarship@Western. It has been accepted for inclusion in Electronic Thesis and Dissertation Repository by an authorized administrator of Scholarship@Western. For more information, please contact [wlsadmin@uwo.ca](mailto:wlsadmin@uwo.ca).

## Abstract

The ANEMI model is an integrated assessment model of global change that emphasizes the role of water resources. The model is based on the principles of system dynamics simulation in order to analyze changes in the Earth system using feedback processes. Securing water resources for the future is a key issue of global change, and ties into global systems of population growth, climate change carbon cycle, hydrologic cycle, economy, energy production, land use and pollution generation.

This thesis focusses on the development of global water supplies necessary to keep pace with a growing population and global economy using an integrated feedback-based approach. The main contributions of this work include: (i) implementation of the energy-economy system based on the principles of system dynamics simulation in the ANEMI model; (ii) incorporation of water supply as an additional sector in the global economy that parallels the production of energy, inclusion of climate change effects on land yield and potentially arable land for food production, and (iii) addition of nutrient cycles of nitrogen and phosphorus to the model as indicators of global water quality, which affect the production of surface water supplies.

With the new structure of the ANEMI model, a series of experiments are conducted in order to examine the impacts of climate change throughout the Earth system, evaluate potential limits to population growth through the depletion of food and water supplies and the generation of pollution, assess the potential impacts of water quality on the development of water supplies, and analyze the role of water supply development of conventional and alternative water supplies in adapting to water stress. The role of alternative water supplies in the form of desalination and wastewater reuse

are assessed to fulfill future water demands beyond conventional water supplies of surface and groundwater.

Evaluation of the model performance demonstrates that the model can reproduce historical trends related to global change within the Earth system. The experimental results show that investment in alternative water supplies on a global scale should be made in advance of conventional water supply depletion, as time delays may result in prolonged increases in global water stress. It was also found that the role of technological change was a greater factor for meeting future food production requirements than the effect of a changing climate. The impact of water quality degradation and the depletion of available water resource on water supply development, was found to be understated when studied on the global scale. It is recommended that the water supply development system developed in this work be extended to a finer spatial scale where the effects of water depletion and water quality degradation can be more thoroughly examined.

## Keywords

global change; integrated assessment modelling; system dynamics simulation; water resources management; water supply; climate change; earth system; feedback

## Summary for Lay Audience

The ANEMI model is a computer simulation model of global change that emphasizes the role of water resources. Securing water resources for the future is a key issue of global change, and ties into global systems of population growth, climate change, carbon cycle, hydrologic cycle, economy, energy production, land use and pollution generation.

This thesis focusses on assessing water supply development within ANEMI from an economic perspective. The main contributions of this work include: (i) the addition of a new energy-economy system in the ANEMI model; (ii) addition of a novel water supply development model, (iii) inclusion of climate change effects on the food production sector, and (iv) addition of a water quality sector which affects the development of surface water supplies.

With the new structure of the ANEMI model, a series of experiments are conducted in order to; examine the impacts of climate change throughout the Earth system, evaluate potential limits to the population through the depletion of food and water supplies and the generation of pollution, assess the potential impacts of water quality on the development of water supplies, and analyze the role of water supply development of conventional and alternative water supplies in adapting to global water stress. The role of alternative water supplies in the form of desalination and wastewater reuse are assessed to fulfill future water demands beyond conventional water supplies of surface and groundwater.

The experimental results show that investment in alternative water supplies on a global scale should be made in advance of conventional water supply depletion, as time delays may result in prolonged increases in global water stress. It was also found that the role of technological change was a greater factor for meeting future food production requirements than the effect of a changing climate. The impact of water quality degradation and the depletion of available water resource on water supply development, was found to be understated when studied on the global scale.

## Co-Authorship Statement

This Monograph format thesis dissertation was written in its entirety by the author. The author also produced all the figures shown herein except where indicated by citation. Although this is an original dissertation, the content contained herein was based on work completed by the author in collaboration with others as follows.

The work presented in Section 3.2.11 of the thesis has been published in a preliminary form in:

Breach P.A. and S.P. Simonovic (2018) *Wastewater Treatment Energy Recovery Potential For Adaptation To Global Change: An Integrated Assessment*. *Environmental Management*, 61:624–636. doi: 10.1007/s00267-018-0997-6.

The conceptualization and development of the global nutrient cycles in ANEMI to represent surface water quality through total phosphorus and nitrogen concentrations was carried out by Breach, along with writing of the research paper. Simonovic provided advice, reviewed the research paper and provided comments prior to submission and during the review process.

## Acknowledgements

First, I would like to thank Professor Slobodan P. Simonovic for his guidance and patience in the culmination of the work presented in this thesis. He has given me many opportunities to learn and grow as a student and individual through many different facets. He has allowed me to take on interesting challenges throughout the entirety of our work together. From helping me gain experience in teaching courses and attending conferences, to managing various aspects of the FIDS office and allowing me to collaborate on research with other students. For this I give my sincerest thanks and I will not forget the many lessons that I have learned during our time working together.

I would also like to thank Professor Jim MacGee for taking the time to help me in aspects of this work that were very foreign to me at first (the field of economics for one). Our discussions were always interesting, and we were able to learn a lot together.

The road to this point has not always been linear. It has been a dynamic process with many feedbacks that involved learning not only about the research and courses that I have completed, but also about myself. The person I was coming into this experience is not the same person I am now, and there are still many opportunities to learn and grow in the future. There are many other people I would like to thank that helped me on this road. Namely, my friends and fellow students for providing much needed relief at times, my family for supporting me unconditionally, and my partner Rebecca Tisdale, who has supported me mentally and emotionally throughout this entire journey.

# Table of Contents

Abstract .....	i
Summary for Lay Audience.....	iii
Co-Authorship Statement.....	iv
Acknowledgements.....	v
List of Figures .....	ix
List of Tables .....	xvii
Chapter 1 .....	1
1. Introduction.....	1
1.1. Global Change in the 21 <sup>st</sup> Century .....	1
1.2. The Role of Water Resources in Global Change .....	5
1.3. Analyzing the Earth System.....	10
Chapter 2.....	15
2. Literature Review.....	15
2.1. Global Scale Research on Modelling Water Resources.....	15
2.2. Fundamentals of System Dynamics Simulation.....	22
2.3. Integrated Assessment Models of Global Change .....	30
2.4. ANEMI Model Evolution.....	38
2.5. Gaps in the Literature .....	46

2.6. Research Objectives and Thesis Contributions.....	47
Chapter 3.....	51
3. Methodology.....	51
3.1. Intersectoral Feedback Structure.....	54
3.2. Description of the ANEMI3 Model Sectors.....	63
3.2.1. Climate Sector.....	63
3.2.2. Carbon Cycle .....	67
3.2.3. Population Sector.....	74
3.2.4. Land Use Sector.....	80
3.2.5. Food Production Sector.....	84
3.2.6. Sea Level Rise Sector .....	93
3.2.7. Hydrologic Cycle Sector.....	94
3.2.8. Water Demand Sector.....	100
3.2.9. Energy-Economy Sector.....	107
3.2.10. Water Supply Development .....	137
3.2.11. Nutrient Cycles.....	153
3.2.12. Persistent Pollution.....	161
3.3. Parameter Estimation .....	168
3.4. Model Implementation.....	170
3.5. Model Validation.....	170



3.5.1. Behaviour Reproduction .....	172
3.5.2. Future Model Performance .....	181
3.5.3. Integration Error.....	198
3.5.4. Sensitivity Analysis and Extreme Conditions.....	200
Chapter 4.....	207
4. Model Experiments.....	207
4.1. Climate Change Impacts .....	208
4.2. Population Dynamics and Limits to Growth.....	216
4.3. Water Quality Effects on Water Supply.....	222
4.4. Water Supply Development in the Context of Global Change .....	228
4.5. Food Production .....	237
Chapter 5.....	248
5. Summary and Discussion.....	248
5.1. Model Performance .....	248
5.2. The Role of Climate in Global Change.....	252
5.3. Considerations for Water Supply Development in the 21 <sup>st</sup> Century .....	254
Chapter 6.....	257
6. Conclusions and Recommendations .....	257
6.1. Findings and Contributions .....	257
6.2. Limitations .....	259

6.3. Future Work .....	261
References.....	263
Appendices.....	275
Appendix A. List of Intersectoral Feedback Loops .....	275
Appendix B. Parameters for the Nutrient Cycles.....	296
Appendix C. Differential evolution algorithm for parameter estimation of ANEMI3 .....	298
Appendix D. VenPy code used for automation of ANEMI3 model runs .....	302
Appendix E. Model Code .....	310
Curriculum Vitae .....	311

## List of Figures

Figure 1.1. Typical (a) domestic and (b) industrial structural water intensities as a function of GDP per capita (after Alcamo et al. (2003a)). .....	6
Figure 2.1. Conceptual illustration of WaterGAP2 model structure (after Alcamo et al. 2003a)	16
Figure 2.2. Causal loop diagram for heating of room with thermostat. ....	23
Figure 2.3. Stock and flow diagramming for heating of room with thermostat. ....	26
Figure 2.4. Basic dynamic system behaviours of (a) positive feedback, (b) negative feedback, (c) oscillation, (d) S-shaped growth, and (e) overshoot and collapse. ....	28
Figure 2.5. Macro-structure of the AIM model (after Matsuoka et al. 2001). ....	33
Figure 2.6. Macro-structure of the IMAGE 3.0 model (after Stehfest et al. 2014). ....	34
Figure 2.7. Macro-structure of IGSM-WRS model (after Strzepek et al. 2013). ....	35

Figure 2.8. Connections between energy, water, land, climate, and socioeconomics in GCAM version 5.1 (after Calvin et al. 2019). .....	36
Figure 2.9. Intersectoral feedback structure of ANEMI (after Davies and Simonovic 2010). .....	41
Figure 2.10. Intersectoral feedback structure of ANEMI2 (after Akhtar et al. 2013). .....	44
Figure 2.11. Feedback structure of wastewater energy-recovery implementation in ANEMI2 (after Breach and Simonovic 2018). .....	46
Figure 3.1. Intersectoral causal loop diagram of the ANEMI3 model. ....	55
Figure 3.2. Causal loop diagram of the ANEMI3 climate sector. ....	64
Figure 3.3. Stock and flow diagram of the ANEMI3 climate sector. ....	65
Figure 3.4. Causal loop diagram of carbon cycle sector in ANEMI3. Red, green, and blue arrows and variables represent connections to climate, land use, and energy production sectors respectively. ....	69
Figure 3.5. Stock and flow diagram of carbon cycle in the ANEMI3 model. ....	70
Figure 3.6. Causal loop diagram of the ANEMI3 population sector. ....	75
Figure 3.7. Stock and flow diagram of the ANEMI3 population sector. ....	77
Figure 3.8. Causal diagram of the ANEMI3 land use sector. ....	81
Figure 3.9. Stock and flow diagram of ANEMI3 land use sector. ....	82
Figure 3.10. Causal loop diagram of the ANEMI3 food production sector. ....	85
Figure 3.11. Stock and flow diagram of the ANEMI3 food production sector. ....	86
Figure 3.12. Relationship between global temperature change and change in potential arable land (after King et al. 2018). Error bars represent 95% confidence interval from the GCMs used in calculating global average temperature change. ....	89

Figure 3.13. Distribution of crop production for the 4 crop types used in (Searchinger et al. 2019) compared to global totals in the years 1980 and 2017.....	91
Figure 3.14. Causal diagram of the ANEMI3 sea-level rise sector. ....	93
Figure 3.15. Causal loop diagram of the ANEMI3 hydrologic cycle sector. ....	95
Figure 3.16. Stock and flow diagram of the AEMI3 hydrologic cycle sector. Items in blue denote processes that have human influence on the hydrologic cycle, while those in red represent the influence of changing climate.....	96
Figure 3.17. Illustration of structural water intensity for domestic water use (after Alcamo et al. 2003a). ....	101
Figure 3.18. Causal diagram of the ANEMI3 water demand sector.....	102
Figure 3.19. GCAM energy production projections for 2005-2100 (after Davies et al. (2013)).	104
Figure 3.20. Causal loop diagram for good production and capital sub-system of the energy-economy sector. ....	110
Figure 3.21. Stock and flow diagram of the ANEMI3 capital sector of the economy .....	111
Figure 3.22. Causal loop diagram for the energy production sub-system of the ANEMI3 energy-economy sector. ....	115
Figure 3.23. Stock and flow diagram for the ANEMI3 energy production sector .....	118
Figure 3.24. Causal loop diagram for the energy capital sub-sector of the energy-economy sector. ....	120
Figure 3.25. Stock and flow diagram of the ANEMI3 energy capital sector .....	121
Figure 3.26. Causal loop diagram for energy requirements sub-system in the ANEMI3 energy-economy sector. ....	125

Figure 3.27. Stock and flow diagram of energy requirements sub-system of ANEMI3 energy-economy sector. ....	126
Figure 3.28. Causal loop diagram of ANEMI3 energy pricing sector.....	130
Figure 3.29. Stock and flow diagram for the energy pricing sub-system of the ANEMI3 energy-economy sector. ....	131
Figure 3.30. Causal loop diagram for the technological change sub-system of the ANEMI3 energy-economy sector. ....	133
Figure 3.31. Stock and flow diagram of energy technology sub-system within the ANEMI3 energy-economy sector. ....	135
Figure 3.32. Causal loop diagram of the ANEMI3 water supply development sector. The dotted arrow from water price to water supply indicates a causality that is neither positive nor negative. ....	139
Figure 3.33. Stock and flow diagram of the ANEMI3 water supply development sector.....	141
Figure 3.34. Water pricing component of the ANEMI3 water supply development sector. ....	142
Figure 3.35. Illustration of Wood's algorithm.....	147
Figure 3.36. Production structure of water supply within the energy-economy-water sector of the ANEMI3. ....	150
Figure 3.37. Goods allocation in the energy-water-economy sector of the ANEMI3. ....	151
Figure 3.38. Stock and flow diagram of the ANEMI3 nitrogen cycle.....	156
Figure 3.39. Stock and flow diagram of the ANEMI3 phosphorus cycle.....	157
Figure 3.40. Causal structure of the ANEMI3 persistent pollution sector.....	162
Figure 3.41. Stock and flow diagram of the ANEMI3 persistent pollution sector. ....	163
Figure 3.42. Simulated vs. historical World population for the period of 1980 to 2019.....	174

Figure 3.43. Simulated vs. historical World population subdivided by age demographic. Solid lines depict ANEMI3 results while dotted lines are historical values.....	175
Figure 3.44. Global temperature change from 1980-2018 comparison between ANEMI3 climate sector and NASA observed data. ....	176
Figure 3.45. Water demand comparison between the ANEMI3 and IHP (2000). Data between the years 2000-2010 for IHP (2000) are extrapolated from the historical data. ....	177
Figure 3.46. Water production comparison between the ANEMI3 and Wada and Bierkens (2014) from 1980 to 2019.....	178
Figure 3.47. Historical energy production comparison between ANEMI3 model results and estimates provided by Ritchie and Roser (2018a) for coal, oil and gas.....	179
Figure 3.48. Historical energy production comparison between ANEMI3 model results and estimates provided by (Ritchie and Roser 2018a) for hydro, nuclear, and renewable energies.	180
Figure 3.49. Land area comparison for agricultural and built areas between ANEMI3 model results and estimates provided by HYDE (2016).....	181
Figure 3.50. ANEMI3 model performance for the period 1980 - 2100.....	183
Figure 3.51. ANEMI3 population projections compared to those in United Nations (2019).....	184
Figure 3.52. Global surface temperature change comparison between ANEMI3 baseline and ANEMI3 running with the RCP scenario GHG emissions.....	186
Figure 3.53. Comparison of atmospheric CO <sub>2</sub> concentration between ANEMI3 baseline and ANEMI3 running with the RCP scenario GHG emissions.....	186
Figure 3.54. ANEMI3 simulated levels of water stress using the withdrawal to availability ratio and alternate formulations.....	188

Figure 3.55. Comparison of gross economic output between ANEMI2, ANEMI3, and DICE2013R models.....	190
Figure 3.56. Comparison of per capita consumption rates between ANEMI2, ANEMI3, and DICE2013R models.....	191
Figure 3.57. Comparison of (a) domestic and (b) industrial water demands from ANEMI3 simulated values and model projections by Wada et al. (2016). Error bars represent the range in water demands resulting from the use of different shared socioeconomic pathways in each projection made in Wada et al. (2016).....	192
Figure 3.58. Comparison of (a) irrigated land area for agriculture and (b) agricultural water demand between ANEMI3 and irrigation scenarios by FAO (2018).....	194
Figure 3.59. Comparison of projected surface and groundwater production rates between ANEMI3 and Wada and Bierkens (2014).....	195
Figure 3.60. Comparison of projected desalinated water production. ....	196
Figure 3.61. Energy production from (a) coal, (b) oil and gas, (c) hydro and nuclear energy, and (d) renewables.....	197
Figure 3.62. Maximum percentage integration error for selected state variables using varying time steps. Error is calculated based on the results provided by a time step that is 1/2048 <sup>th</sup> of a year. ....	200
Figure 3.63. Sensitivity of selected state variables using Monte Carlo sensitivity simulation. Shaded areas represent confidence level associated with simulated model variable output. ....	204
Figure 3.64. Total sensitivity of selected state variables using Monte Carlo sensitivity simulation. Shaded areas represent confidence level associated with simulated model variable output. ....	205

Figure 4.1. Global surface temperature change resulting from the baseline ANEMI3 run and RCP scenario runs. ....	210
Figure 4.2. Changes of precipitation, evapotranspiration, and available surface water with five climate change scenarios.....	211
Figure 4.3. Effect of climate change on (a) net arable land and factors affecting food production including (b) increase in arable land through boreal forest conversion, (c) impacted agricultural land by the sea level rise, and (d) land yield.....	213
Figure 4.4. Net effect of climate change on food production including the effects of changes in net arable land and land yields.....	214
Figure 4.5. Climate damage functions. ....	215
Figure 4.6. Life expectancy values for ANEMI3 baseline and UN WPP scenarios.....	217
Figure 4.7. Life expectancy multipliers in ANEMI3 for (a) baseline and (b) constant fertility scenarios.....	219
Figure 4.8. Influence of population change on (a) domestic, (b) industrial, and (c) agricultural water demands. ....	221
Figure 4.9. Total nitrogen and phosphorus input to surface water under the ANEMI3 baseline scenario. Left axis represent number of moles of nitrogen and phosphorus inputs to surface water per year.....	223
Figure 4.10. Treated and untreated wastewater inputs to the nutrient cycles over time.....	224
Figure 4.11. Surface water nutrient concentrations of nitrogen and phosphorus. ....	225
Figure 4.12. Surface water nutrient concentrations under the ANEMI3 baseline and constant wastewater treatment scenarios.....	226



Figure 4.13. Development of water supplies under the baseline and constant wastewater treatment scenarios for (a) conventional water supplies and (b) alternative water supplies.....	227
Figure 4.14. Development of water supplies in the ANEMI3 model. The upper scale labels are used for surface water and groundwater supply while the lower labels are for wastewater reuse and desalination. ....	229
Figure 4.15. Depletion effects on conventional water supplies for (a) 10%, (b) 25%, and (c) 50% reduction in available water resources compared to the ANEMI3 baseline scenario.....	231
Figure 4.16. Effect of conventional water supply depletion on alternative water supplies for (a) 10%, (b) 25%, and (c) 50% reduction in available water resources compared to the ANEMI3 baseline scenario. ....	232
Figure 4.17. Prices ranges shown by shaded areas for depletion scenarios of 10%, 25%, and 50% reduction of available water resources for surface water and groundwater supply.....	233
Figure 4.18. Maximum production capacities based on the capital accumulation of water supply under depletion scenarios of conventional water resources.....	235
Figure 4.19. Change in water stress values for each depletion scenario.....	236
Figure 4.20. Effect of technological change on (a) food production and (b) land yield from 1980 to 2050. ....	239
Figure 4.21. Effect of climate change on food production through isolated impacts of (a) land yield (b) sea-level rise, and (c) increase in arable land. Combined effect shown in (d).....	241
Figure 4.22. Projections of (a) land yield, (b), land fertility, (c) land fertility degradation rate, (d) climate change effect on land yield. ....	243

Figure 4.23. Projected irrigation agricultural area from scenarios based on FAO (2018). "Middle of the road scenario was added which represents the midpoint between "Business as Usual" and "Towards Sustainability" scenarios. ....	244
Figure 4.24. Effect of irrigation scenarios on (a) food production, (b) fraction of irrigated agriculture, (c) agricultural water demand, and (d) total water stress. ....	245

## List of Tables

Table 2.1. Sectoral comparison of Integrated Assessment Models from the literature. ....	32
Table 3.1. Connections between different model sectors in ANEMI3. Highlighted rows represent the intersectoral connections that have been added or modified in this work. ....	58
Table 3.2. Illustration of intersectoral connection in the model including total number of incoming (from) and outgoing (to) connections. ....	62
Table 3.3. Initial transfer matrix for area between land use/cover types in [Mha/year]. ....	83
Table 3.4. Effect of temperature change on crop yields for wheat, rice, maize, and soybean. ....	90
Table 3.5. Initial stock values for hydrologic cycle sector. All values are in units of [km <sup>3</sup> ]. ....	97
Table 3.6. Percentages of water reallocation in the hydrologic cycle after human withdrawal and consumption. ....	98
Table 3.7. Water withdrawal rates for energy production of various types (Larsen and Drews 2019). ....	104
Table 3.8. Parameters used nutrient inputs to nutrient cycles. ....	159
Table 3.9. Parameters values used in the persistent pollution sector. ....	166
Table 3.10. Model constants and their optimal values with corresponding sectors. ....	167
Table 3.11. Model testing procedures based on Sterman (2000). ....	170

Table 3.12. Comparison datasets for baseline model run. ....	172
Table 3.13. Datasets used for comparison of the ANEMI3 model future behaviour. ....	181
Table 3.14. Parameters used to test the sensitivity of key state variables in the ANEMI3. ....	200
Table 4.1. Links between model experiments and research objectives. ....	206
Table B.6.1. Initial values and residence times of carbon, nitrogen, and phosphorus stocks in their respective cycles from Mackenzie et al. (1993).....	295
Table B.6.2. Rate constants used to describe flow in the cycles of carbon, nitrogen, and phosphorus from Mackenzie et al. (1993).....	296

# Chapter 1

## 1. Introduction

Human impacts on the environment at global scales are being realized through our ability to alter atmospheric concentrations of greenhouse gases and consequently global climate, creating the need to consider environmental problems and their interactions with the Earth as a system. The Earth system is composed of biological, physical, chemical, and human elements that form a network of feedbacks through their interconnections (Steffan et al. 2004). The concept of global change becomes increasingly important as the components of the Earth system such as population, economic productivity, climate, food production, and hydrology are interlinked through dynamic non-linear feedback processes (Davies 2007). Within this system, changes in one component inevitably lead to changes in another. This is why global change research focusses on interactions between components of the Earth system as a whole, as opposed to only those of climate (Cox and Nakicenovic 2004; Steffan et al. 2004).

### 1.1. Global Change in the 21<sup>st</sup> Century

The concept of global change was first formally discussed on an international stage at the symposium titled “Man’s Role in Changing the Face of the Earth”, organized by the Wenner-Gren Foundation for Anthropological Research, held in Princeton, New Jersey in 1955 (Thomas 1956). This meeting led to further discussions such as “Man’s Impact on the Global Environment” which was sponsored by the Massachusetts Institute of Technology, and took place at Williams College in Williamstown, Massachusetts during the year of 1970 (Price 1989). The goal of these meetings

was to engage in cross-disciplinary thoughts and ideas about how humans are affecting various systems on a global scale ranging from agriculture, geochemistry, climatology, forestry, and engineering, to sociology, economics, and philosophy. Around the same time in 1968 the Club of Rome was created consisting of over 30 European scientists, economists and industrialists with the purpose of furthering understanding of global multi-disciplinary issues. As a result, “Limits to Growth” (Meadows et al. 1972) was published which popularized the notion of Earth as a closed system where natural resources and environment imposed severe limits on population and economic growth. Increased awareness of global environmental issues and our role in them has led to the formation of numerous scientific organizations dedicated to studying different aspects of global change (International Group of Funding Agencies for Global Change Research 2011).

These include the:

- International Biosphere-Geosphere Program (IGBP), running from 1986 with the goal of providing information needed to assess various aspects of the Earth system over the next 100 years to facilitate decision making processes related to global change (IGBP 2010). The program focussed on the biogeochemical cycles of the Earth at a time when they were not being considered by other organizations (Price 1989).
- World Climate Research Programme (WCRP), founded in 1980 focusing on analysis and prediction of Earth system change and the involvement of and impact that it has on human activities (WCRP 2020). This program includes the Coupled Model Intercomparison Project (CMIP) which has become a vital resource to climate change assessment works by providing numerous global climate model runs from various modelling groups.

- International Human Dimension Program on Global Environmental Change (IHDP), running from 1990 functioned as an interdisciplinary science program focusing on human interactions with different aspects of the natural environment (UIA 2020). This program had an emphasis on the social sciences by bringing global change research into policy, planning and law-making on an international stage.
- DIVERSITAS – International Program of Biodiversity Science, created in 1991 was established to study the ecosystem functions of biodiversity with the goal of linking biological, ecological, and social sciences (DIVERSITAS International 2011). This allowed for building an understanding of biodiversity loss with policy implications for conservation and sustainable use of biodiversity on a global scale.

These programs individually have largely operated as silos in the past, focussing on increasing knowledge and understanding of only certain aspects of global change as opposed to the feedbacks that drive it (Price 1989). The Amsterdam Declaration marked a milestone for the Earth system science programs. The declaration was made between the IGBP, IHDP, WCRP, and DIVERSITAS programs at the 2001 Global Change Open Science Conference in Amsterdam (Steffan et al. 2004). From the conference it was agreed that new approaches are needed to study the Earth as a system, because the concept of global change cannot be understood through simple cause and effect. The dynamics of the Earth system were thought to be driven by the presence of critical thresholds of key environmental variables, some of which have moved far beyond the range of natural variability (Steffan et al. 2004). The outcome of the conference was the Earth System Science Partnership,

which signified a collaboration between the global change research groups of IGBP, IHDP, WCRP, and DIVERSITAS (PAGES 2019).

The programs mentioned above have since been subsumed by the Future Earth program established in 2015 (Haines et al. 2017). The goal of Future Earth is to combine these programs and their research networks in order to bring together research from different disciplines as they relate to sustainable development with the purpose of bridging the science-policy interface (Haines et al. 2017). This could be an indication that research targeting global change from an interdisciplinary, feedback-based approach is becoming more valuable and necessary as the subsystems of the Earth become increasingly connected and even competitive.

Changes to the Earth system and its subsystems is occurring on unprecedented scales. One way to quantify the dynamic nature of these changes is by looking at them through a perspective of sustainability. Sustainable development has been defined by the 1987 Brundtland Commission of the United Nations report *Our Common Future* as, "...development that meets the needs of the present, without compromising the ability of future generations to meet their own needs." (World Commission on Environment and Development 1987). Viewing changes to the Earth system in terms of environmental footprint allows us to link pollution and consumption of natural resources to the levels of human activity and economic development.

Recently, it has been shown that human usage of bioproductive area has been exceeded by available biocapacity by 50% (Borucke et al. 2013). This means that the ecosystem resources and services of 1.5 Earths are were needed to sustain the path of human development in 2013. This

number was previously 0.7 Earths in 1961. In the field of sustainability science this would be classified as ‘overshoot’, indicating that the stocks of ecological capital are being depleted and waste is accumulating, which could act as a limiting factor to future human development. The consumption of water resources has been shown to exceed supply in half of the World’s river basins during at least parts of the year, while in two thirds of the World’s river basins water pollution has been shown to exceed assimilation capacity leading to accumulation of waste. The focus of the work addressed in this thesis lies in further understanding the role of water resources in global change.

## 1.2. The Role of Water Resources in Global Change

Water can be considered one of, if not the most, important drivers for human life as well as social and economic development (Rogers et al. 1998). Water resources provide for the most basic human needs of drinking and sanitation, while allowing for irrigated agriculture to take place, and industrial activities such as thermal power generation, mining, and manufacturing. Therefore, the use of, management, and availability of water resources plays a crucial role in the progression of global changes in the Earth system as without it, our society cannot function.

A growing global population has put stress on water resources in many regions around the World. This problem will continue to grow as the population is projected to increase 42% by the year 2100 to 10.9 billion people (United Nations 2019a). The demand for water increases not only with the population but also with the consumption of water on a per capita basis. In Alcamo et al. (2003a), it was shown that countries with higher gross domestic product (GDP) per capita generally have



higher water usage in the domestic sector, and follow a type of S-curve, while in the industrial sector, water usage decreases exponentially to an equilibrium value (Figure 1.1).

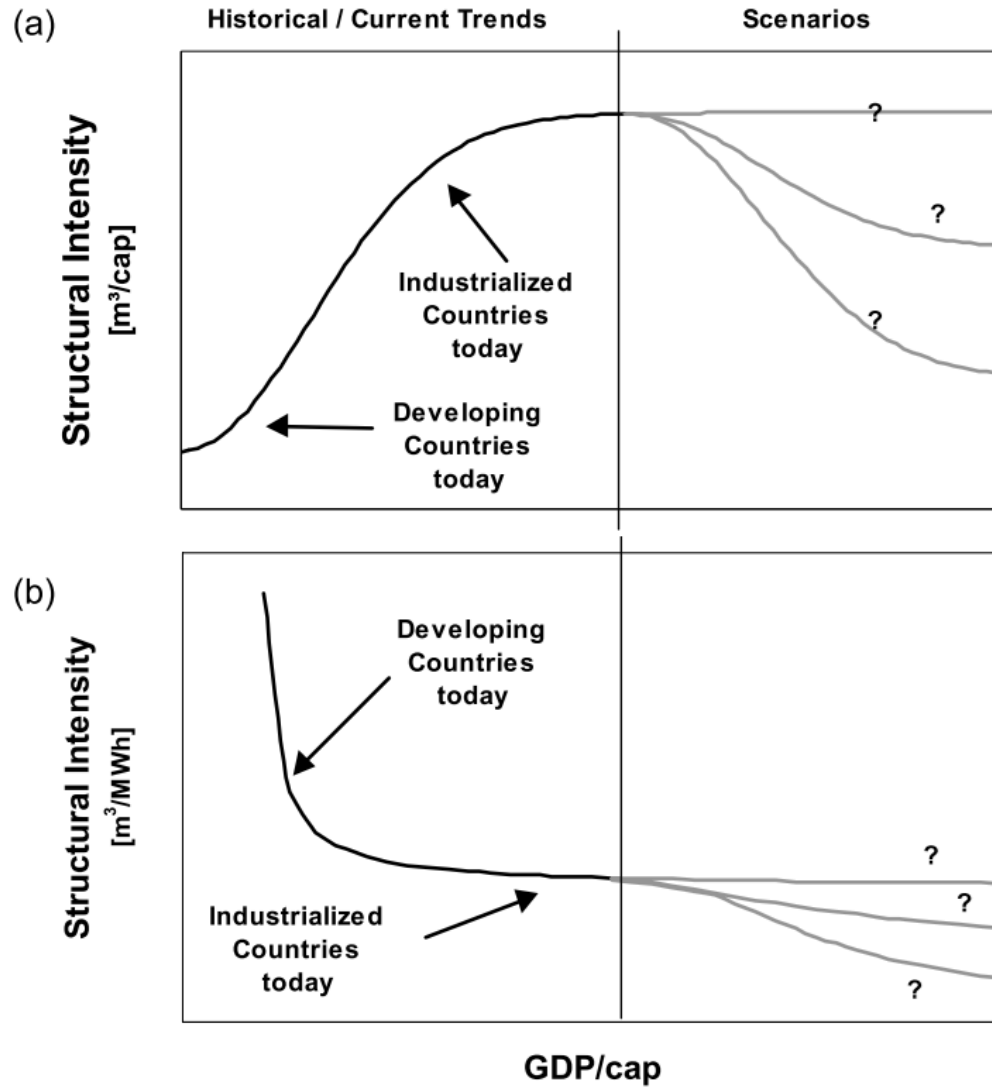


Figure 1.1. Typical (a) domestic and (b) industrial structural water intensities as a function of GDP per capita (after Alcamo et al. (2003a)).

Therefore, as countries continue to develop economically the water usage patterns will change. By continuing with the current trends in global population, economics, and technological change, water demands will continue to increase in most developing countries due increased domestic

water usage as well as agricultural production. In developed countries domestic and industrial demands saturate and the expansion of irrigated land stagnates (Alcamo et al. 2003b).

Water stress is often defined as the ratio of water withdrawals to the availability of water resources in a given region. The hydrologic cycle along with changes made to it through anthropogenic means dictates the amount of water resources that are available for use. Although natural variability in weather patterns can determine if a region will experience wet or dry seasons, human influence on hydrologic cycles such as the construction and operation of dams and reservoirs, water diversions, and water withdrawals redistribute the water availability in time and space. Climate change is expected to alter the spatial and temporal distribution of water resources on top of what is observed naturally and through direct human influence (Simonović 2012). Increased global temperatures through the greenhouse effect are expected to intensify the hydrologic cycle, leading to higher evapotranspiration rates, more frequent and heavier storms, and faster flowing rivers, along with the potential for longer periods of drought. Because of this, there exists the potential for the availability of water resources to be changed for better or worse in different areas of the world (Schlosser et al. 2014).

Water resources may be available in a given point in time and space; however, the quality of that water can sometimes dictate whether or not it is available for a certain type of use. For example, according to a national report from the US Environmental Protection agency almost half of rivers and streams across the US are categorized in “poor biological condition” as a result of nutrient and sediment pollution. The condition of the rivers and streams mentioned are deemed unfit for fishing

and recreational use (US-EPA 2010). In China, the situation is even worse with more than 70 percent of rivers and lakes being polluted, and almost half may contain water unfit for human consumption or contact (Aulakh 2014). Seasonal and daily fluctuations in source water quality can affect the quality of treated water intended for human consumption as well. In North China, more than half of the rivers do not meet minimum national water standards due to pollution and are not even suitable for agricultural use (Olmstead 2010). Because of this, it is estimated that the cost of water scarcity due to pollution is 1 – 3% of local GDP in water scarce areas of China (Kahrl and Roland-Holst 2008).

Degrading water quality over time has been shown to cause maintenance and treatment issues in drinking water treatment plants. There is evidence that increases in dissolved organic matter can lead to fouling and blocking membranes and filters, cause harmful disinfection by-products, facilitate biological re-growth in distribution systems, and transport pesticides, pharmaceuticals, and heavy metal into treatment systems (Eikebrokk et al. 2004). This in turn could necessitate changes to treatment processes and significantly increase operational costs that are likely to further increase with climate change (Ritson et al. 2014). A study done on Philadelphia's drinking water system linked gastrointestinal illness in elderly citizens to fluctuations in source water turbidity, even though the water treatment facility in this study and several other studied in the United States met Environmental Protection Agency standards (Schwartz et al. 2000). This study highlights that changes in water quality can have impacts on the water treatment, which can lead to water supplies inadequate for human consumption. Changes in water quality on a global scale could be a significant concern for our ability to maintain clean and sufficient water supplies.

The combined effect of socioeconomic growth and climate change are projected to lead to an increase of 1–1.3 billion people living in regions experiencing water stress by 2050 (Schlosser et al. 2014). Therefore, the ability to adapt to water stress through securing freshwater resources will be a key issue for the future. This has been identified as one of the main objectives for prospective global change research in the Belmont Challenge (International Group of Funding Agencies for Global Change Research 2011). Solutions to ensuring freshwater security vary from managing water demands, and more accurately modelling water resource availability (surface and ground water), to technological solutions such as desalination and water reuse.

Desalination involves the use of thermal evaporation or membrane separation technology to remove dissolved solids that are present in saline water sources. Thermal evaporation involves boiling ocean or brackish waters to evaporate freshwater thereby leaving the solids behind. Membrane separation technology on the other hand applies pressure to semi-permeable membrane filters which allow freshwater to be separated from the dissolved solids. Both methods are highly energy intensive and can be costly when compared to traditional water supplies. Currently, there are approximately 16 thousand operational desalination plants around the World producing over 95 million m<sup>3</sup>/day of desalinated water for human use (Jones et al. 2019). The cost associated with producing this type of water supply is estimated to be between 0.45 to 2.51 \$/m<sup>3</sup>, which is still 2 to 3 times higher than conventional water supply (Ziolkowska 2014). However, the cost of desalination has decreased by approximately a factor of 10 since the 1960s and is expected to continue to become cheaper as the technology is improved (Advisian Worley Group 2019).

Water reuse technologies involve the treatment of waste waters from a variety of different uses such as agricultural, municipal and industrial. The level of treatment necessary is dependent on the composition of waste waters being treated as well as the type of reuse that is under consideration. For non-potable reuse, waste water is treated to a lower standard while potable uses require more advanced treatment methods capable of removing emerging pathogens, endocrine disrupting chemicals, and pharmaceuticals (Gude 2017). Treatment options vary from simple low-energy solutions such as lagoons which allow wastewater to filter through media, to high-energy advanced treatment plants employing activated sludge treatment along with different levels of disinfection ranging from ultra-violet to membrane filtration (Hudman 1999).

Water resources management in the context of global change involves many different disciplines ranging from climate science, economics, hydrology, biology, engineering, governance, agriculture, and social sciences as outlined above. In order to address the problem of dealing with future water stress, these disciplines must be put together in a comprehensive framework. This will allow decision makers to explore policy options that consider the Earth system as a whole.

### 1.3. Analyzing the Earth System

Assessment of various aspects of global change often requires the use of models from different domains and a way to combine them so that the relationships and interactions between these models can be studied. When it comes to global change research, the goal is often to analyze the effect of policies or scenarios on different aspects of global change. This in turn provides the information necessary to help inform the policies of decision makers. This has necessitated the use

of new tools and modelling paradigms to analyze complex interactions in the Earth system at a variety of spatial and temporal scales.

The concept of integrated assessment (IA) has been defined as an interdisciplinary process of bringing together knowledge from different disciplines, adding value in contrast to a single disciplinary approach in order to provide information to decision and policy makers (Rotmans and Dowlatabadi 1998). It is performed to bring about understanding of an issue regardless of the discipline. IA is often applied to issues that involve physical, biological, and/or social elements to bring together knowledge from different fields. Environmental issues have been the main focus of IA, specifically with regards to climate change and natural resource management (Rotmans and van Asselt 1999).

Tol and Vellinga (1998) describe the process of IA in a set of stages. The first stage involves structuring the problem that is to be assessed. Due to the complex nature of the issues for which IA is typically applied, this can be a considerable task. The boundary of the problem must be defined in a way that encompasses all the important components of the problem, as well as components that may become important to the problem under different conditions or over time. Stage 2 involves the use of participatory and modelling methods for assessment. Participatory methods engage stakeholders that play a role in the problem at hand. This could be done in the form of focus groups or expert panels in order to gain a better understanding of the problem. In the case of climate change, the Intergovernmental Panel on Climate Change (IPCC) plays this role in curating scientific evidence and information about climate change.

The integrated assessment modelling (IAM) approach involves the coupling of disciplinary models. This is done by exchanging inputs and outputs that would otherwise be exogenous to the separate disciplinary models. Connections can be made in one direction (from one disciplinary model to another) or in both directions which creates a feedback loop between the two models. Due to the increased complexity in the combined model, simplified forms of the disciplinary models are often used. For example, the study of Holden and Edwards (2010) details an approach that was used to reduce the complexity of an atmosphere-ocean global climate model in order to incorporate it into an integrated assessment model of global change.

There are many different methods that can be used to form a model for integrated assessment. Connections between disciplinary models can be made statically (output of one model is first obtained then given as input to another), or dynamically (both models running at the same time). The latter of which, is the only way that feedback loops can be created and studied. Dynamic connections can be made by using a computer program to facilitate the exchange of information while the models are running, or both models can be combined into the same computer code (Tol and Vellinga 1998). The field of system dynamics focusses specifically on analyzing the dynamic nature of systems that are composed of feedback loops. Therefore, the use of system dynamics is ideal for the construction of integrated assessment models of global change.

System dynamics simulation implements the principles of systems thinking to decompose real world problems into systems built of interconnected elements. Systems thinking facilitates the

conceptualization of system dynamics simulation models through the formulation of dynamic hypotheses (how a system will behave over time). This process involves the use of causal loop diagramming to map out the feedback loops that are driving system behaviour. This is effectively describing the boundary of the problem as well as the components that are responsible for reproducing it. Systems thinking provides a formalized way of implementing Step 2 of the integrated assessment process described in Tol and Vellinga (1998) through the mapping of feedback loops. System dynamics simulation builds from the conceptual models developed through systems thinking by adding structure to them. The addition of stocks or state variables, and the flows that affect them take the system from a conceptual model to a mathematical model through stock and flow diagramming. Stock and flow diagrams illustrate the configuration of stocks and flows which is essentially a visual representation of a system of first order differential equations. Most, if not all, IAMs can be represented in this way from a high level. For these reasons the system dynamics simulation approach is ideal for the construction of IAMs and provides a formalized way for creating feedback loops between disciplinary models of global change. More details regarding system dynamics simulation is given in Section 2.2.

Anthropogenic influence on the Earth system in the form of a growing population with increased usage of natural resources and pollution of the air and water is causing global changes in climate and the availability and quality of freshwater supplies. The use of alternative water supplies such as desalination and water reuse technologies provide a potential means to alleviate water stress. Improving the security of freshwater resources has been identified as one of the main objectives of prospective global change research, which is becoming increasingly integrated amongst various disciplines. Therefore, an integrated approach is needed to address research in this area. Integrated



assessment modelling was originally developed for the assessment of issues related to global change such as climate change and lends well to analyzing water supply development within the Earth system. System dynamics simulation provides a practical approach for the implementation of integrated assessment models. This work aims to assess the development of water supplies both conventional (surface water and groundwater) and alternative (desalination and water reuse) within the Earth system using an integrated, feedback-based approach.

## Chapter 2

### 2. Literature Review

#### 2.1. Global Scale Research on Modelling Water Resources

In the past two decades several attempts to model global water resources have been made. Much of the research in this area deals with modelling water and energy budgets on global grids that are driven by climate data and socioeconomic trends as exogenous inputs. Many of the global hydrologic models to date have been developed to assess the impact of changes in the hydrologic cycle as a result of climate change and human influence (Sood and Smakhtin 2014).

Alcamo et al. (2007) used the WaterGAP2 model to investigate the spatial variation of several indicators of water stress in the future. The climate input to the model was driven by Global Climate Models (GCMs), while a corresponding set of socioeconomic scenarios from IPCC's fourth assessment report were used to calculate water use as a function of population and GDP for domestic and industrial water users respectively at the national level (Figure 2.1). Through this analysis it was found that global water stress was mainly driven by changes in water use as a result of increasing domestic withdrawals in developing nations as per capita water use rates increased. Climate change had a much smaller impact and, in some regions, provided relief to water stress through higher amounts of annual precipitation. This study highlights the importance of considering socioeconomic drivers for sustainable water resource management on a global level. However, from Figure 2.1 it is apparent that the socioeconomic drivers were modelled as

exogenous inputs (population, income, technology, and climate). This eliminates the ability to investigate the feedback effects of water stress on the rest of the system.

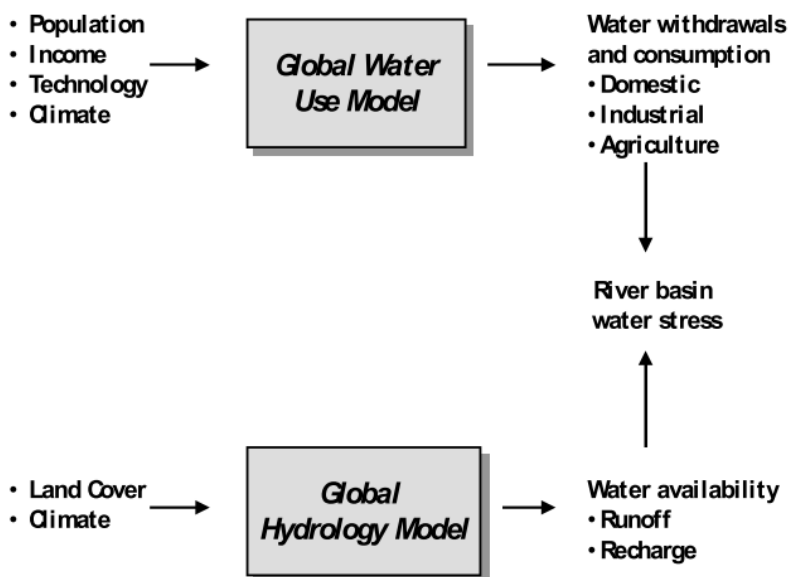


Figure 2.1. Conceptual illustration of WaterGAP2 model structure (after Alcamo et al. 2003a)

Vörösmarty et al. (2010) found a similar result when modelling human water security threat on a global scale and goes a step further by assessing the ability to cope with water stress through investing in water savings technology at a national level. Through their analysis it was found that the highest levels of water stress generally occur in regions with higher populations and associated water withdrawals. When the ability for nations to invest in water saving technologies was considered, there existed a stark contrast in levels of water stress directly related to national GDP. Countries in Europe where human water security was under threat were mostly remedied when a potential investment benefit factor was applied for the future. Central African countries that were

under low human water security threat under historical conditions then moved to moderate to high levels even after a potential investment benefits factor was applied. Therefore, the economic ability to adapt to water stress is a crucial consideration for freshwater security on a global scale.

Water resource systems are being added to integrated assessment models in order to bring together elements of global change that are modelled endogenously to study impacts on water resources such as water stress. Strzepek et al. (2013) details the water resources system added to the Integrated Global System Model (IGSM) developed at the Massachusetts Institute of Technology (Sokolov et al. 2005). This system includes domestic and industrial water usage as a function of population and GDP values from the IGSM model. Irrigation water demand is driven by the incorporation of temperature and precipitation from the IGSM model into an agricultural crop simulation model. Water supplies were considered in the form of natural runoff and renewable groundwater amounts, as well as desalination from the installed capacity in each basin. Taking into consideration the water supplies and demands, water stress was calculated on a basin scale. Human capacity to manage water stress was taken into consideration by minimizing spillage and utilizing all surface water runoff before groundwater was used.

Both studies focus primarily on representing the global hydrologic system in detail, to assess water stress with subsequent calculation of water use driven exogenously by socioeconomic scenarios. Socioeconomic variables at national scales, such as population and GDP, were used to compute water use; however, feedback effects on these variables as a result of water stress were not considered. For example, as water stress is encountered there is an associated effect on economic

productivity due to limitations in water withdrawals for agricultural and industrial production thereby creating the potential for GDP to decrease. Although these studies and several others mentioned in Sood and Smakhtin (2014) represent detailed processes of the hydrologic system, the inability to incorporate feedback during periods of water stress inhibits the development of realistic future impact scenarios for the global system.

Schlosser et al. (2014) used the IGSM water resource system from Strzepek et al. (2013) with different climate models socioeconomic scenarios to emphasize the effects of changes in climate and economic growth separately and then combined. The results from this study have shown that water demands increase at a much faster rate in developing countries due to larger population growth and per capita water demands. Overall, it was found that socioeconomic drivers of population and economic growth had the strongest effect on water stress in the future as in Alcamo et al. (2007), but regional changes in climate provide exceptions to this case. For example, in some areas of China and India increased precipitation reduces water stress through increased surface water availability.

The WorldWater model of Simonovic (2002a) added a global water resources sector to the WORLD3 model of Meadows et al. (1974). This was done to assess potential limits to human development resulting from limited water resources. By incorporating water resources into WORLD3's model structure it was found that the use of clean water for diluting and transporting wastewater has the potential to contribute to water stress on a global scale (Simonovic 2002b). As a result, food production becomes limited, result in increased mortality rates and an overall

reduction in global population. The WorldWater model provided a unique insight in how water resources could affect the global dynamics presented in WORLD3, however there are a considerable amount of limitations with both models.

The WORLD3 and WorldWater models included a limited number of sectors to represent the state of the World and were highly aggregated in both time and space. Because of this, the utility of them is limited to analyzing the interactions between a small subset of horizontally aggregated long-term processes occurring on a global scale. Due to the limited amount of model sectors only a small subset of the feedbacks, which we consider important in the Earth system today, were included. For example, environmental systems associated with climate, hydrology, biogeochemical cycles, and land cover were not included, thereby limiting the degree to which global environmental change can be studied.

The WORLD3 and WorldWater models were constructed on a globally aggregated scale, meaning that every variable in the model was one that was either globally averaged or summed, and the temporal scale considered was annual. Because of this, any heterogeneity in the subsystems that are represented (water resources, industrial growth, agriculture and food production, pollution, non-renewable resource, and population dynamics) would fail to be captured. Concepts such as water stress would be understated at this degree of aggregation because it is based on the discrepancy between water demand and water supply which vary in time and space, and the shifting patterns of global climate (and as a result the hydrologic cycle) could not be captured.

Another study, done by Wada and Bierkens (2014), combined a global distributed hydrological model (PCR-GLOBWB) with a global water demand model to study the interactions between water availability and water demand allowing for feedbacks to arise between them for the period of 1960 to 2010. Water demand was broken down into withdrawal and consumptive use for domestic, industrial, and agricultural users, and water availability was separated into surface and groundwater resources. Desalination was also included using available country level data. The results show an increasing reliance on groundwater resources over the analysis period, suggesting that surface water has been extensively exploited in past periods. As a result, more groundwater depletion is expected in areas that are already experiencing high rates of groundwater use. When this methodology was used to project the use of water resources in the future it was found that there was an increase of 30% use in non-sustainable surface water and non-renewable groundwater (Wada and Bierkens 2014).

Depletion of groundwater resources and its economic impacts were studied on a global scale by Turner et al. (2019). The GCAM model was coupled with a global hydrological model developed in Liu et al. (2017) in order to determine the amount of renewable and non-renewable groundwater available for use at the basin scale. Groundwater aquifer thickness reduces with groundwater withdrawals from the GCAM model and becomes more costly to pump according to predetermined supply curves. The results of this study show that contrary to much of the current literature, groundwater depletion rates may decrease by the end of the 21<sup>st</sup> century. This was due to economic limitations regarding pumping and extraction cost in groundwater aquifers that experience significant amounts of drawdown. This is an important finding, because it suggests that even though groundwater resources are available, they can become un-economical. The study suggests

that it may be more beneficial investing in additional surface water supplies via reservoir expansion, but this is not without limitations as well.

Hanasaki et al. (2016) developed a model to estimate the areas where seawater desalination is likely to be used for incorporation in global hydrological models that incorporate human water withdrawal and consumption. Changes in technology have begun to make desalination an increasingly viable option in some areas, allowing for competition with conventional water sources such as surface water and groundwater resources. In this study relationships were developed between gridded aridity datasets (as the ratio between potential evapotranspiration and precipitation), distance to coastlines, population, and GDP data to desalination capacity over time. The relationship was used to project desalination production into the future, with global values increasing from 2.8 km<sup>3</sup>/year in 2005 to between 18.7 and 49 km<sup>3</sup>/year in 2055 based on the assumptions used.

This value is still small in comparison to the total amounts withdrawn from conventional water resources but is a considerable increase from the base year. Desalination becomes much more important for areas that are arid, close to coastlines, with higher populations and economic capacity to make the technology feasible. Previous studies incorporating desalination into global hydrologic models have only either used constant values or assumed increasing values with population (Wada et al. 2016). Hanasaki et al. (2016) shows the importance of taking an economic approach to alternative water supplies such as desalination, however the implementation is based on the use of



exogenous data sources for population and GDP. Incorporating endogenous estimates would allow for feedbacks to take place.

## 2.2. Fundamentals of System Dynamics Simulation

A system can be generally defined as a collection of structural and non-structural elements that are connected and interact with each other to function as a whole (Kauffman 1980; Simonović 2012). This definition encompasses many types of systems that could be physical, organizational, social, or abstract. A system typically has an input which through a series of transformations generates an output. In open systems, the output leaves the system boundary while in closed systems the output goes on to affect the input, thus creating a feedback loop.

A space heater used to warm a room is an example of an open system. The input of turning the unit on adds heat from warm air being pushed into room thereby increasing the temperature to a preferred level. The same problem of heating the room could be addressed with the addition of a thermostat, creating a closed system. The input of warm air into the room increases the room temperature to the desired level thus affecting the input by causing the heater to turn off when the desired temperature is reached. Inputs to open systems are exogenous (value is determined outside of the model), while inputs that are affected by the outputs in closed systems are endogenous (value is determined from within the model).

The study of system dynamics seeks to find endogenous explanations of system behaviour (Sterman 2000). What this means is the source of the problem being investigated lies within the system structure. Exogenous explanations of system behaviour do not explain the dynamics of the system responsible for the problem – they only pose further questions on what caused the exogenous variable to change as they did (Sterman 2000). Endogenous system behaviour can be mapped out using causal loop diagramming in order to identify feedback relationships. An example of a causal loop diagram is given below for the case of the heating problem mentioned previously using a thermostat (Figure 2.1).

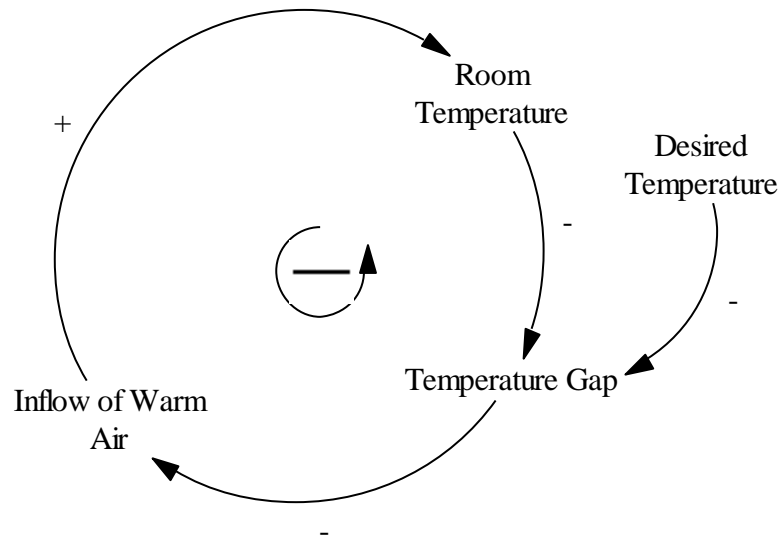


Figure 2.2. Causal loop diagram for heating of room with thermostat.

Causalities are denoted by information arrows which link together the variables included in the description of the system dynamics. The information arrows can be thought of mathematically as,

$$\text{Inflow of Warm Air} = f(\text{Temperature Gap}) \quad (2.1)$$

Where each connection indicates which variable is a function of one another. The direction of causality is denoted by the polarity (+/-) that is assigned to each information arrow. For example, it is shown in Figure 2.2 that an increase in the *Inflow of Warm Air* would cause a decrease in the *Room Temperature* as indicated through the negative polarity assigned to this link.

Feedbacks that drive system behaviour are identified by following the connections from a given variable in the causal loop diagram back to itself. The polarity for a feedback loop can either be positive or negative. Positive or reinforcing feedback loops signify a change in a given variable in the loop which thereby causes further change in the same direction as the initial change. This type of system behaviour signifies exponential growth processes (Simonović 2012). A negative or balancing feedback loop responds to a change in a given variable in the loop with another change in the opposite direction, thereby dampening the initial effect. Negative feedback loops always have either an implicit or explicit goal for which the system will tend towards.

In the case of Figure 2.1, a negative feedback loop is formed between *Inflow of Warm Air*, *Room Temperature*, and *Temperature Gap*. An increase in the *Inflow of Warm Air* results in an increase in the *Room Temperature* which will result in a smaller *Temperature Gap* from the *Desired Temperature*, thus resulting in smaller *Inflow of Warm Air*. The polarity of this feedback loop is indicated by negative sign shown inside the loop. In this case the goal of the negative feedback is explicit. The

*Desired Temperature* would be reached as the *Temperature Gap* approaches a value of zero, causing the heater to turn off.

Causal loop diagramming helps illustrate the dynamics that act to drive system behaviour from a conceptual standpoint. The construction of the causal loop diagrams can be developed with stakeholders using a participatory approach to help uncover important dynamics in systems that have social elements or decision-making components (Kotir et al. 2016). However, the problem with causal loop diagrams is that they do not contain any information about the structure of the systems they describe (Richardson 1986). Variables that describe the system state cannot be distinguished from those that are derived from it. For example, in the case of Figure 2.1 the variable *Temperature Gap* is used to denote the difference between *Room Temperature* and the *Desired Temperature*. However, the gap assumes implicitly that *Room Temperature* is lower than the *Desired Temperature* initially. Otherwise the *Temperature Gap* would take on a negative value thereby reducing *Inflow of Warm Air* to a negative value, which physically does not make sense.

Stock and flow diagrams build from the causal loop diagram by adding structural elements that denote the system state variables (stocks or levels) and those which affect them (rates or flows). Stock variables represent accumulations within the system and represent conservative quantities such as mass or energy for example. The values of stock variables represent the state of the system in a snapshot in time. Flow variables are the only variables that can affect the values of stocks. They represent actions within a system, and their units are that of the corresponding stock variable

divided by a unit of time. The stock and flow diagramming for the heating of a room with a thermostat is shown in Figure 2.2 below.

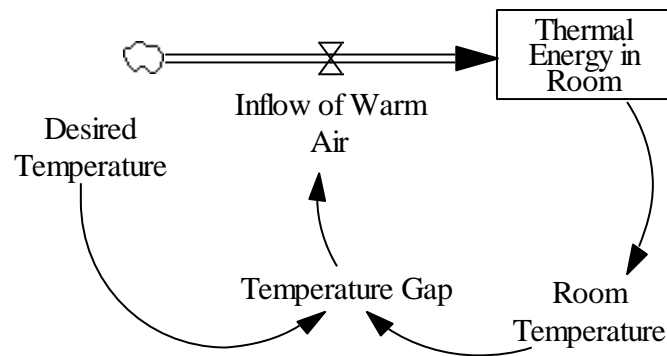


Figure 2.3. Stock and flow diagramming for heating of room with thermostat.

The stock variable is chosen to represent the amount of thermal energy in the room as opposed to the room temperature. This is because temperature is not a conserved quantity. Degrees of temperature cannot be accumulated whereas energy can. The amount of energy in the room denoted by the variable *Thermal Energy in Room* is converted to the *Room Temperature*. The *Inflow of Warm Air* from the heater is a flow variable, and acts to influence the stock of *Thermal Energy in Room* directly. The stock and flow diagram shown here represents a first order differential equation,

$$\frac{d(\text{Thermal Energy in Room})}{dt} = \text{Inflow of Warm Air} \quad (2.2)$$

Where all variables that are not in this equation are deemed auxiliary variables and only act to further define *Inflow of Warm Air*. This contrasts with the mathematical equivalent for the causal loop diagram in Equation 2.1. Stock and flow diagrams provide a visual depiction of a system of differential equations, or the structure of the system, while causal loop diagrams only show causality.

The presence of time delays in dynamic systems is an important element to consider when analyzing the system behaviour. In the most general terms, delays are used to represent the amount of time between the response of a system to a corresponding stimulus (Simonović 2012). Practically speaking, this type of phenomenon can occur in different forms. It takes time to measure and report information necessary to act, creating an informational delay (Sterman 2000). An example of an informational delay in the context of the heating system discussed above could exist through the thermostat reading. If the readings are taken in 10-minute intervals, there is an information delay of 10 minutes for the reading of the *Room Temperature* before the heating unit can respond with *Inflow of Warm Air*. Material delays also exist as it takes time to move from one location to another or change form. For example, the planning and construction of infrastructure takes time from initial planned investments.

By combining positive and negative feedback mechanisms as well as time delays many different types of system behaviours can be expressed (Figure 2.4).

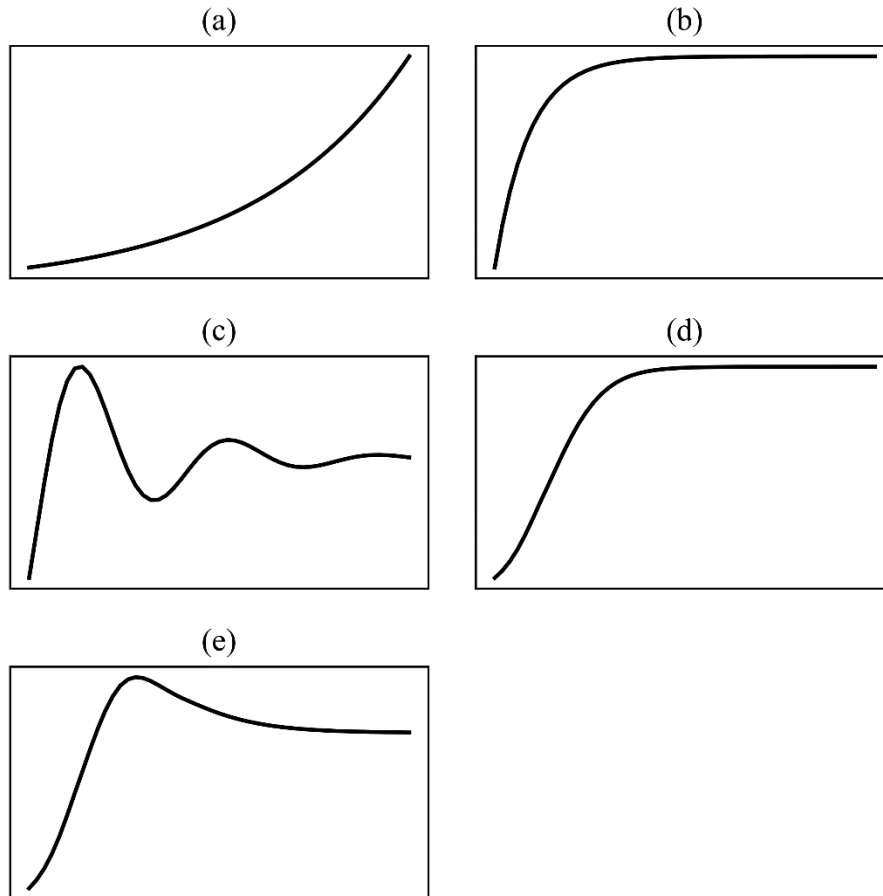


Figure 2.4. Basic dynamic system behaviours of (a) positive feedback, (b) negative feedback, (c) oscillation, (d) S-shaped growth, and (e) overshoot and collapse.

Combining the goal-seeking behaviour of negative feedback loops, along with a delay in the perception of the goal, results in an oscillatory system behaviour (Figure 2.2c). In the case of the room heating example, this type of system behaviour could result from a delay in the thermostat reading of the *Room Temperature*. As the room is being heated, the *Desired Temperature* would be reached and then overshoot until the thermostat reading indicates a temperature greater than or equal to this value. From this point, the heating unit would turn off and the temperature would decrease below the desired temperature until the next thermostat reading.

Combining both positive and negative feedback loops together can result in a system behaviour termed “S-shaped” growth (Figure 2.2d). This type of behaviour occurs when the system state variable follows a sigmoidal curve. At the initial system state, positive feedback dominates causing exponential growth. As the system state variable grows, the negative feedback begins to dominate at an inflection point, causing goal-seeking behaviour to an equilibrium value where the inflows and outflows of the stock variable are equal. This behaviour is common in systems that represent constrained growth. This is why the equilibrium value is often referred to as the “carrying capacity of the S-shaped growth curve (Goodman 1989). For example, the growth of rabbit populations can follow this behaviour. As the population grows exponentially the density of the population in a given area increases. This results in reduced mortality rates due to the effects of crowding, eventually reaching an equilibrium population value.

The “overshoot and collapse” behaviour is similar to that of S-shaped growth, where positive and negative feedback loops are combined to simulate constrained growth patterns (Figure 2.2e). However, in this case there is also a delay that is incorporated into the negative feedback loop. An overshoot of the carrying capacity or equilibrium value of the S-shaped growth curve occurs due to the delay in the negative feedback. The negative feedback acts more strongly than it would in the case of S-shaped growth because the system is being pushed beyond its equilibrium value. As a result, there is a collapse in the system stock.



Systems that have multiple coupled stocks, feedbacks, and delays are known as complex systems. Complex systems can exhibit any or all of the system behaviours listed previously. There are three key properties of complex systems which include irreversibility, inertia, and transitional phenomena (Mackenzie 1999). The property of irreversibility states that a system does not return to its previous state when subject to a disturbance. This means that the point of equilibrium, or the balance of inflows and outflows for the stock variables, can be altered when the system is subject to external influences. The property of inertia refers to perpetual change of the system state through positive and negative feedback processes. Finally, the property of transitional phenomena refers to the altered behaviour of a system that emerges as dominance shifts between feedback loops. An example of this is S-shape growth patterns which represent a shift of positive feedback to negative feedback dominance.

### 2.3. Integrated Assessment Models of Global Change

Understanding the interactions between sub-systems of the Earth system is a demanding task and involves communication between diverse areas of study (Hamilton et al. 2015; Dunford et al. 2014; Janetos 2008). To gain an understanding of the interactions between different sub-systems of the Earth system, integrated assessment models are employed. IAMs use simplified representations of various sectors within the Earth system including; social-economy, climate, ecology, water resources, land use and cover, carbon cycle, and energy production and demand for example, to represent complex feedback structures between them which evolve through time (Akhtar et al. 2013; Hamilton et al. 2015). It is within this framework that global change can be assessed in response to various scenarios regarding policy, technological developments, and socioeconomic

trends. IAMs are used to develop scenarios for greenhouse gas emissions and land use/cover for GCMs to simulate climate change (Moss et al. 2010).

The representation of water resources in integrated assessments of global change vary widely in the amount of detail that is included, and the level of integration with other components of the Earth system. In addition, the spatial scales at which components are represented and interact vary in each IAM. The concept of dealing with mismatching spatial scales in integrated assessment research has been recognized as one of the major challenges, as it defines the way in which regional to local scale processes interact with the global system (Scholes et al. 2013). For example, in water resources management, this effect could be manifested through impacts on global economy as agricultural and industrial production is limited by regional water stress.

Several integrated assessment models of global change were examined in the literature. The common sectors that are represented endogenously (internally linked with other system components) in each model are CO<sub>2</sub> emissions and energy production and demand (Table 2.1). This finding likely stems from the fact that the first IAMs used to study human influence on climate change focussed primarily on the feedback relationships between these two sectors (Capellán-Pérez et al. 2014). As IAMs continue to evolve there becomes a tighter integration between these sectors and biogeophysical cycles of the Earth system (Fiddaman 2002). Part of this integration has led to more comprehensive representations of the hydrologic cycle to assess impacts on water stress through comparisons of water availability and demand (Strzepek et al. 2013). The models that currently integrate water availability and demand are: AIM (Asia-Pacific Integrate Model)

(Matsuoka et al. 2001), IMAGE (Integrated Model to Assess the Global Environment) (Stehfest et al. 2014), IGSM-WRS which is a modification of the Integrated Global System Model that includes a Water Resource System component (Strzepek et al. 2013), GCAM (Global Change Assessment Model) (Calvin et al. 2019), and ANEMI (Davies and Simonovic 2010; Akhtar et al. 2013).

Table 2.1. Sectoral comparison of Integrated Assessment Models from the literature.

	MESSAGE	AIM	GCAM	IMAGE	DICE/RICE	FREE	IGSM-WRS	ANEMI
Agriculture	x	x	x	x	x	---	x	x
Land Use	o	x	x	x	o	o	x	x
Demography	x	o	o	o	o	o	x	x
Climate	---	x	x	x	x	x	x	x
Water Quality	---	x	---	x	---	---	x	x
Water Availability	---	x	x	x	---	---	x	x
Water Demand	---	x	x	x	---	---	x	x
Water Supply	---	---	x	o	---	---	o	x
Energy	x	x	x	x	x	x	x	x
Sea Level Rise	---	x	x	x	---	---	x	x
Economy	x	o	x	o	x	x	x	x
Emissions	x	x	x	x	x	x	x	x

x Internally linked      o Externally driven      --- N/A

The AIM and IMAGE models (Figure 2.5 and Figure 2.6) are similar in that the Earth system is driven by a set of socioeconomic scenarios which are defined by future population, GDP, and technological trends as exogenous input to the model. These inputs drive feedback processes between land use, energy supply and demand, and CO<sub>2</sub> emissions, which in turn are used to assess regional impacts on water resources such as flood risk and water stress among other impacts on biodiversity, agricultural productivity, and ecosystems. The way in which these models are driven

by exogenously through future assumptions in social-economy does not allow for cross-sectoral feedbacks between water resources systems and the dynamic evolution of global change. A combination of regional and grid based spatial disaggregation methods are used to resolve changes in the Earth system to finer spatial scales, however in both models there is no ability to for regional impacts on finer scales to feedback into the global system.

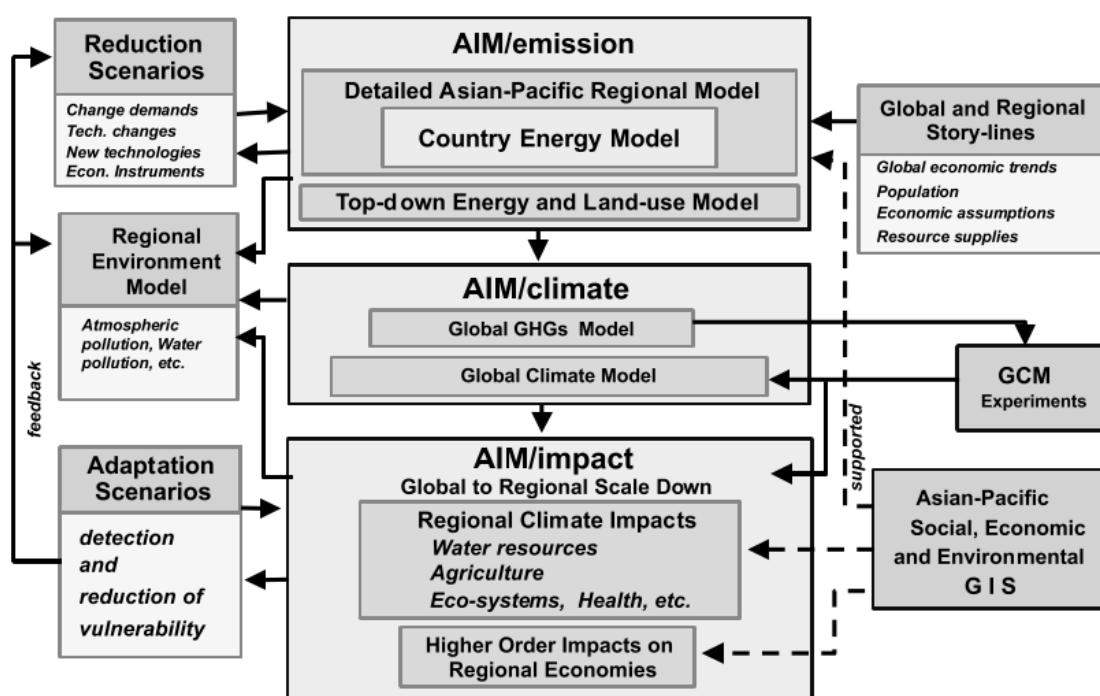


Figure 2.5. Macro-structure of the AIM model (after Matsuoka et al. 2001).

IGSM-WRS is a modified version of IGSM, which allows for the coupling of IGSM's Earth system model to a detailed water resource system (WRS) (Strzepek et al. 2013) as shown in Figure 4. This WRS calculates water availability from surface storage and groundwater sources within a set of 282 large river basins around the World using a global hydrologic model on a 2x2.5-degree grid. Alternative water sources are also accounted for through water diversion from neighboring

grid cells, and desalination capacity in coastal environments. Although the model includes a comprehensive water sector and allows for assessment at the regional scale in the context of the global system, it was noted that the water sector is related to the economy-climate sector via a “one-way” relationship (Strzepek et al. 2013).

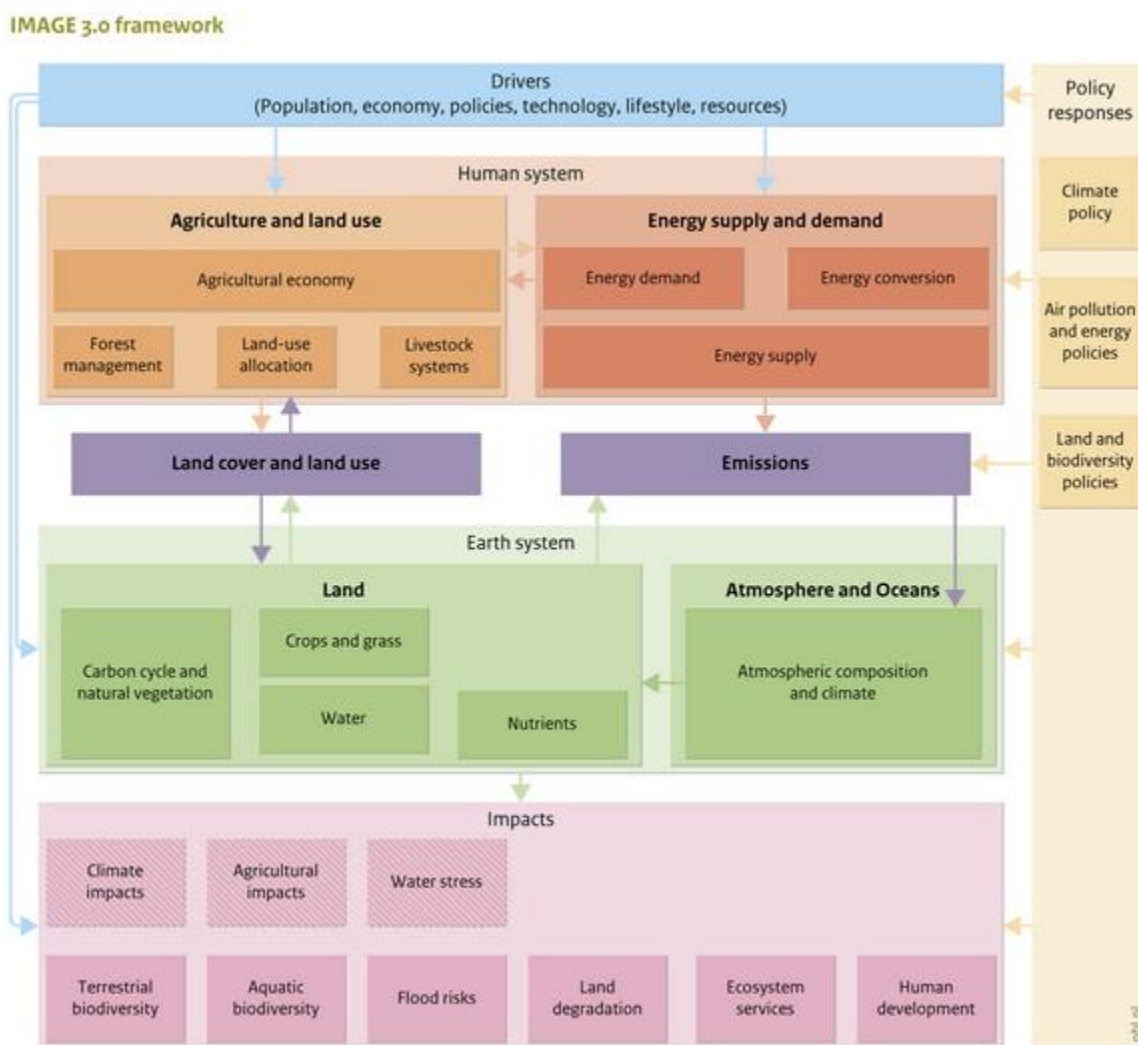


Figure 2.6. Macro-structure of the IMAGE 3.0 model (after Stehfest et al. 2014).

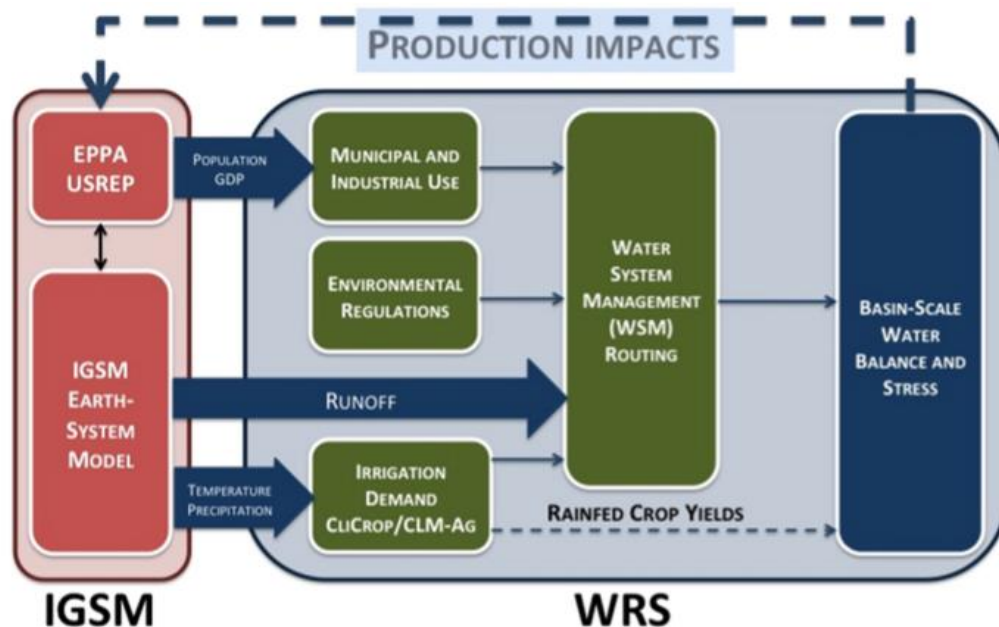


Figure 2.7. Macro-structure of IGSM-WRS model (after Strzepek et al. 2013).

The GCAM model has undergone recent updates which greatly improve the representation of water resources for assessments of global change (Calvin et al. 2019). A water resources system was added which represents water availability, supply, and demand at a basin level consisting of 235 sub-basins globally. Availability of water is simulated using a global hydrological model, while demands are based on gridded estimates of electricity production for industry, and irrigation demands for agriculture. Municipal demands are based on exogenous gridded values for population and GDP. Water supplies are represented by consumption of surface water and groundwater resources in the hydrologic model, as well as seawater.

The production of these supplies is dependent on the economics of each supply type in a given region. For example, desalination is used in places where surface water and groundwater are not abundant, and desalination is cheaper (i.e. closer to coastlines). Groundwater depletion and

changes in surface water availability also affect water price allowing for the use of these supply options to change (Turner et al. 2019). Feedback effects between model sectors is shown in Figure 2.8.

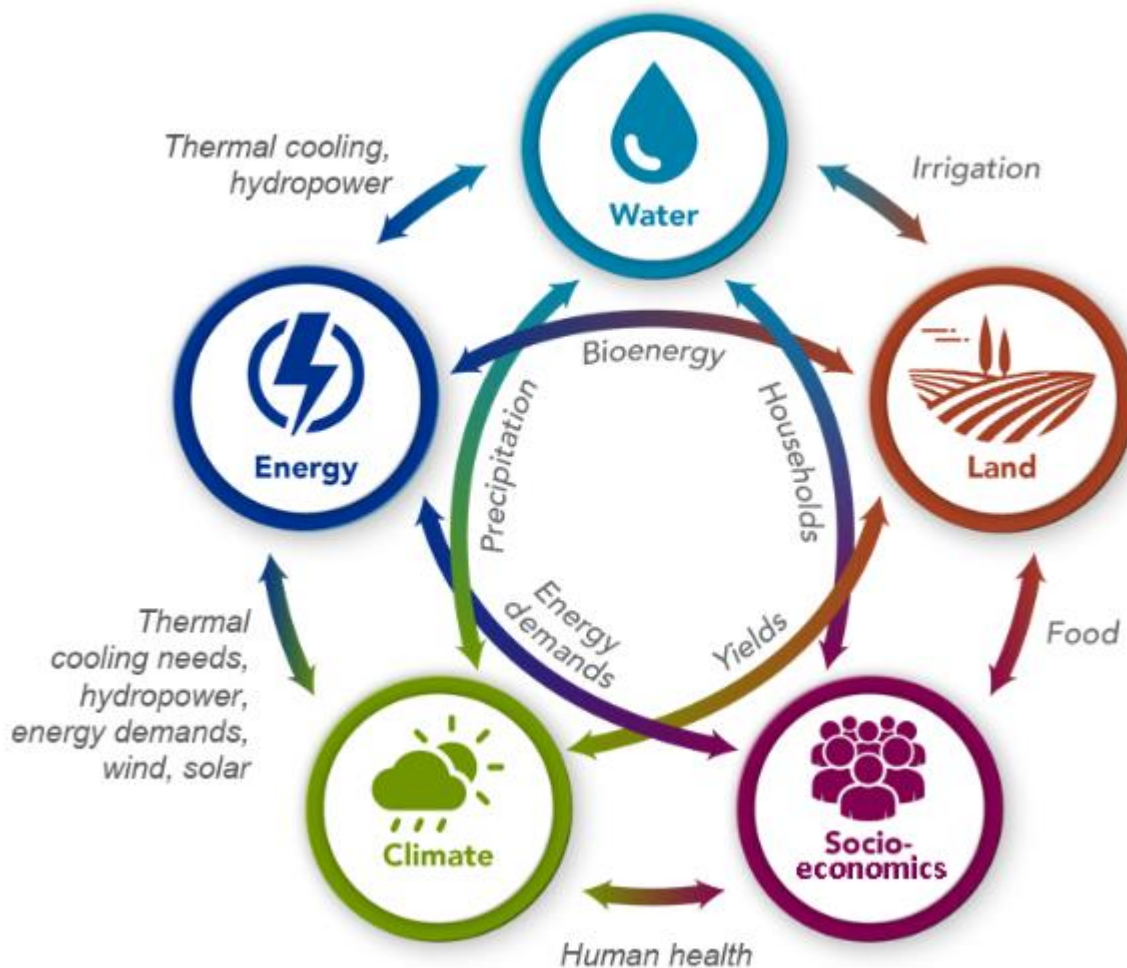


Figure 2.8. Connections between energy, water, land, climate, and socioeconomics in GCAM version 5.1 (after Calvin et al. 2019).

The incorporation of water resources in GCAM is a major improvement, however representations of water quality and water reuse are currently not included. Furthermore, population is still an

exogenous policy variable which limits potential negative feedback from resource constraints and pollution, such as water stress and quality degradation.

The current version of the ANEMI integrated assessment model developed at Western University is made up of 9 sectors including: population, land use, food production, carbon cycle, climate, energy-economy, and three water sectors composed of water quality, demand, and availability through modelling of the global hydrological cycle (Akhtar et al. 2013). In this approach the Earth system is modelled as a series of feedback processes linking the 9 sectors or sub-systems. The model is driven endogenously from an initial state as opposed to the scenario driven approach in the other models mentioned. The benefit to this approach is that the feedbacks between the model sectors can be studied, allowing for the integrated assessment of global change from an entirely endogenous perspective.

The spatial scale used in the ANEMI model is aggregated to the global level. This allows for long-term feedback processes to be examined; however, this level of aggregation limits the level of detail that can be represented. For example, without a spatial dimension, regional processes affecting water stress through variations in water demand and availability cannot be examined. Such effects might include regional per capita water usage, population growth rates and migration, as well as regional hydrologic processes used to determine water availability. This could lead to underestimating the impacts of global change on water stress due to only the globally aggregated values being used. For example, global water stress may appear to be low while extreme levels of



water stress in agricultural areas of China might exist. This could negatively affect regional food production and have global impacts on food markets (Wang et al. 2017).

Models such as DICE/RICE, FREE, and MESSAGE are focussed mainly on interactions between climate, energy, economy and emissions with no real focus on global environmental change. GCAM, IMAGE, and IGSM-WRS include water resources components, however there are still key feedback relationships missing. Water is typically treated as an assessment variable rather than a key driver in integrated assessment models. ANEMI is the only integrated assessment model that considers water quality, availability, demand, and water supply simultaneously allowing for feedbacks to take place between the model sectors. Studying the role of water resources in global change with the ANEMI model is the focus of this thesis. More details on the ANEMI model development is provided in the next section.

## 2.4. ANEMI Model Evolution

The word *anemi* is a Greek word that translates to “the winds of change”. The choice of this word for the integrated assessment model used in this work was to capture the dynamic and feedback driven nature of the model which makes it unique in the domain of integrated assessment modelling. The ANEMI model was inspired by the WorldWater model of Simonovic (2002), which was based on the WORLD3 model of Meadows and Jorgen (1992). The WORLD3 model was created to assess potential limits to the growth of human civilization through natural resource and pollution effects which were explored using system dynamics simulation techniques. This work showed that overshoot and collapse behaviours in our global system are expected in the

future due to the coupling of economic growth and material consumption. This was later expanded upon in the WorldWater model to include the World's water resources as another potential limit to growth. Conceptually, the ANEMI model builds upon that of WorldWater by developing a model that is purely based on system dynamics (model is constructed using stocks and flows to represent feedback processes), which places an emphasis on the role of water resources in the Earth system.

The ANEMI model is developed at the Facility for Intelligent Decision Support, at Western University. It brings together 8 simplified global models of climate, carbon, land use, population, energy-economy, water use, water quality and the natural hydrologic cycle. The climate sector models the change and interaction between atmospheric and ocean temperatures in response to radiative forcing from changes in atmospheric greenhouse gas concentrations. The carbon sector provides atmospheric carbon dioxide concentrations to the climate sector by modelling the carbon cycle on a globally aggregated scale. This includes carbon stocks for land biomass, litter, humus, stable humus and charcoal, and several ocean layers. The transfer of carbon in the carbon cycle is influenced anthropogenically by changes in land use, and industrial carbon dioxide emissions. The changes in land use are driven primarily by population growth rates resulting in conversion of temperate forest, and semi-desert and tundra biomes to agricultural land, and agricultural land to human developed areas. Anthropogenic greenhouse gas emissions are driven by the production of energy which is closely tied to economic development. The economic sector models economic output as a function of the global capital stock, and labor from the working population.

In the ANEMI model, water resources are represented through the three water sectors mentioned above, including water quality, water demand, and the hydrologic cycle. The hydrologic cycle component determines the amount of water resources available for human consumption, by modelling the movement of water through atmosphere, land, groundwater, ice, and ocean stocks. Water demand is driven through population and economic development as well as irrigation in the case of agricultural demand. A portion of water withdrawals and consumption are driven by the water demand and act to reallocate water in the hydrologic cycle. Water quality is represented simply by allowing for polluted water in the form domestic and industrial wastewaters, as well as agricultural returnable waters to displace freshwater resources. This is done by using the rule of thumb mentioned in Shiklomanov (2000), where 1 unit of polluted water renders 8-10 units of water unsuitable for human consumption, contributing to water stress. Water stress acts as the primary driver for the development of alternative water resources in the form of wastewater reuse and desalination. However, it is assumed that these resources can be established immediately without any consideration for the cost of implementation.

The first version of the ANEMI model was developed in Davies and Simonovic (2010), and established the basic feedback structure of the society-biosphere-climate system. This was accomplished by bringing together separate sub-systems available in the literature in order to represent the model sectors listed above, and establish inter-sectoral feedbacks used to drive the system (Figure 2.9).

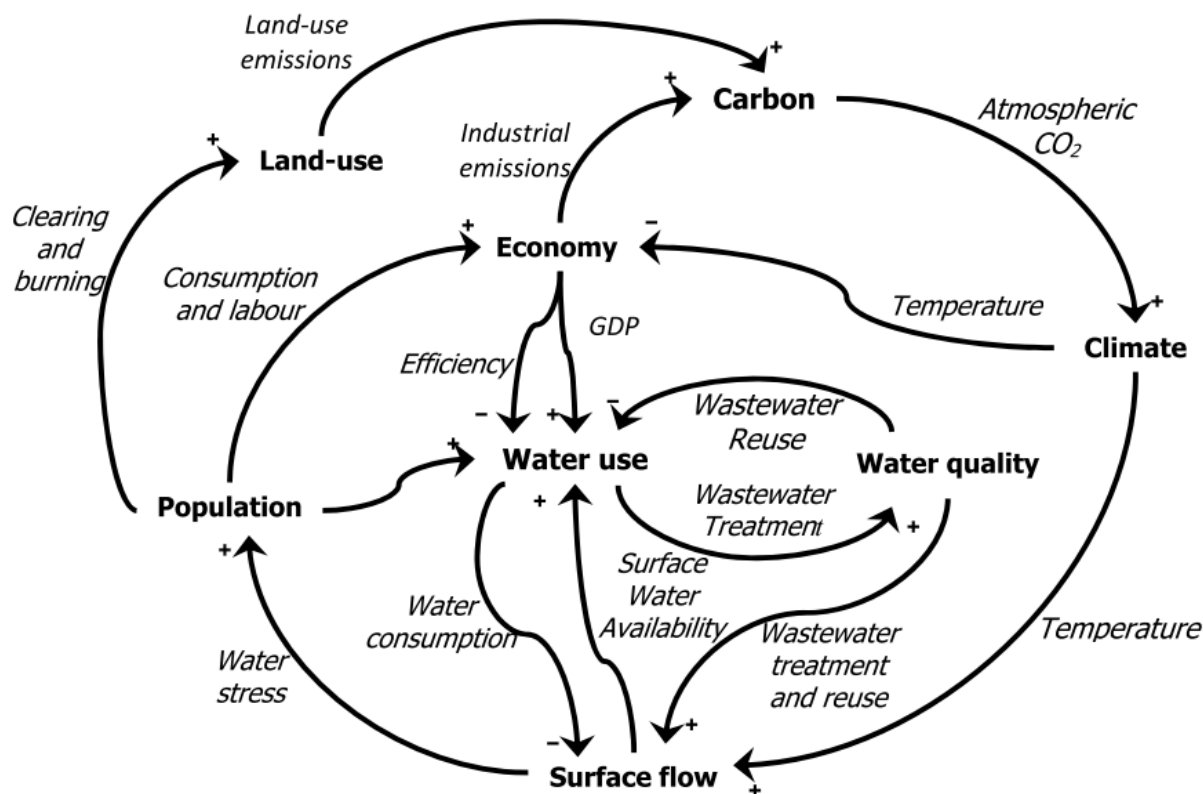


Figure 2.9. Intersectoral feedback structure of ANEMI (after Davies and Simonovic 2010).

The climate sector is based on the Box-Advection-Diffusion model of Harvey and Schneider (1985), while the carbon cycle and land use sector were modified from Goudriaan and Ketner (1984). Population growth is modelled based on the approach taken by Fiddaman (1997) with the addition of water stress as an additional limitation to growth. The economic sector is based on the Dynamic Integrated model of Climate and Economy (DICE) of Nordhaus (1992). The water quality, water demand, and hydrologic cycles sectors were developed in such a way that allows for their integration with the sub-systems that were adapted from the literature.

The purpose of this work was to increase the understanding of socio-economic policies and scientific uncertainties of the Earth system by focusing on system structure and function rather than specific predictions. Using several policy scenarios and sensitivity simulations it was found that water pollution resulting from low levels of wastewater treatment may lead to severe levels of water stress on a global scale. It was recommended that greater reuse of treated wastewater and slowing the rate of irrigation expansion could help alleviate water stress in the future. In this work the role of feedbacks on the development of global change are emphasized as feedback interactions between socio-economic and physical systems are used to drive the model.

In Davies and Simonovic (2011) the first version ANEMI model was improved by incorporating more detail into the agricultural and food production sectors as well as how this relates to water pollution. Food production was made to be driven by per capita caloric consumption which varies over time, along with the total caloric consumption which with population. Fodder crops and pasture-based production are simulated separately from food crops due to different water requirements. This allows for more accurate quantification of virtual or green water requirements needed from the agricultural sector of the model. The dilution of green water from agricultural runoff was then incorporated into the definition of water stress by acting as an additional source of water consumption. The results from this study showed that increased levels of irrigation versus rain-fed crops reduced green water consumption and agricultural area by the year 2100. This in turn led to higher water stress values from greater consumption of blue water and more water pollution from agricultural runoff. In other words, in order to meet the demands for food of a growing population water becomes increasingly scarce.

The second version of ANEMI (ANEMI2), published in Akhtar et al. (2013) incorporates a computable general equilibrium model to represent energy production within the global economy as well as a new disaggregated population sector, sea-level rise impacts on agriculture, and includes the effect of more greenhouse gases on climate. The disaggregation of the population sector into four age demographics allowed for the working population (ages 15 to 64) to represent the labor force in the economic model, and allowed for heat stress effects driven by changes in climate to affect mortality rates in the old and young (ages 15 or less and 65+). The energy-economy sub-system allowed for a carbon tax scenario to be analyzed. The application of a carbon tax on fossil fuels initially showed a heavier reliance on hydropower and nuclear energy production, as well as a drop in energy consumption due to higher prices. This policy resulted in a 0.4°C by the year 2085 compared to baseline. However, carbon emissions were only delayed, leading to higher emission rates by the year 2100. The feedback structure of ANEMI2 is shown in Figure 2.10.

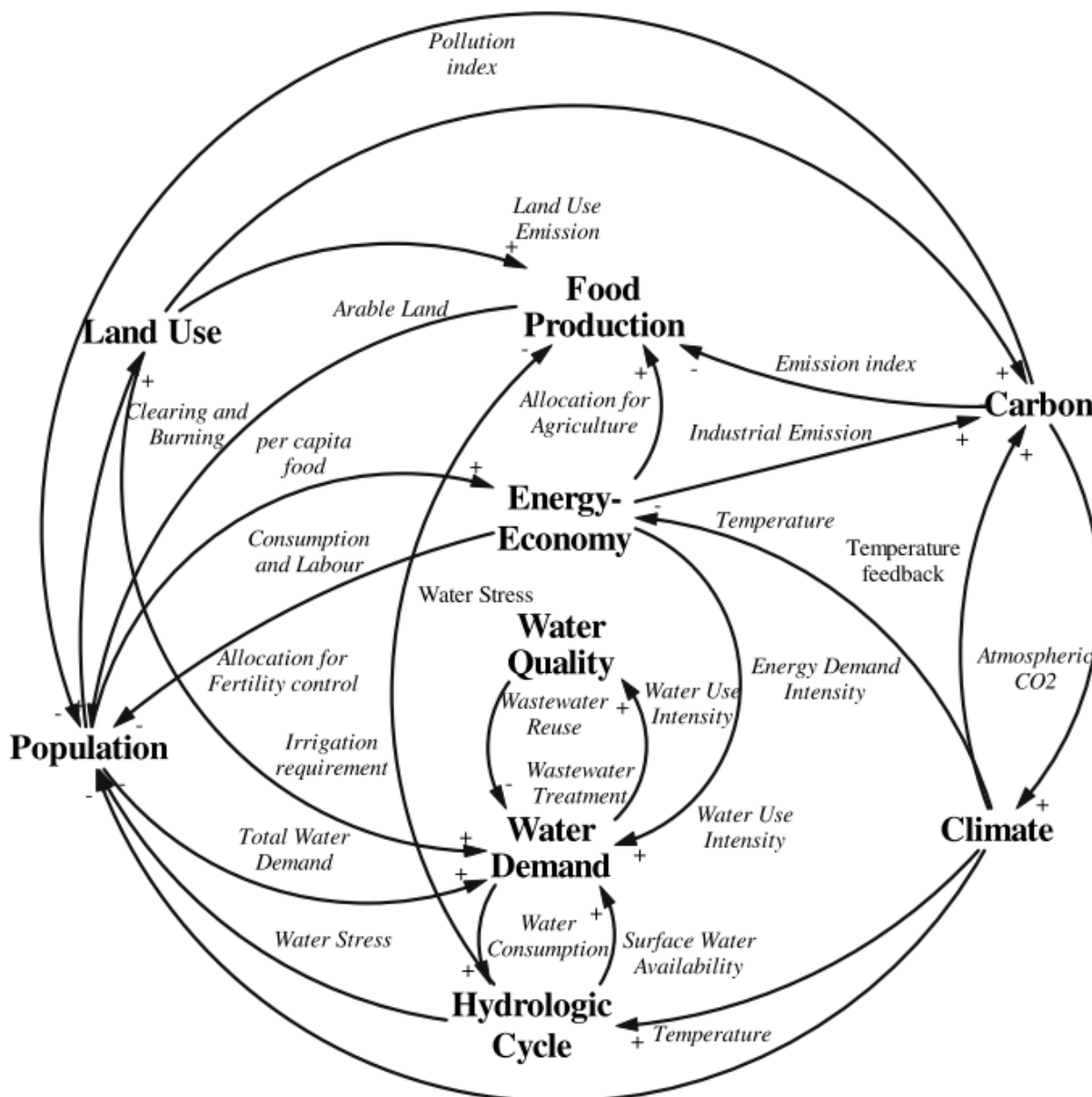


Figure 2.10. Intersectoral feedback structure of ANEMI2 (after Akhtar et al. 2013).

The ANEMI2 model was regionalized for Canada using a top-down approach for population, land use, hydrologic cycle, water demand, water quality, food production, and energy-economy sectors (Akhtar 2011; Davies et al. 2011). In order to accomplish this, the stock variables in this sector were disaggregated to represent Canada and the rest of World (ROW) as two regions which make

up the whole. A small open economy model of Canada was used in combination with the ANEMI model. Three scenarios were run including the implementation of a carbon tax as well as carbon capture and storage technology, increased water use, and increase in agricultural land conversion. The carbon tax scenario showed an initial decrease in GDP of the Canadian economy; however, GDP slowly rebounds and increases relative to the baseline while emissions were greatly reduced. An increase of water usage of 15% had little effect on water stress in Canada due to an abundance of freshwater, while increasing agricultural land by 15% resulted in greater food production and relatively little impact on available water resources.

Building from the structure of ANEMI2, Breach and Simonovic (2018) added energy recovery from wastewater in the form of biosolids incineration and biogas utilization. The recovered energy is treated as an additional energy source in the energy-economy sector of ANEMI2, creating a feedback that acts to boost wastewater treatment over time with re-investment from energy recovery. In this work, the level of wastewater treatment is represented by a stock that contains a number of uniform treatment plants providing a level of wastewater treatment capacity. Investment boosts the number of plants while the processes of aging and decommissioning causes the stock to decrease. Energy recovered from the wastewater treatment processes provides for a portion of energy production in the energy-economy sector and re-investment is proportional to the energy supplied. The feedback structure of this work is shown in Figure 2.11. The results show that by viewing the construction of wastewater treatment plants as a type of investment in recovered energy, wastewater treatment could increase globally by 34% despite increases in wastewater volumes due to a growing population with improved access to sanitation.





ability to adapt to future water stress in certain regions through investment in infrastructure, effective water allocation management, and water saving technologies (Vörösmarty et al. 2010).

Studies that have modelled the development of surface water and groundwater supplies only included coupled hydrologic and water demand models while socioeconomic aspects of the Earth system remainder exogenous, as is the case in Wada and Bierkens (2014). The newly added water supply sector in the GCAM model includes the use of alternative water supplies as the price of conventional water supplies increase due to depletion. However, the socioeconomic aspects of the GCAM model such as population and GDP growth are scenario based thereby limiting many potential feedback processes.

The development of water supplies as a way to adapt to water stress from an economic point of view considering both conventional and alternative water supplies has not yet been represented in a fully integrated way on the global scale. The main objective of this thesis is to address this gap in the literature through the development of a water supply model that is economically based within the highly endogenous ANEMI integrated assessment model.

## 2.6. Research Objectives and Thesis Contributions

Water resources management plays an integral role in the process of global change, acting as a potential limit to growth of human development in the long term (Simonovic 2002b). Water pollution, availability, and production of water resources both, conventional and alternative, will

play a key role on the level of future water stress. Adapting to such water related issues in the face of global change will require significant economic investment and/or changes to the way that water is managed on a global scale.

Water resources are linked to various aspects of global change, such as climate change affecting the availability of water resources, population growth, industrial development, and energy requirements affecting water demand, and pollution affecting water quality. Because of the integrated nature of water resource management on a global scale, an integrated solution is required. Integrated assessment modelling provides a way to bring together multidisciplinary models of global change and is an important tool for analyzing the impacts and feedbacks of water resource management on global change and vice versa. The system dynamics simulation approach is ideal for the implementation of an integrated assessment model and will facilitate the inclusion of additional disciplinary models to study global change dynamics within the Earth system.

Taking these factors into account the research objectives of this work are to:

1. Construct a model of water supply development that is economically based and driven by feedbacks within the Earth system in ANEMI.
2. Analyze the feedbacks between water supply development and the Earth system.
3. Analyze the role of water supply development for both conventional and alternative water supply in adapting to water stress. Water supply in this context refers to the rate at which available water resources can be utilized to satisfy water demands through supply infrastructure of surface water, groundwater, wastewater reuse, and ocean water resource.

4. Improve the representation of water quality in the ANEMI model to include the effects of water quality on the development of surface water supplies.
5. Perform future model experiments with the improved ANEMI model pertaining to key aspects of global change including:
  - a. Evaluating potential limits to population growth through the depletion of natural resources (food and water) and the generation of pollution.
  - b. Assessment of the potential impacts of water quality on the development of water supplies.
  - c. Climate change impacts throughout the Earth system.

The research objectives have been addressed in this work in the following ways:

1. Integrating a new water supply development model in ANEMI. The model is based on the development of capital stocks for surface water, groundwater, wastewater reuse, and desalination water supplies through investment in each. The value of the capital stocks is used to represent water supply capacity. Production is influenced by the available water resources, water demand, and water quality, creating a tight coupling to the rest of the ANEMI model feedback structure.
2. Analyzing the impact of changes in water quality on water production through corresponding changes in the price of providing surface water supplies, as well as the capacity for alternative water supplies to develop in response to increasing water demand and stress.
3. The role of alternative water supplies is assessed by altering the level of available water resources for the conventional water supplies of surface water and groundwater, thereby

driving up production prices. This allows for the viability of alternative water supplies in adapting to water stress to be assessed.

4. The assembled model has been used to assess feedbacks within the Earth system through the development of future global change scenarios. The selected scenarios are closely tied to water supply development, including those related to climate change, population dynamics, water quality, and food production.

The research contributions of this work are as follows:

1. The water supply development model provides an entirely new perspective on the development of water supply, by linking the capacity of different sources (surface water, groundwater, water reuse, and desalination) to their respective capital stocks. The capital stocks represent the level of water supply infrastructure for a given source and represents the supply capacity. This approach grounds the development of water supply in economic terms, which has been shown to be a limiting factor for future water security.
2. The inclusion of alternative water resources in this research in the form of desalination and water reuse from an endogenous, economically based perspective is a novel concept in the realm of integrated assessment modelling.
3. Establishment of a link between water quality and water supply through impacts to surface water treatment. This link has not been addressed in the realm of integrated assessment modelling, and has the potential to increase treatment costs with degrading future water quality and climate change (Eikebrokk et al. 2004; Ritson et al. 2014), potentially making alternative water supplies more viable in the future.

The next Chapter details the modification made to the structure of the ANEMI model in order to address the research objectives discussed here.

## Chapter 3

### 3. Methodology

This chapter presents the ANEMI3 model, which is built upon the first two iterations of ANEMI. The model shares the same system dynamics simulation paradigm that was used in the previous iterations of ANEMI, in that feedbacks and delays are used to drive system behaviour. ANEMI3 is a type of integrated assessment model that describes the state of and interactions between model sub-systems that compose the Earth system. The main sub-systems or ‘sectors’ used are that of the climate system, carbon, nutrient, and hydrologic cycles, population dynamics, land use, food production, sea level rise, energy production, global economy, persistent pollution, water demand, and water supply development.

Each individual sector in the model describes the relevant feedbacks that drive the state variables in the sector. Connections between sectors form intersectoral feedbacks responsible for the functioning of the Earth system. It is the intersectoral feedbacks that allow us to represent feedbacks that drive global changes in the Earth system. Feedbacks driving global change are now evident, while it is expected that negative feedbacks acting on population and economic growth may be more evident in the future. From a system dynamics perspective, effective policymaking should be based on addressing the feedback structure of a system, not only on modifying the system parameters. This viewpoint is what makes the ANEMI3 model unique and useful in a time when global modelling is becoming progressively more complex.

The boundary of the model is defined by the problem that is being explored. In this case, we are modelling the role of water resources in various aspects of global change. Therefore, the spatial scale of the model is mainly one that is global. In some sectors, the stocks are disaggregated to capture material flows on a sub-global scale, but not at a level that is location specific. For example, in the nutrient cycles different stocks are used to denote the flow of nutrients from atmosphere to land, humus, rivers, coastal water, and oceans, however each of these individual stocks are globally aggregated. This spatial scale limits the level of detail that can be used to describe the flows that act to change the model stocks, however it allows us to accomplish our research objective to analyze feedbacks between water resources and other model sectors on a global scale.

The time horizon used in the model is from the year 1980-2100. This is in part due to the incorporation of models from different studies into the sub-sectors of ANEMI which had initial time horizons close to the year 1980, while the year 2100 is one that is often used as a benchmark for global change phenomenon such as climate change. Roberts et al. (1983) that the selected time step should  $1/3^{\text{rd}}$  to  $1/4^{\text{th}}$  of the halving time of negative feedback loops and  $1/5^{\text{th}}$  to  $1/10^{\text{th}}$  of the doubling time of positive feedback loops in system dynamics models. Results are report on an annual time step; however, the stocks are integrated using a time step of  $1/128^{\text{th}}$  of a year. This represents the largest possible time step that could be used while avoiding numerical instabilities when integrating the system of first order differential equations. Simple Euler integration is used to solve the system of equations in the model. This was done to reduce model computation time when performing sensitivity analyses.

One of the objectives of this work is to examine the development of global water supplies from an economic perspective, allowing for the role of both conventional and alternative water supplies to be assessed with regards to offsetting future water stress on a global scale. Another is to assess the potential influence of water quality degradation on the development of surface water supplies. With the assembled model, experiments are to be carried out in order to; a) assess the relationship between water supply and food production to sustain a growing population, b) assess the potential impacts of water quality on the development of water supplies, and c) analyze the impacts of climate change on various aspects of the Earth system.

These objectives are addressed by incorporating the following key changes to the ANEMI model through this research:

- Addition of a model sector to represent global nutrient cycles of nitrogen, and phosphorus.
- Addition of a nutrient emissions to surface waters sector in order to provide an indicator of surface water quality.
- Incorporation of global surface temperature change effects on arable land in the food production sector.
- Addition of persistent pollution sector from WORLD3.
- Removal of the computable general equilibrium model used in the previous economic sector of ANEMI.
- Addition of the Feedback-Rich Energy Economy (FREE) model into ANEMI3.
- Incorporation of water supply into the FREE model to simulate the development of water supplies from an economic perspective.



The changes and additions to the ANEMI model are detailed in Sections 3.1 and 3.2 below and form the foundation for the main research contributions of this work, which were not able to be assessed in the previous versions of the ANEMI model. This includes the analysis of water supply from a novel perspective which integrates the global economy, water quality degradation and the distinction of conventional and alternative water supplies through the use of a feedback-driven, system dynamics simulation model.

### 3.1. Intersectoral Feedback Structure

The highly endogenous structure and coupling of sub-systems in the ANEMI3 model are part of its novelty in the realm of integrated assessment modelling. Because of this, feedback processes are responsible for the behaviour that is exhibited in model runs. The model sectors that comprise the ANEMI3 model are that of the climate system, carbon, nutrient, and hydrologic cycles, population dynamics, land use, food production, sea level rise, energy production, global economy, persistent pollution, water demand, and water supply development. Feedback loops between sectors, or intersectoral feedback loops are responsible for global change in this Earth system.

Creating a causal loop diagram from these connections between model sectors allows us to view the feedbacks that are created by combining model sectors in this way (Figure 3.1). Intersectoral feedbacks in the ANEMI3 model allow for the representation of various aspects of global change. In this diagram alone there is a total of 89 possible intersectoral feedback loops. The size of the feedback loops range from 2 to 9 sectors included out of the 10 that are shown.

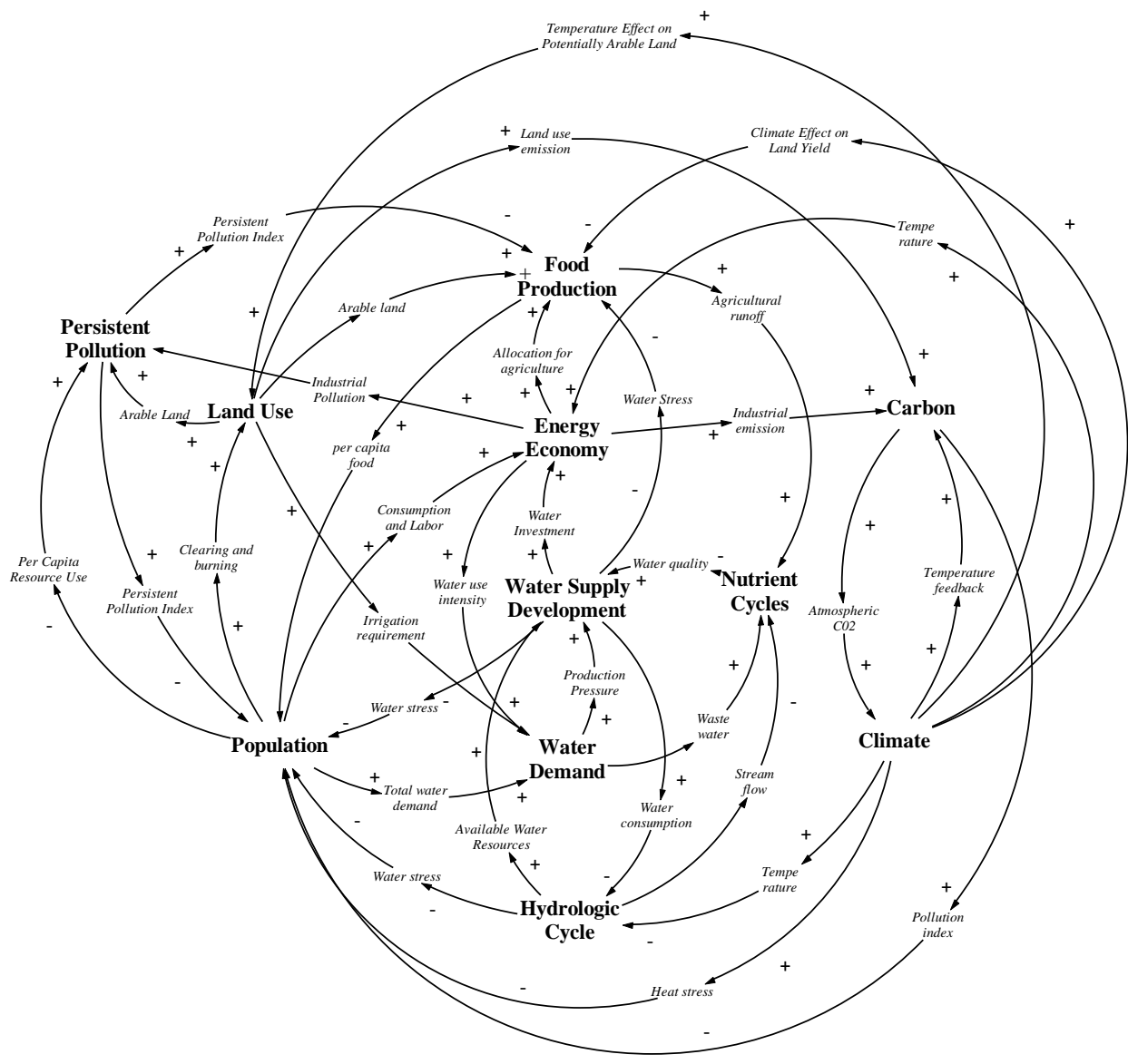


Figure 3.1. Intersectoral causal loop diagram of the ANEMI3 model.

These sectors are selected in order to represent the dynamics of global change at the global scale with an emphasis on the development of water supplies. By organizing the components of the Earth system in this way, feedback processes that drive global change can be represented. An

example is that of a growing global economy, which drives energy production and industrial growth, thereby resulting in more greenhouse gas emissions and climate change. This in turn results in negative feedbacks on economic growth through climate damages, which can represent economic damages as a result of land and structures lost to coastal flooding, for example. This feedback loop is present in other feedback-based integrated assessment models. With the modified feedback structure of the ANEMI3 model in this thesis, global scale feedbacks are created in addition to those present in the previous iteration. These include:

- Water supply development increases water consumption, thereby reducing water availability, resulting in reduced water supply development.
- Increased water supply development results in a decrease in water stress, thereby reducing mortality rates allowing for increased population levels and water demand thereby increasing pressure to develop additional water supply.
- Investment in water supply capital stocks increases the global aggregate capital stock, thereby increasing water usage intensity and water demand, creating more pressure for the development of water supply.
- The development of water supplies alleviates water stress on food production thereby increasing agricultural runoff to the nutrient cycles. This in turn has a negative impact on water supply through reduced water quality and increased cost of water supply for surface water.
- Persistent pollution adds additional negative feedbacks to population mortality rates by acting as a multiplier of life expectancy. With increased population, the total use of resources and pollution generation increase. The increase in persistent pollution levels after some time and reduces population levels.

- Increased population has a positive effect on global economy by boosting the labor force, resulting in more industrial pollution generation. This in turn has a limiting effect on population growth through the life expectancy multiplier from persistent pollution.
- Increased population also provides more labor input which supports the economic growth. This affects water demand by reducing withdrawal intensities in the domestic and industrial sectors, resulting in less water consumption and more available water resources. This supports water supply development thereby limiting water stress and supporting further population growth.

The additional intersectoral feedback loops in the new ANEMI3 model are used to accomplish the research objectives of analyzing water supply development within the Earth system, inclusion of water quality degradation on the development of surface water supplies, and allows for the assessment of global scale feedback related to water supply development.

1. Develop a model of water supply development that is economically based and driven by feedbacks within the Earth system in the ANEMI3 integrated assessment model.
2. Analyze the feedbacks between water supply development and the Earth system.
3. Analyze the role of water supply development for both, conventional and alternative water supply in adapting to water stress.
4. Improve the representation of water quality in the ANEMI3 model to include the effects of water quality on the development of surface water supplies.

5. Perform future model experiments with the improved ANEMI3 model pertaining to key aspects of global change including:
- a. The need for water supply development and food production to sustain a growing population.
  - b. Assessment of the potential Impacts of water quality on the development of water supplies.
  - c. Climate change impacts throughout the Earth system.

One of the goals of this work is to identify new feedback processes that may be of importance to global change, particularly with regards to water supply development. All the connections between model sectors in the ANEMI3 model are listed below in Table 3.1.

Table 3.1. Connections between different model sectors in ANEMI3. Highlighted rows represent the intersectoral connections that have been added or modified in this work.

Influencing Model Sector	Affected Model Sector	Types of Influence
Climate	Hydrologic Cycle	<ul style="list-style-type: none"> <li>• Surface temperature change increases evapotranspiration and melting of ice and snow</li> </ul>
Climate	Economy	<ul style="list-style-type: none"> <li>• Reduces economic output through temperature change in climate damage function</li> </ul>
Climate	Population	<ul style="list-style-type: none"> <li>• Surface temperature change increases heat stress effects on young and old</li> </ul>
Climate	Food Production	<ul style="list-style-type: none"> <li>• Increased global temperature have a positive effect on potentially arable land thus more food production</li> </ul>
Climate	Carbon Cycle	<ul style="list-style-type: none"> <li>• Increased surface temperatures stimulate carbon uptake from litter, humus, charcoal sinks, and ocean sinks</li> </ul>
Climate	Sea Level Rise	<ul style="list-style-type: none"> <li>• Surface temperature change is used as an indicator for the relationship used to represent sea level rise</li> </ul>
Carbon Cycle	Climate	<ul style="list-style-type: none"> <li>• Higher atmospheric carbon concentration increases radiative forcing on the climate system</li> </ul>

Hydrologic Cycle	Water Supply	<ul style="list-style-type: none"> <li>• Available water resources determine depletion effect in supply development</li> </ul>
Hydrologic Cycle	Nutrient Cycles	<ul style="list-style-type: none"> <li>• Changes in streamflow, rainfall, and groundwater percolation rates affect nutrient transfer rates</li> <li>• Increased river flow rates reduce the concentration of nutrients</li> </ul>
Water Supply	Population	<ul style="list-style-type: none"> <li>• Water stress increases mortality rates through life expectancy</li> </ul>
Water Supply	Economy	<ul style="list-style-type: none"> <li>• Water supply development is aggregated within total economic capital and output</li> <li>• A portion of global investment funds are allocated to water supply development</li> </ul>
Water Supply	Food Production	<ul style="list-style-type: none"> <li>• Water stress acts as a limit to food production</li> </ul>
Water Demand	Water Supply	<ul style="list-style-type: none"> <li>• Increased water demand creates water stress thereby increasing production pressure on water supplies</li> </ul>
Water Demand	Nutrient Cycles	<ul style="list-style-type: none"> <li>• Higher industrial and domestic water demand result in the generation of more nitrogen and phosphorus in the form of wastewater</li> </ul>
Water Demand	Hydrologic Cycle	<ul style="list-style-type: none"> <li>• Domestic, industrial, and agricultural water demands consume available water resources</li> </ul>
Nutrient Cycles	Water Supply	<ul style="list-style-type: none"> <li>• Water quality influences surface water supply development</li> </ul>
Population	Water Demand	<ul style="list-style-type: none"> <li>• Growing population increases domestic water demands</li> </ul>
Population	Land Use	<ul style="list-style-type: none"> <li>• Growing population increase forest and grassland clearing and burning for agriculture</li> </ul>
Population	Economy	<ul style="list-style-type: none"> <li>• Increased population boosts available labour</li> </ul>
Population	Food Production	<ul style="list-style-type: none"> <li>• Increased population creates the need for more food production</li> </ul>
Population	Persistent Pollution	<ul style="list-style-type: none"> <li>• Greater population increases the generation of industrial persistent pollution amounts</li> </ul>
Economy	Population	<ul style="list-style-type: none"> <li>• Increased economic output results in higher quality health services and life expectancy thereby reducing mortality rates</li> </ul>
Economy	Water Demand	<ul style="list-style-type: none"> <li>• More economic output increases domestic water demands</li> </ul>
Economy	Food Production	<ul style="list-style-type: none"> <li>• Higher economic output results in greater agricultural input per hectare and higher food production</li> </ul>
Economy	Energy Production	<ul style="list-style-type: none"> <li>• Increased global capital results in higher energy requirements thus boosting energy production</li> </ul>
Economy	Persistent Pollution	<ul style="list-style-type: none"> <li>• Increased consumption results in higher per capita persistent pollution generation</li> </ul>

Energy Production	Emissions	<ul style="list-style-type: none"> <li>• Energy production from fossil fuels increases carbon emissions</li> </ul>
Energy Production	Economy	<ul style="list-style-type: none"> <li>• Increased energy capital boosts total capital and economic output</li> </ul>
Energy Production	Water Demand	<ul style="list-style-type: none"> <li>• Production of energy is used as an indicator of industrial activity and associated water demands</li> </ul>
Land Use	Food Production	<ul style="list-style-type: none"> <li>• Increased agricultural lands boosts potential food production</li> </ul>
Land Use	Carbon Cycle	<ul style="list-style-type: none"> <li>• Clearing and burning of forest and grasslands release carbon stored in litter, humus, and charcoal stocks to the atmosphere</li> </ul>
Land Use	Persistent Pollution	<ul style="list-style-type: none"> <li>• Increased agricultural lands result in greater persistent pollution generation from agriculture</li> </ul>
Food Production	Water Demand	<ul style="list-style-type: none"> <li>• More food production results in higher agricultural water demands</li> </ul>
Food Production	Population	<ul style="list-style-type: none"> <li>• Greater food per capita results in higher life expectancy</li> </ul>
Food Production	Nutrient Cycles	<ul style="list-style-type: none"> <li>• More net arable land results in higher emissions of nutrients from agricultural effluents</li> </ul>
Emissions	Carbon Cycle	<ul style="list-style-type: none"> <li>• More CO<sub>2</sub> emissions boost atmospheric carbon content</li> </ul>
Emissions	Climate	<ul style="list-style-type: none"> <li>• Increased emission of methane, nitrogen dioxide, and chlorofluorocarbons increases radiative forcing on the climate system</li> </ul>
Persistent Pollution	Population	<ul style="list-style-type: none"> <li>• Higher levels of persistent pollution act as a multiplier to decrease life expectancy</li> </ul>
Persistent Pollution	Food Production	<ul style="list-style-type: none"> <li>• Increased persistent pollution has a negative effect on land fertility thus reducing food production rates</li> </ul>
Sea Level Rise	Food Production	<ul style="list-style-type: none"> <li>• Sea level rise reduced net arable land for food production</li> </ul>

Viewing the number of intersectoral connections to and from each sector provides an indication of their degree of coupling within the ANEMI3 model. Table 3.2 shows the connections to and from each model sector. If a sector has no outgoing connections and only incoming connections, there would be no potential for feedbacks, and it would mainly be for assessment purposes. A sector with a high number of incoming and outgoing connections is likely to have more intersectoral feedbacks. Finally, if a sector has all outgoing connections and no incoming connections then it

can be considered as exogenous input to the model and no feedbacks are present. The sectors with the highest number of combined incoming and outgoing connections are population, economy, climate, and food production indicating that they have a high degree of connectivity to other sectors in the model and potentially more feedbacks.



Table 3.2. Illustration of intersectoral connection in the model including total number of incoming (from) and outgoing (to) connections.

To \ From	Population	Economy	Climate	Carbon Cycle	Food Production	Energy Production	Emissions	Water Supply	Water Demand	Hydrologic Cycle	Nutrient Cycles	Land Use	Persistent Pollution	Sea Level Rise	Total #
Population		x			x				x			x	x		5
Economy	x				x	x			x				x		5
Climate	x	x		x	x					x				x	5
Carbon Cycle			x												1
Food Production	x								x		x				3
Energy Production		x					x		x						3
Emissions			x	x											2
Water Supply	x	x			x					x					4
Water Demand								x		x	x				3
Hydrologic Cycle								x			x				2
Nutrient Cycles								x							1
Land Use				x	x								x		3
Persistent Pollution	x				x										1
Sea Level Rise					x										1
Total #	5	4	2	3	6	1	1	3	4	3	3	1	3	1	

## 3.2. Description of the ANEMI3 Model Sectors

### 3.2.1. Climate Sector

The climate sector of ANEMI3, as in previous versions, is based on the DICE model of Nordhaus (1994). In this sector, the dynamics of heat exchange between the deep ocean and the combined upper ocean and atmospheric layers are modelled, along with a cooling effect that acts to limit the rate of temperature increase. Identifying the feedbacks that drive this simple climate system allow us to speculate on how the system will function over time. The climate sub-system is driven by two feedback loops (Figure 3.2). The first being a feedback cooling effect, while the second represents the diffusion of heat in the atmospheric stock to the ocean stock. Both negative feedbacks act to dampen the systems response to radiative forcing which comes from increased greenhouse gas concentrations in the carbon cycle and greenhouse gas sub-systems. Based on the structure of this simplified climate system, one might expect it to predict global temperature values on the lower end of the spectrum. This is because positive feedbacks related to climate change such as methane release from tundra regions and change in albedo as global ice cover melts are not included, which have the potential to accelerate increases in global temperatures.

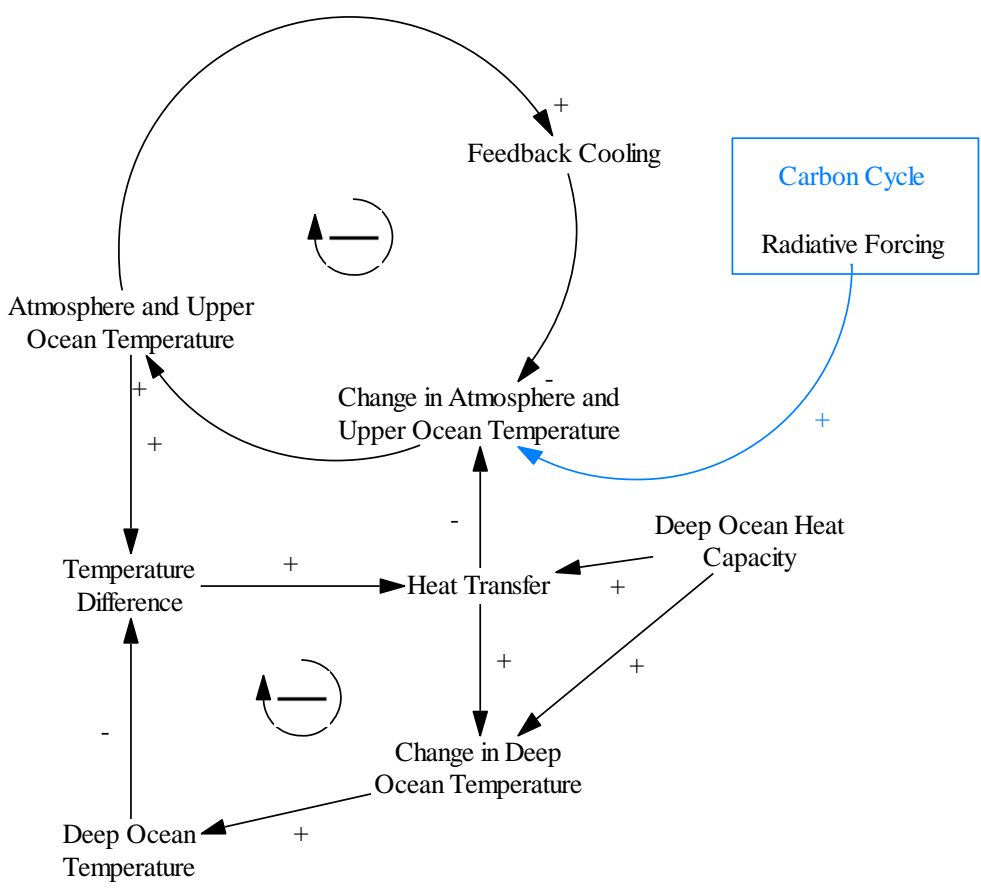


Figure 3.2. Causal loop diagram of the ANEMI3 climate sector.

The stock and flow diagram of this model is given in Figure 3.3. Two stocks are used to quantify the current global temperature of the atmosphere and oceans in response to external radiative forcing caused by greenhouse gases that are divided into CO<sub>2</sub>, methane, nitrogen dioxide, chlorofluorocarbons, and others. Diffusion of heat between these two stocks results in heat being transferred from the atmosphere stock to the ocean stock which acts as a heat sink.

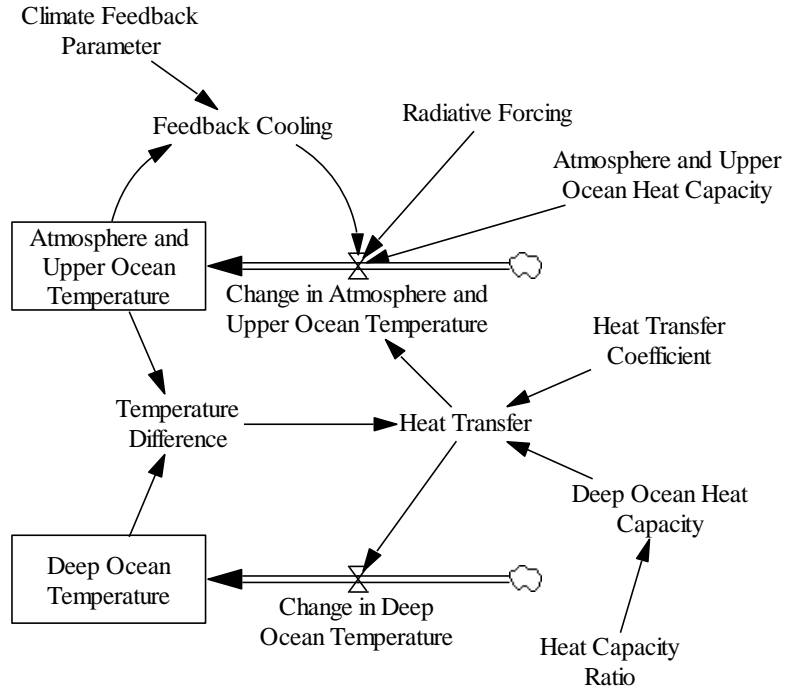


Figure 3.3. Stock and flow diagram of the ANEMI3 climate sector.

Radiative forcing acts to increase the flow that changes the temperature of the atmosphere stock and is based on the relative change of the greenhouse gases considered from their preindustrial levels.

The mathematical description of the atmospheric and upper ocean temperature stock is given by,

$$T_{AUO} = \int CT_{AUO} \cdot dt \quad [^{\circ}C] \quad (3.1)$$

Where  $T_{AUO}$  represents the temperature of the atmosphere and upper ocean and  $CT_{AUO}$  is the rate at which  $T_{AUO}$  is changing ( $^{\circ}C/year$ ). The deep ocean temperature,  $T_{DO}$  is defined as,

$$T_{DO} = \int CT_{DO} \cdot dt \quad [^{\circ}\text{C}] \quad (3.2)$$

Where  $CT_{DO}$  is the change in temperature of the deep ocean stock ( $^{\circ}\text{C}/\text{year}$ ). The change in temperature of the atmospheric and upper ocean stock is calculated based on the difference between radiative forcing, heat transfer from the deep ocean stock and the heat capacity of the atmospheric and upper ocean stock,

$$CT_{AUO} = \frac{F - f_H - HT}{HC_{AUO}} \quad [^{\circ}\text{C}/\text{year}] \quad (3.3)$$

$F = \text{Radiative forcing } [W/m^2]$

$f_H = \text{Feedback cooling effect } [W/m^2]$

$HT = \text{Heat transfer between atmosphere and upper ocean to deep ocean } [W/m^2]$

$HC_{AUO} = \text{Heat capacity of atmosphere and upper ocean } [W \cdot \frac{\text{year}}{^{\circ}\text{C} \cdot \text{m}^2}]$

The change in temperature of the deep ocean stock,  $CT_{DO}$  depends on the heat transfer from the atmosphere and upper ocean layer above, and the heat capacity of the deep ocean stock,

$$CT_{DO} = \frac{HT}{HC_{DO}} \quad [^{\circ}\text{C}/\text{year}] \quad (3.4)$$

$HC_{DO} = \text{Heat capacity of deep ocean layer } [W \cdot \frac{\text{year}}{^{\circ}\text{C} \cdot \text{m}^2}]$

Heat capacity of the deep ocean layer is calculated by,

$$HC_{DO} = R_{HC} \cdot C_{HT} \quad \left[ W \cdot \frac{\text{year}}{^{\circ}\text{C} \cdot \text{m}^2} \right] \quad (3.5)$$

$R_{HC}$  = Heat capacity ratio [ $W/(m^2 \cdot ^\circ C)$ ]

$C_{HT}$  = Heat transfer coefficient [year]

The transfer of heat between the atmosphere and upper ocean and deep ocean layers is dependent upon the difference in temperature between them, the heat capacity of the deep ocean layer and heat transfer coefficient.

$$HT = (T_{AUO} - T_{DO}) \frac{HC_{DO}}{C_{HT}} \quad [W/m^2] \quad (3.6)$$

### 3.2.2. Carbon Cycle

The carbon cycle in the ANEMI3 model is based on Goudriaan and Ketner (1984). It is used to model the flow of carbon through the Earth system from atmosphere to land and oceans. By incorporating the entire carbon cycle, atmospheric concentration can more realistically be simulated to drive changes in climate through the greenhouse effect. Feedbacks between the carbon cycle and climate system can also be represented through increased solubility of carbon dioxide in the ocean and fertilization effects of plant material with increased global temperatures. Finally, by modelling the cycle of carbon, connections can be made with the land use sector by separating the land stock of carbon into different biome types. This allows for changes in land use such as the burning and clearing of grasslands and forests, to contribute CO<sub>2</sub> emissions to the atmosphere.

The causal loop diagram of the carbon cycle sector is given in Figure 3.4. The chain of negative feedback loops passing through each of the terrestrial carbon stocks from the atmosphere and back

again act as positive feedback loop in the carbon cycle. This is because more atmospheric carbon results in higher uptake of carbon in the biomass, which results in greater transfer of carbon through the chain (litter, humus, stabilized humus and charcoal) thereby resulting in more decay and transfer of carbon back to the atmosphere. Although these are positive feedback loops, carbon in this cycle is conserved, but the release or storage of carbon in the terrestrial stocks will be dependent on the balance between uptake and decay. The last feedback loop in the diagram is a negative feedback loop that represents the diffusion of carbon dioxide between the two ocean layers.

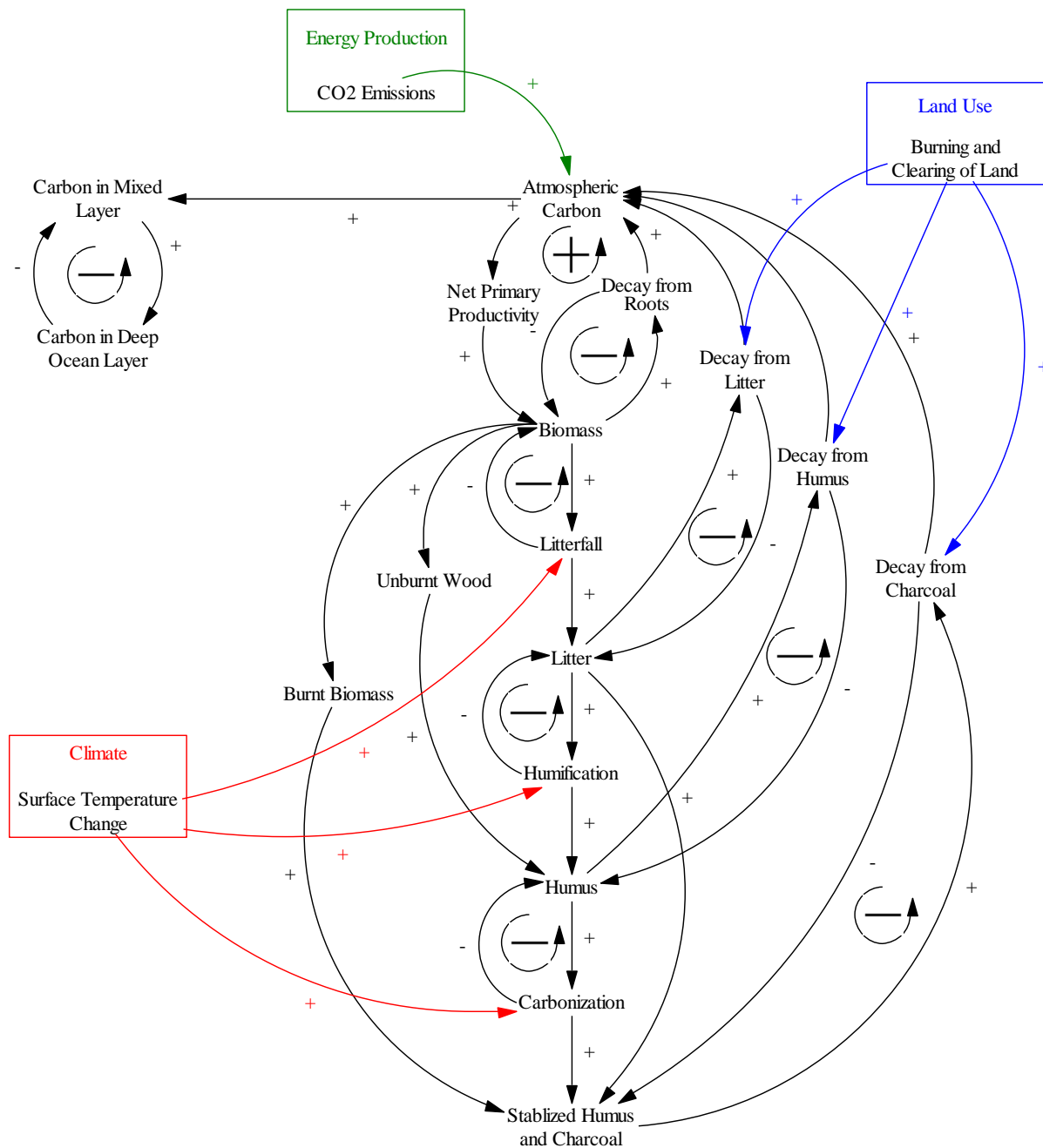


Figure 3.4. Causal loop diagram of carbon cycle sector in ANEMI3. Red, green, and blue arrows and variables represent connections to climate, land use, and energy production sectors respectively.



The cycle of carbon from the atmosphere through land and oceans is shown in the stock and flow diagram of Figure 3.5. The atmosphere, ocean layers, and terrestrial components of the carbon cycle are represented as stocks while the processes of net primary production (carbon uptake by living biomass), rates of dead biomass decay, and dissolution of carbon into the ocean are represented as flows.

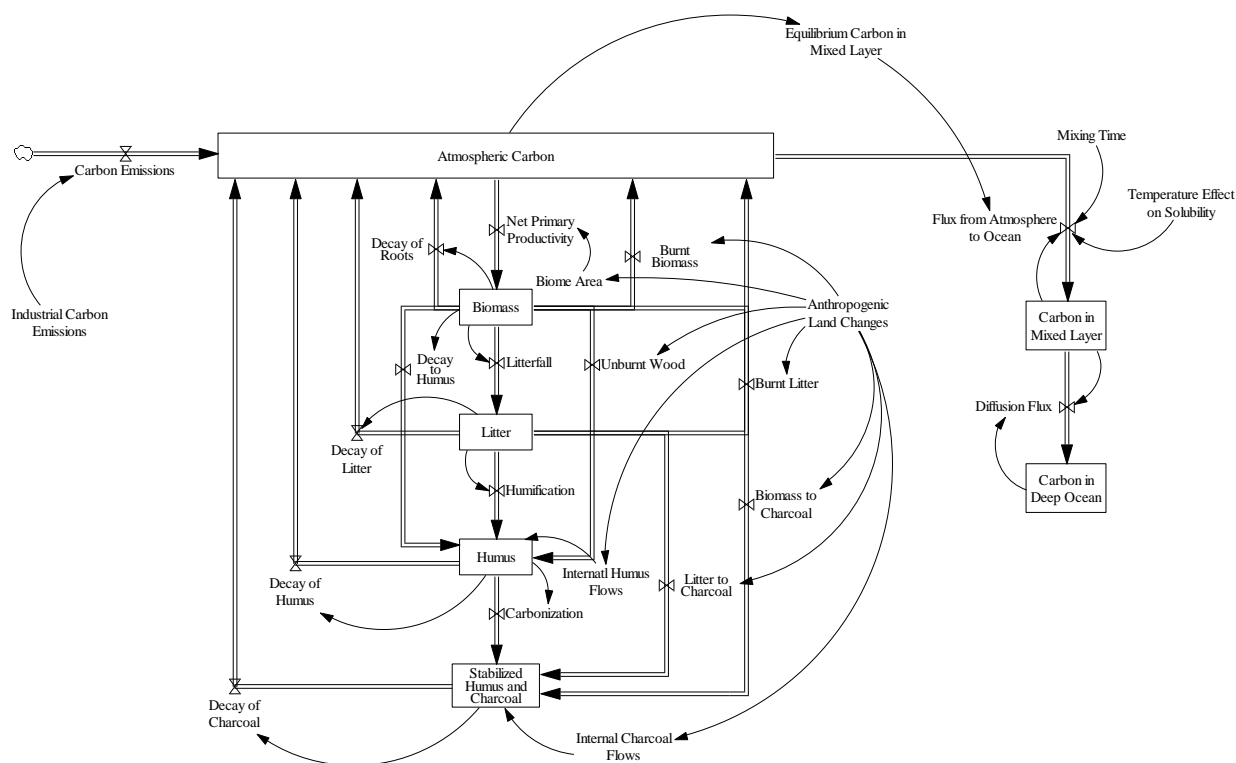


Figure 3.5. Stock and flow diagram of carbon cycle in the ANEMI3 model.

The biome (or land use) types that are represented in the model are 1) tropical forests, 2) temperate or boreal forests, 3) grasslands, 4) agricultural lands, 5) deserts and tundra, and 6) settled areas. Living biomass of each biome is sub-divided into leaves, branches, stems and roots. Decaying biomass is separated in litter, humus, charcoal, and stabilized humus and charcoal. This subdivision allows for atmospheric carbon uptake and decay rates to be specified for each carbon

sink. The ocean stock of carbon is sub-divided into two separate layers: one mixed layer and one deep ocean layer. The mixed layer is used to represent diffusion of carbon between ocean and atmosphere based on the difference in concentration. CO<sub>2</sub> is highly soluble in seawater and dissolves into the mixed layer from the atmosphere according to Henry's Law (Masterson and Hurley 2009).

The mathematical description of the carbon cycle sector is summarized from Davies (2007). The accumulation of carbon in the atmosphere can be expressed as,

$$N_A = \int (D_B + D_L + D_H + D_K - NPP + B_B + B_L + E - F_0) \cdot dt \quad [Gt C] \quad (3.7)$$

$N_A$  = Atmospheric carbon [Gt C]

$D_B$  = Decay of biomass [Gt C/y]

$D_L$  = Decay of litter [Gt C/y]

$D_H$  = Decay of humus [Gt C/y]

$D_K$  = Decay of charcoal [Gt C/y]

$NPP$  = Net primary productivity [Gt C/y]

$B_B$  = Burning of biomass [Gt C/y]

$B_L$  = Burning of litter [Gt C/y]

$E$  = Industrial emissions [Gt C/y]

$F_0$  = Carbon absorbtion by oceans [Gt C/y]

Net primary productivity is computed as,

$$NPP_{jk} = p_{jk} \cdot \sigma(NPP_j) \cdot \frac{A_j}{10^{15}} \quad [Gt C/y] \quad (3.8)$$

$j$  = Biome type

$k$  = Biomass component

$p_{jk}$  = Fraction of biomass partitioned to component  $k$  of biome  $j$

$\sigma(NPP_j)$  = Variable surface density of net primary production [Gt C/(m<sup>2</sup> · y)]

$A_j$  = Biome area [m<sup>2</sup>]

The biome (or land use) type  $j$  refers to the set of biomes represented in the model and the biomass component  $j$  refers to the leaves branches stems and roots that make up a given biome type. The variable surface density of net primary production is represented as,

$$\sigma(NPP_j) = \sigma(NPP_j)_0 \cdot \left( 1 + \beta \cdot \ln \left( \frac{C_A}{C_{A_0}} \right) \right) \quad [Gt C / (m^2 \cdot y)] \quad (3.9)$$

$\sigma(NPP_j)_0 =$  base surface density [Gt C / (m<sup>2</sup> · y)]

$\beta =$  CO<sub>2</sub> fertilization factor

$C_A =$  Current atmospheric CO<sub>2</sub> [Gt C]

$C_{A_0} =$  Initial atmospheric CO<sub>2</sub> [Gt C]

The amount of carbon stored within each component the biomass stock for each biome type is represented as,

$$B_{jk} = \int \left( NPP_{jk} - FL_{B_{jk}} - FH_{B_{jk}} - FK_{B_{jk}} - B_{B_{jk}} - UB_{B_{jk}} \right) \cdot dt \quad [Gt C] \quad (3.10)$$

$FL_{B_{jk}} =$  Amount of litter falling from biomass to litter layer [Gt C/y]

$FH_{B_{jk}} =$  Decay of biomass to humus [Gt C/y]

$FK_{B_{jk}} =$  Burning of biomass [Gt C/y]

$B_{B_{jk}} =$  Burning of biomass from human land use [Gt C/y]

$UB_{B_{jk}} =$  Unburned remainder of biomass [Gt C/y]

Carbon accumulation in the litter stock is represented as,

$$L_j = \int \left( \sum_{k=1}^4 FL_{B_{jk}} - D_{L_j} - FH_{L_j} - BL_j - FL_{K_j} \right) \cdot dt \quad [Gt C] \quad (3.11)$$

$\sum_{k=1}^4 FL_{B_{jk}} =$  Total litter fall [Gt C/y]

$D_{L_j} =$  Decay of carbon from litter to atmosphere [Gt C/y]

$FH_{L_j}$  = Decomposition of litter into humus [Gt C/y]

$B_{L_j}$  = Flow of carbon from litter to atmosphere [Gt C/y]

$FL_{K_j}$  = Carbon flow from litter directly to charcoal [Gt C/y]

The humus carbon stock can be expressed as,

$$H_j = \int \left( \sum_{k=1}^4 FH_{B_{jk}} + FH_{L_j} - FK_{H_j} - D_{h_j} + \sum_{k=1}^4 UB_{jk} + FH_{H_j} \right) \cdot dt \quad [Gt C] \quad (3.12)$$

$\sum_{k=1}^4 FH_{B_{jk}}$  = Decay of biomass to humus [Gt C/y]

$FH_{L_j}$  = Decomposition of litter to humus [Gt C/y]

$FK_{H_j}$  = Decomposition of humus to charcoal [Gt C/y]

$D_{H_j}$  = Decay of humus to the atmosphere [Gt C/y]

$\sum_{k=1}^4 UB_{jk}$  = Unburned remainder of biomass [Gt C/y]

$FH_{H_j}$  = Internal flow of humus [Gt C/y]

The charcoal carbon stock can be expressed as,

$$K_j = \int \left( FK_{H_j} - D_{k_j} + \sum_{k=1}^4 FK_{B_{jk}} + FK_{L_j} - FK_{K_j} \right) \cdot dt \quad [Gt C] \quad (3.13)$$

$FK_{H_j}$  = Flow of carbon from humus to charcoal [Gt C/y]

$D_{k_j}$  = Decay of charcoal [Gt C/y]

$\sum_{k=1}^4 FK_{B_{jk}}$  = Burning of biomass [Gt C/y]

$FK_{L_j}$  = Carbon flow from litter to charcoal [Gt C/y]

$FK_{K_j}$  = Internal flow of charcoal from one biome to another [Gt C/y]

For initial values for each of the carbon stocks as well as parameters used in defining the flows from one to another the reader is referred to (Davies 2007). The mixed layer ocean carbon stock is represented as,

$$C_{ML} = \int (FO_A - DF_o(0)) \cdot dt \quad [Gt C] \quad (3.14)$$

$C_{ML}$  = Carbon in mixed layer ocean stock [Gt C/y]

$FO_A$  = Absorbtion of carbon dioxide from atmosphere [Gt C/y]

$DF_o(0)$  = Diffusive flow of carbon dioxide to deep ocean [Gt C/y]

The deep ocean carbon stock is divided into 10 layers of varying depth with the top 5 layers having a thickness of 200m and the bottom 5 layers having a thickness of 560m each. This is done to slowly transfer carbon deep into the ocean carbon stock based on diffusive flow. The deep ocean carbon stock is represented mathematically by,

$$C_o(h) = \int (DF_o(h) - DF_o(h + 1)) \cdot dt \quad [Gt C] \quad (3.15)$$

$DF_o(h)$  = Diffusive flow of carbon from upper layer to current layer [Gt C/y]

$DF_o(h + 1)$  = Diffusive flow of carbon to lower layer from current layer [Gt C/y]

$h$  = current layer of 10 deep ocean layers

### 3.2.3. Population Sector

The causal loop diagram in Figure 3.6 illustrates the feedbacks associated with the population sector. There is one positive feedback loop which drives the system and is responsible for

exponential growth of the human population. A higher population results in a higher growth rate through more births and therefore a higher population. The rest of the population sector details a series of negative feedbacks that act as limits to population growth. The negative feedbacks include from the effects of crowding, water stress, extreme temperatures, food production, persistent pollution, and wealth represented as global GDP. All of which are always active but to different degrees and affect either the life expectancy and thus mortality rates of the population, or fertility thereby reducing birth rates. Each of these effects act as multipliers and are related through look-up tables that could be associated with a significant amount of uncertainty, the degree of which is tested in the model experimentation section of this thesis.

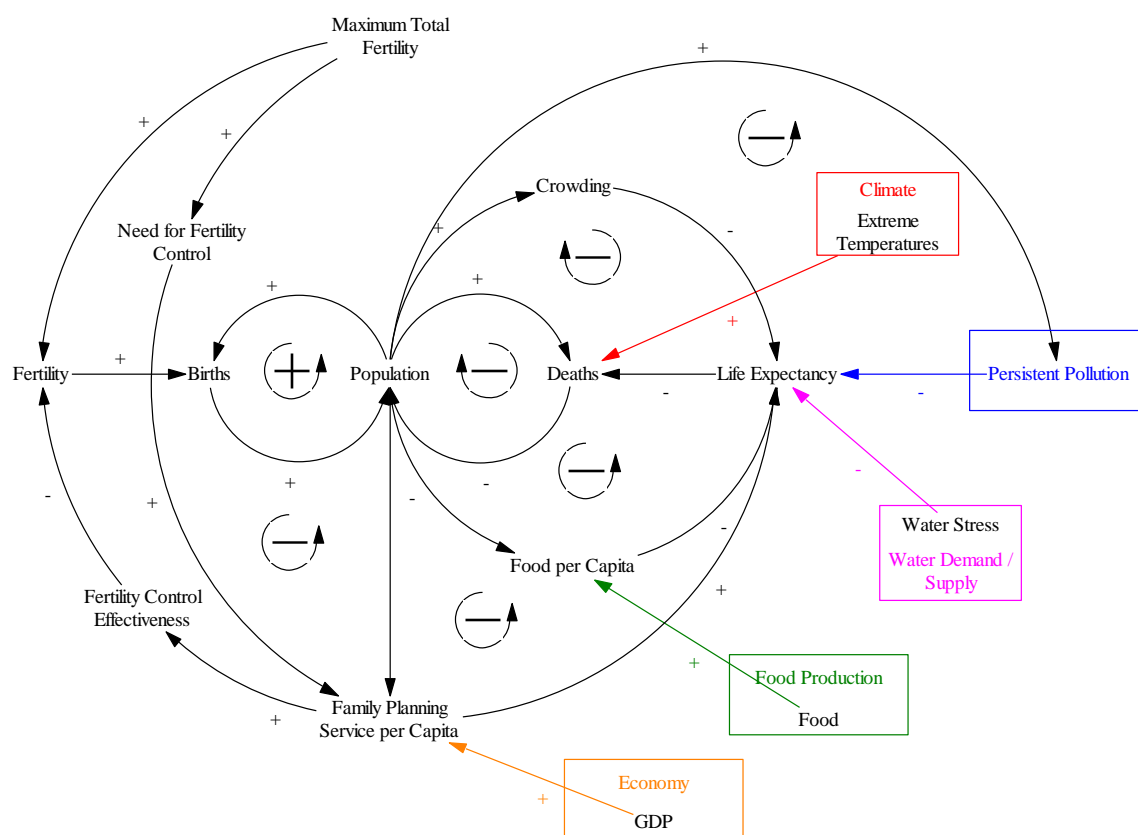


Figure 3.6. Causal loop diagram of the ANEMI3 population sector.

The population sector of ANEMI3 uses separate stocks to split the population into different demographics of ages 0 to 14, 15 to 44, 45 to 65, and 65+. This was done to capture the effects of delays in demographic responses to changes in external conditions which thereby affect birth and death rates. It allows for the growth of the total population to retain some inertia as external conditions change which more closely captures the dynamics of population growth in the real world. This structure also allows for the population of different age groups to be used in other areas of the model. For example, the 15 to 44 and 45 to 65 population groups are combined and used as the labour force in the energy-water economy sector. Another reason as to why these groups were used is so that age group specific factors that influence mortality can be applied. Climate change is included as an influence on mortality rate by a temperature multiplier that acts to influence deaths due to the presence of more frequent heat waves causing heat stress. Factors influencing fertility and birth rates are also included and will be discussed further below.

The stock and flow structure of the population sector includes stocks that represent the number of people currently in each age group (Figure 3.7). Flows are used to move people from the younger to older age groups over time, and the flow of people from each stock outside of the model boundary denotes deaths. This structure of stock and flows is often referred to as an “aging chain”, which is used to capture delays in the movement of information or material from one cohort to another over time. This is a generic structure that can be applied to a range of problems capturing higher order delays of material or information. It is often used in production processes representing the movement of a product through different production stages but could also be used to represent physical processes such as the routing of streamflow in a semi-distributed hydrologic model. Applied to population cohorts the aging chain takes a more literal meaning and represents the delay

associated with individuals in each population cohort aging over time and moving in older cohort groups.

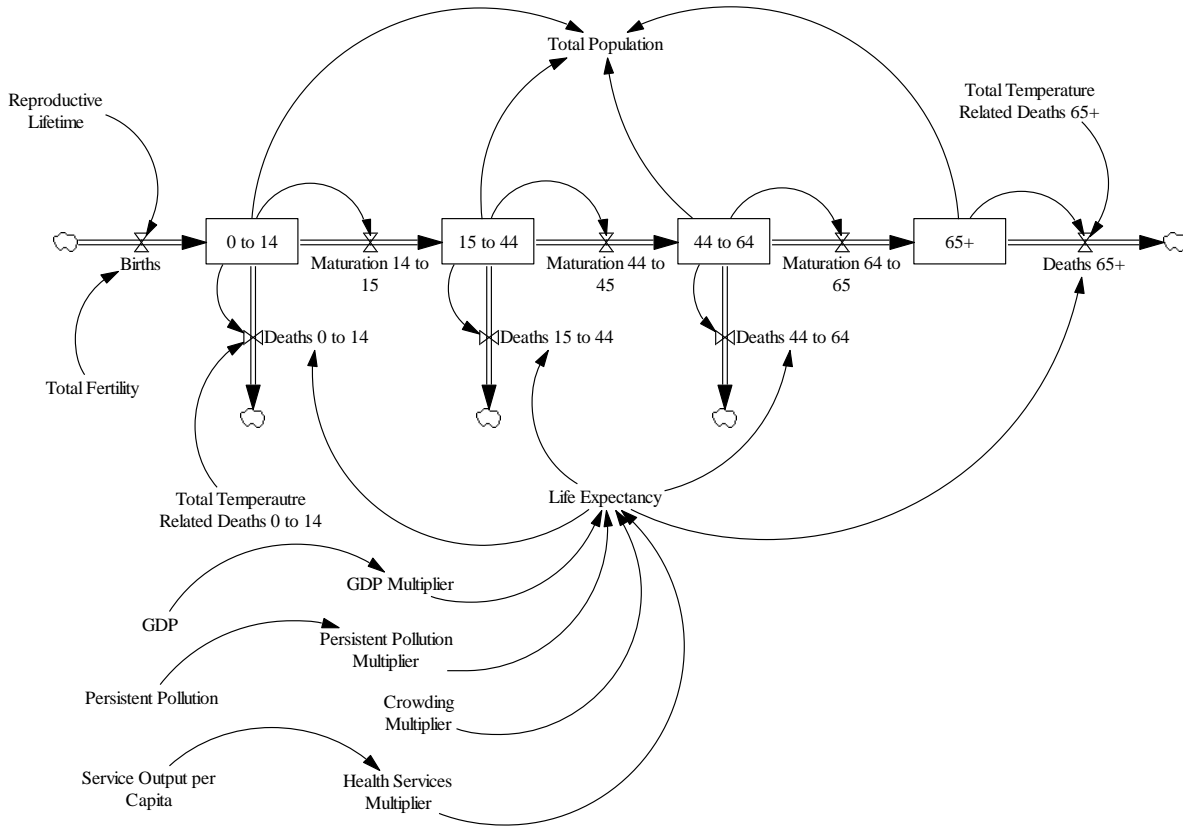


Figure 3.7. Stock and flow diagram of the ANEMI3 population sector.

The aging chain of population groups can be represented mathematically by,

$$P_1 = \int Births - P_1 M_1 - \frac{P_1(1 - M_1)}{\tau_1} - T_{deaths_1} \quad [persons] \quad (3.16)$$

$$P_2 = \int P_1 M_1 - \frac{P_2(1 - M_2)}{\tau_2} - P_2 M_2 \quad [persons] \quad (3.17)$$



$$P_3 = \int P_2 M_2 - \frac{P_3(1 - M_3)}{\tau_3} - P_3 M_3 \quad [\text{persons}] \quad (3.18)$$

$$P_3 = \int P_3 M_3 - P_4 M_4 - T_{deaths_4} \quad [\text{persons}] \quad (3.19)$$

$P_i = \text{Population}$  [persons]

$M_i = \text{Mortality rate}$  [1/y]

$\tau_i = \text{Length of time spent in sub-demographic}$  [y]

$T_{deaths_i} = \text{Temperature related deaths}$  [persons]

Where  $i$  refers to the sub-demographic in the aging chain (1 being 0 to 14 age group and 4 being 65+). The birth rate is dependent on fertility rate, and the half of the size of the reproductive population (assumes equal proportion of gender),

$$\text{Births} = F_{total} \cdot \frac{P_2}{2\tau_2} \quad [\text{persons/y}] \quad (3.20)$$

$F_{total} = \text{Total fertility}$

Total fertility is calculated based on the maximum fertility rate multiplied by the level of desired total fertility and fertility control effectiveness.

$$F_{total} = \text{MIN}(F_{M_{total}}, F_{M_{total}} \cdot (1 - F_{e_{cont}}) + F_{e_{cont}} \cdot F_{D_{total}}) \quad (3.21)$$

$F_{M_{total}} = \text{Maximum total fertility}$

$F_{e_{cont}} = \text{Fertility control effectiveness}$

$F_{D_{total}} = \text{Desired total fertility}$

Mortality rates for each sub-demographic are based on empirical relationships adopted from Meadows et al. (1974) and Keyfitz and Flieger (1971) which are a function of life expectancy,

$$L_E = L_{EN} \cdot L_{MF} \cdot L_{MHS} \cdot L_{MP} \cdot L_{MC} \quad [y] \quad (3.22)$$

$L_E$  = Life expectancy

$L_{EN}$  = Life expectancy normal [y]

$L_{MF}$  = Lifetime multiplier from food

$L_{MHS}$  = Lifetime multiplier from health services

$L_{MP}$  = Lifetime multiplier from pollution

$L_C$  = Lifetime multiplier from crowding

$L_{WS}$  = Lifetime multiplied from water stress

The calculation of life expectancy is based on a “normal” life expectancy that is multiplied by several factors that increase or decrease it from the normal value based on a set of empirical relationships.  $L_{MF}$  is a function of food supply from the food production sector,  $L_{MHS}$  is a function of GDP from the economic sector,  $L_{MP}$  is a function of persistent pollution from the pollution sector,  $L_C$  is a function of urban population which varies with the total population, and  $L_{WS}$  varies based on the current level of water stress from the water demand and water supply sectors in ANEMI3. Temperature related deaths  $T_{deaths_i}$ , are only applicable to the 0 to 14 and 65+ age groups because they are the most susceptible to heat stress induced by climate change related increases in severe heat waves. This is dependent on another empirical relationship that is a function of global temperature change in the climate sector.

An increasingly important dynamic that is currently not included in the ANEMI3 model is the migration of human population driven by the climate change. The issue is not new, and there are examples of climate driven migrations dating back as far as 45,000 years in the past (Ionesco et al. 2017). However, changes in climate are occurring much faster than they have been in the recent

past, accelerated through anthropogenic greenhouse gas emissions. It has been estimated that the number of climate migrants could reach 200 million by the year 2050 as a result of shoreline erosion, coastal flooding, and agricultural displacement (Piguet 2008). Climate migration on such a scale could have far reaching effects on all aspects of the Earth system. Water demands will shift to accommodate changes in the spatial distribution of water resources due to climate change. However, barriers that prevent migration such as political or economic boundaries may exacerbate the impacts on affected populations that are not able to relocate from areas that experience climate related disasters. This is why it is a priority of the Global Compact for Migration to find solutions that allow for populations to adapt to changing environmental conditions and provide flexible pathways for migration to occur when absolutely necessary (United Nations 2019b).

### 3.2.4. Land Use Sector

The land use sector is used to describe the global distribution of land use and cover over time. This is done by modelling the rates at which one land use or cover type is changing into another. Six land use and cover classes or biome types are used, namely, tropical forest, temperate forest, grassland, agricultural land, semi-desert and tundra, and urban area. Accounting for changes in land-use and cover is an important component in ANEMI3 as it determines the conversion of land for agricultural purposes and thus the production of food to support growing populations. Additionally, there is a release of CO<sub>2</sub> as one land type converts to another. For example, as forests are converted to agricultural land there is a release of CO<sub>2</sub> associated with the loss of vegetation, which makes the effect of land cover change an important source of CO<sub>2</sub> emissions in the model contributing to the greenhouse effect.

There is no feedback structure in the land use and cover sector when considered in isolation from the rest of the ANEMI3 model. It acts purely as an open system that is driven by changes in population which drive land use and cover change rates Figure 3.8. The main function of this sector is to use population growth input to modify biome change rates. This allows for the current biome values to be updated and give estimates of land-based CO<sub>2</sub> emissions and changes in agricultural area for the food production sector.

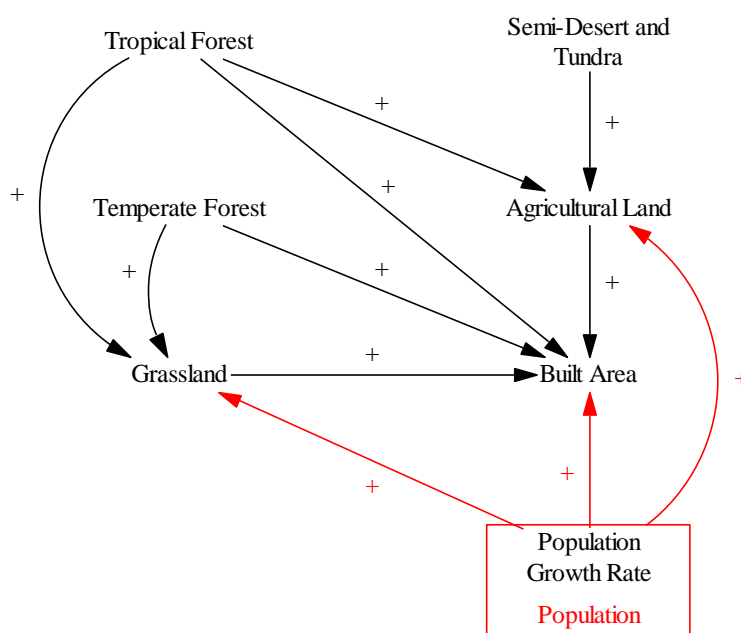


Figure 3.8. Causal diagram of the ANEMI3 land use sector.

Changes in land use and cover are modelled using a transfer matrix which contains the rate at which one land use and cover type changes into another. This matrix only considers anthropogenic influence on each biome type and the rates of change are a linear function of population. This

formulation assumes that the natural ecosystem is resilient to disturbance. It is adopted from ANEMI1 (Davies 2007) which was originally based on the model of Goudriaan and Ketner (1984).

The stock and flow diagram of the land sector in ANEMI3 is given in Figure 3.9.

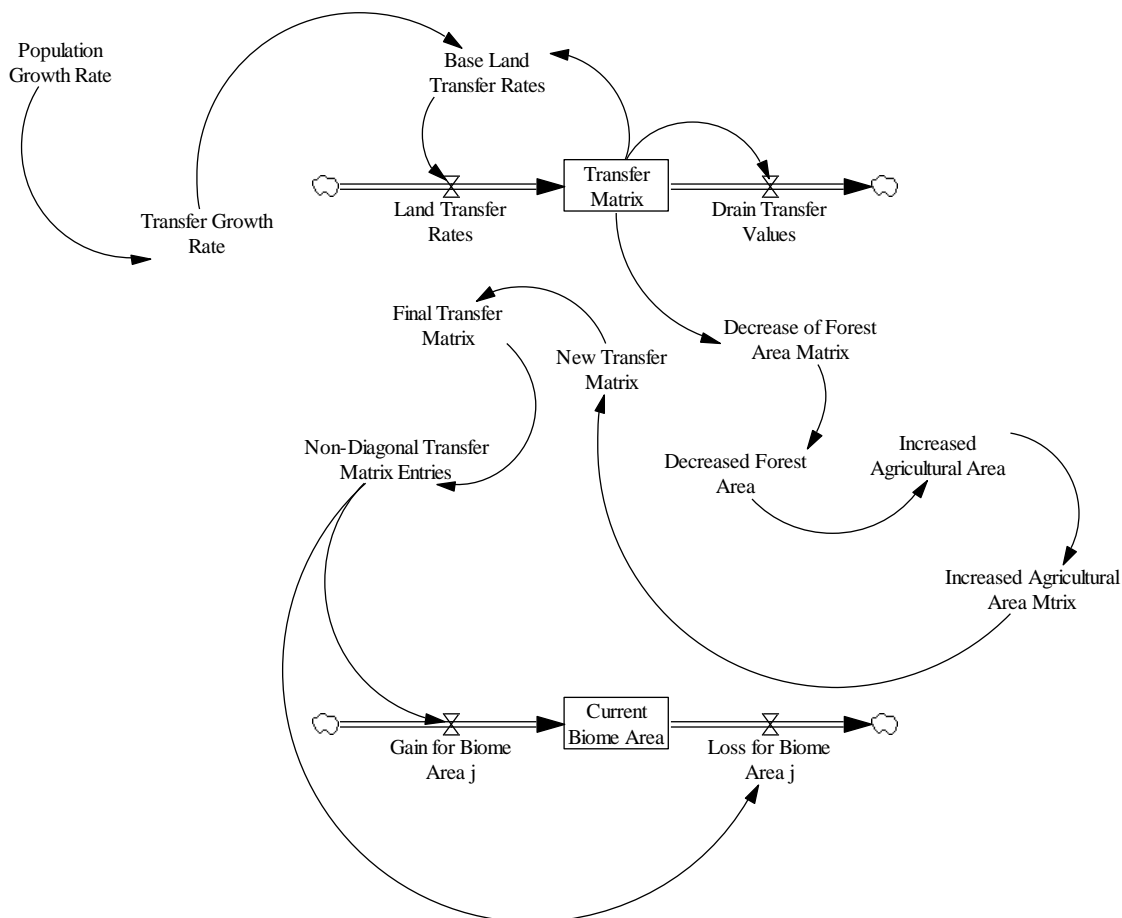


Figure 3.9. Stock and flow diagram of ANEMI3 land use sector.

There are two stocks in this formulation. The first is the transfer matrix which represents the current rate of change for each biome. This is then altered by population growth and temperature change which represent anthropogenic influence on each biome. The values of the updated transfer matrix are then applied to the current biome area. The initial transfer matrix shown in Table 3.3.

The values in this table can be interpreted as the rate of transfer from the biome type in row  $i$ , to biome type in column  $j$ . The non-diagonal elements are the base land transfer rates from one biome type to another, while diagonal elements are used to represent shifts in biome areas that do not change from one type to another.

Table 3.3. Initial transfer matrix for area between land use/cover types in [Mha/year].

	<b>Tropical Forest</b>	<b>Temperate Forest</b>	<b>Grassland</b>	<b>Agricultural Land</b>	<b>Human Area</b>	<b>Semi-Desert and Tundra</b>
<b>Tropical Forest</b>	15	0	0	0	0	0
<b>Temperate Forest</b>	0	2	0	0	0	0
<b>Grassland</b>	6	1	400	0	0	0
<b>Agricultural Land</b>	6	0	0	400	0	2
<b>Human Area</b>	0.5	0.5	1	1	0	0
<b>Semi-Desert and Tundra</b>	0	0	0	0	0	0

The land transfer rate of the non-diagonal elements is represented as,

$$L_{trans (non-diag)} = L_{tm} \cdot r \quad [Mha/y^2] \quad (3.23)$$

$L_{trans (non-diag)}$  = Land transfer rate of non-diagonal elements [Mha/y<sup>2</sup>]

$L_{tm}$  = Land transfer matrix [Mha/y]

$r$  = Population growth rate [1/y]

Land transfer rates along the diagonal direction are calculated as,

$$L_{trans} (diag) = L_{tm} \cdot r^{\frac{1}{2}} \quad [Mha/y^2] \quad (3.24)$$

The land transfer matrix is considered as a stock, which represents the state of land transfer at a given point in time. The land transfer matrix changes based on the land transfer rates in Equations 13 and 14 and drain transfer values ( $L_{tdr}$ ), which are used to eliminate the possibility of negative transfer rates.

$$L_{tm} = \int (L_{trans} - L_{tdr}) \cdot dt \quad [Mha/y] \quad (3.25)$$

The land transfer matrix is ultimately used to drive the change in biome area at a rate equal to the sum of the transfer rates from biome  $i$  to biome  $j$ , minus the sum of transfer rates from biome  $j$  to biome  $i$ ,

$$\frac{dA_j}{dt} = \sum_{i=1}^6 (a_{ij} - a_{ji}) \quad [Mha/y] \quad (3.26)$$

$A_j$  = Current area of biome  $j$  [Mha]

$a_{ij}$  = Rate of transition of area from biome  $i$  to biome  $j$  [Mha/y]

### 3.2.5. Food Production Sector

The food production sector in ANEMI3 models global food production which is ultimately used to determine the level of food per capita as an indicator for limitations of population growth. The production of food is affected by several factors including land fertility, arable land, water, and nutrients. The food production sector is based on that of the WORLD3 model (Meadows et al. 1974). The feedback structure of the food production sector is shown by the causal loop diagram in Figure 3.10.

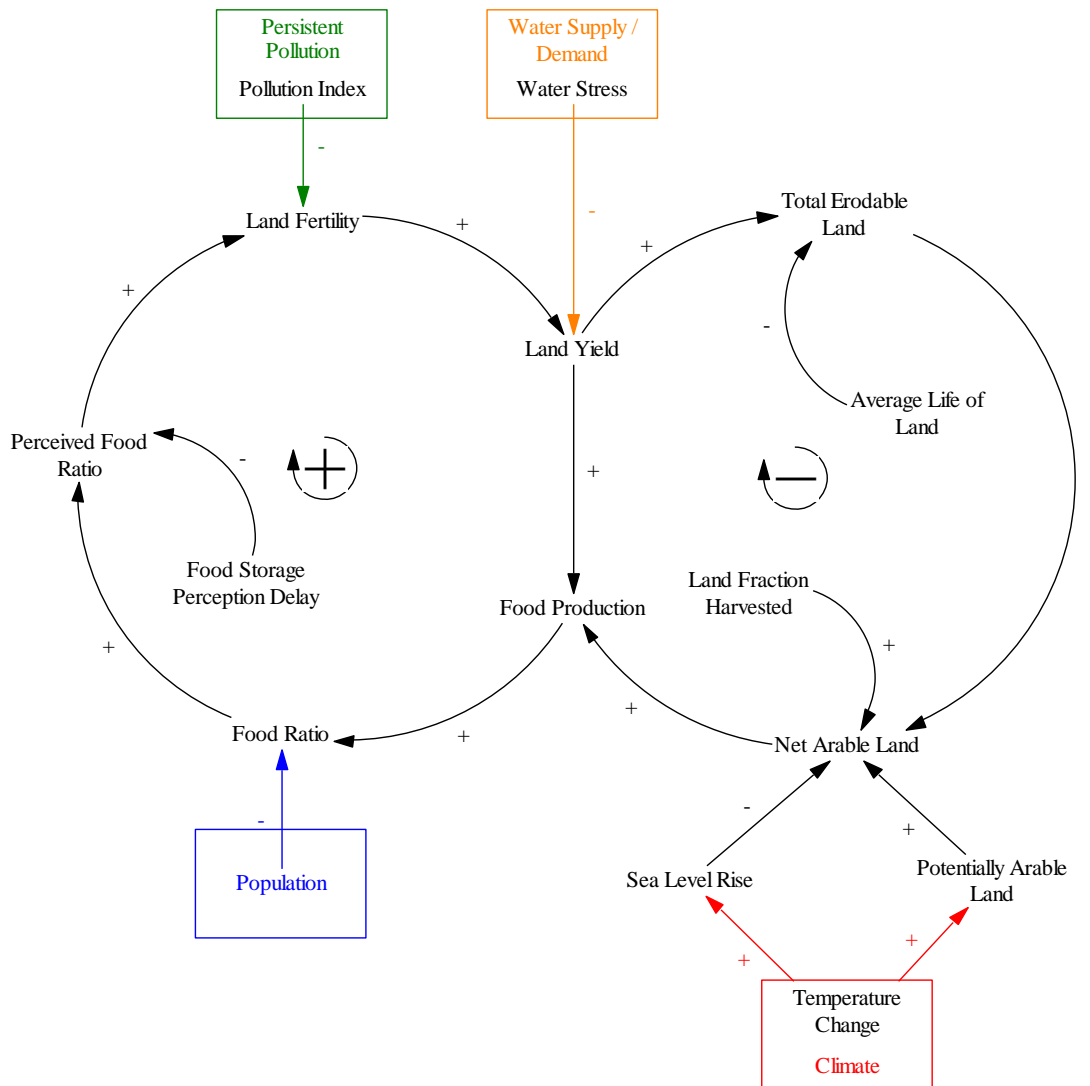


Figure 3.10. Causal loop diagram of the ANEMI3 food production sector.

There are two main feedback loops which drive the food production. The positive loop represents the effect of increased food production driving more reinvestment in increasing land fertility and thus food production again. The negative loop represents decreasing land yield due to food production which lead to more land erosion and then less arable land available for food production.

The corresponding stock and flow structure is shown in Figure 3.11.



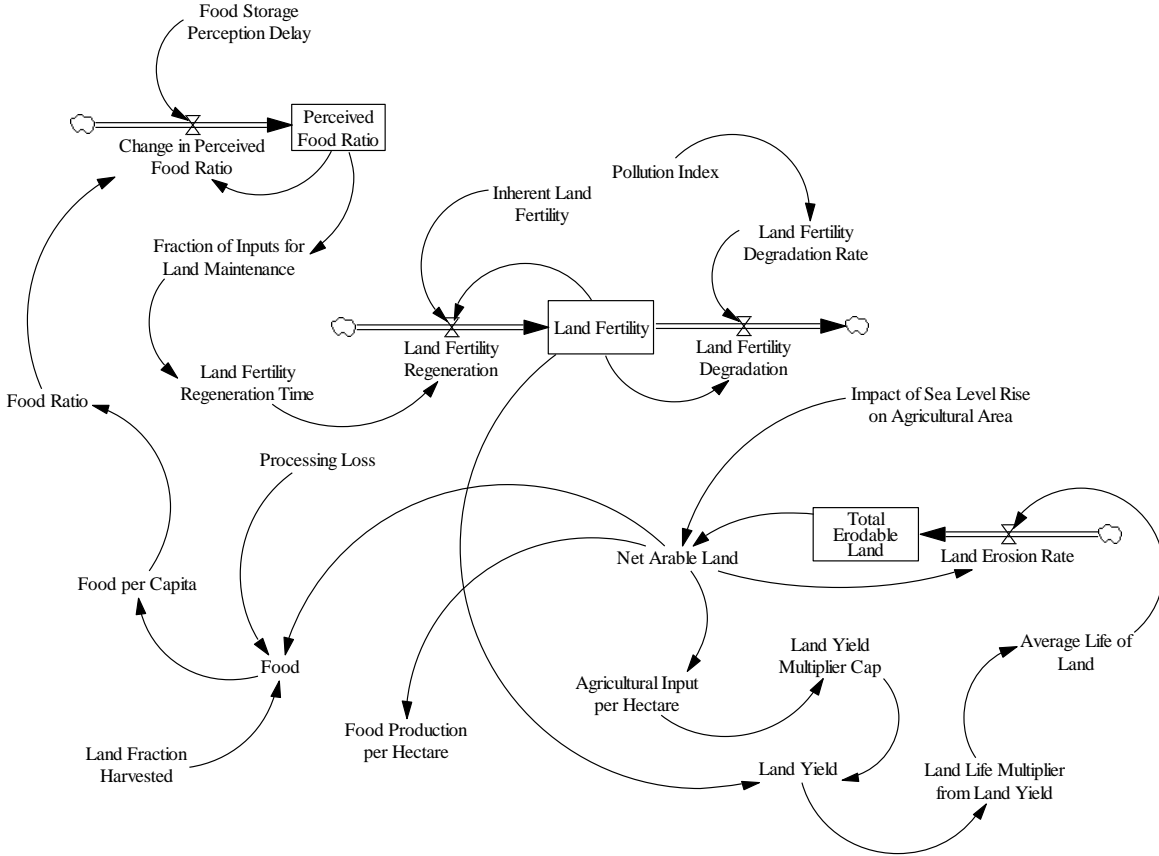


Figure 3.11. Stock and flow diagram of the ANEMI3 food production sector.

Food production can be increased in two ways through this representation. Either the amount of arable land can be increased by cultivating more land for agriculture, or the yield of that land can be increased through the application of modern agricultural inputs. In ANEMI3, climate change through increased temperatures can affect the level of potentially arable land, as changes in the number of growing days available in a given region can allow for agricultural activities to become feasible in areas where they were not. Two main factors limit the food production in the model. The first being that the production of food is reduced by land erosion, which limits the ability to produce food from the stock of arable land. The second is reduced land fertility, which arises from water stress as well as pollution.

Food production in units of vegetable equivalent kilograms per year is calculated based on the equations from Meadows et al. (1974),

$$F_p = L_y \cdot A_l \cdot L_{fh} \cdot (1 - P_l) \quad [\text{Veg. eq. kg/y}] \quad (3.27)$$

$F_p$  = Amount of food production [Veg. eq. kg/y]

$L_y$  = Land yield [Veg. eq kg/(ha · y)]

$A_l$  = Net arable land [ha]

$L_{fh}$  = Land fraction under harvesting

$P_l$  = Processing loss (assumed as 10%)

The land yield represents the total weight of crop production on average per hectare of land each year. The base amount of land yield is the land fertility, which can be modified by capital inputs which represent the use of modern agricultural inputs such as fertilizers and the efficiency for which they are applied. Water stress is also included as a factor that affects the land yield because insufficient water resources needed for irrigated agriculture will reduce crop output.

$$L_y = L_{yf} \cdot L_{fert} \cdot L_{ymc} \cdot L_{ymw} \quad [\text{Veg. eq. kg/(ha · y)}] \quad (3.28)$$

$L_{yf}$  = Land yield factor

$L_{fert}$  = Land fertility [Veg. eq. kg/(ha · y)]

$L_{ymc}$  = Land yield multiplier from capital

$L_{ymw}$  = Water stress to land yield factor

The fertility of the land used for food production is dependent on several different factors including soil chemistry, moisture content, and the type of crops being grown. Any processes that affect these factors will in turn influence the rate of degradation and regeneration of land fertility. Land fertility is represented as a stock, governed by the following equation,

$$L_{fert} = \int (L_{fr} - L_{fd}) \cdot dt \quad [Veg.eq.kg/(ha \cdot y)] \quad (3.29)$$

$L_{fr}$  = Land fertility regeneration [Veg.eq.kg/(ha · y<sup>2</sup>)]

$L_{fd}$  = Land fertility degradation [Veg.eq.kg/(ha · y<sup>2</sup>)]

The net amount of arable land that can be used for food production depends on the level of arable or agricultural land from the land use sector, the amount of erodible land which progresses over time with food production, as well as the amount of agricultural land that has been impacted by sea level rise. The amount of land area used for fodder and animal crop is subtracted from this value, as only that used for crop production is considered.

$$A_l = (L_{ar} - L_{ero}) \cdot L_{obs} - L_{slr} - L_{fa} \quad [ha] \quad (3.30)$$

$A_l$  = Net Arable Land [ha]

$L_{ar}$  = Arable land [ha]

$L_{ero}$  = Net erodible land [ha]

$L_{obs}$  = Obstacle to land conversion [ha]

$L_{slr}$  = Impacted agricultural land due to sea level rise [ha]

$L_{fa}$  = Land area used for fodder and animal crop [ha]

Climate change is expected to bring warmer climates to northerly regions over time, and may create the potential for regions that have not been exploited for agricultural purpose in the past to be considered for the future (Zabel et al. 2014; King et al. 2018). The WORLD3 model, from which the food production sector in ANEMI3 comes from, did not include a sector for climate change, let alone the potential effects of climate change on food production. King et al. (2018) used a set of seven global climate models to estimate the changes in land area that has growing degree days above 5 degrees Celsius with an annual sum of over 1200 degrees Celsius as an

indicator of potentially arable land. Based on this study the change in global temperature from the same set of GCMs used in the study is related to the change in potentially arable land. Figure 3.12 shows this relationship.

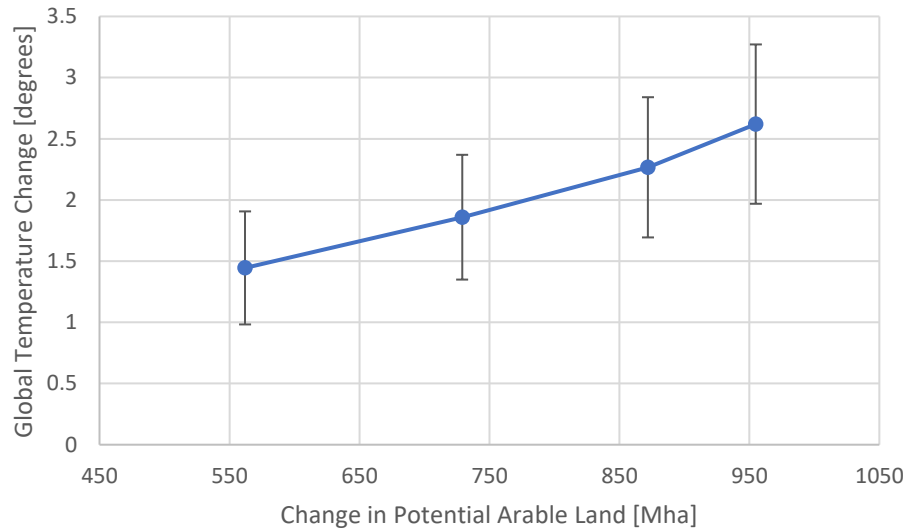


Figure 3.12. Relationship between global temperature change and change in potential arable land (after King et al. 2018). Error bars represent 95% confidence interval from the GCMs used in calculating global average temperature change.

This relationship is used as a multiplier to the land transfer rates from the semi-desert and tundra biome to the biome for agricultural land. However, this relationship is only between surface temperature change and *potential* arable land. In order to become agricultural land, the newly discovered amounts of potential arable land would need to be cultivated based on updated information of the land becoming available for cultivation as the climate changes. Therefore, an information delay is applied to this relationship with a baseline value of 20 years. The sensitivity to this assumed information delay is tested in Section 3.5.4.

In addition to increasing potentially arable land as a result of climate change mentioned in Section 3.2.4, it is expected that global crop yields will decrease to the occurrence of more severe and frequent temperature extremes, thereby causing heat and water stress (Zhao et al. 2017; King et al. 2018; Searchinger et al. 2019). In Searchinger et al. (2019), a comprehensive analysis was carried out to examine the impact of changes in climate on crop yields of four major crop types including wheat, rice, maize, and soybean. The analysis compiled, results from different methods that include global grid and point based models, statistical regressions, and field warming experiments. The results showed that on average, for each degree of temperature change global yields of wheat, rice, maize, and soybean would be reduced by 6.0%, 3.2%, 7.4%, and 3.1%, respectively. The ANEMI3 model only includes the total food production including all crop types. In order to incorporate these potential climate related effects on land yield, a weighted average was taken from these percentage reductions based on the total number of tonnes produced in the model base year of 1980. Crop production data was taken from the FAOSTAT database (FAO 2019b).

Table 3.4. Effect of temperature change on crop yields for wheat, rice, maize, and soybean.

Crop Type	Temperature Yield Reduction	Production Levels in 1980	Weighted Average of Temperature Yield Reduction
	%/°C	billion tonnes	%/°C
Wheat	6.0	1.98	5.34
Rice	3.2	1.96	
Maize	7.4	1.75	
Soybean	3.1	0.33	

The weighted average of temperature yield reductions for wheat, rice, maize, and soybean crops based on the 1980 production levels is 5.34% per degree Celsius of global surface temperature change (Table 3.4). These four crops are only a subset of the all crop types grown. However, their use in the ANEMI3 model for total yield reduction values is justified by the fact that their proportion of global food production has remained relatively constant over time (Figure 3.13).

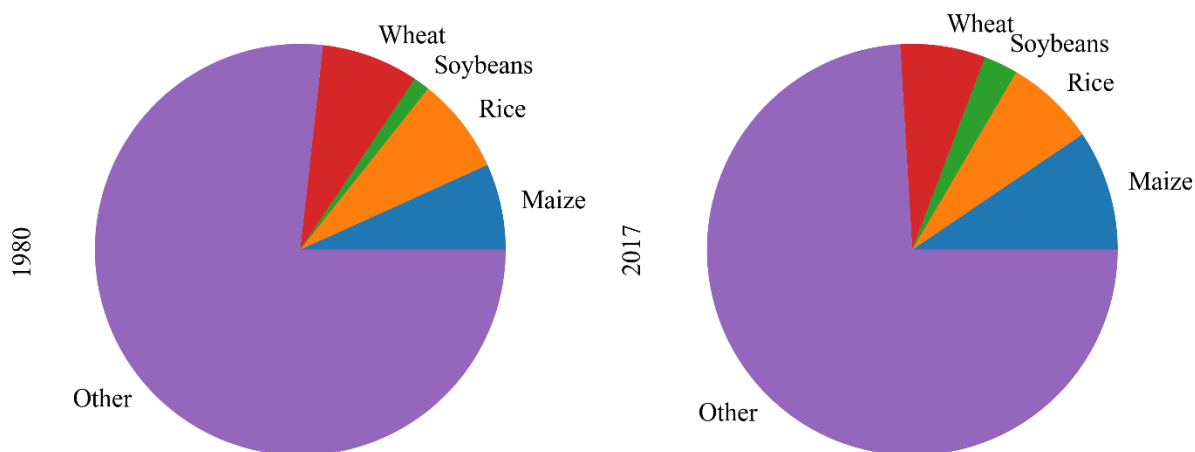


Figure 3.13. Distribution of crop production for the 4 crop types used in (Searchinger et al. 2019) compared to global totals in the years 1980 and 2017.

This number is used as a scenario to assess the influence of climate change on food production, along with the effect of increased potentially arable land derived from King et al. (2018).

The previous model versions included irrigation as an exogenous driver of water demands for agriculture. However, evidence has shown that crop yields from irrigated agriculture are consistently higher than those from rain-fed agriculture in the developing world (Lipton et al. 2003; Döngert 2010; Jin et al. 2012). Increasing levels of irrigation in the future are a key factor to increasing agricultural land yields despite limited expansion potential for agricultural land use.

Irrigated agriculture allows for increased land yields by allowing crops to receive a constant stream of dissolved nutrients from soils for optimal vegetative growth and development for crop production. Irrigation has the most potential to increase crop yields in areas where large seasonal and interannual fluctuation in rainfall patterns exist (Klohn et al. 2003). Due to the potential for shifts in the spatial and temporal distributions of rainfall patterns as a result of climate change, it is possible that the potential for irrigated agriculture may increase in the future. In the ANEMI3 model, a tighter coupling of irrigation and food production is made to assess the ability of intensified irrigation and agricultural land use to satisfy the increased demand on food production in the future. The effect of irrigation on food production is incorporated through a multiplier effect on land yield, based on the fact that crop yields from irrigated agriculture are higher than rainfed by a factor of 2.3 on average (Dowgert 2010). The effect of changes in food production and agricultural water demand are tested by implementing exogenous scenarios taken from FAO (2018). Details of these scenarios are provided in Section 4.5.

In this sector the effects of climate change on food production have been enhanced from the previous version of ANEMI, which only considered the impact of sea level rise through reduced arable land. In ANEMI3, the effect of changes in global air temperatures now affect food production by reducing land yields through the effect of heat stress based on the findings of Dowgert (2010). In addition, air surface temperatures now have an affect on food production through the northward shift of potentially arable lands into boreal forests based the functional relationship derived from King et al. (2018). The modifications to the food production sector allow for the research objectives 5a and 5c from Section 2.6 to be addressed.

### 3.2.6. Sea Level Rise Sector

During the period of 1901 to 2010, the average sea level has risen approximately 0.2m due to the melting of arctic sea ice and ocean expansion (IPCC 2013). The rate at which polar ice is melting and sea levels are rising is projected to accelerate in the 21<sup>st</sup> century with climate change. The amount of projected sea level rise under a variety of different scenarios is likely to be between 0.26m and 0.82m relative to the baseline (1986 – 2005) period. Rising sea levels has the potential to impact agriculture and fresh groundwater resources through the inundation of agricultural lands and saltwater intrusion into groundwater aquifers. The resulting impacts to the global economy are projected to be on the scale of 14 trillion USD per year by 2100 due to flood damages if no adaptation measures are adopted (Jevrejeva et al. 2018). Additional economic impacts may arise on the municipal level from increased water elevations in coastal outfalls for drainage systems, causing the potential for back ups in stormwater drainage systems and wastewater treatment plants (IPCC 2014).

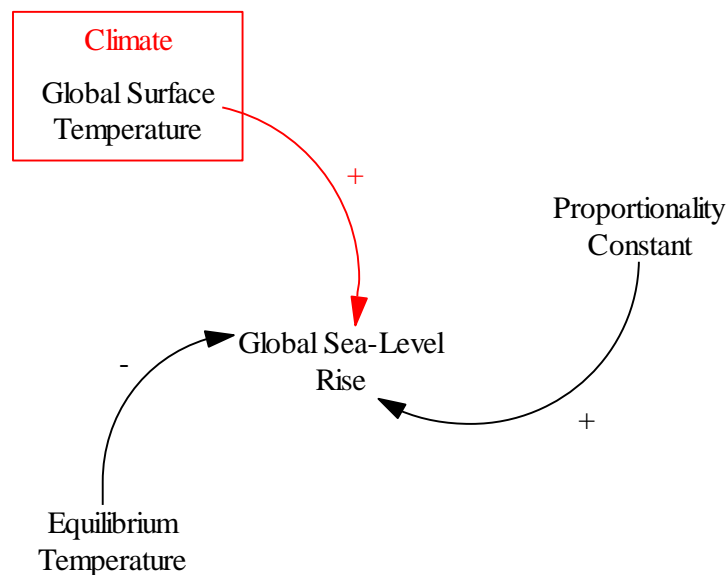


Figure 3.14. Causal diagram of the ANEMI3 sea-level rise sector.



In ANEMI3, the global average near surface air temperature change is used as a driver for sea level rise. The projected mean sea level rise is approximated as linear function of the temperature change,

$$H = a(T - T_0) \quad [m] \quad (3.31)$$

*H = Mean sea level rise [m]*

*T = Global mean temperature [°C]*

*T<sub>0</sub> = Reference temperature [°C]*

*a = Slope of correlation [m/°C]*

This equation is based on the work of Rahmstorf (2007) who demonstrated a highly significant correlation of global temperature changes and mean sea level rise ( $r=0.88$ ,  $p=1.6e-8$ ). The slope ( $a$ ) of which was found to be 3.4mm/(year.°C). Although this representation of mean sea level rise is simple, the impacts of which are important for food production in ANEMI3 by limiting the amount of land available for agriculture.

### 3.2.7. Hydrologic Cycle Sector

The hydrologic cycle describes the flow of water from oceans to atmosphere, onto the land surface and through the groundwater back to the ocean again as a continuous cycle. Each point in the hydrologic cycle can be considered as a kind of reservoir from which water flows to and from. The causal loop diagram in Figure 3.15 illustrates the feedback loops at work that drive the hydrologic cycle.

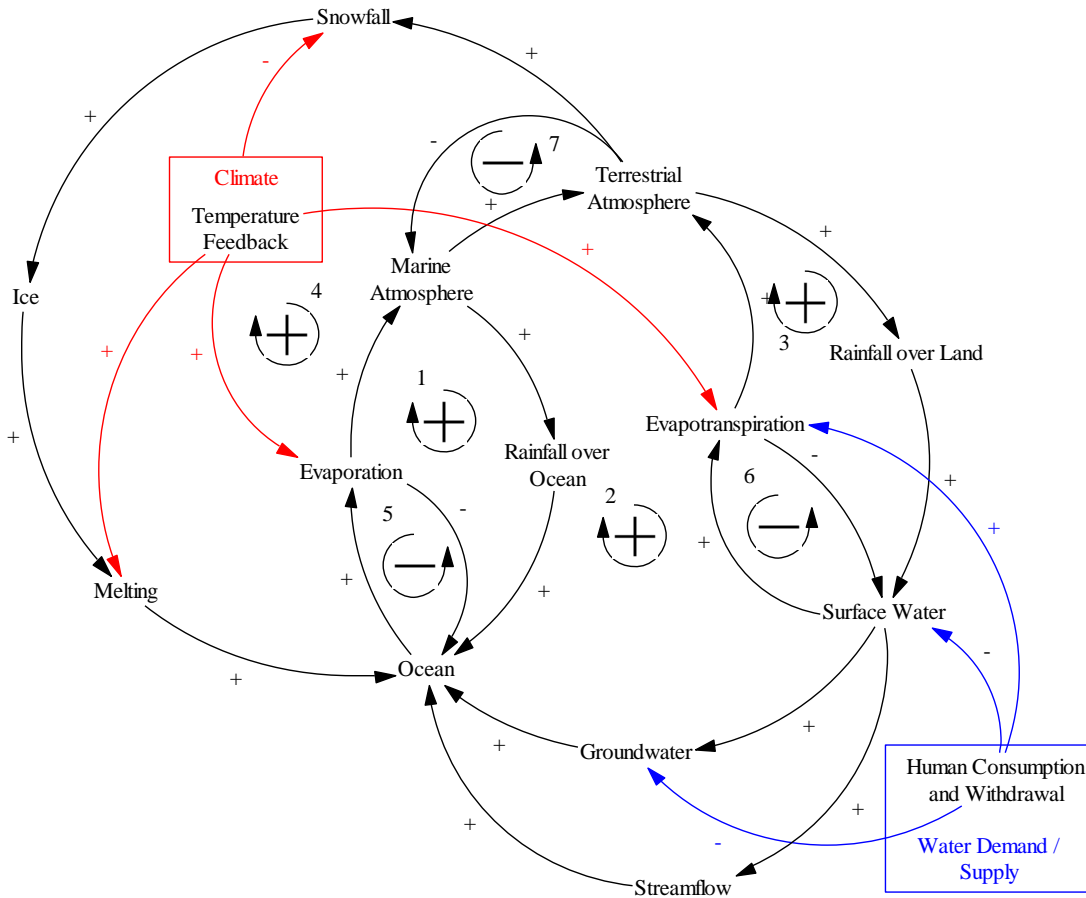


Figure 3.15. Causal loop diagram of the ANEMI3 hydrologic cycle sector.

Feedback loops number 1- 4 in Figure 3.15 illustrates the movement of water from the atmosphere (terrestrial or marine) to the surface (ocean or land) as rainfall or snowfall and then back to the atmosphere (through evaporation and evapotranspiration). These are positive feedback loops because more water in oceans and surface waters results in larger surface area and thus more evaporation leading to more atmosphere and rainfall then more water in oceans and surface waters once again. The positive loops are balanced by negative loops 5 and 6 which regulate increases in land and ocean water volumes by increased evaporation. Loop number 7 illustrates the balance between advection of atmospheric water over oceans and land surfaces as this process depends

upon the difference in water content between them. The configuration of stocks and flows in the hydrologic cycle sector of the model are shown in Figure 3.16.

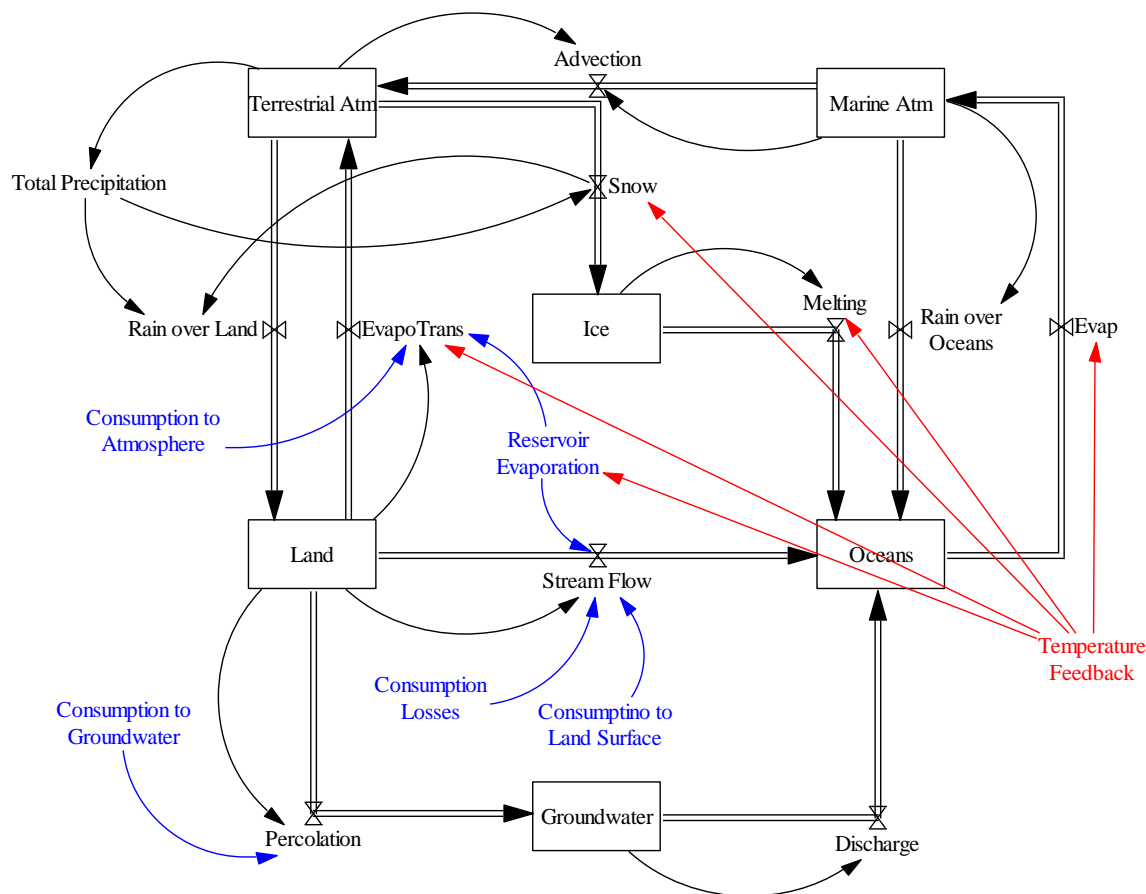


Figure 3.16. Stock and flow diagram of the AEMI3 hydrologic cycle sector. Items in blue denote processes that have human influence on the hydrologic cycle, while those in red represent the influence of changing climate.

In the ANEMI3, six reservoirs or stocks are used consisting of oceans, ice, land, groundwater, terrestrial atmosphere and marine atmosphere. The processes modelled that move water to and from these stocks are snowfall, ice melt, evaporation and evapotranspiration, rain over land and oceans, stream flow, percolation, and groundwater discharge. These processes all act as flows that influence the stocks. Initial values for the stocks in the hydrologic cycle are chosen in a way that

allows the system to start at a pseudo steady state condition in Table 3.5 from Davies (2007). From this initial point, the hydrologic cycle is influenced by anthropogenic means.

Table 3.5. Initial stock values for hydrologic cycle sector. All values are in units of [km<sup>3</sup>].

<b>Hydrologic Stock</b>	<b>Literature Value</b>	<b>ANEMI3 Model Value</b>
<b>Marine Atmosphere</b>	9.4 – 11 * 10 <sup>3</sup>	9.4 * 10 <sup>3</sup>
<b>Terrestrial Atmosphere</b>	4.0 – 4.5 * 10 <sup>3</sup>	4.0 * 10 <sup>3</sup>
<b>Oceanic Water Content</b>	1338 * 10 <sup>6</sup>	1338 * 10 <sup>6</sup>
<b>Land Surface Water</b>	118 – 360 * 10 <sup>3</sup>	200 * 10 <sup>3</sup>
<b>Ice and Permafrost</b>	24 – 43 * 10 <sup>6</sup>	24.5 * 10 <sup>6</sup>
<b>Groundwater</b>	10.5 – 23.4 * 10 <sup>6</sup>	10.6 * 10 <sup>6</sup>

Anthropogenic influence on the hydrologic cycle is implemented in two ways. The first, takes into consideration water withdrawals and consumption, while the second represents the influence of changing climate. The effect of withdrawals and consumption for domestic, industrial, and agricultural water users involves the removal of water resources in the form of surface water (from stream flow) and groundwater (from the groundwater stock). The total amount of withdrawals is based on water production in the water supply sector, while the way that withdrawals are allocated across the hydrologic cycle is based on the composition of water demand across users. The proportions of which are given in Table 3.6.

Table 3.6. Percentages of water reallocation in the hydrologic cycle after human withdrawal and consumption.

Water User	Evaporation	Land	Groundwater	Lost
Agriculture	70	10	20	0
Domestic	50	0	50	0
Industry	70	0	15	15

Most of the water is not removed from the cycle at any point, it is only reallocated among the different stocks in order to maintain conservation of mass. However, in the case of industrial water consumption, water can be effectively separated from the hydrologic cycle in cases where water makes up a portion of the final product in the production process. Climate change influences the hydrologic cycle by superimposing a temperature feedback effect that affects several processes within it as the temperature change increases by acting as a multiplier. As a result, a larger portion of precipitation becomes rainfall instead of snow, and the melting of ice is increased along with evaporative processes.

The mathematical formulation of the hydrologic cycle in the ANEMI3 starts with the water content stored in the atmosphere over land and oceans,

$$A_M = \int (E_M - Adv - P_O) \cdot dt \quad [km^3] \quad (3.32)$$

$A_M$  = Marine atmospheric moisture [ $km^3$ ]

$E_M$  = Evaporation from oceans [ $km^3/y$ ]

$Adv$  = Advective flow of moisture between land and oceans [ $km^3/y$ ]

$P_O$  = Precipitation over oceans [ $km^3/y$ ]

$$A_L = \int (Adv + ET - P_R - P_S) \cdot dt \quad [km^3] \quad (3.33)$$

$A_L$  = Atmospheric moisture over land [ $km^3$ ]

$ET$  = Evapotranspiration from land surface [ $km^3/y$ ]

$P_R$  = Precipitation over land in the form of rain [ $km^3/y$ ]

$P_S$  = Precipitation over land in the form of snow [ $km^3/y$ ]

Water storage in the terrestrial environment or land surface is represented as,

$$LS = \int (P_R - ET - SF - GP) \cdot dt \quad [km^3] \quad (3.34)$$

$LS$  = Water storage on land surface [ $km^3$ ]

$SF$  = Streamflow of water from land surface to ocean [ $km^3/y$ ]

$GP$  = Groundwater percolation [ $km^3/y$ ]

Water storage in the oceans is given by the following equation,

$$O = \int (SF + GD + P_O + M - E_M) \cdot dt \quad [km^3] \quad (3.35)$$

$GD$  = Groundwater discharge [ $km^3/y$ ]

$M$  = Melting of ice sheets [ $km^3/y$ ]

Finally, groundwater and ice storage are expressed as,

$$GS = \int (GP - GD) \cdot dt \quad [km^3] \quad (3.36)$$

$GS = \text{Groundwater storage } [km^3]$

$$IS = \int (P_s - M) \cdot dt \quad [km^3] \quad (3.37)$$

$IS = \text{Ice storage } [km^3]$

### 3.2.8. Water Demand Sector

Water demand sector in the ANEMI3 is based on the desired water withdrawals of agricultural, domestic, and industrial water users. Base domestic water withdrawals are dependent on structural water intensities which relate economic factors such as GDP to withdrawal rates per person. This concept is based on the conceptual model presented in Alcamo et al. (2003a), and has been confirmed by the IHP (2000) data (see Figure 3.17. Illustration of structural water intensity for domestic water use (after Alcamo et al. 2003a).).

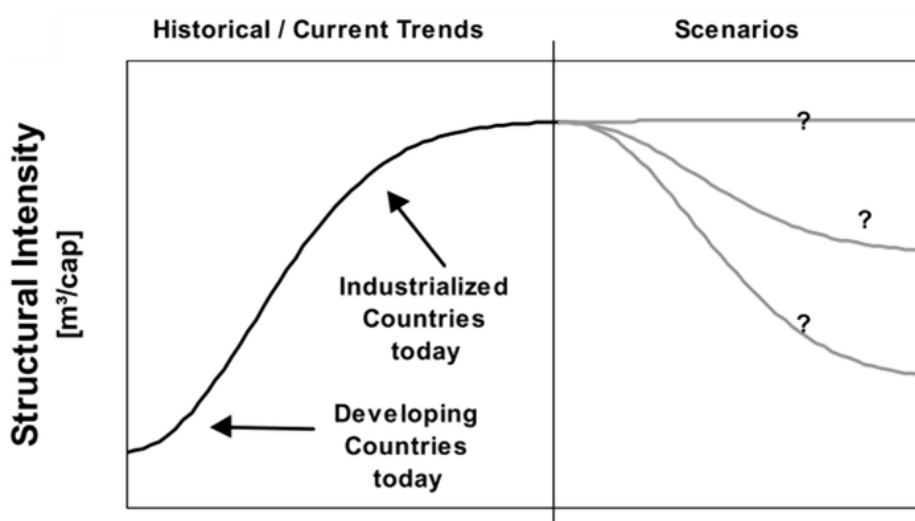


Figure 3.17. Illustration of structural water intensity for domestic water use (after Alcamo et al. 2003a).

The relationships presented indicate that there are established trends in water usage as countries become developed using an indicator of economic development such as GDP per capita. Domestic water use in terms of water volume per capita tends to increase as more water is needed for improved sanitation and use of more water-using appliances such as dishwashers and washing machines. This trend stabilizes in the developed countries. The causal diagram in Figure 3.18 shows the water demand sector including domestic, industrial, and agricultural water users.

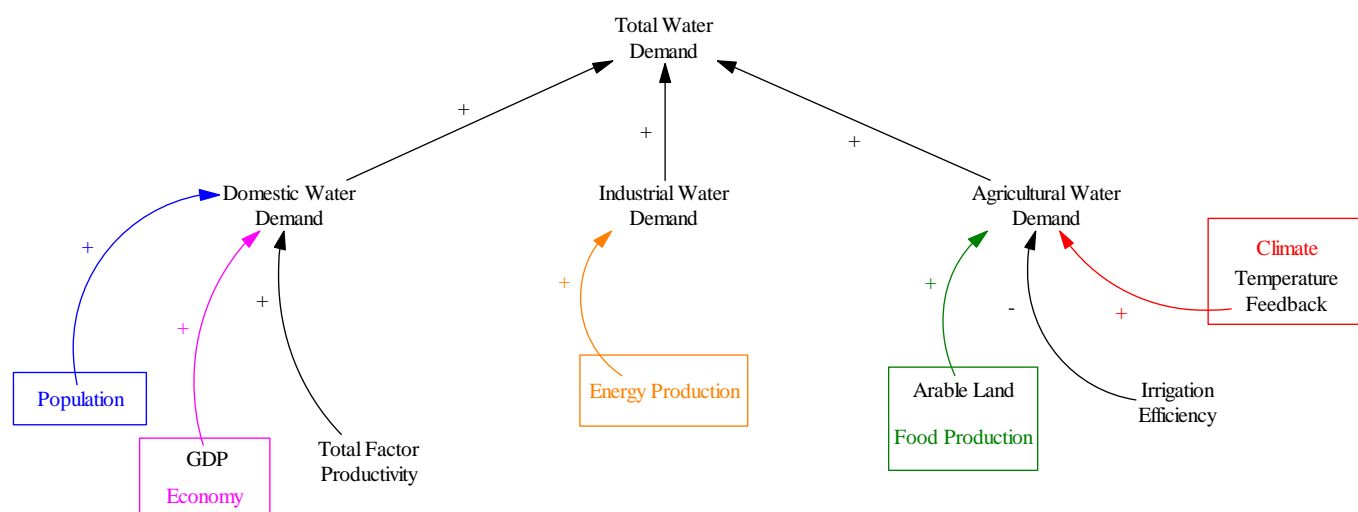


Figure 3.18. Causal diagram of the ANEMI3 water demand sector.

Although there are no feedback loops within the water demand sector itself, there are many intersectoral connection and feedbacks associated with water demand discussed previously in Section 3.1.



Domestic structural water intensity from this conceptual model is represented by the following equation,

$$DSWI = DSWI_{min} + DSWI_{max}(1 - \exp(-\gamma_d GDP^2)) \quad [m^3/person] \quad (3.38)$$

$$DSWI = \text{Domestic structural water intensity } [m^3/person]$$

Where domestic structural water intensity is a function of GDP and  $DSWI_{min}$ ,  $DSWI_{max}$ , and  $\gamma_d$  are calibrated parameters based on the country for which the domestic structural water intensity is to be estimated. This equation is designed for the use of country level inputs, however in the ANEMI3 it is calibrated and applied to the global scale. The reasoning behind this is that conceptually this equation fits the trends that are taking place globally for domestic water use as discussed above. This concept is also ideal for application to the global scale as the input of global GDP is readily available in the ANEMI3 model. Using the domestic structural water intensity, water demand is calculated as,

$$W_{dom} = DSWI \cdot P_{total} \cdot \Delta TFP \quad [km^3] \quad (3.39)$$

$$W_{dom} = \text{Domestic water demand } [km^3]$$

$$P_{total} = \text{Total population } [persons]$$

$$\Delta TFP = \text{Change in total factor productivity}$$

The change in total factor productivity is from the economic sector in the ANEMI3 and represents changes in domestic water use efficiency. This can be in the form of more efficient water distribution systems and water-using home appliances, for example.

The generation of electricity typically dominates water withdrawals in the industrial sector as a country develops. The trend in energy use starts with a high usage of water per unit of energy consumption due to the usage of mostly thermal power plants and water for cooling. Over time, more developed countries generally have a mix of thermal and non-thermal power generation plants thus reducing water usage per unit of energy consumption. The representation of industrial water withdrawal in the ANEMI3 takes into consideration projected changes in the mix of energy supply by incorporating projections from the Global Change Assessment Model (GCAM) presented in Figure 3.19.

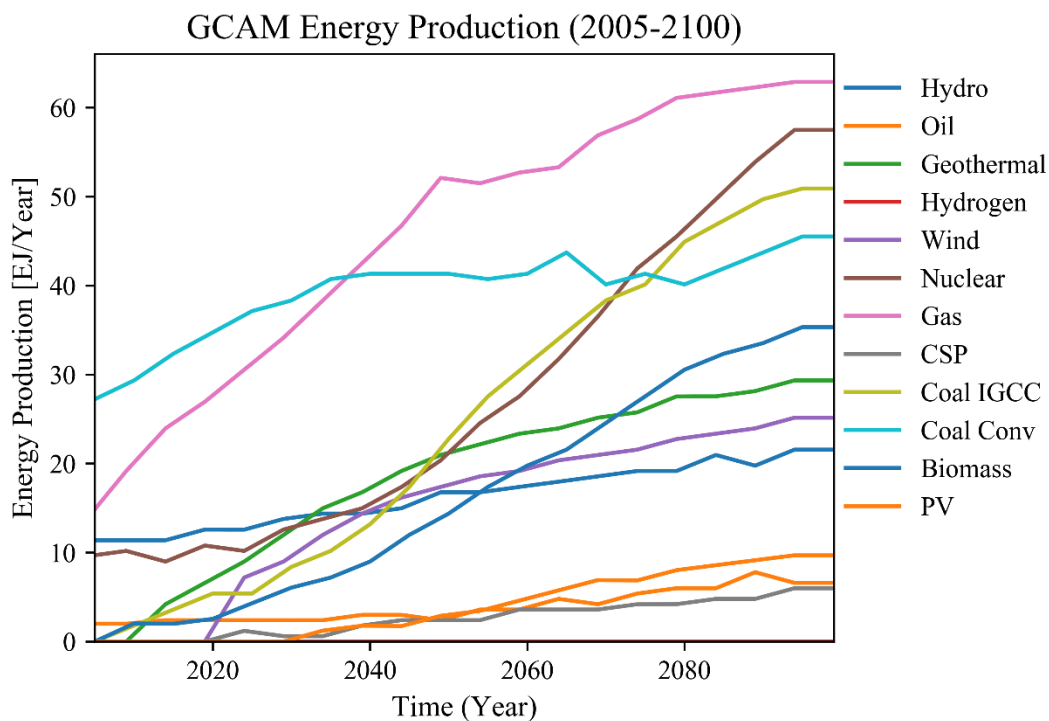


Figure 3.19. GCAM energy production projections for 2005-2100 (after Davies et al. (2013)).

In the ANEMI3 energy sector, energy production is considered for four different energy sources consisting of coal, oil and gas, hydro and nuclear power, and renewables. The fuel types from GCAM shown in Figure 3.19 were aggregated to their corresponding types in the ANEMI3, along with the water withdrawals for each of the GCAM energy production type as shown in Table 3.7.

Table 3.7. Water withdrawal rates for energy production of various types (Larsen and Drews 2019).

ANEMI3 Energy Type	GCAM Energy Type	Water Withdrawal Factor (L/MWh)
Coal	Coal IGCC (Integrated Gasification Combined Cycle)	1612
	Coal Conv (Conventional Coal)	103694
Oil and Gas	Oil	95890
	Gas	43502
Hydro and Nuclear	Hydro	0
	Nuclear	151628
Renewables	Geothermal	7586
	Hydrogen	0
	Wind	0
	CSP (Concentrated Solar Power)	3165
	Biomass	104806
	PV (Photovoltaic)	10

The industrial water demand is therefore represented by the following equation,

$$W_{ind} = \sum_{i=1}^4 \left( E_{p_i} \cdot \sum_{j=1}^n EWF_j \cdot \left( \frac{GCAM_j}{Total\ GCAM_i} \right) \right) \quad [km^3/y] \quad (3.40)$$

$W_{ind}$  = Industrial water demand [ $km^3/y$ ]

$E_{p_i}$  = Energy production in ANEMI3 for energy source  $i$  [ $GJ/y$ ]

$EWF_j = \text{Energy withdrawal factor for energy source } j \text{ [km}^3/\text{GJ]}$

$GCAM_j = \text{GCAM energy production for energy source } j \text{ [GJ/y]}$

$\text{Total } GCAM_i = \text{Total GCAM energy production of energy sources } i \text{ [GJ/y]}$

By reformulating the industrial water withdrawal in this way, energy production is connected to water demand in the ANEMI3 model, and projected technological changes for industrial water demand are incorporated from the GCAM projections.

Agricultural water demand depends on the amount of agricultural area that is being used for food production, as well as the level of technological change with respect to water usage for food production. Change in global surface temperature is also included as an additional factor affecting water demand for food production. Increased temperatures will lead to higher evapotranspiration rates in agricultural soils thereby leaving less water for utilization for the crops and thus boosting irrigation water requirements (Yuan et al. 2016). Agricultural water demand is represented mathematically as,

$$W_{agr} = PHW \cdot A_l \quad [\text{km}^3/\text{y}] \quad (3.41)$$

$W_{agr} = \text{Agricultural water demand [km}^3/\text{y]}$

$PHW = \text{Per hectare water withdrawals [km}^3/(\text{ha} \cdot \text{y})]$

$A_l = \text{Net arable land [ha]}$

Where per hectare water withdrawals are represented as,

$$PHW = BW_{agr} \cdot Technology_{agr} \cdot T_{feedback} \quad [\text{km}^3/(\text{ha} \cdot \text{y})] \quad (3.42)$$

$BW_{agr}$  = Base specific water withdrawals for agriculture [ $km^3/(ha \cdot y)$ ]

$Technology_{agr}$  = Exogenous technological change factor for irrigation

$T_{feedback}$  = Temperature feedback multiplier from climate sector

The modifications to the water demand sector from the previous version include improvements to the representation of industrial water demand. Originally, the industrial water demand was based on the product of the industrial structural water demand curve, representing the water demand from per unit of electricity production (Figure 1.1b), and the electricity production represented by an exogenous growth rate. In ANEMI3, the industrial water demand is determined through the use of modelled energy production amounts for coal, oil and gas, hydro and nuclear, and renewables, combined with water withdrawal factors for these energy types from Larsen and Drews (2019). This modification allows for the research objectives number 2 and 3 from Section 2.6 to be addressed, as it creates another feedback water supply development and the energy-economy sectors, as well as provides more plausible industrial water demand projections.

### 3.2.9. Energy-Economy Sector

The energy-economy sector used in ANEMI2 was based on the traditional Solow neoclassical growth model where economic output is represented as a function of capital and labor in the form of a Cobb-Douglas production function (Prescott 1988). The growth of capital is dependent on investment, which is determined by a Solow rule where a fraction of output is invested in new capital every time period, while population growth increases the labor force, thereby boosting output and the capital stocks over time. This reinforcing behaviour on the output is combined with a computable general equilibrium (CGE) model where the global economy consists of a representative household and a representative firm. The representative household encapsulates the

World's population whose preferences are captured by a utility function based on consumption. The household generates income by renting capital and selling energy services to the firm, as well as earning income from the labor force. This income provides a budget constraint to the household for which it maximizes its utility function. The firm on the other hand, seeks to minimize the total cost of producing energy amongst different sources. As these two dynamics unfold, prices for energy production move to clear the market and achieve equilibrium between energy supply and demand for each time step. The structure of this model allows for the examination of long run economic growth of aggregate capital stock as well as the production paths for fossil fuels and renewable energies.

In ANEMI3, water supply was to be added as an additional service to be sold to the firm, and the firm would seek to minimize the total cost of production by considering the prices of supplying water. This would have been based on the current level of capital stocks in water supply infrastructure for surface water, groundwater, wastewater reuse, and desalination water supplies. The capital stocks include infrastructure such as reservoirs, treatment plants, and distribution networks for example in the case of surface water supplies. Connections between energy and water production would have been incorporated into the model by including energy as a key component in the production of water and vice-versa, forming a nexus between energy and water production in the global economy. The implementation of this structure into the energy-economy sector of ANEMI2 however, proved difficult as the clearing of the energy and water markets had a very narrow pathway and was extremely unstable. Therefore, in ANEMI3 a new energy-economy model was incorporated for which water supply could be integrated.

The new energy-economy sector in the ANEMI3 model is based on that developed by Fiddaman (1997), which incorporates the energy and economy models from Sterman (1980; 1981), and Nordhaus (1992). Many of the dynamics related to economic growth and resource depletion from previous approach are captured now, but there are some key structural differences. The first being that the macroeconomic assumption of market equilibrium that is used previously is no longer present, as the model being used here is a disequilibrium model. Instead of energy prices being set to equate supply and demand at every time step, there are negative feedbacks which constantly drive supply to meet the demand as they change over time.

The following sub-sections summarize the new energy-economy sector that is incorporated into the ANEMI3 model based on the Feedback-Rich Energy Economy Model (FREE) from Fiddaman (1997) as a basis for the new water supply development sector.

### 3.2.9.1. Goods Production and Capital

The dynamics of the aggregated capital stock of the global economy is shown in in Figure 3.20, consisting of five main feedback loops. The first and second loop depict the adjustment of the desired capital stock in response to the relative cost and marginal production of capital. The gap between the desired and actual capital stock is corrected in the third loop. The fourth loop illustrates the incorporation of expected output growth rate on investment, and the fifth loop factors capital depreciation into investment in additional capital.

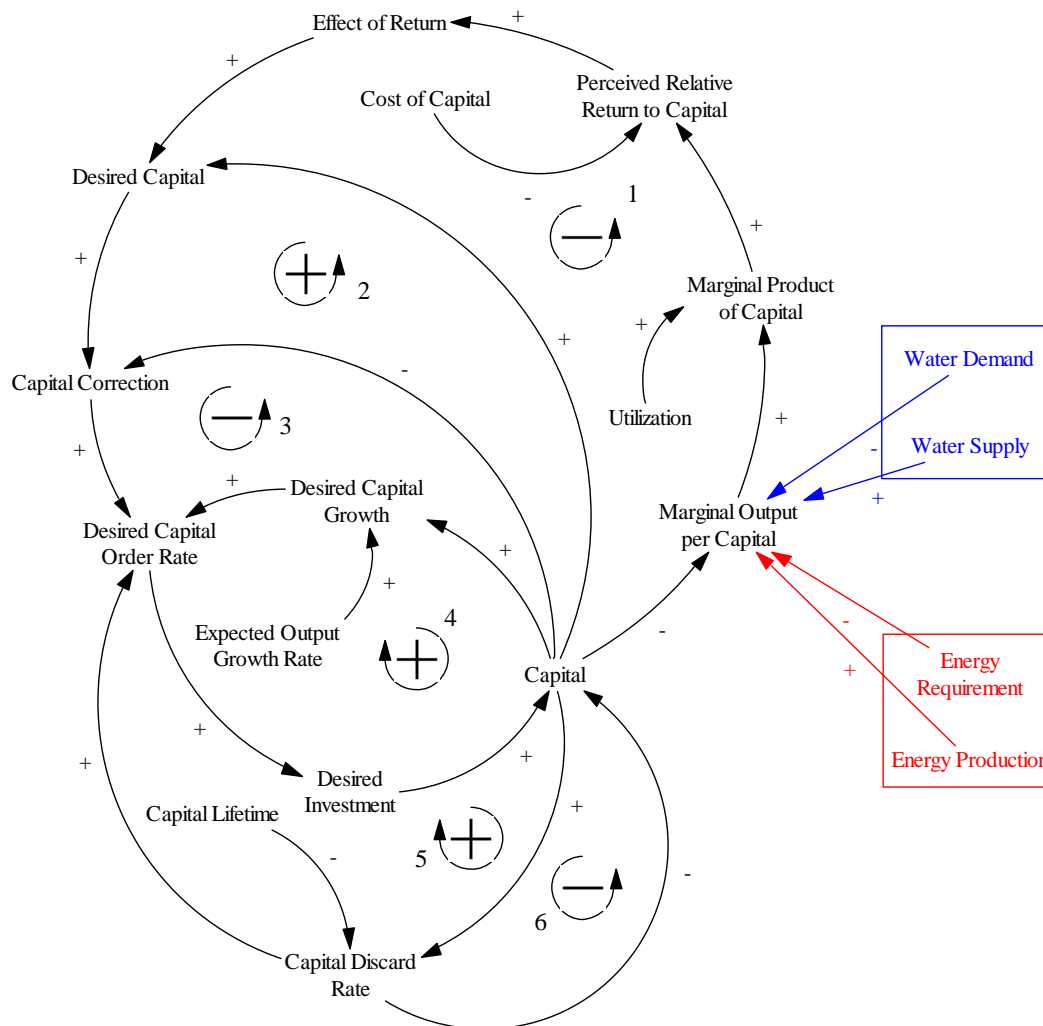


Figure 3.20. Causal loop diagram for good production and capital sub-system of the energy-economy sector.

The stock and flow structure that is used to drive the global capital stock is shown in Figure 3.21.

The capital stock is the main state variable which is affected by investment and depreciation, corresponding to the flows of investment and capital discard rates.



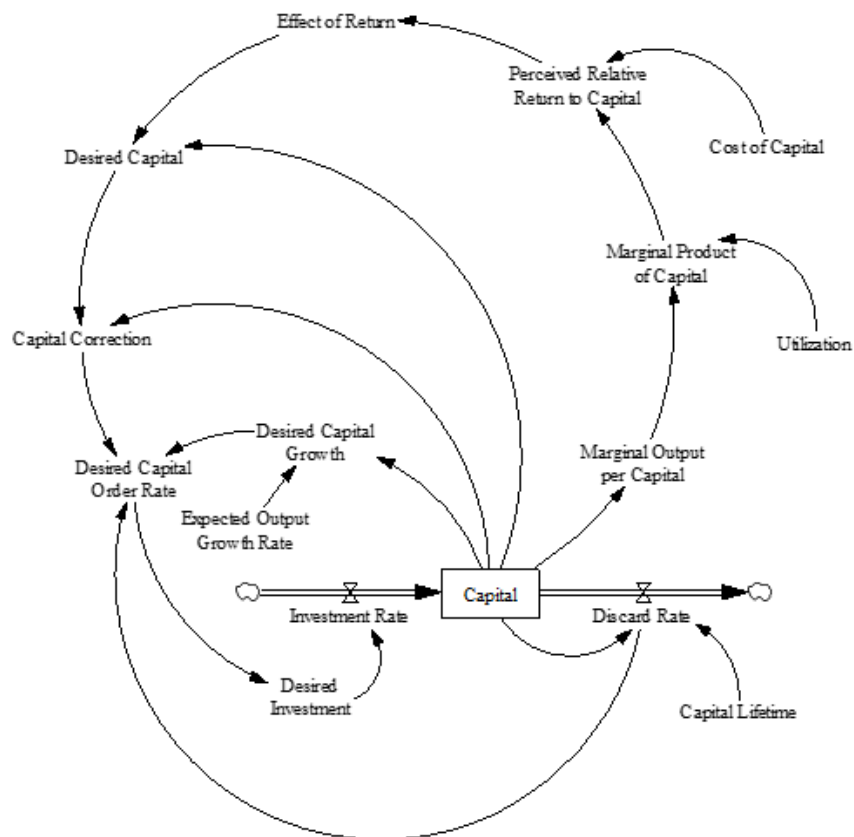


Figure 3.21. Stock and flow diagram of the ANEMI3 capital sector of the economy

Economic output is determined using a Cobb-Douglas production function in the following form,

$$Y = Y_0 A_t \Omega \left( \frac{L}{L_0} \right)^\alpha \left( \frac{KO}{KO_0} \right)^{1-\alpha} \quad [$/year] \quad (3.43)$$

$Y$  = Gross output [\$/year]

$Y_0$  = Reference gross output [\$/year]

$A_t$  = Factor productivity

$\Omega$  = Climate damages

$\alpha$  = Value share of labor

$L$  = Labor [persons]

$L_0$  = Initial labor [persons]

$KO$  = Operating capital [\$/]

$KO_0$  = Initial operating capital [\$/]

Labor will increase over time as the working population increases, as will capital as the economy grows thereby increasing economic output. As global temperatures increase, so too will climate damages and will reduce economic output through the following equation:

$$\Omega = \frac{1}{1 + \theta} * \left( \frac{T - T_a}{T_{ref}} \right)^\phi \quad (3.44)$$

$\theta$  = Climate damage scale factor  
 $T$  = Atmospheric temperature [°C]  
 $T_a$  = Adapted temperature [°C]  
 $T_{ref}$  = Reference temperature [°C]  
 $\phi$  = Climate damage non – linearity factor

This formulation allows for economic climate damages to take place only when there is a deviation from the adapted temperature. The adapted temperature approaches the current atmospheric temperature with a delay according to the fractional adaptation rate,  $T_{frac}$  in units of °C:

$$T_a(t) = \int (T_{frac} \cdot (T - T_a)) \cdot dt \quad [°C] \quad (3.45)$$

The aggregate capital stock for the production of goods increases with investment and is depleted by depreciation, which is a fixed fraction of capital,

$$K(t) = \int (I - \delta K) \cdot dt \quad [\$] \quad (3.46)$$

$K$  = Capital aggregate [\$]  
 $I$  = Investment rate [\$/year]  
 $\delta$  = Fractional depreciation rate

Depreciation acts as a first-order exponential decay, and is compensated by the first term of the investment equation which takes the following form,

$$I = \delta K + \frac{(K_D - K)}{\tau_k} + KG \quad [$/year] \quad (3.47)$$

$K_D = \text{Desired capital } [\$]$

$\tau_k = \text{Capital correction time } [y]$

$G = \text{Perceived fractional growth rate of output}$

In addition to compensating for depreciation, investment is driven by the perceived growth in output. Otherwise, capital would lag the optimal value for each time step. Lastly, investment in capital is determined by the deviation between desired capital and its current value over a correction time. Desired capital is defined as,

$$K_D = \frac{KM_k}{r} \quad [\$] \quad (3.48)$$

$M_k = \text{Marginal product of capital } [$/($ \cdot \text{year})]$

$r = \text{Interest rate}$

which amounts to the current level of capital adjusted for the relative cost and marginal product of capital.

### 3.2.9.2. Energy Production

Energy is produced to meet the demands for the production of goods and services (i.e. economic output). The production of energy is disaggregated into four types: coal, oil and gas, hydro and nuclear power, and renewables. Hydro and nuclear energy sources are combined into a single

energy source because they have similar carriers (i.e. generation of electricity to a grid) and long-term characteristics including diminishing returns to expansion as the best sites are used first, and are subject to political and environmental constraints (Fiddaman 1997).

The capacity of energy production is set by the amount of capital stock that has been accumulated into each energy source and is influenced by production pressures and profit incentives. The rate of variable inputs determines the utilization of production capacity. Limitations on energy production are in the form of depletion and saturation for non-renewable and renewable energy sources. Depletion refers to the use of limited resource stocks (i.e. fossil fuels) thereby increasing effort and cost required to extract the resources. Saturation in this context refers to diminishing returns to energy production effort. For example, the most ideal sites are taken first to implement wind and solar farms or dams for hydropower generation, thereby making it more difficult and/or expensive to implement additional sites. These concepts are illustrated in the causal loop diagram in Figure 3.22.

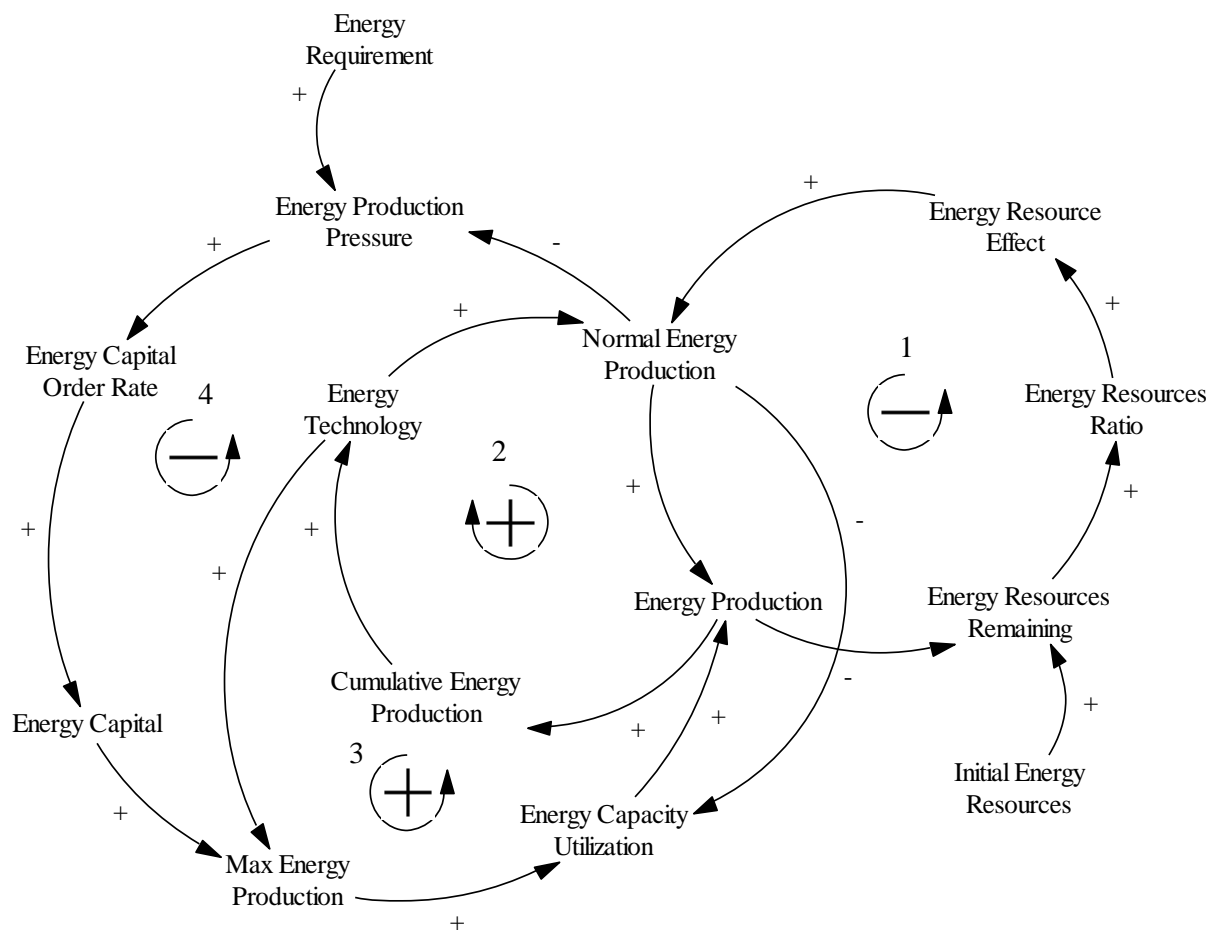


Figure 3.22. Causal loop diagram for the energy production sub-system of the ANEMI3 energy-economy sector.

Feedback loop number 1 illustrates the effect of resource depletion on energy production. As more energy is produced, energy resources begin to deplete. This affects the ratio of energy resources remaining which acts as a reduction factor on energy production, creating a negative feedback loop. The second loop is a positive loop, which illustrates the increasing efficiency of energy production through technological improvements over time, driven by cumulative energy production. The third loop represents the perpetual production of energy to meet demand. As energy is produced resources begin to deplete, causing a reduction in production through the

resource depletion effect. This in turn causes production pressure to meet demand, resulting in further investment in energy capital stocks thereby increasing production again. The fourth loop is a negative feedback loop, which limits the increase in energy production as technological improvements are made thereby boosting energy production and reducing production pressure.

The equation used to represent energy production in the model takes the following form:

$$EP_i = EP_{i,0} \left( \alpha_i \left( \frac{R_i}{R_{i,0}} \right)^{\rho_i} + (1 - \alpha_i) EII_i^{\rho_i} \right)^{\frac{1}{\rho_i}} \quad [GJ/y] \quad (3.49)$$

$EP_i$  = Energy production [GJ/year]

$EII_i$  = Effective input intensity

$EP_{i,0}$  = Initial energy production [GJ/year]

$\alpha_i$  = Resource share

$R_i$  = Resource remaining [GJ]

$\rho_i$  = Resource substitution coefficient

$R_{i,0}$  = Initial resource remaining [GJ]

In this equation,  $i$  is used to denote the energy source under consideration. The resource share provides an upper limit on energy production by representing the minimum time required for resource extraction in the case of non-renewables, and the maximum resource flux in the case of renewables.

$$\alpha_{nonrenewable} = \left( \frac{R_{i,0}}{\tau_r EP_{i,0}} \right)^{\rho_{nonrenewable}} \quad \alpha_{renewable} = \left( \frac{R_{i,0}}{EP_{i,0}} \right)^{\rho_{renewable}} \quad (3.50)$$

Where  $\tau_r$  is the minimum resource depletion time in years. As energy resources are consumed for example in the case of fossil fuels, there is a depletion effect present that acts to decrease energy production unless there is a change in the effective input intensity. The effective input intensity

depends on the level of technology development as well as capital and variable inputs put into production.

$$EII_i = TE_i \left( \frac{KE_i}{KE_{i,0}} \right)^{\beta_{i,kv}} \left( \frac{V_i}{V_{i,0}} \right)^{1-\beta_{i,kv}} \quad (3.51)$$

$TE_i = \text{Energy technology}$

$V = \text{Variable input}$

$KE_i = \text{Energy capital [\$]}$

$V_{i,0} = \text{Initial variable input}$

$KE_{i,0} = \text{Initial energy capital [\$]}$

$\beta_{i,kv} = \text{Capital share}$

The stock and flow diagram for the energy production sector is depicted in Figure 3.23. The production of energy depletes the energy stock over time thereby accumulating into the cumulative energy production. In the case of coal production and oil and gas production, depleted energy resources results in an energy resource effect that reduces the normal energy production rate over time, creating a negative feedback loop on production with a goal of zero in the case of full depletion.

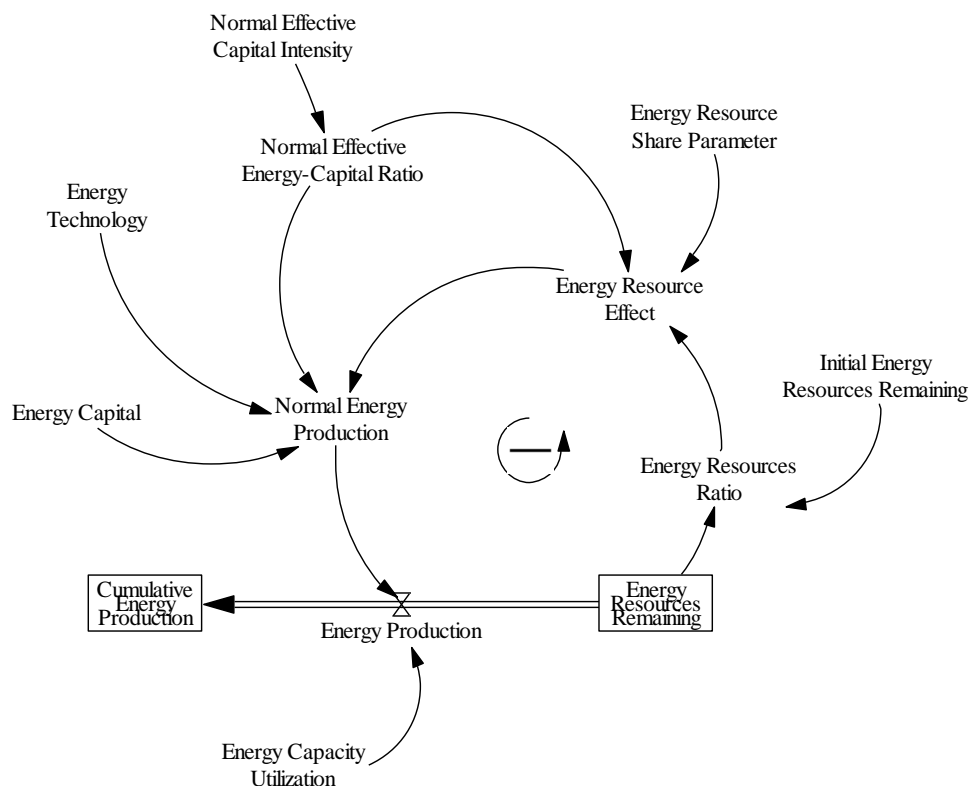


Figure 3.23. Stock and flow diagram for the ANEMI3 energy production sector

### 3.2.9.3. Energy Capital

The capital stocks for the different energy sources are structured in a similar way to that of the goods production capital stock. The main difference is that there is a stock which represents energy capital under construction which after a delay time becomes new energy capital.

There are six feedback loops in total in the energy capital sector (Figure 3.24). The first loop is a negative feedback loop that drives the process of energy capital depreciation which slowly depletes the energy capital stock. The second loop, being a positive feedback loop compensates for depreciation by factoring it into the desired energy capital order thus boosting the energy capital



order rate and energy capital. The third loop moves energy capital from the construction phase to the completion phase. The fourth loop reduces energy orders by taking into consideration capital that is currently under construction when determining the desired energy capital order rate. The fifth loop is a positive feedback loop which increases capital investment based on perceived returns. The sixth loop reduces the effect of perceived returns, thereby limiting the positive effect of the fifth. This is because more energy capital results in reduced the marginal product of capital, thereby reducing the return on energy capital investment. These feedback loops in combination drive the energy production of the ANEMI3 model.

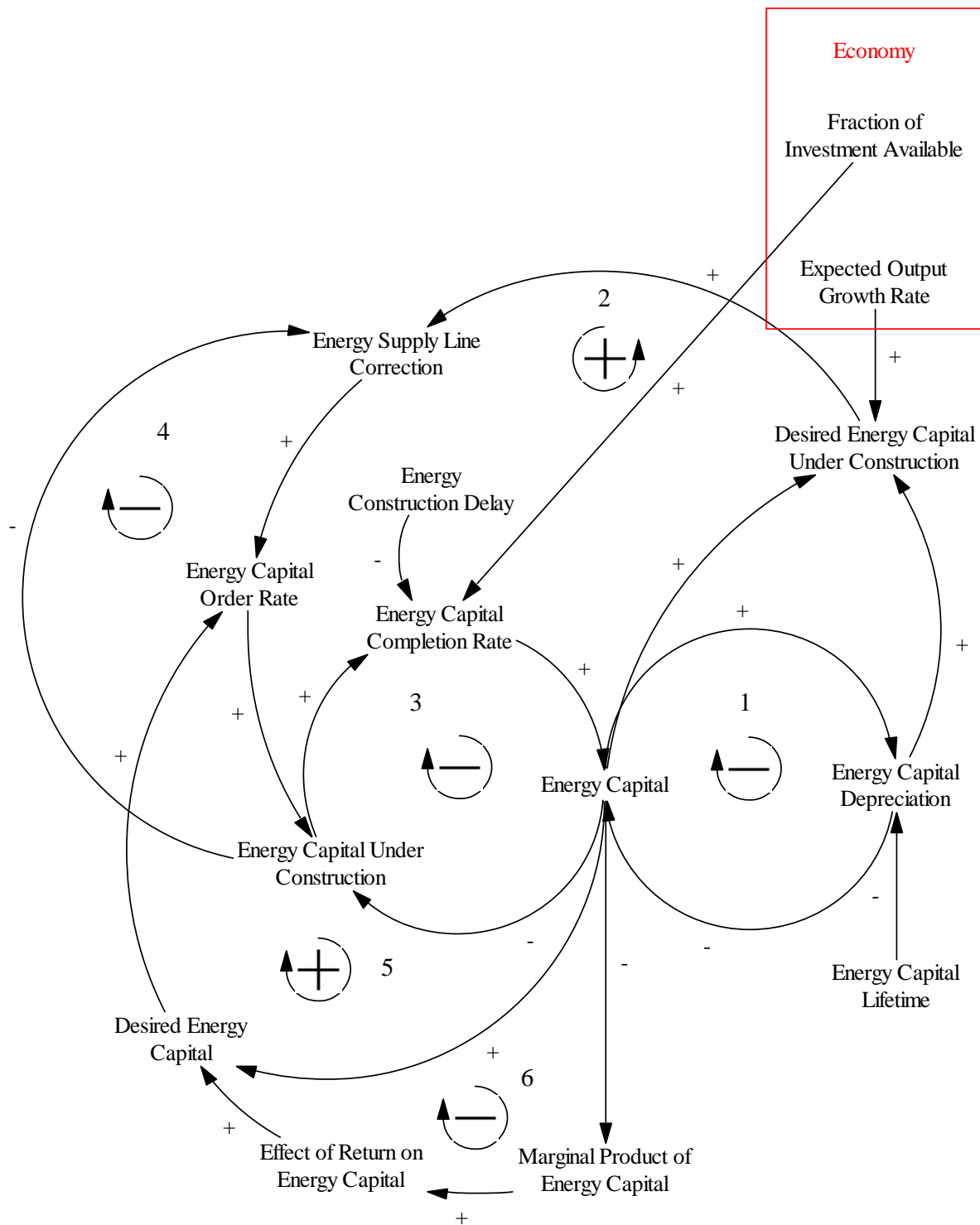


Figure 3.24. Causal loop diagram for the energy capital sub-sector of the energy-economy sector.

The corresponding stock and flow diagram is depicted in Figure 3.25. It illustrates the main feedbacks present in the energy capital sector. There are two stocks which denote energy capital that is either under construction or completed. By dividing the capital stock in this way, a delay is formed from the time that investment in energy supply is made, to when it is completed and contributing to energy production.

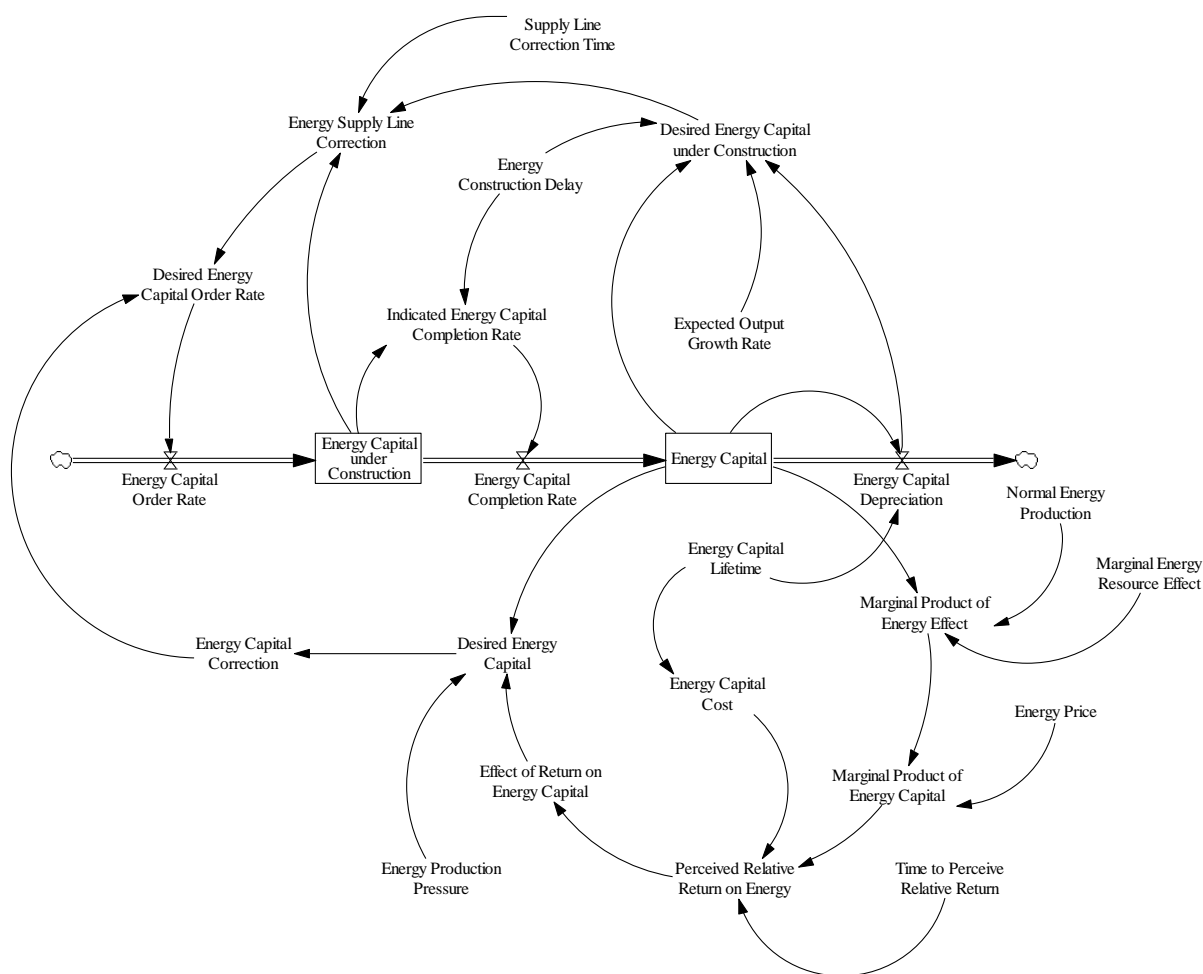


Figure 3.25. Stock and flow diagram of the ANEMI3 energy capital sector

The energy capital stock can be represented mathematically by,

$$KE_i = \int \frac{KC_i}{\tau_c} - \frac{KE_i}{\delta_i} \quad [\$] \quad (3.52)$$

$KE_i =$  Energy capital for energy source  $i$  [\\$]

$KC_i =$  Energy capital under construction for energy source  $i$  [\\$]

$\tau_c =$  Capital construction delay [y]

$\delta_i =$  Energy capital lifetime [y]

$$KC_i = \int EKO_i - \frac{KC_i}{\tau_c} \quad [\$] \quad (3.53)$$

$EKO_i =$  Energy capital order rate [\$/y]

The energy capital order rate prompts the construction of new capital and thereby increases the capacity for energy production. It is formulated in the same way as capital investment for goods production in that it compensates for capital depreciation, adjusts for perceived growth in energy orders, and responds to discrepancies in desired versus current energy capital stock.

$$EKO_i = \delta_i KE_i + \frac{DKC_i - KC_i}{\tau_{kc}} + \frac{DKE_i - KE_i}{\tau_k} + KE_i * GE_i \quad [$/year] \quad (3.54)$$

$DKC_i =$  Desired energy capital under construction [\\$]

$DKE_i =$  Desired energy capital [\\$]

$\tau_{kc} =$  Time to correct capital under construction [y]

$GE_i =$  Perceived growth rate of energy orders

$$DKE_i = \frac{KE_i M_{i,k} EO_i}{r NEP_i} \quad [\$] \quad (3.55)$$

$M_{i,k}$  = Marginal product of energy capital [\$/(\$·y)]

$EO_i$  = Energy order rate [\$/y]

$r$  = Interest rate

$NEP_i$  = Normal energy production [GJ/y]

$$DKC_i = KE_i (\delta_i + GE_i) \tau_{kc} \quad [\$] \quad (3.56)$$

### 3.2.9.4. Energy Requirements

One of the unique features of the FREE model in contrast to other climate-energy-economy models of its kind is the embodiment of energy requirements, or demand, in the capital stock (Fiddaman 1997). This means that when capital is constructed, it has a fixed energy intensity. In the real world, this equates to energy consumption being dependent on products that persist with time. For example, once an electric stove is manufactured its energy efficiency cannot be changed. This contrasts with other models like DICE (Nordhaus 1994) which assume that appliances like an electric stove could be converted to one that uses natural gas. In the FREE model, transitioning between energy sources requires gradual substitution of energy capital due to price changes even if the current allocation of capital is suboptimal.

The feedbacks that are governing the energy requirement subsystem are shown in Figure 3.26. Five main feedback loops govern the behaviour of this subsystem. The first, represents a negative feedback of diminishing energy requirement. The second is a negative feedback loop where an

increase in energy requirements (or demand), results in an increase in price and thus a lower energy requirement install rate. The third loop acts in a similar way as the second, but the energy price is decreased, creating a positive feedback loop on energy requirement. The fourth is a positive feedback loop which shows that an increase in energy requirement causes energy intensity of capital to increase thereby resulting in greater energy requirements.

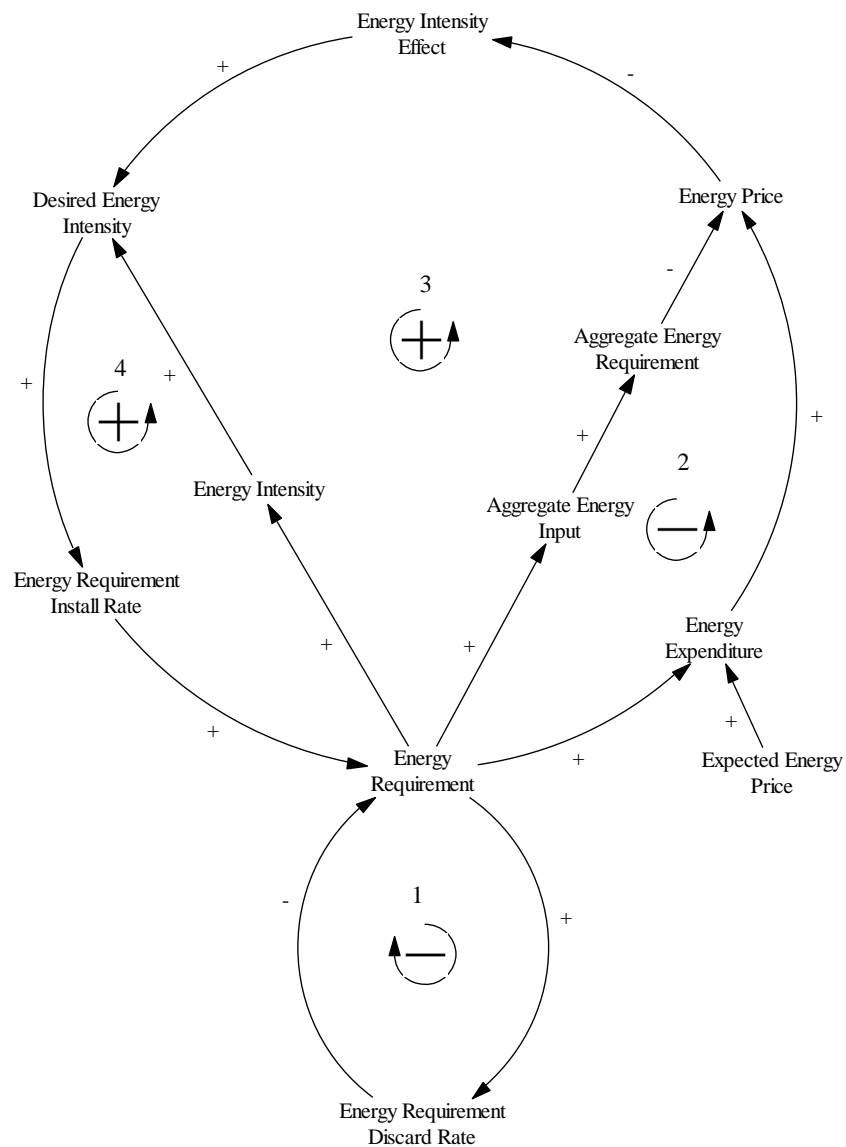


Figure 3.26. Causal loop diagram for energy requirements sub-system in the ANEMI3 energy-economy sector.

The corresponding stock and flow diagram is presented in Figure 3.27.

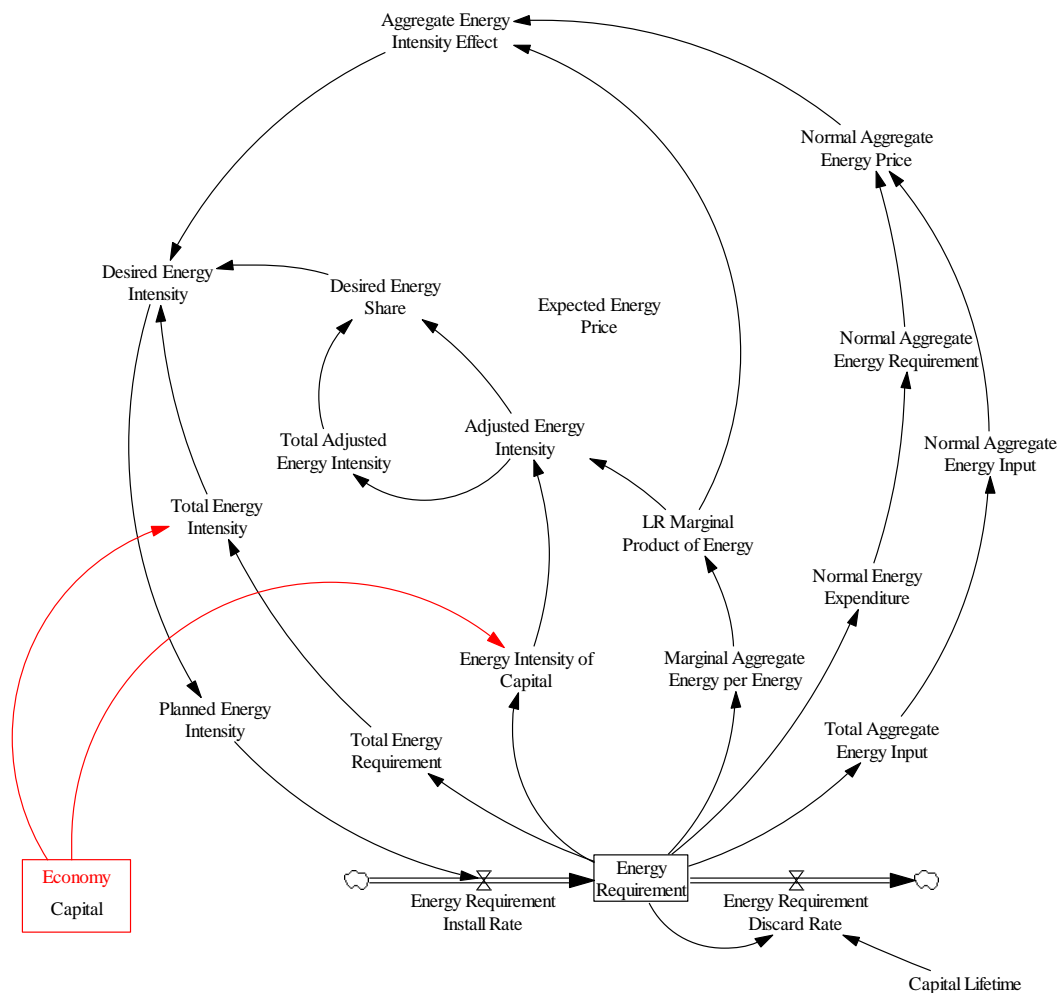


Figure 3.27. Stock and flow diagram of energy requirements sub-system of ANEMI3 energy-economy sector.

Changes in energy requirements are co-flows with capital investment and depreciation of the energy capital stocks, and retrofitting can gradually adjust the energy intensity of existing capital to that of the planned energy intensity of new capital,

$$ER_i = \int (N_i(I + \varepsilon K) - (\delta + \varepsilon)ER_i) \cdot dt \quad [GJ/y] \quad (3.57)$$



$ER_i = \text{Energy requirements for capital corresponding to energy source } i \text{ [GJ/y]}$

$N = \text{Planned energy intensity of new capital corresponding to energy source } i \text{ [GJ/(\$} \cdot \text{y)]}$

$I = \text{Investment rate [$/y]}$

$\varepsilon = \text{Fractional retrofit rate [1/y]}$

$\delta = \text{Fractional discard rate [1/y]}$

Planned energy intensity adjusts to the desired intensity with a delay period. The delay period is meant to represent the time taken to incorporate the desired energy intensity into new products,

$$N_i = \int \frac{ND_i - N_i}{\tau_n} \cdot dt \quad [\text{GJ}/(\$ \cdot \text{y})] \quad (3.58)$$

$ND_i = \text{Desired energy intensity of new capital } i \text{ [GJ}/(\$ \cdot \text{y)]}$

$\tau_n = \text{Energy intensity planning delay [y]}$

The energy intensity is adjusted based on the aggregate energy intensity and the relative shares of individual energy sources. This is done by introducing multipliers for relative price and the marginal product of energy to the current energy intensity,

$$ND_i = N_T \cdot AE \cdot DS_i \quad [\text{GJ}/(\$ \cdot \text{y})] \quad (3.59)$$

$N_T = \text{Total energy intensity of capital [GJ}/(\$ \cdot \text{y)]}$

$AE = \text{Aggregate energy intensity adjustment}$

$DS_i = \text{Desired share for energy source } i$

where,

$$N_T = \frac{\sum_i ER_i}{K} \quad [GJ/(\$ \cdot y)] \quad (3.60)$$

The adjustment to aggregate energy intensity is calculated by comparing the long-run marginal product of the aggregate energy good to that of the perceived aggregate energy price from all sources,

$$AE = \left( \frac{M_T}{P_T} \right)^{\omega \sigma_{ke,lr}} \quad (3.61)$$

$M_T$  = Long-run marginal product of aggregate energy [\$/GJ]

$P_T$  = Normal aggregate energy price for energy source  $i$  [\$/GJ]

$\omega$  = Energy intensity adjustment coefficient

$\sigma_{ke,lr}$  = Long-run capital-energy substitution elasticity

With this formulation, higher marginal product of aggregate energy (more economic output per unit of energy) or lower prices will result in a higher desired energy intensity of new capital. The desired share for energy source,  $i$  is calculated as the share of adjusted energy intensity that energy source  $i$  has compared against the total for all energy sources.

$$DS_i = \frac{AI_i}{\sum_i AI_i} \quad (3.62)$$

$AI_i$  = Adjusted energy intensity of energy source  $i$  [\$/( $y \cdot GJ$ )]

$$AI_i = \frac{ER_i \cdot \left(\frac{M_{i,lr}}{P_i}\right)^{\omega\sigma_{ke,lr}}}{K} \quad [\$/(y \cdot GJ)] \quad (3.63)$$

$M_{i,lr}$  = Long-run marginal product of energy [\$/GJ]

$P_i$  = Perceived energy price [\$/GJ]

If  $\omega$  in Equation 49 and 51 is set to a value of 1, the substitution of energy sources will behave in a similar way to a general equilibrium model. That is, a change to the energy prices will result in immediate changes to the energy intensity of new capital.

### 3.2.9.5. Energy Pricing

Energy pricing varies with the cost of energy producer prices along with distribution costs, total taxes, and depletion rent. The dynamics of the energy pricing sub-system are illustrated by the causal loop diagram shown in Figure 3.28. There are three feedback loops that govern the behaviour of energy pricing in the model. The first feedback loop regulates the energy price. An increase in energy price results in a decrease in the order rate, thereby reducing production pressure and dampens the initial increase. The second is a positive feedback loop, where an increase in producer price is perpetuated by increasing the indicated price, thereby reinforcing the initial increase. The third loop regulates the second by gradually allowing the gap between the current and indicated producer price over time. This sub-system has connections with the energy production sub-system in establishing the level of production pressure as the ratio of energy production (supply) to the energy order rate (demand), as well as the energy capital sub-system in establishing the average energy cost.

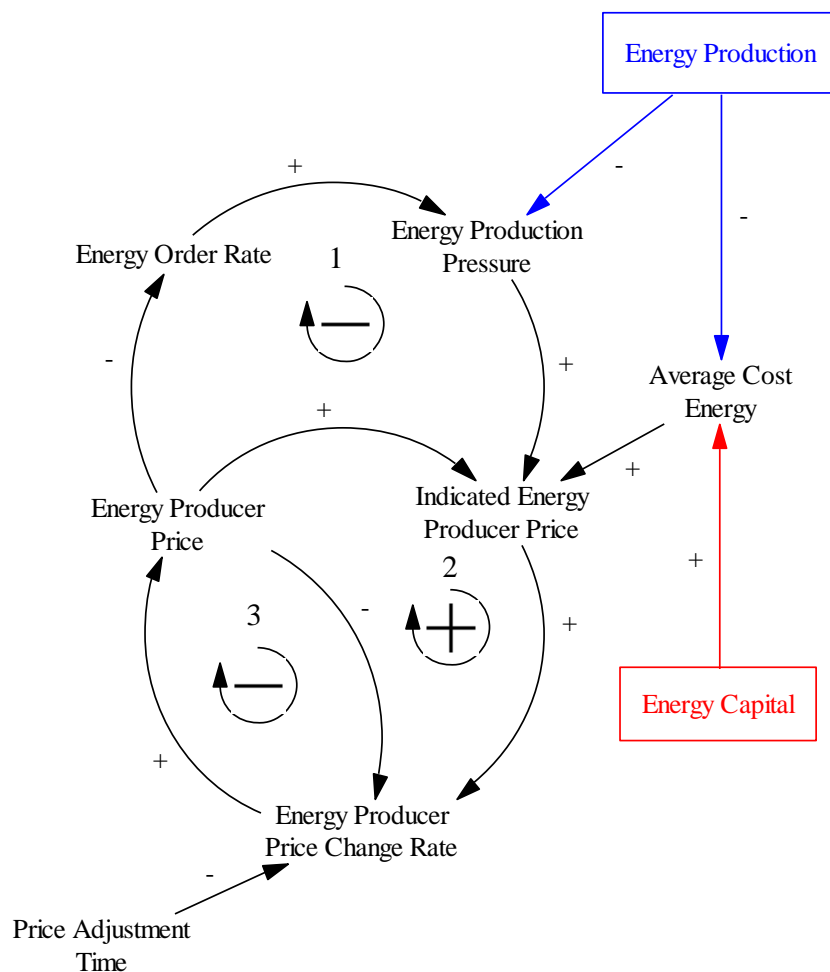


Figure 3.28. Causal loop diagram of ANEMI3 energy pricing sector.

The stock and flow diagram for the energy pricing sub-system is presented in Figure 3.29. From this diagram it is shown that the price acts as a stock or state variable which is changing in response to the indicated price over the price adjustment time. The final energy price is determined by the producer price in addition to distribution costs and total taxes on energy source. This could include the implementation of a carbon tax on fossil fuel production, however this is not considered in this work.

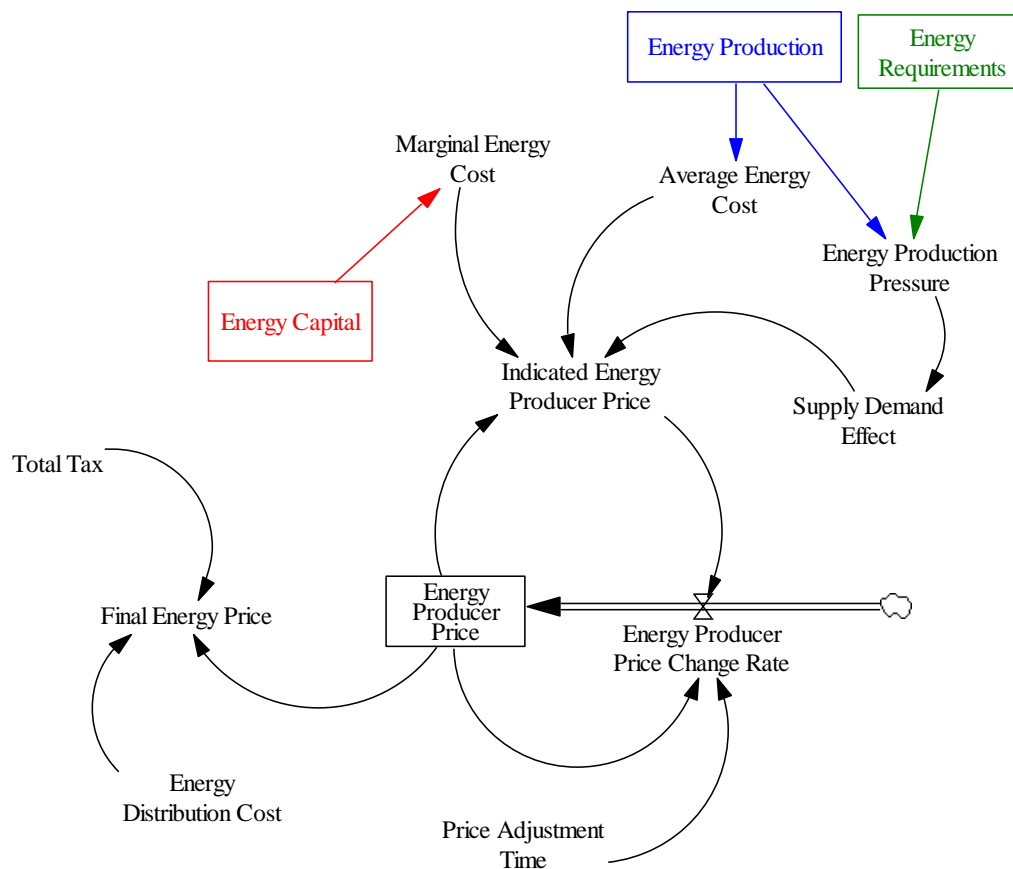


Figure 3.29. Stock and flow diagram for the energy pricing sub-system of the ANEMI3 energy-economy sector.

The energy price can be represented mathematically by,

$$P_i = PP_i + \mu_i + D_i + T_i \quad [$/GJ] \quad (3.64)$$

$P_i = \text{Energy price } [$/GJ]$

$D_i = \text{Distribution cost } [$/GJ]$

$PP_i = \text{Producer price } [$/GJ]$

$T_i = \text{Total taxes } [$/GJ]$

$\mu_i = \text{Depletion rent } [$/GJ]$

$$PP_i = \int \frac{IP_i - PP_i}{\tau_p} \quad [$/GJ] \quad (3.65)$$

$IP_i =$  Indicated producer price [\$/GJ]

$\tau_p =$  Price adjustment time [y]

The producer price is adjusted by its previous value to approach the indicated producer price over an adjustment time,  $\tau_p$ . The indicated producer price changes with the average and marginal costs of energy production as well as with the ratio of energy orders to production. This is where supply and demand of energy are equated to influence the price in place of a market clearing mechanism that would be used in traditional macroeconomic models.

$$IP_i = PP_i \left( \frac{AC_i}{PP_i} \right)^{\gamma_a} \left( \frac{MC_i}{PP_i} \right)^{\gamma_m} \left( \frac{EO_i}{NEP_i} \right)^{\gamma_d} \quad [$/GJ] \quad (3.66)$$

$AC_i =$  Average cost of energy production [\$/GJ]

$\gamma_a =$  Weight to average cost [\$/GJ]

$MC_i =$  Marginal cost of energy production [\$/GJ]

$\gamma_m =$  Weight to marginal cost

$EO_i =$  Energy order rate [GJ/y]

$NEP_i =$  Energy production at normal capacity utilization [GJ/y]

$\gamma_d =$  Weight to demand pressure

### 3.2.9.6. Energy Technology

Technological progression plays a role in the production of energy through the effective input intensity, which acts to increase the production of energy for the same level of inputs. The causal loop diagram illustrates the feedbacks involved that govern the endogenous representation of energy technology in the model (Figure 3.30).

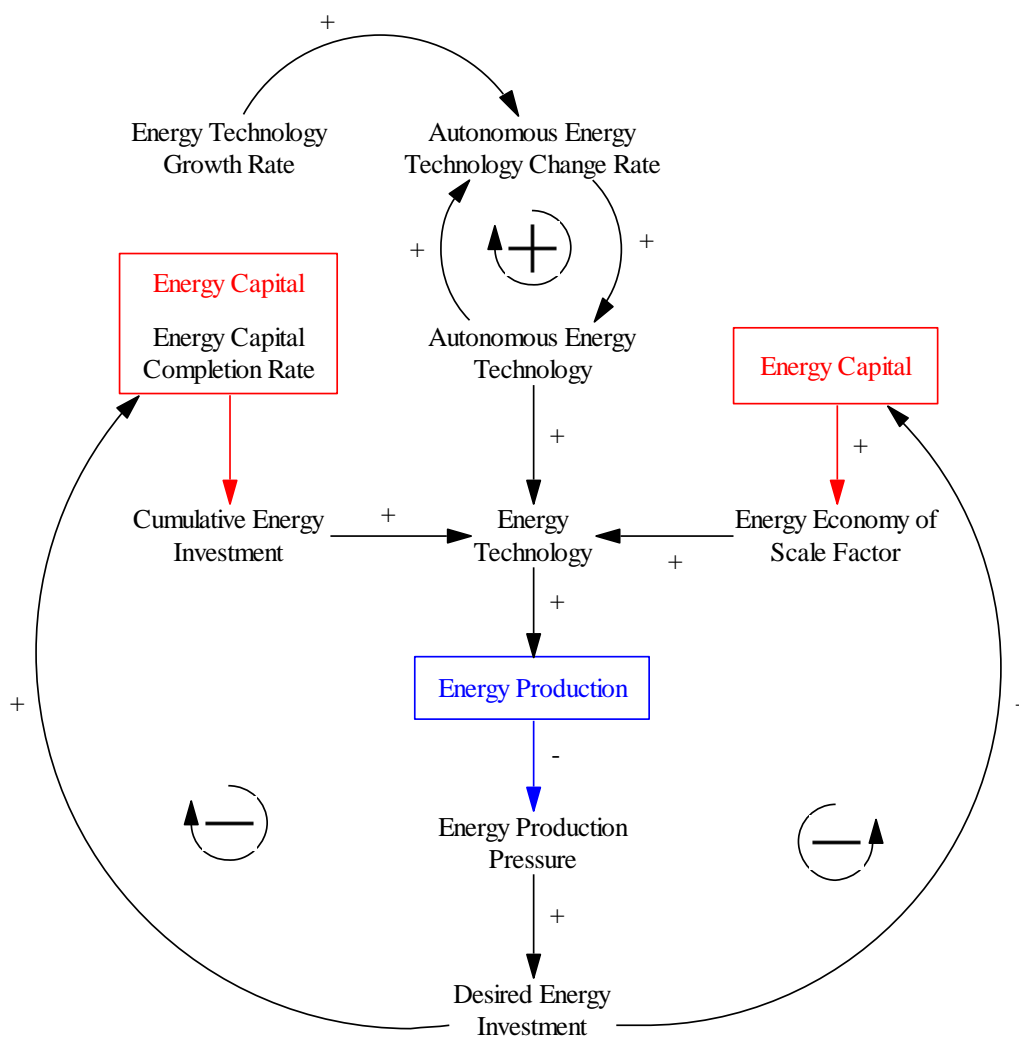


Figure 3.30. Causal loop diagram for the technological change sub-system of the ANEMI3 energy-economy sector.

The positive feedback loop drives technological progress in energy production exogenously over time with the application of a growth rate factor. As energy is produced, the production pressure which considers the ratio of supply to demand, acts to decrease the level of desired investment in new energy capital. This decrease in desired energy investment slows the rate at which the cumulative energy investment grows, thereby slowing down technological advancement in energy production. Economy of scale (the proportionate saving in costs through increased production) is also factored into energy technology. As desired energy investment decreases with increased production, the growth in economy of scale will increase at a slower rate, thereby creating another negative feedback loop on the progression of energy technology.

The corresponding stock and flow diagram illustrates the system structure of the technological change sub-system (Figure 3.31). The level of autonomous energy technology is represented as a stock and grows exogenously based from its initial value and the specified growth rate. This is the only feedback loop that exists directly within this sub-system, while the other come from different sub-systems within the energy-economy sector. The endogenous portion of the energy technology sub-system is represented by incorporating cumulative energy investment stock as an indicator of technological change, as it is assumed that more investment in a given energy source over time will result in faster rates of technological change.



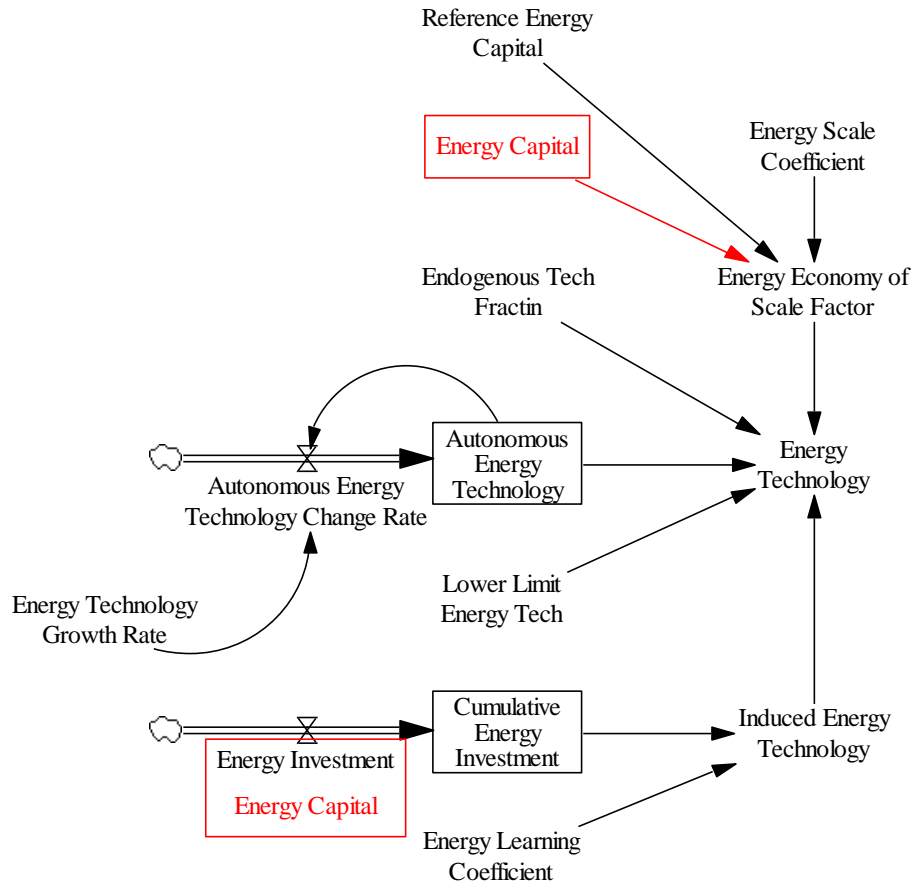


Figure 3.31. Stock and flow diagram of energy technology sub-system within the ANEMI3 energy-economy sector.

Here, technological change is represented by a standard learning curve, that progresses with cumulative investment in energy capital. The functional form is given as,

$$ET_i = \beta_t \ln \left( \frac{C_i}{C_{i,0}} \right) \quad (3.67)$$

$ET_i$  = Endogenous technological change

$\beta_t$  = learning curve coefficient

$C_i$  = Cumulative investment [\$]

$C_{i,0}$  = Initial cumulative investment [\$]

The learning curve function for technological change in energy production is then used to calculate the energy technology level which factors into energy production (Equation 3.49).

$$TE_i = \frac{1}{LL_i + \frac{(1 - LL_i)}{ET_i^v AT_i^{1-v} S_i}} \quad (3.68)$$

$TE_i$  = Energy technology level

$LL_i$  = Lower limit to cost reductions from technology

$ET_i$  = Endogenous learning curve

$AT_i$  = Autonomous technology

$S_i$  = Scale economy effect

$v$  = Fraction of technology endogenous

$$AT_i = e^{\alpha_t t} \quad (3.69)$$

$\alpha_t$  = Fractional autonomous energy technology growth rate

$$S_i = \left( \frac{KE_i}{KE_{i,0}} \right)^{\gamma_s} \quad (3.70)$$

$KE_i$  = Energy capital [\$]

$KE_{i,0}$  = Initial energy capital [\$]

$\gamma_s$  = Scale coefficient

This formulation allows for the energy technology level to increase over time as more capital is invested into energy production.

This sector is a new addition to the ANEMI3 model based on that of Fiddaman (1997). In the previous version of ANEMI, a computable general equilibrium model was used to represent the energy-economy as discussed at the beginning of Section 3.2.9. This modification to the ANEMI model structure allows for research objective 1 from Section 2.6 to be addressed by providing a means to incorporate the water supply development sector into the production structure of the energy-economy model, which is discussed in the following section.

### 3.2.10. Water Supply Development

The new water supply sector in ANEMI3 was developed by incorporating water supply as a new production sector within the newly added energy-economy sector. This has been achieved by adding capital stocks to produce water supply in the form of surface, ground, wastewater reclamation, and desalination water sources. The basic structure of the energy sector, described in the previous section of the document, was adopted as a starting point from which changes were made to accommodate the development of water supply.

The causal loop diagram presented in Figure 3.32 illustrates the dynamics that are governing the behaviour of the water supply development sector. The first feedback loop acts as a negative feedback on water supply capital through depreciation. With regards to water supply, this would represent the cost of maintaining supply infrastructure including pumps, distribution networks, dams and reservoirs, and treatment facilities. The second feedback loop counteracts the first, by

having a positive feedback effect on water supply capital. With more water supply capital there is more depreciation, which in turn increases the water capital order rate (investment in water supply) thus adding more water supply capital. The third feedback loop counteracts water stress by prompting investment in water capital to increase water supplies. The fourth and last feedback incorporates the effects of depletion and saturation into water supply development.

As available water resources become depleted, the water supply is reduced for the same input intensity. This means that more effort is required to produce the same rate of water supply, which also makes a given type of water supply that is depleted more expensive. For example, when the groundwater elevation decreases from over abstraction, more pumping is required to extract the same amount of water resource. The effect of saturation is also included in this relationship, assuming the best or most cost-effective sites are used first for water supply infrastructures. An example of which could include the construction of additional reservoirs, source water intakes, of groundwater wells in areas that are less suitable or cost effective than those that were previously constructed.

The dotted causal link from water price to the capital order rate in Figure 3.32 indicates a connection that is neither positive nor negative. Instead, this link is used to determine the amount of investment that is made in the capital stocks of the different supply types (surface, ground, wastewater reclamation, and desalination water sources). Inputs from the nutrient cycle, hydrologic cycle, and water demand sectors are used to define the water price, water stress, and water resource ratio variables respectively in the water supply development sector.

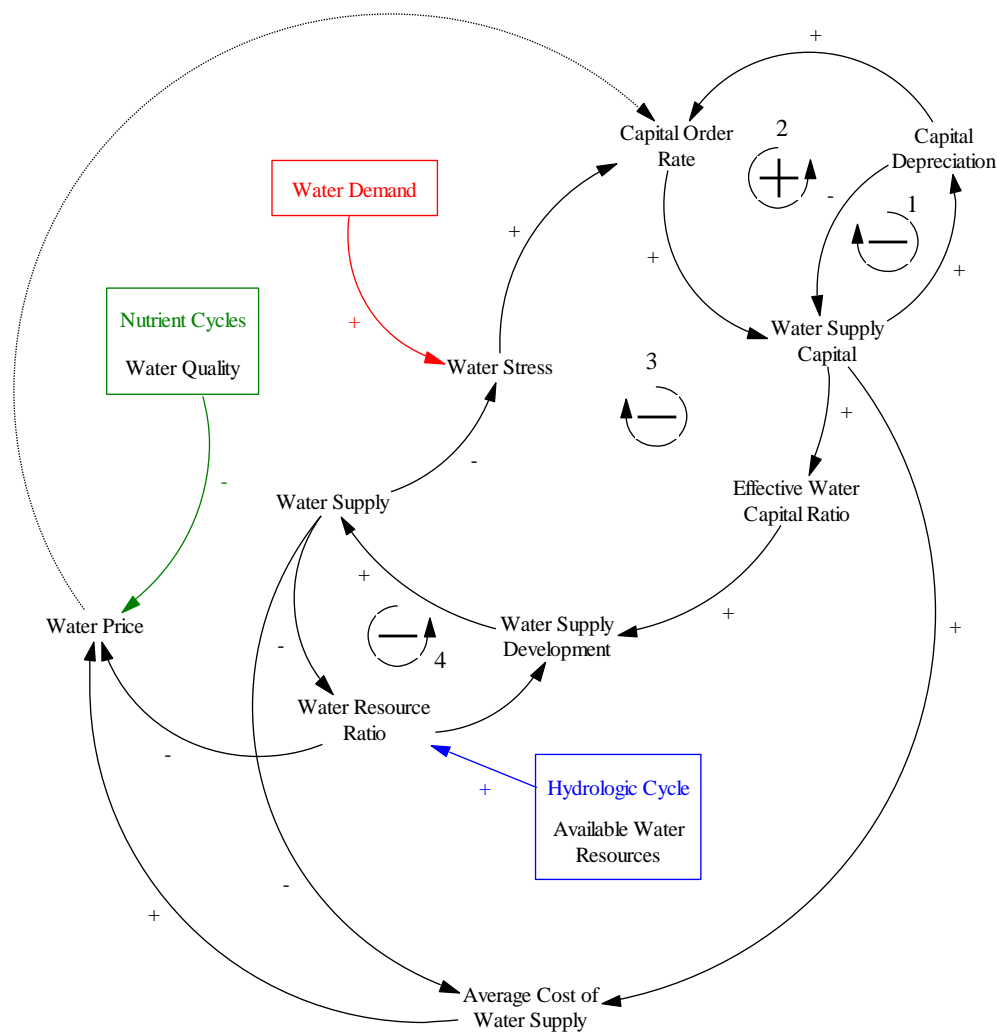


Figure 3.32. Causal loop diagram of the ANEMI3 water supply development sector. The dotted arrow from water price to water supply indicates a causality that is neither positive nor negative.

The stock and flow diagram for the water supply development sector is shown in Figure 3.33. The main stocks in the water supply development sector consist of those for the water supply, water supply price, and water supply capital, both established and under construction. The purpose of having two stocks to represent water supply under construction and currently established is to add

a time delay to the water development of water supplies. The time delay represents a lag in water capital in response to the stimulus of investment, which in this case is the water supply capital order rate. Water supply is represented as a stock, even though this value is a rate, or flow variable that represents the volume of water being supplied by a given source in a year. This was done to mitigate the occurrence of circular references in the model, as the development of water supplies is dependent on the water resource ratio and vice versa. Water supply does not accumulate, only the capital that represents the level of infrastructure associated with water supply. Because of this, an additional unnamed outflow is added which releases the current value of water supply from the water supply stock, preventing any accumulation.

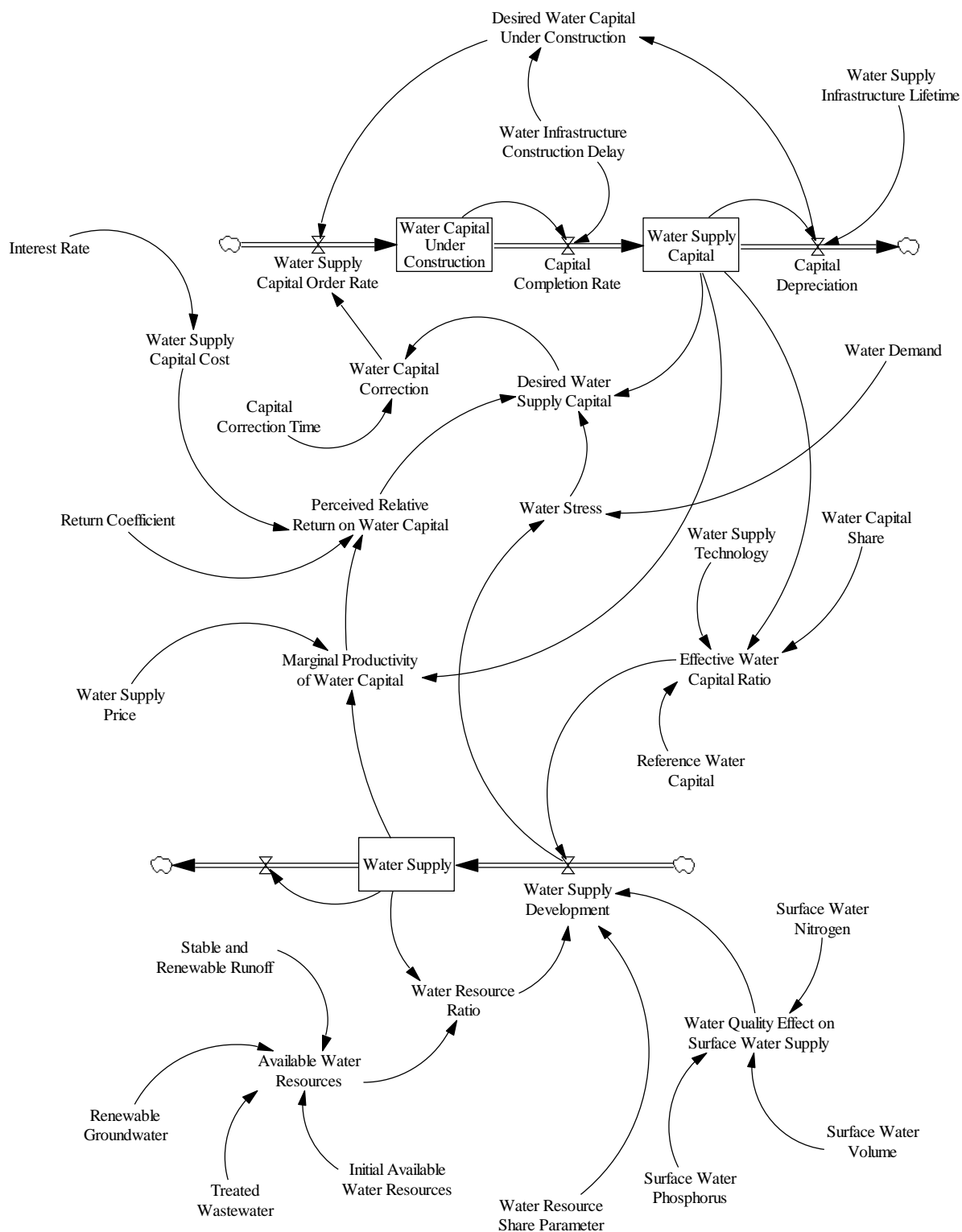


Figure 3.33. Stock and flow diagram of the ANEMI3 water supply development sector.

Water pricing within the water supply development sector is shown in Figure 3.34.

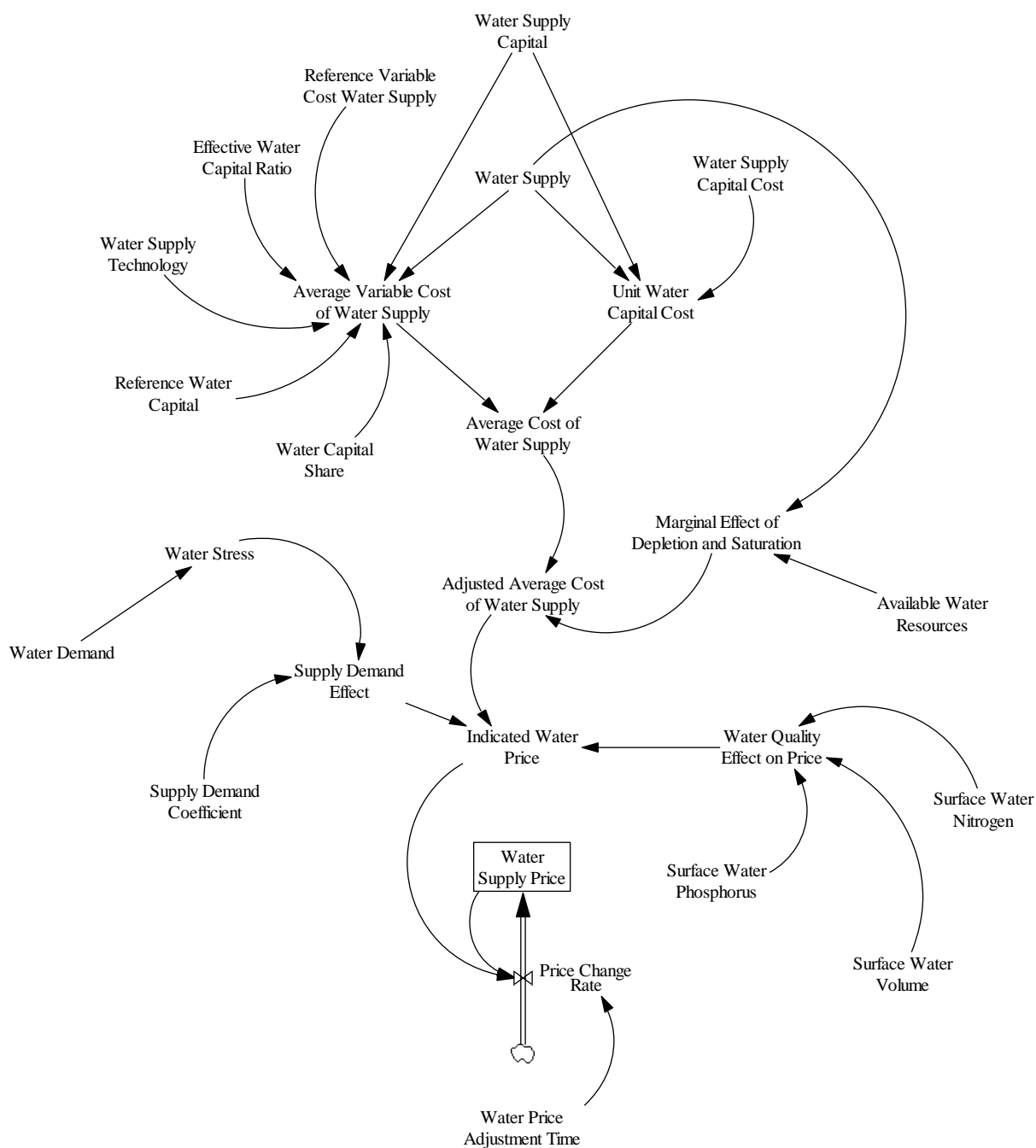


Figure 3.34. Water pricing component of the ANEMI3 water supply development sector.



Water resources,  $R_i$  are used in the production of water supplies, where the subscript  $i$ , denotes the type of water supplies for which the water resources are being used.

$$R_{sw} = S_r * TRF - URW * WPF \quad [km^3/y] \quad (3.71)$$

$$R_{gw} = Q_{perc} - Q_{discharge} \quad [km^3/y] \quad (3.72)$$

$$R_{ww} = TDW + TIW \quad [km^3/y] \quad (3.73)$$

$$R_{ds} = Oceans \quad [km^3] \quad (3.74)$$

$R_{sw}$  = Surface water resources [ $km^3/y$ ]

$R_{gw}$  = Groundwater resources [ $km^3/y$ ]

$R_{ww}$  = Wastewater resources [ $km^3/y$ ]

$R_{ds}$  = Desalination water resources

$S_r$  = Stable and reusable runoff fraction

$TRF$  = Total renewable flow [ $km^3/y$ ]

$WPF$  = Wastewater pollution factor

$Q_{perc}$  = Percolation to groundwater [ $km^3/y$ ]

$Q_{discharge}$  = Groundwater discharge [ $km^3/y$ ]

$TDW$  = Treated domestic wastewater [ $km^3/y$ ]

$TIW$  = Treated industrial wastewater [ $km^3/y$ ]

$URF$  = Untreated Returnable Waters [ $km^3/y$ ]

The amount of water resources available for the development of water supplies is dependent on the hydrologic cycle, water demand, and water quality sectors of the model. In the case of surface water, the stable and reusable portion of runoff is taken from the total renewable streamflow and is adjusted for untreated wastewater discharge. The adjustment for wastewater discharge is based on IHP (2000) which estimates that for every cubic meter of contaminated wastewater discharged into water bodies and streams, makes unsuitable 8-10 cubic meters of fresh water. The difference in groundwater percolation and discharge is used for the consideration of groundwater resources

as this refers to renewable groundwater. Only renewable groundwater resources are considered for the global scale. The inclusion of non-renewable or fossil groundwater resources should be considered at the regional scale. For the potential reuse of wastewater, industrial and domestic wastewaters are considered. Although the reuse of wastewater is highly dependent on the type of wastewater and the use for which it is being treated, it is considered here as a supplementary type of water supply in the case of groundwater and surface water depletion. Water resources used for desalination are considered primarily from the ocean stock in the hydrologic cycle. This results in a virtually limitless supply; however, it is very energy intensive resulting in a high effective input intensity thereby limiting production.

The concept of resource depletion in energy production is also applicable to water supply development. For example, in the case of surface water and groundwater resources, depleted water resources will mean less suitable locations for water extraction and treatment plants. This might mean that source waters could be further from where the water is being used, thus increasing distribution costs. Pumping costs could also be increased by using deeper aquifers or surface water supplies that have a greater difference in elevation from their point of use. Water resource depletion factors into the water supply development process in much the same way as energy production, however there is one key difference. The depletion effect for energy production in Equation 3.49 is based on the ratio of current energy resources remaining to the initial amount. In contrast, water resources are renewable to varying degrees. Therefore, simply taking the ratio of the available water resources to the initial water resources is insufficient. Here, the ratio of available water resources to the current production level is used. In order to accomplish this structure, water

production was changed to a stock variable (Figure 3.33) to avoid creating an indeterminate system (introduction of a new negative feedback by making water production a function of itself).

$$WS_i = \int WS_{i,0} \left( \alpha_{w_i} \left( \frac{WS_i}{AW_i} \right)^{\rho_{w_i}} + (1 - \alpha_{w_i}) EWII_i^{\rho_{w_i}} \right)^{\frac{1}{\rho_{w_i}}} \cdot dt \quad [km^3/y] \quad (3.75)$$

$WS_i$  = Water supply from water resource  $i$  [ $km^3/y$ ]

$WP_{i,0}$  = Initial water production [ $km^3/y$ ]

$AW_i$  = Available water resource remaining [ $km^3/y$ ]

$EWII_i$  = Effective water input intensity

$\alpha_{w_i}$  = Water resource share

$\rho_{w_i}$  = Resource substitution coefficient

In the case of surface water, the available water resources are a rate (runoff minus water quality depletion effects) rather than a stock that can be depleted over time. If production equals this rate, then there is no more surface water that can be utilized at this time step. For wastewater reuse if the rate of reuse is equal to that of the amount of treated wastewater, then no more wastewater can be reused unless wastewater treatment percentage increases.

In the energy capital sub-system of the energy-economy sector, Equation 3.55 is used to define the desired energy capital, which determines the amount of investment to be made in each type of energy source. In this equation, the desired energy capital for each source is determined by the perceived return on investment, and the production pressure defined as the ratio of the energy order rate or demand to energy production for each source.

In the case of water supply, the term for perceived return on investment is removed, thereby making the primary drive for new water supply capital based on production pressure, which resembles the definition of water stress (withdrawal or demand to availability ratio). This value is multiplied by the current water capital stocks to obtain the desired water capital stocks,

$$DKW_i = KW_i \cdot \frac{W_{d_i}}{WS_i} \quad [\$] \quad (3.76)$$

$DKW_i =$  Desired water capital for water source  $i$  [ $km^3$   
/y]

$W_{d_i} =$  Demand for water supply  $i$  [ $km^3$ /y]

$WS_i =$  Water supply from water source  $i$  [ $km^3$ /y]

Where  $i$  denotes the type of water supply for which desired water capital is being determined. In order to obtain the demand for water supply from each source, Wood's algorithm (Wood and Wollenberg 1996) is used to allocate the total water demand (sum of domestic, industrial, and agricultural water demand) to each supplier. The geometric representation of Wood's algorithm is illustrated in Figure 3.35., where each rectangle represents a different supplier (surface, ground, wastewater reclamation, and desalination water supplies). The area of each rectangle represents the capacity for a given supplier to fulfil the demand for a product, while the position and width of each rectangle is based on the "attractiveness" value and "width" parameters respectively. Here, the inverse water supply price is used to represent the attractiveness value, and the area of each rectangle would be the water supply capacity for a given supply type. The total water demand is allocated to each supplier by the black line in Figure 3.35. which moves from right to left until the area to the right of the line fulfils the demand. The area of each rectangle that lies on the right of the black line represents the level of demand satisfied by each supplier, therefore a water supply

type with a high price would be placed farther to the left on the attractiveness scale, and would receive less of the total water demand.

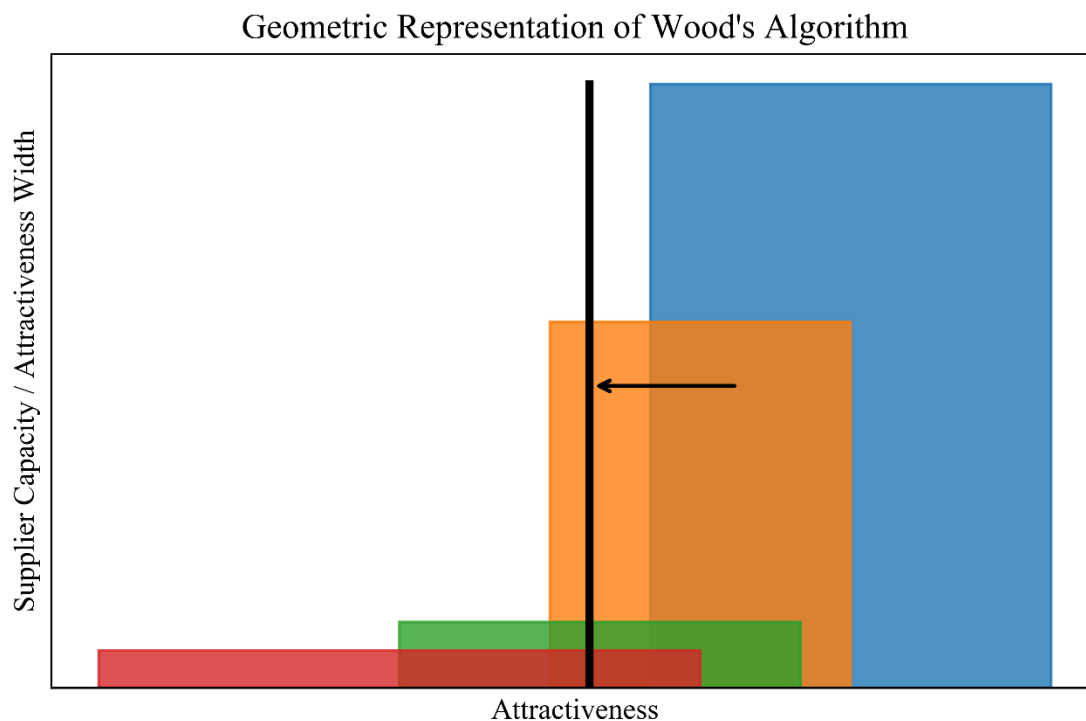


Figure 3.35. Illustration of Wood's algorithm.

The inverse water supply price was chosen as the main driver for changes in supplier attractiveness as this will vary with technological improvements, depletion, saturation, and water quality in the case of surface water supply. This formulation encapsulates the effects of global changes in technology, water resource availability, and water quality on the allocation of capital investments in different types of water supply. The width factor determines how this allocation is distributed to suppliers which are not necessarily the cheapest option. For example, on the global scale, although the use of surface water supplies is likely the most cost-effective option in many regions, groundwater, water reuse, and desalination supplies are all being used simultaneously. For

example in areas where surface and groundwater supplies are scarce, desalination is a much more feasible option (Gao et al. 2017). Estimation of the width parameter is discussed in Section 3.3.

The concept of endogenous technological change applied to energy production has analogies to water supply development. In the case of surface water and groundwater supplies, it is assumed that pumping, distribution and treatment technologies will remain largely the same but will show some improvement over time. However, alternative water supplies such as wastewater reuse and desalination are likely to see vast improvements in the near future as mentioned in Chapter 2 of the thesis. Factoring technological change into the water supply development process is what will help make alternative water supplies more feasible in the future, along with depletion and saturation of conventional water supplies. The dynamics and structure for the implementation of technological change in water supply development is the same as that of energy technology in Section 3.2.9.6, however different parameters are used for desalination and water reclamation technologies and are discussed in Section 3.3.

A unique attribute of water resources when considering water supply development is water quality. Degraded water quality can impact the functioning of water treatment facilities as well as maintenance costs and the necessary configuration of unit processes (Schwartz et al. 2000; Eikebrokk et al. 2004; Cisneros et al. 2014). This may also influence the ability to secure adequate source waters for extraction of water resources in the future as a result of pollution and climate change (Ritson et al. 2014). This could negatively impact production of conventional water

supplies by increasing the cost of implementing new capital as well as variable inputs needed for treatment and distribution including energy, chemicals, and labor.

In ANEMI3, nutrient concentrations in surface waters are used as an indicator of water quality on a global scale. Wastewater and agricultural inputs are used as the main contributors to water quality degradation, and changes in the levels of nutrients in the form of total nitrogen and phosphorus are used as indicators of water quality from the nutrient cycle sector of the model. The ratio of current to initial nutrient concentrations for surface water resources is used as a multiplier on the water supply price,

$$P_{w_{sw}} = PP_{w_{sw}} \cdot \left( \frac{NCE}{NCE_0} \right)^{\gamma_w} \quad [$/km^3] \quad (3.77)$$

$P_{w_{sw}}$  = Water supply price for surface water [\$/km<sup>3</sup>]

$PP_{w_{sw}}$  = Producer price for surface water [\$/km<sup>3</sup>]

$NCE$  = Nutrient concentration effect [(nN · nP)/(km<sup>3</sup>/y)<sup>2</sup>]

$NCE_0$  = Initial nutrient concentration effect [(nN · nP)/(km<sup>3</sup>/y)<sup>2</sup>]

$\gamma_w$  = Influence of water quality on surface water supply price

Where the nutrient concentration effect takes into consideration the concentration of both total nitrogen and phosphorus,

$$NCE = \frac{N_{N_{River}} \cdot N_{P_{River}}}{SF^2} \quad [(nN \cdot nP)/(km^3/y)^2] \quad (3.78)$$

$N_{N_{River}}$  = Nitrogen content of river stock [nN]

$N_{P_{River}}$  = Phosphorus content of river stock [nP]

$$SF = \text{Streamflow [km}^3/\text{y]}$$

In order to include water supply development as an additional component within the energy-economy sector, key connections needed to be made with the energy-economy sector of the model. Those connections are detailed below and relate to variables mentioned in Section 3.2.9. Establishing these connections effectively closes several feedback loops for water supply development to fit into this sector. Water supply development is treated as an additional horizontal disaggregation of the global capital stock alongside the energy sector (Figure 3.36).

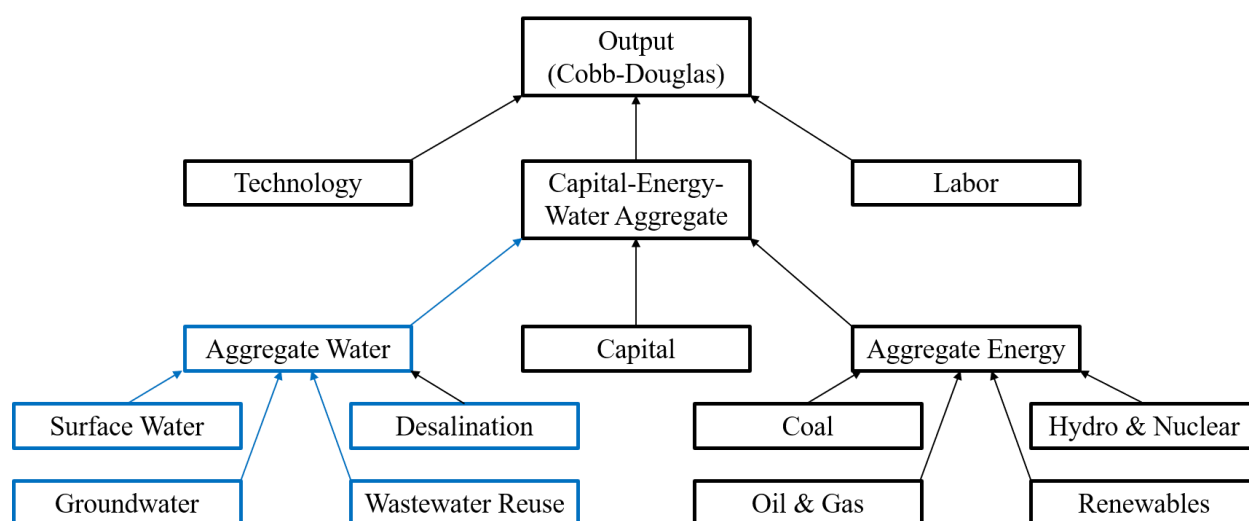


Figure 3.36. Production structure of water supply within the energy-economy-water sector of the ANEMI3.

To accomplish this production structure, water production, capital, technological change, and pricing structures were replicated from that of the energy economy sector. Capital stocks were created to represent water supply infrastructures for surface water, groundwater, wastewater reuse,



and desalination. The level of capital for each source refers to any infrastructure that relates to the global capacity of the system to provide water supply. This includes reservoirs, pumping systems, treatment systems, and distribution networks. Economic output in the energy-economy sector is distributed amongst energy and water production, investment, and consumption. The inclusion of water supply development adds an additional consumer of economic output (Figure 3.37).

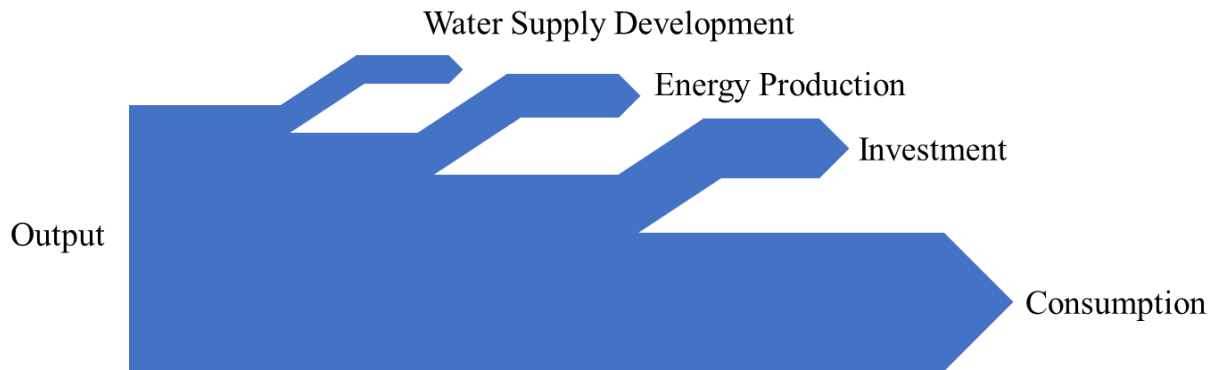


Figure 3.37. Goods allocation in the energy-water-economy sector of the ANEMI3.

The operating capital,  $KO$  signifies the portion of the global capital stock,  $K$  that is used for generating economic output or the production of goods and services in the economic sector. It is represented by the following equation:

$$KO = KO_0 * U * \left( \frac{Aggr_{norm}}{Aggr_{ref}} \right) \quad [\$] \quad (3.79)$$

$U = Utilization$

$Aggr_{norm} = Output\ of\ capital-energy-water\ aggregate\ good\ at\ normal\ capacity\ utilization\ [\$]$

$Aggr_{ref} = Reference\ output\ of\ capital-energy-water\ aggregate\ good\ [\$]$

Utilization refers to the degree to which installed production capacity is being used, or the level of current production versus potential maximum production with full utilization of capital. This was initially only a function of energy production and needed water supply development to be included. To do this, an average is taken between the utilization of energy and water production capacities,

$$U = \frac{1}{2} * (EOC^{\frac{1}{\varepsilon_e}} + WOC^{\frac{1}{\varepsilon_w}}) \quad (3.80)$$

*EOC = Energy operating coefficient*

*WOC = Water operating coefficient*

$\varepsilon_e$  = Energy elasticity coefficient

$\varepsilon_w$  = Water elasticity coefficient

The output of the capital-energy-water aggregate good at normal capacity utilization,  $Aggr_{norm}$  also needed to be modified to include the contribution water supply development to changes in output. This modification is included as the final term in the following equation,

$$Aggr_{norm} = Aggr_{ref} * \left( \alpha_k \left( \frac{K}{K_0} \right)^\gamma + \alpha_e \left( \frac{E_{demand}}{E_{production}} \right)^\gamma + \alpha_w \left( \frac{W_{demand}}{W_{supply}} \right)^\gamma \right)^{\frac{1}{\gamma}} \quad [\$] \quad (3.81)$$

$Aggr_{norm}$  = Normal capital-energy-water aggregate [\$]

$Aggr_{ref}$  = Reference capital-energy-water aggregate [\$]

$\alpha_k$  = Capital share parameter

$\alpha_e$  = Energy share parameter

$\alpha_w$  = Water share parameter

$\gamma$  = Capital-energy-water substitution coefficient

The water supply development sector is an entirely new addition to the ANEMI model and is the main contribution of this thesis. The previous version of ANEMI did not include any distinction between available water resources and water supply for surface and groundwater resources and had no economic component to the development of alternative water resources. In ANEMI3, the addition of the water supply development sector allows for the representation of water supply development from an economic perspective, including both conventional and alternative water supplies. This addition to the ANEMI model addresses research objective 1, 2, and 4 from Section 2.6.

### 3.2.11. Nutrient Cycles

The biogeochemical cycle describes the movement of chemical compounds which drive the biological and geological processes that shape the face of the Earth. These compounds move from various reservoirs including vegetation, soils, rivers and lakes, coastal waters and oceans, and the atmosphere. The processes that drive the movement of these compounds are extremely diverse and occur across widely varied scales of time and space. For example, uplift of the Earth's crust occurs over millions of years, while the delivery of Nitrogen compounds from atmosphere to land through lightning strikes can occur in seconds. Some of the most important cycles to consider on a global scale are those associated with Nitrogen (N), and Phosphorous (P). These are some of the main elements that make up living matter, and are inextricably linked through the biological processes of respiration and decay (Mackenzie 1999). It is not a coincidence that their cycles are also closely tied to human activities and play a vital role for life on Earth in general.

The cycle of N is important to global change research as it has been identified to be an important rate-limiting element with respect to the biological uptake of CO<sub>2</sub> for land and ocean vegetation, helping to 'balance the budget' of carbon through what is known as the 'fertilization effect' (den Elzen et al. 1997). Most of the processes included in the nitrogen cycle mirror those of the carbon cycle (although the chemical reactions are different). However there are a few key differences: the land and ocean plants and organisms also fixate nitrogen from the air in addition to biological uptake; and rain and lightning are important processes for delivering nitrogen from the atmosphere to the Earth's surface and oceans. Additionally, it should be noted that most of the nitrogen is stored in the air and atmosphere in contrast to the carbon where most of it is stored in the ocean.

Phosphorous compounds act as essential nutrients that supports plant life around the globe. The Phosphorous cycle also follows that of the carbon cycle in that the sources and transport processes are similar. The main difference arises in the fact that the primary mechanism associated with the transport of Phosphorous compounds occurs through the attachment to sediments which are transported as runoff or in aerosol form. This is partly why the cycle of Phosphorous does not typically include an atmospheric component. Phosphorous rarely exists in a gaseous state unlike nitrogen and carbon but can temporarily form as an aerosol which is deposited relatively quickly. Phosphorous also acts as a rate limiting factor for the biological uptake of carbon and nitrogen especially for photosynthesizing marine organisms (den Elzen et al. 1997).

Humans are now having a profound influence on the major nutrient cycles of N, and P with increasing development and industrialization. In many cases N, and P are extracted, consumed,

and discharged as waste. This has caused an increase in the amount of these compounds in certain reservoirs, thereby accelerating the flow to others. In addition, many of the processes mentioned previously have been bypassed, thus affecting the timing of the cycles themselves. Examples include increasing fertilizer application and soil erosion rates via intensified agriculture, discharging wastewater to streams, and mining P ore for use on land. These human activities have the potential to destabilize the nutrient cycles in ways that have not been seen previously. As a result we are now able to detect impacts such as climate change, loss of aquatic biodiversity as a result of poor water quality and limited water quantity (Schuster-Wallace et al. 2008), and acid deposition due to the oxidation of sulfur and nitrogen gases in the atmosphere increasing the pH of rainwater (Mackenzie 1999). The extent of these impacts is largely unknown today and even more unknown in the future. However, their potential to impact various aspects of the Earth system, such as population, economy, water quality, land cover, food production, and climate are likely.

The structure of the N and P nutrient cycle model of Mackenzie et al. (1993) that captures the natural processes that move these elements through their respective cycles at various timescales, is used as the basis for the development of nutrient cycles in the ANEMI3 (Breach and Simonovic 2018). This part of the model is based on the assumption of an initial quasi-steady state condition from which the model is to be perturbed to account for human influence on the element cycles. The stock and flow diagrams for the nutrient cycles of N and P are shown in Figure 3.38 and Figure 3.39 respectively.

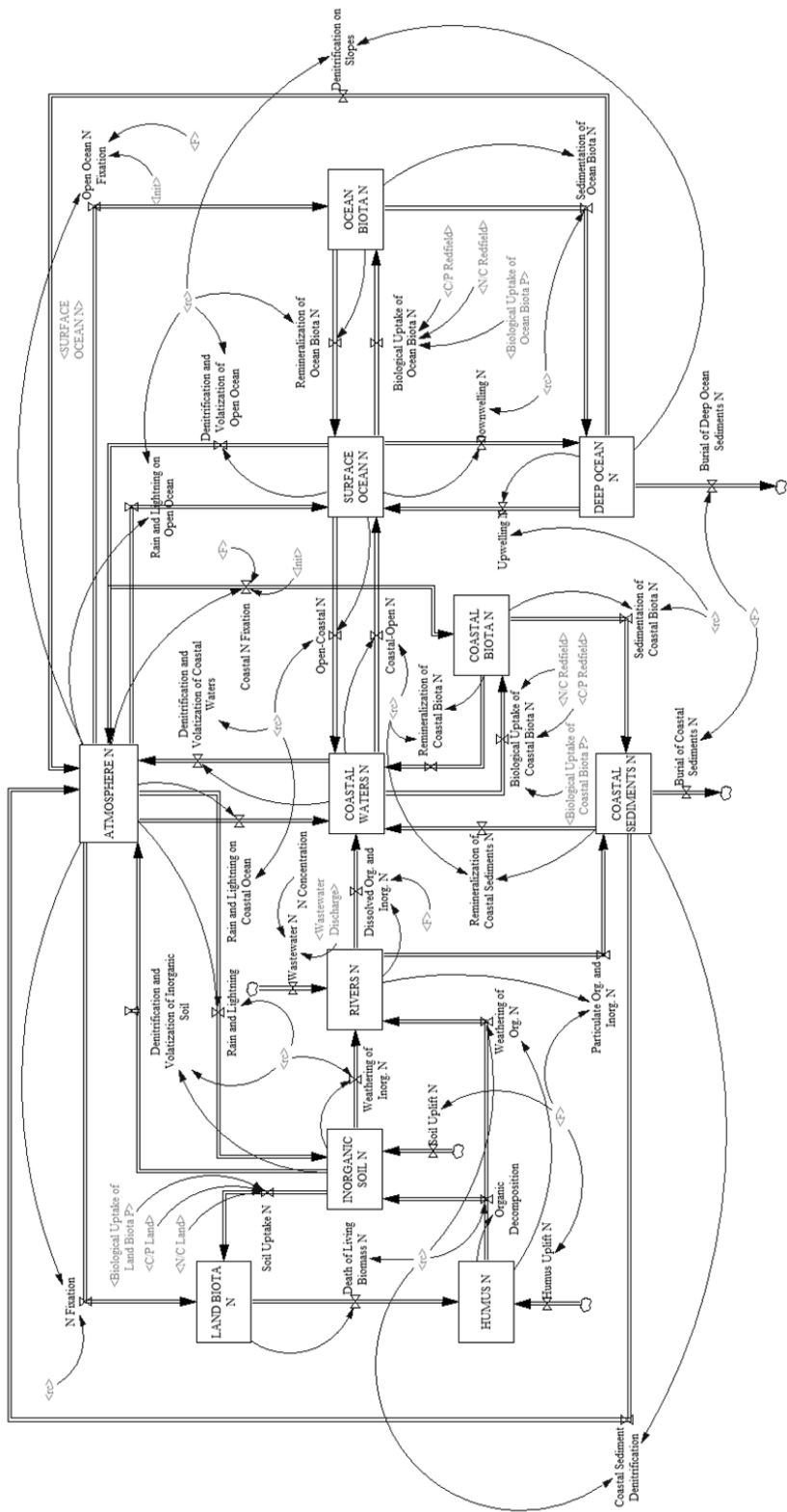


Figure 3.38. Stock and flow diagram of the ANEMI3 nitrogen cycle.

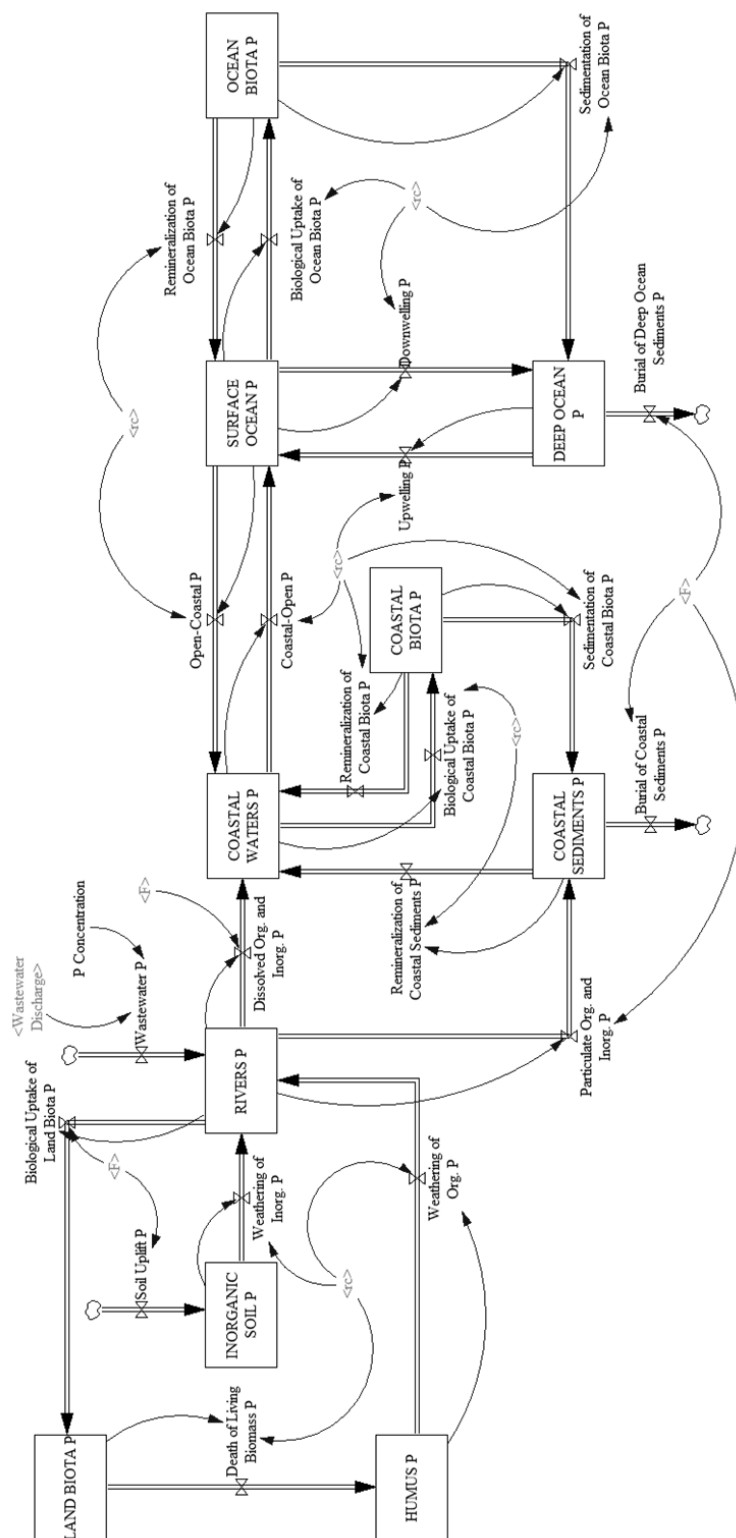


Figure 3.39. Stock and flow diagram of the ANEMI3 phosphorus cycle.

Each flow in the model is represented as a negative feedback with a first-order material delay and an implicit goal of zero. The mathematical representation of the nutrient cycles is given as,

$$N_i = \int (k_{ijN} \cdot N_i + F_{ijN}) \cdot dt \quad [nN] \quad (3.82)$$

$$P_i = \int (k_{ijP} \cdot P_i + F_{ijP}) \cdot dt \quad [nP] \quad (3.83)$$

*i* = Index for originating nutrient reservoir

*j* = Index for receiving nutrient reservoir

$k_{ijN}$  = Rate constant matrix for N flows from nutrient reservoir *i* to *j* [1/y]

$k_{ijP}$  = Rate constant matrix for P flows from nutrient reservoir *i* to *j* [1/y]

$N_i$  = Nitrogen reservoir *i* [nN]

$P_i$  = Phosphorus reservoir *i* [nP]

$F_{ijN}$  = Constant nitrogen flow from reservoir *i* to *j* [nN/y]

$F_{ijP}$  = Constant phosphorus flow from reservoir *i* to *j* [nP/y]

As each stock is drained it will be transferred to another in a continuous chain of higher order delays. Because the represents a continuous cycle of negative feedbacks, it will attempt to reach an equilibrium under natural conditions. Anthropogenic influences on this system in the form of wastewater discharge to the N and P river stocks affects this equilibrium and drives global change in the nutrient cycles. Due to the presence of higher order delays, the system is also likely to be susceptible to large fluctuations and oscillations when perturbed. Initial values for the stocks to create the initial steady state condition in the model and rate constants (or decay fractions) describing the flow of a particular element from one stock to another. The inverse of the rate constant is the time constant, which represents the time associated with the first-order delay for one mole of a particular element to travel from a particular stock. The initial values for the nutrient reservoirs as well as rate constants and constant flows are given in Appendix B.



The input of N and P in the nutrient cycles from wastewater is calculated for domestic and industrial wastewaters as well as agricultural returnable waters. For domestic and industrial wastewaters, the nutrient input is calculated based on the amount of untreated wastewater adjusting for wastewater reuse, as well as treated wastewater with exogenous removal efficiencies applied,

$$NE_{N_{dom}} = \left( DW_{untreated} - W_{ww_{dom}} + DW_{treated} \cdot (1 - N_{removal_{eff}}) \right) \cdot N_{conc_{dom}} [nN/y] \quad (3.84)$$

$$NE_{P_{dom}} = \left( DW_{untreated} - W_{ww_{dom}} + DW_{treated} \cdot (1 - P_{removal_{eff}}) \right) \cdot P_{conc_{dom}} [nP/y] \quad (3.85)$$

$$NE_{N_{ind}} = \left( IW_{untreated} - W_{ww_{ind}} + IW_{treated} \cdot (1 - N_{removal_{eff}}) \right) \cdot N_{conc_{ind}} [nN/y] \quad (3.86)$$

$$NE_{P_{ind}} = \left( IW_{untreated} - W_{ww_{ind}} + IW_{treated} \cdot (1 - P_{removal_{eff}}) \right) \cdot P_{conc_{ind}} [nP/y] \quad (3.87)$$

*NE* = Nutrient emission

*DW* = Domestic wastewater [ $km^3/y$ ]

*IW* = Industrial wastewater [ $km^3/y$ ]

*W<sub>ww</sub>* = Wastewater reuse from water production sector [ $km^3/y$ ]

*N<sub>removal<sub>eff</sub></sub>* = Exogenous N removal efficiency

*P<sub>removal<sub>eff</sub></sub>* = Exogenous P removal efficiency

*N<sub>conc</sub>* = Concentration of N in wastewater [ $nN/km^3$ ]

*P<sub>conc</sub>* = Concentration of P in wastewater [ $nP/km^3$ ]

Agricultural nutrient inputs to surface water are based on the net amount of arable land that is used for food production. This is paired with nutrient leaching factors that are used to determine the amount of nutrients that reach surface waters,

$$NE_{N_{agr}} = A_l \cdot N_{leaching} \quad [nN/year] \quad (3.88)$$

$$NE_{P_{agr}} = A_l \cdot P_{leaching} \quad [nP/year] \quad (3.89)$$

$A_l$  = Net arable land [ha]

$N_{leaching}$  = Leaching factor for N from net arable land [nN/y]

$P_{leaching}$  = Leaching factor for P from net arable land [nP/y]

The input of nutrients to surface waters in the nutrient cycle is based only on the excess amount from the initial nutrient inputs. This is because the nutrient cycle sub-system is assumed to start at a quasi-steady state solution. The parameter values used in calculation nutrient inputs to the nutrient cycles are given below in Table 3.8.

Table 3.8. Parameters used nutrient inputs to nutrient cycles.

Parameter	Value	Units	Source
Nitrogen concentration of domestic wastewater	60	g/L	Henze and Comeau (2008)
Nitrogen concentration of industrial wastewater	60	g/L	
Phosphorus concentration of domestic wastewater	15	g/L	
Phosphorus concentration of industrial wastewater	15	g/L	
Nitrogen leaching coefficient of agricultural runoff	18.65	kg/ha/year	FAO (2019a)
Phosphorus leaching coefficient of agricultural runoff	0.415	kg/ha/year	

The nutrient cycles sector is an entirely new addition to the ANEMI model. In the previous version, water quality was represented only by the subtracting wastewater and agricultural runoff from the available water resources with a dilution factor applied. In ANEMI3, the nutrient concentration of surface waters provides an indicator of water quality that is used to influence the development of surface water supplies as discussed in Section 3.2.10. This addition to the model is used to address research objective number 4 and 5b from Section 2.6.

### 3.2.12. Persistent Pollution

An additional sector to represent the level of persistent pollution in the Earth system was added in ANEMI3. This sector is used to describe the generation and assimilation of pollutants over time that may be harmful to the global biosphere (Thissen and De Mol 1978). It is based on the persistent pollution sector of the WORLD3 model and is used to form an additional negative feedback on population growth (Meadows et al. 1974). The main drivers for the generation of persistent pollution are industrial and agricultural activity, while the current population and economic output are used to scale these effects in global system. Technological change acts as a reduction factor for the levels of persistent pollution generation from these activities, while natural rate of assimilation represents the environmental capacity to cope with and break down these pollutants over time. The causal structure of the persistent pollution sector is shown in Figure 3.40.

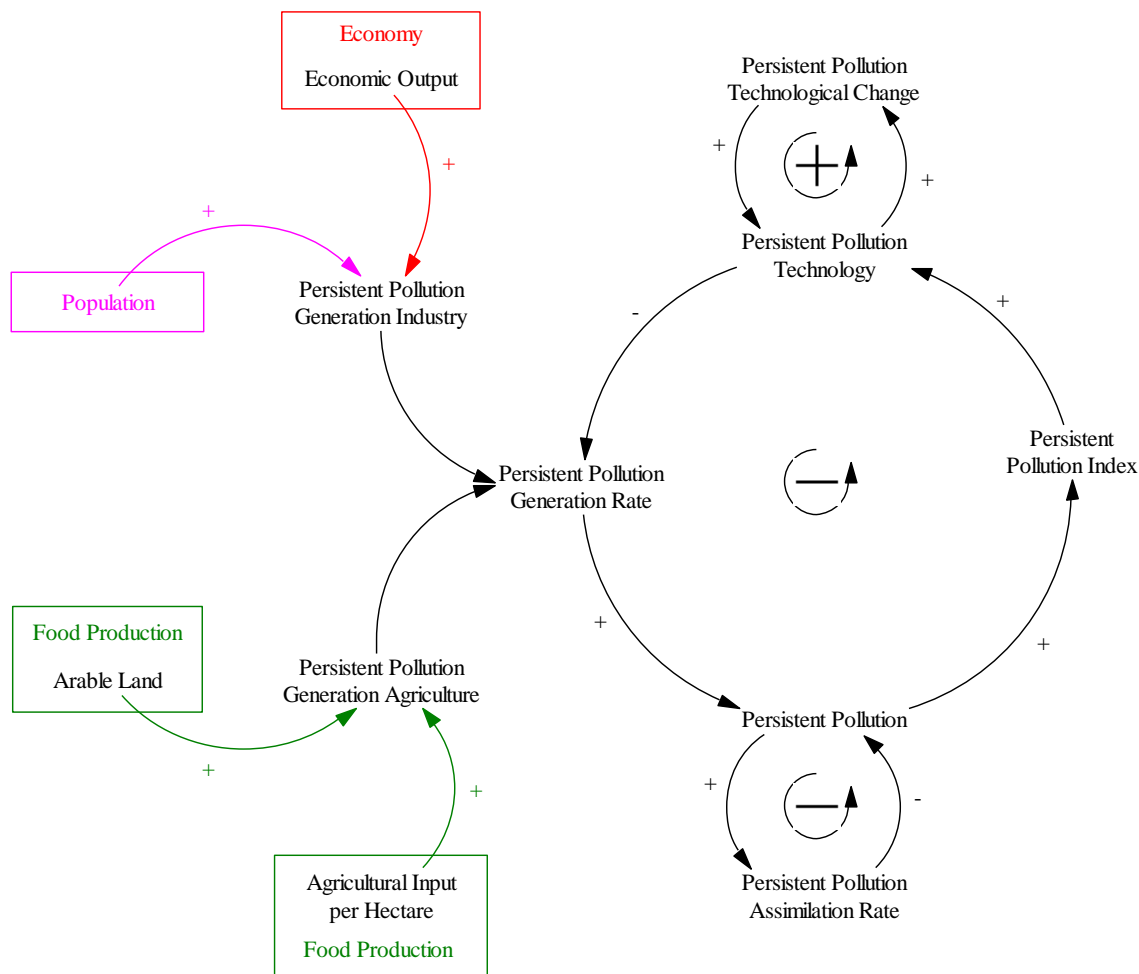


Figure 3.40. Causal structure of the ANEMI3 persistent pollution sector.

There are three feedback loops that drive the dynamics of persistent pollution. The loop connecting persistent pollution with persistent pollution technology acts as a negative feedback on persistent pollution. As the levels of persistent pollution increase, so too does the persistent pollution index, creating a greater need for technological change for dealing with pollution. The changes in technology reduce the generation rate from industry and agriculture, which results in less persistent pollution. The positive loop driving technological change represents an accumulation of knowledge, whereby more technological progress leads to a faster accumulation of new

developments in persistent pollution technology. The final loop represents a negative feedback on persistent pollution through the natural assimilation rate. Overtime, assimilation leads to a decrease in persistent pollution, acting as a form of exponential decay.

The stock and flow diagram for the persistent pollution sector is presented in Figure 3.41.

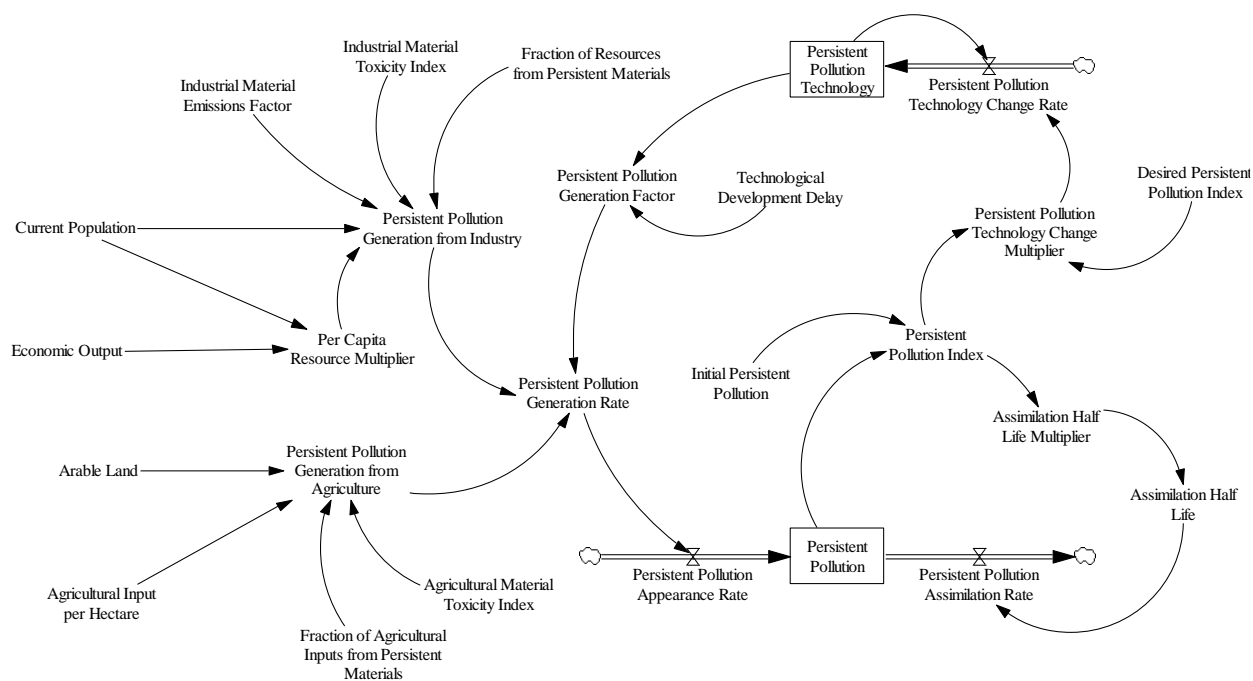


Figure 3.41. Stock and flow diagram of the ANEMI3 persistent pollution sector.

The state of the persistent pollution sub-system is represented by the two stock variables of persistent pollution and persistent pollution technology. The flows that alter the state of the system are based on the rates at which pollution is generated by the industrial and agricultural sectors as well as the natural assimilation rate in the case of persistent pollution. For persistent pollution

technology, the rate of change is driven by the previous level of technology as well as the current level of persistent pollution.

The persistent pollution stock can be represented mathematically by the following equation,

$$PP = \int (PP_{Appearance} - PP_{Assimilation}) \cdot dt \quad [Pollution\ units] \quad (3.90)$$

$PP = Persistent\ pollution\ [Pollution\ units]$

$PP_{Appearance} = Persistent\ pollution\ appearance\ rate\ [Pollution\ units]$

$PP_{Assimilation} = Persistent\ pollution\ assimilation\ rate\ [Pollution\ units]$

The assimilation rate is calculated based on the current level of persistent pollution along with the assimilation half-life,

$$PP_{Assimilation} = \frac{PP}{\tau_{assimilation}} \quad [Pollution\ units/y] \quad (3.91)$$

$\tau_{assimilation} = Assimilation\ half-life\ [y]$

The assimilation half life changes with the persistent pollution index,

$$\tau_{assimilation} = f(PP_{index}) \quad [y] \quad (3.92)$$

$PP_{index} = Persistent\ pollution\ index$

The  $PP_{index}$  is simply calculated as the current  $PP$  divided by its initial value. The rate at which persistent pollution is accumulated is defined below,

$$PP_{appearance} = \frac{PP_{gr}}{\tau_{transmission}} \quad (3.93)$$

$PP_{gr}$  = Persistent pollution generation rate [Pollution units/y]

$\tau_{transmission}$  = Persistent pollution transmission delay [y]

The generation rate depends on persistent pollution generated from agriculture, industry, and includes a generation factor that encapsulates the effect of technological change,

$$PP_{gr} = PP_{gr_{factor}} (PP_{gr_{ind}} + PP_{gr_{agr}}) \quad [Pollution\ units/y] \quad (3.94)$$

$PP_{gr_{factor}}$  = Persistent pollution generation factor

$PP_{gr_{ind}}$  = Persistent pollution industrial generation [Pollution units/y]

$PP_{gr_{agr}}$  = Persistent pollution agricultural generation [Pollution units/y]

Industrial generation is driven by population,

$$PP_{gr_{ind}} = M_{resource} \cdot P_{total} \cdot F_{pm} \cdot M_{e_{ind}} \cdot M_{t_{ind}} \quad [Pollution\ units/y] \quad (3.95)$$

$M_{resource}$  = Per capita resource use multiplier [Resource unit/(person · y)]

$P_{total}$  = Total population [persons]

$F_{pm}$  = Fraction of resources from persistent materials

$M_{e_{ind}}$  = Industrial material emissions factor

$M_{t_{ind}}$  = Industrial material toxicity index [Pollution unit/Resource unit]

Agricultural pollution generation is calculated in a similar way, except it is based on the arable land and agricultural inputs,

$$PP_{gr_{agr}} = Ag_{input} \cdot L_{ar} \cdot F_{pm_{ind}} \cdot M_{t_{agr}} \quad [Pollution\ units/y] \quad (3.96)$$

$Ag_{input}$  = Agricultural input per hectare [ $\$/(\text{ha} \cdot \text{y})$ ]

$L_{ar}$  = Arable land [ha]

$F_{pm_{ind}}$  = Fraction of agricultural inputs from persistent materials

$M_{t_{agr}}$  = Agricultural material toxicity index [Pollution units/y]

The persistent pollution generation factor is equal to the level of persistent pollution technology with an information delay of  $\tau_{technology}$ , that is applied in the form of exponential smoothing. This is done to represent the time it takes for technological change to take effect,

$$PP_{gr_{factor}} = SMOOTH(PP_{tech}, \tau_{technology}) \quad (3.97)$$

$PP_{tech}$  = Persistent pollution technology

$\tau_{technology}$  = Technology development delay [y]

The level of persistent pollution technology is an accumulation of the persistent pollution technology change rate,

$$PP_{tech} = \int PP_{tech_{rate}} \cdot dt \quad (3.98)$$

$PP_{tech_{rate}}$  = Persistent pollution technology change rate

The rate of change of persistent pollution technology is a function of the persistent pollution index,



$$PP_{techrate} = f \left( 1 - \frac{PP_{index}}{DPP_{index}} \right) \quad [1/y] \quad (3.99)$$

$PP_{index}$  = Persistent pollution index

$DPP_{index}$  = Desired persistent pollution index

The values of the parameters used in the persistent pollution sector are given in Table 3.9 below.

Table 3.9. Parameters values used in the persistent pollution sector.

Parameter	Symbol	Units	Value
Persistent pollution transmission delay	$\tau_{transmission}$	year	20
Technology development delay	$\tau_{technology}$	year	20
Industrial material emissions factor	$M_{eind}$	dimensionless	0.1
Industrial material toxicity index	$M_{tind}$	pollution units/resource units	10
Agricultural material toxicity index	$M_{tagr}$	pollution units/\$	1
Fraction of agricultural inputs from persistent materials	$F_{pmagr}$	dimensionless	0.001
Fraction of resources from persistent materials	$F_{pmind}$	dimensionless	0.02

This sector is an entirely new addition to the ANEMI model. The inclusion of the persistent pollution sector in ANEMI3 provides an additional negative feedback on population growth based on the work of Meadows et al. (1974). The addition of the persistent pollution sector is used to address research objective 5a from Section 2.6.

### 3.3. Parameter Estimation

Due to the large number of feedbacks in the ANEMI3 model any changes made in one sector affects all others. This is also true when incorporating and coupling new sectors into the model as additional feedbacks are formed. In order to ensure that realistic values and system behaviours are generated, some of the parameters needed to be re-estimated. Parameters within the water supply development sector and the energy production sector were re-estimated as they are newly added sectors in the model and have an influence on the other sectors. The population sector also contained parameters relating to life expectancy and fertility that needed to be re-estimated so that more realistic population values could be obtained, as population growth is a key driver for every sector of the model. The re-estimation process starts with the identification of key parameters to be estimated. In this case, the parameters listed in Table 3.10 were selected as they are relatively uncertain at the global scale and influence the dynamics of the model sectors mentioned above. The objective function for the for this procedure uses global datasets for population, energy production, and water supply listed in Table 3.12 to calculate relative errors against the corresponding model variables in the table.

Table 3.10. Model constants and their optimal values with corresponding sectors.

<b>Model Sector</b>	<b>Decision Variable</b>		<b>Optimal Value</b>	<b>Units</b>
Water Supply	Specific Water Intake Factor		0.95	-
	Water Resource Elasticity	Surface water	0.469	-
		Groundwater	0.413	-
		Wastewater	0.770	-
		Desalination	0.691	-
	Water Capital Share	Surface water	0.987	-
		Groundwater	0.01	-
		Wastewater	0.937	-
		Desalination	0.658	-
	Initial Water Producer Price	Surface water	15740	\$/km <sup>3</sup>
Groundwater		68509	\$/km <sup>3</sup>	

		Wastewater	119114	\$/km <sup>3</sup>
		Desalination	132786	\$/km <sup>3</sup>
	Short-Run Water Elasticity		0.239	-
	Water Quality Share Parameter		0.097	-
Energy Production	Energy Adjustment Coefficient		0.133	-
	Energy Order Adjustment Coefficient		0.050	-
	Energy Return Coefficient		1.07	-
	Energy Substitution Elasticity		2.25	-
	Energy Resource Elasticity	Coal	0.700	-
		Oil and Gas	0.700	-
		Hydro and Nuclear	0.650	-
		Renewables	0.520	-
	Initial Energy Production	Coal	7.58e10	GJ/year
		Oil and Gas	2.01e11	GJ/year
		Hydro and Nuclear	1.00e10	GJ/year
		Renewables	3.32e8	GJ/year
	Initial Energy Producer Price	Coal	1.28	\$/GJ
Oil and Gas		1.37	\$/GJ	
Hydro and Nuclear		10	\$/GJ	
Renewables		50	\$/GJ	
Population	Crowding Factor		0.86	-
	GDP Factor		1.41	-
	Lifetime Perception Delay		22.4	years
	Social Adjustment Delay		18.7	years
	Max Total Fertility		13.1	-
	Reproductive Lifetime		33.2	years

The objective function is non-linear due to the coupling of feedback processes in the model. Modifying any of the decision variables listed in Table 3.10 will affect all other aspects of the model to some degree. The solution space is assumed to be one that has many valleys and peaks creating the potential for local optima to exist, leading to suboptimal solutions. Because of this, a global optimization algorithm is used, rather than a gradient based method. The differential evolution algorithm (Storn and Price 1995) was selected for this reason, in addition to the fact that derivatives are not needed for the objective function. This algorithm is evolutionary and stochastic by nature, which can lead to results that are close to the global optimum but not necessarily exact. The minimum solution obtained by the differential evolution algorithm was used as a starting point

for a deterministic local minimizer to finish the optimization. Details regarding this algorithm and the procedure for how it was applied can be found in Appendix C, along with the software developed to link the algorithm to the Vensim system dynamics simulation software in Appendix D.

### 3.4. Model Implementation

The ANEMI3 model is built and simulated within the object-oriented Vensim simulation software. Within Vensim, stock and flow diagrams are automatically converted to systems of differential equations. The user must specify the values of constants, initial conditions (for stock or state variables) and equations (for the rate or flow variables) in order to run the model. The time horizon, time step, and integration methods can all be specified by the user. Vensim also provides additional functions to represent common model structures that are used in system dynamics models. These include functions to conveniently represent material and information delays, look up tables, pulse and linearly increasing inputs, and many more. The ANEMI model consists of over 450 constants, 160 unique differential equations (not including subscripts) and 1000 auxiliary equations. Although the ANEMI3 model is relatively large, the software can efficiently integrate the system of equations and can be run on a desktop computer in a matter of minutes. The efficient run-time of the model allows for performing sensitivity analysis and policy simulations that require multiple model runs to complete. More information on where the model can be obtained is provided in Appendix E.

### 3.5. Model Validation

System dynamics simulation models can be constructed to represent purely physical systems for which an input can be given to generate an output that can be compared to data in the real world

or analytical solutions of the system. However, this modelling approach is often used to analyze all types of systems that could include social elements or decision-making processes that can be more abstract or where a high degree of uncertainty exists in measurements. That is why in the field of system dynamics simulation true validation and verification are deemed impossible. Sterman (2000) states that:

*“The goal of modeling, and of scientific endeavor more generally, is to build shared understanding that provides insight into the world and helps solve important problems... Instead of seeking a single test of validity models either pass or fail, good modelers seek multiple points of contact between the model and reality ...”*

With this in mind, a series of tests from Sterman (2000) will be used to evaluate the ANEMI3 plausibility of the baseline scenario with regards to the dynamics that take place. The absolute values are important, however the emphasis here is on the model behaviour so that we can analyze the feedback mechanisms that are driving the model to future states. Each test will be performed for a selection of the ANEMI3 model variables in each model sector. They are presented in Table 3.11.

Table 3.11. Model testing procedures based on Sterman (2000).

<b>Test</b>	<b>Purpose of Test</b>	<b>Procedure</b>
<b>Behaviour Reproduction</b>	Compare modelled variables to historically observed data.	Plot modelled and historical observed variables in each model sector to ascertain whether modelled variable exhibits similar behaviour when compared to observed.  Compute statistical measures of correspondence between model and data.

<b>Projected Comparison</b>	Compare ANEMI3 modelled variables to projected variables in other studies.	Plot ANEMI3 results for variables in each sector against projections from other studies. Identify if ANEMI3 results are within the range of other studies. If not, explain why.
<b>Integration Error</b>	Test the extent to which changes in the model time step affect the results.	Half the time step and run ANEMI3. Plot the result for model variables in each sector. Use different integration methods.
<b>Sensitivity Analysis</b>	Test for changes in behavioural modes when assumptions about parameters, model boundaries, and aggregations are varied over the plausible range of uncertainty.	Identify variables in each sector that are uncertain, may have a high degree of heterogeneity in the Earth system, or are assumed constant but could change over time. Apply Monte Carlo simulation to test the likelihood that these variables could alter model behaviour.
<b>Extreme Conditions</b>	Test whether the model responds plausibly when subjected to extreme policies, shocks, or parameter changes.	Test the response to extreme values in key inputs, alone and in combination.

Specific details related to each test and how they are applied to the ANEMI3 model in each of the model sectors are presented in the upcoming sections for each test.

### 3.5.1. Behaviour Reproduction

Many of the variables in ANEMI3 do not have historically observed counterparts on a global scale, but there are key variables in each sector that can be compared to historical data. One thing to note in this comparison is that on a global scale, there are many datasets that are incomplete (data is only recorded for certain regions), inconsistent (different recording methodologies used across

regions, recording is done at irregular intervals), and at times, unreliable. However, there is still value in comparing the model to the real world in any way possible to see that it reproduces the behaviour of the sub-systems that are being represented. With this being said, the goal is not to reproduce the numbers from the data, but build confidence in the model's ability to generate realistic system behaviours in order to build confidence in future behaviours that arise, as well as policies that are implemented to alter them. The ANEMI3 variables that have been selected, along with the datasets used for comparison are in Table 3.12.

Table 3.12. Comparison datasets for baseline model run.

<b>Model Sector</b>	<b>Variable</b>	<b>Datasets</b>
Population	Total Population	UN World Population Prospects 2019
	Population (0-14)	UN World Population Prospects 2019
	Population (15-44)	UN World Population Prospects 2019
	Population (45-65)	UN World Population Prospects 2019
	Population (65+)	UN World Population Prospects 2019
Climate	Global Atmospheric Temperature	NASA (2019)
Economy	World GDP	World Bank and OECD National Accounts
Water Demand	Domestic Water Withdrawal	International Hydrological Programme (2000)
	Industrial Water Withdrawal	
	Agricultural Water Withdrawal	
Water Supply	Surface Water Withdrawal	Wada and Bierkens (2014)
	Ground Water Withdrawal	
Energy Production	Coal Energy Production	Wada and Bierkens (2014)
	Oil and Gas Energy Production	

	Hydro and Nuclear Energy Production	World Nuclear Association (2018) Ritchie and Roser (2018)
	Renewable Energies	Ritchie and Roser (2018)
Land Use and Cover	Agricultural Area	HYDE (2016)
	Urban Area	

The growth of the human population is one of the most important feedback loops in the ANEMI3 model as it is a key driver of the global change. When comparing the simulated and observed total

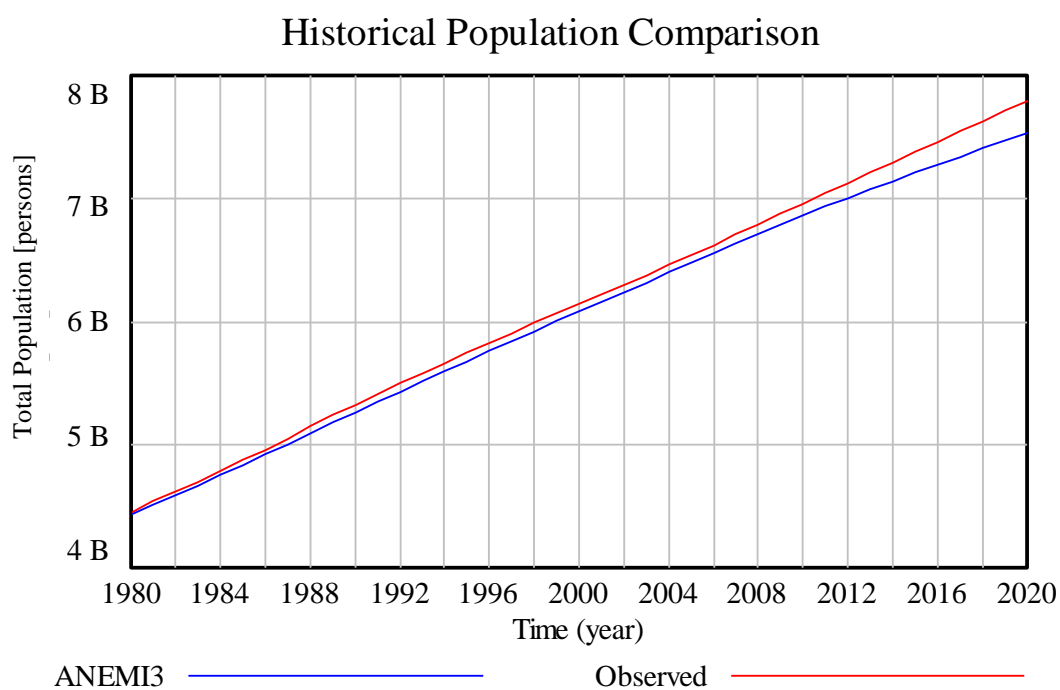


Figure 3.42. Simulated vs. historical World population for the period of 1980 to 2019.

population in Figure 3.42, we see that they start at the same initial value and follow a similar path to 2019. However, the paths start to diverge slightly between the years 2010 to 2019. This discrepancy is relatively minor and there is not a major difference in the overall behaviour of the



historical population. When the population is subdivided further (Figure 3.43), it is shown that the simulated population for all age groups except for 15 to 44, follow historical trends, where the 15 to 44 age group is slightly underestimated. This underestimation of the 15 to 44 age group accounts for the difference in total population from historical data.

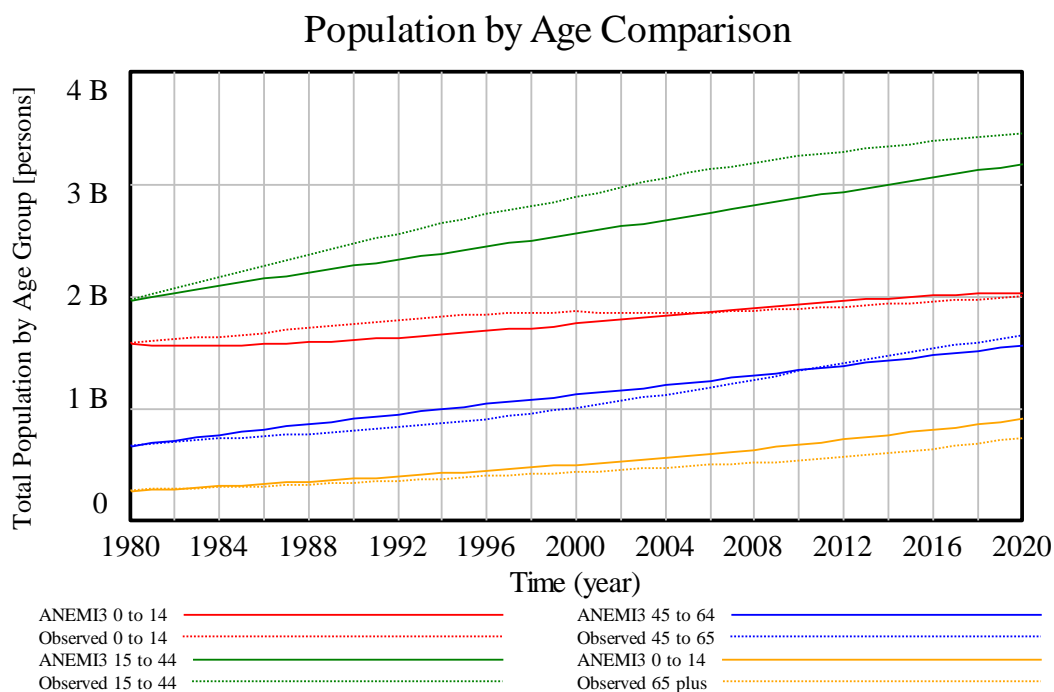


Figure 3.43. Simulated vs. historical World population subdivided by age demographic. Solid lines depict ANEMI3 results while dotted lines are historical values.

The variation in global temperatures due to climate change from the year 1980 are shown in Figure 3.44. From 1980 to 2018 the ANEMI3 model predicts a global temperature change of 0.87 degrees, while the observed NASA data reports a value of 0.6 degrees. The simplified climate system in ANEMI3 is not able or designed to capture the annual variation in global temperatures that are present in the observed NASA data. The behavioural mode is similar, with a slightly higher slope

shown by the ANEMI3. More comparisons are made in Section 4.1 with regards to projected change in global temperature change.

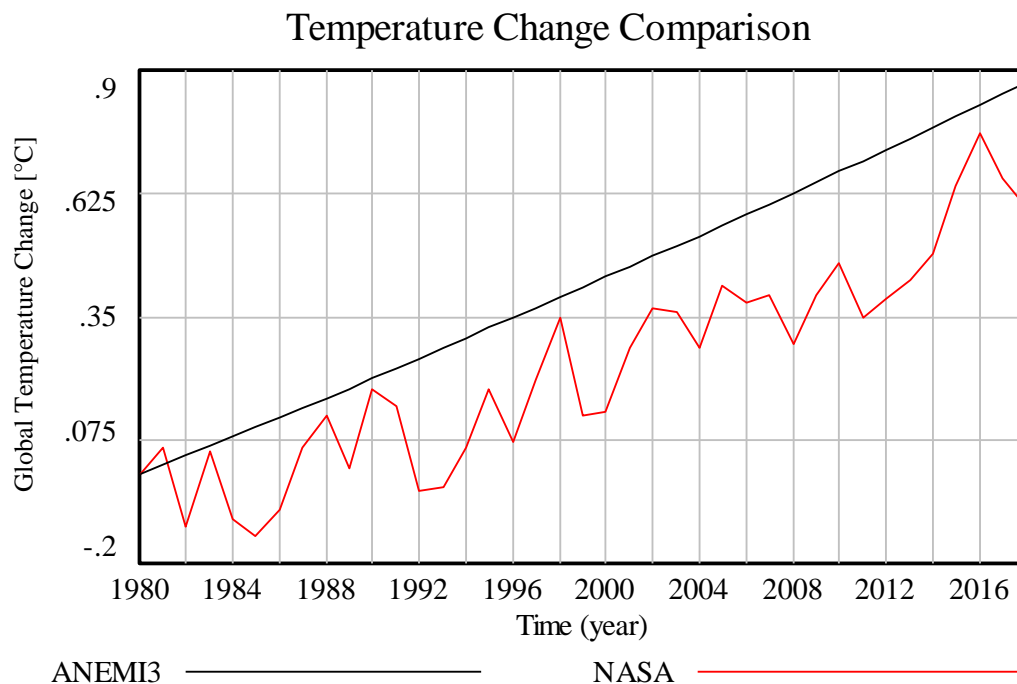


Figure 3.44. Global temperature change from 1980-2018 comparison between ANEMI3 climate sector and NASA observed data.

Water demand projections from ANEMI3 are compared to estimates from IHP (2000) in Figure 3.45. Agricultural demand in 1980 and 2010 is slightly lower than the historical values before the year 1990 and slightly higher after, while industrial water demand provides a good match and domestic water demand is slightly lower than historical. The water demand values are driven by food production in the case of agricultural demands, energy production for the industrial water demand, and population along with economic output for domestic demand. Considering the integrated nature of water demand in ANEMI3, the trend of increasing water demands is sufficiently accurately captured from 1980-2010.

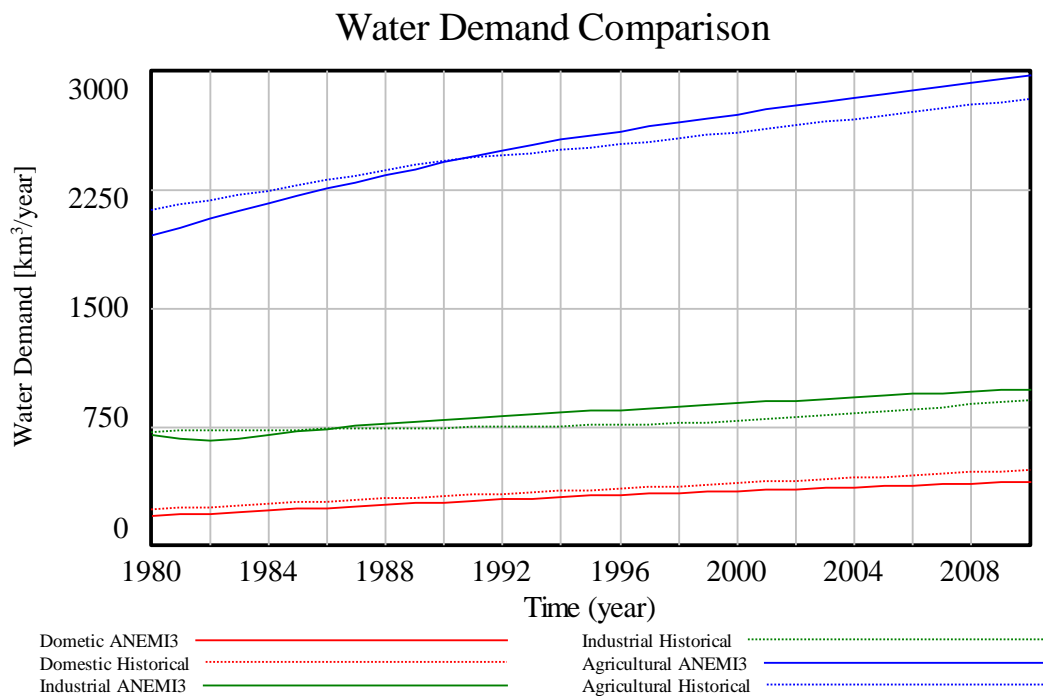


Figure 3.45. Water demand comparison between the ANEMI3 and IHP (2000). Data between the years 2000-2010 for IHP (2000) are extrapolated from the historical data.

The new water production sector in ANEMI3 is compared against estimates provided by Wada and Bierkens (2014). Available global data for the withdrawal of surface water and groundwater is scarce, however in Wada and Bierkens (2014) a global hydrologic model was used in conjunction with a global water demand model to generate estimates for surface water and groundwater withdrawal amounts. Comparison between the ANEMI3 simulated values and the estimates shows good agreement in the trends although the ANEMI3 value for surface water withdrawal is slightly lower (Figure 3.46).

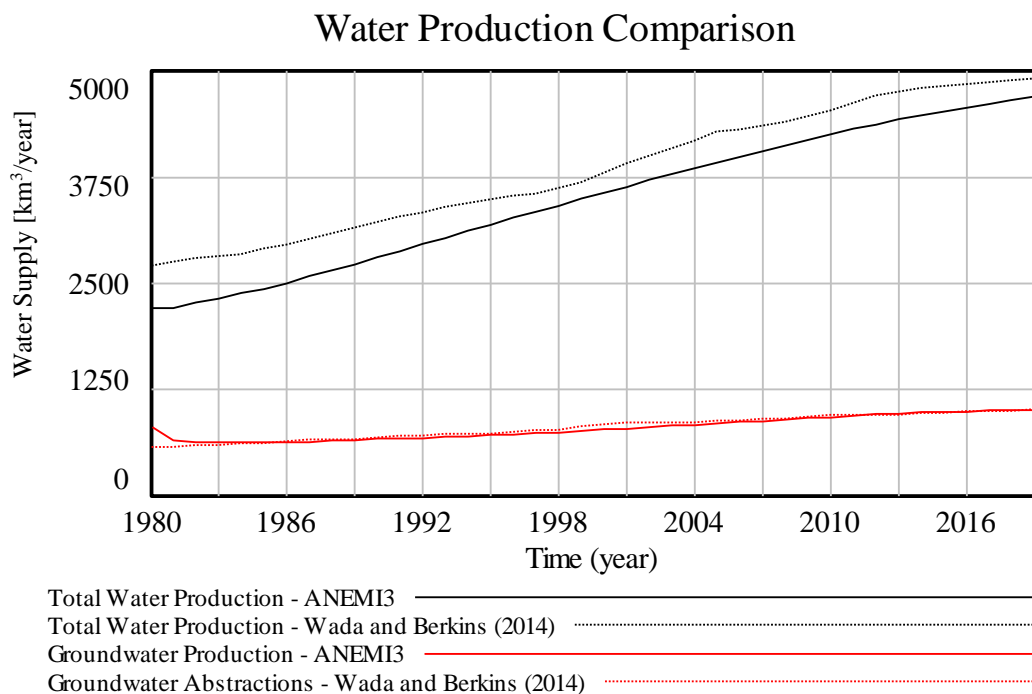


Figure 3.46. Water production comparison between the ANEMI3 and Wada and Bierkens (2014) from 1980 to 2019.

Energy production in the ANEMI3 model is based on that of the FREE model in Fiddaman (1997) which is intended for long term simulations of energy production for the purpose of policy analysis (such as for example, the application of carbon taxes on fossil fuels.) FREE does not accurately captures short term fluctuations in energy production as these are dependent on more detailed market interactions (Fiddaman 1997). The simulated values for oil and gas production are presented in Figure 3.47. There is an initial drop in production in the year 1986. From this point onward, the trajectory of oil and gas production is sufficiently captured. Capturing historical data in the case of energy production from coal, the simulated values are close to observed and have a similar trend, although minor fluctuations over time are not captured. by the ANEMI3. The simple dynamics used to represent energy production in the ANEMI3 model do not capture complex

market interactions that drive energy production, but would allow for examining the change in energy production composition in the case that oil and gas start to become depleted, or when technological changes allow for renewable energies to become more economically feasible.

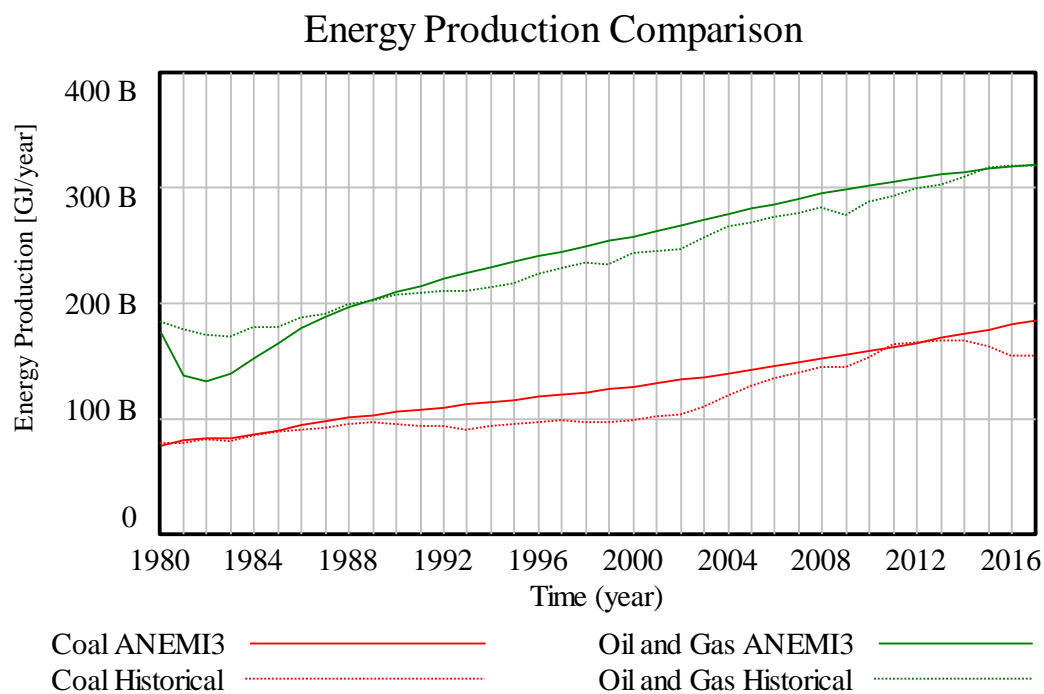


Figure 3.47. Historical energy production comparison between ANEMI3 model results and estimates provided by Ritchie and Roser (2018a) for coal, oil and gas.

Hydro and nuclear energy production are very close to the historical data, capturing the absolute values and trend over time (Figure 3.48). However, in the case of renewable energy production the simulated renewable energy values show an increase, but not on the scale that has been observed. The reason for this is most likely the sensitivity of the ANEMI3 model to initial conditions for renewable energy production, because the initial values are small relative to the amount of growth that is made in a short period of time.

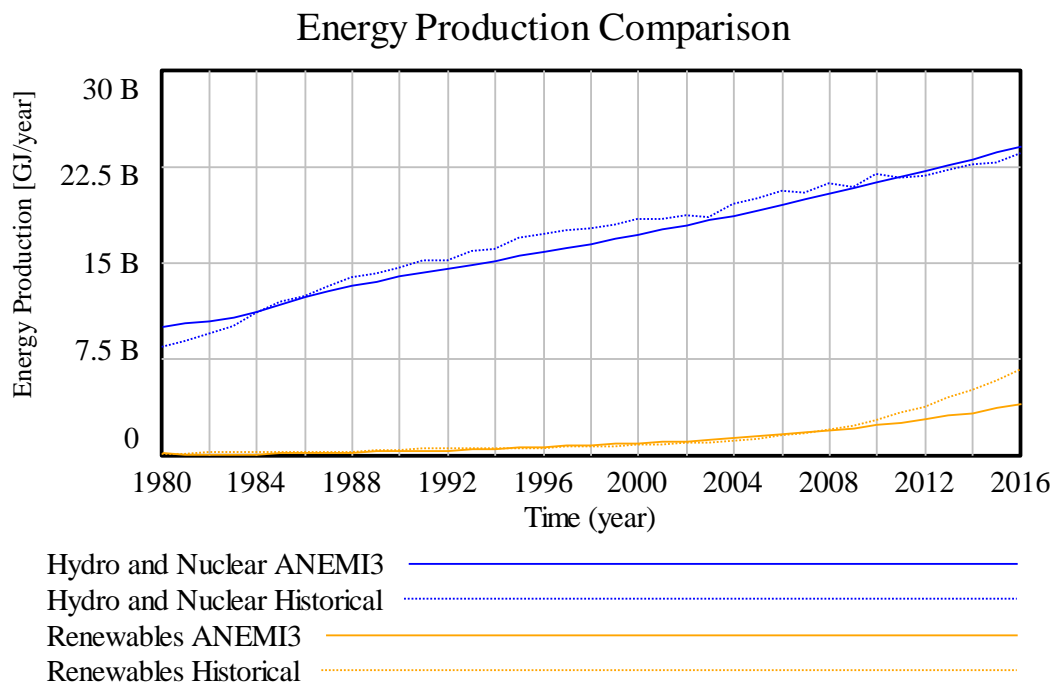


Figure 3.48. Historical energy production comparison between ANEM13 model results and estimates provided by (Ritchie and Roser 2018a) for hydro, nuclear, and renewable energies.

Land area comparisons are made between the ANEM13 model results and data obtained from HYDE (2016) for agricultural and built land areas during the historical period in Figure 3.49. Simulated values for cropland, grazing land, and human built areas appear to be slightly overestimated by the ANEM13 when compared to the historical values. This may be due to minor differences in the categorization of land use types embedded in the initial land values used in ANEM13 from (Goudriaan and Ketner 1984). However, the rates of change in each category are similar.

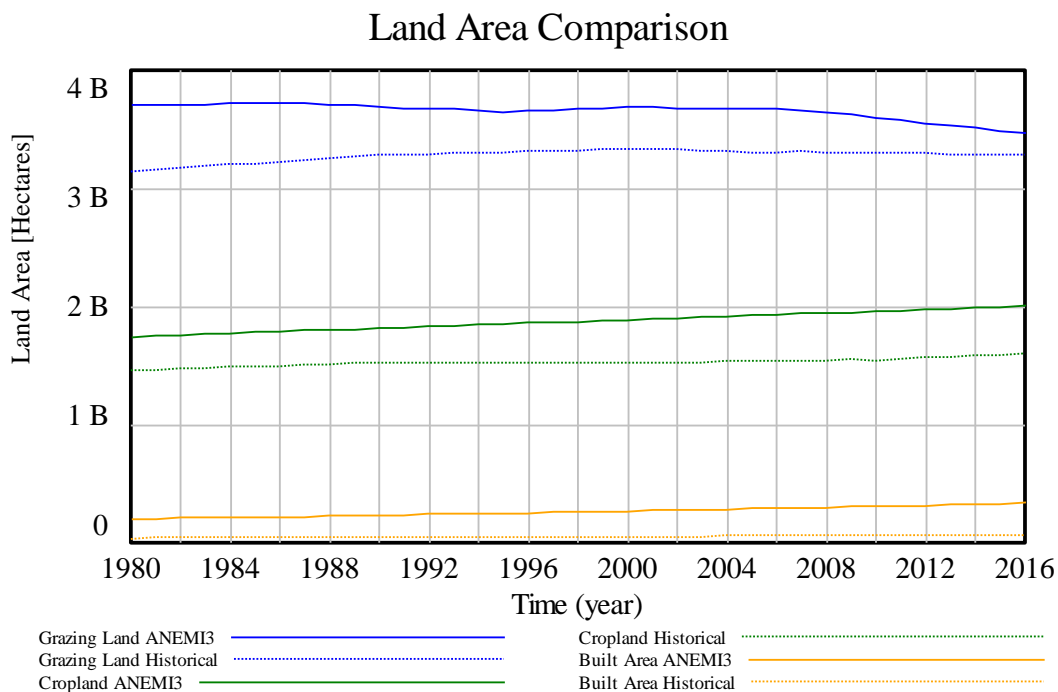


Figure 3.49. Land area comparison for agricultural and built areas between ANEMI3 model results and estimates provided by HYDE (2016).

### 3.5.2. Future Model Performance

Models and data have been used to make predictions on various components of the Earth system that are also being modelled by ANEMI. Comparing the ANEMI3 projections to these predictions provides some context as to where the ANEMI3 results lie amongst the range of predictions available, as well as providing an additional test of plausibility for the model. The goal is not to reproduce the results shown from the other models. The models are using different datasets, time horizons, and model structures in comparison to ANEMI3. Table 3.13 indicates the variables that are being used from each sector in ANEMI3 for comparison with other projections available in the literature.

Table 3.13. Datasets used for comparison of the ANEMI3 model future behaviour.

<b>Model Sector</b>	<b>Variable</b>	<b>Dataset</b>
Population	Total Population	UN World Population Prospects 2019
Climate	Global Atmospheric Temperature	Krinner et al. (2013)
Economy	Gross Economic Output	DICE 2013R
	Per Capita Consumption	ANEMI2
Water Demand	Domestic Water Withdrawal	Wada et al. (2016)
	Industrial Water Withdrawal	Chaturvedi et al. (2013)
	Agricultural Water Withdrawal	
Water Supply	Surface Water Production	Wada and Bierkens (2014)
	Groundwater Production	
	Desalination Production	Hanasaki et al. (2016) Fichtner GmbH (2011)
Energy Production	Total Energy Production	ANEMI2
	Coal Energy Production	Ito et al. (2000)
	Oil and Gas Energy Production	Mohr et al. (2009)
	Hydro and Nuclear Energy Production	
	Renewable Energies	

The trajectories of the main stocks in the baseline scenario that define the state of the ANEMI3 model are shown in Figure 3.50. The total population varies from 4.4 billion to 9.5 billion in 1980 and 2100 respectively. Population increases almost linearly at the start of the simulation, then the increase slows down as negative feedbacks on population begin to limit the growth. The peak population is reached in the year 2085. After this point the death rate exceeds that of the birth rate and there is a gradual decrease in population until the end of the simulation.



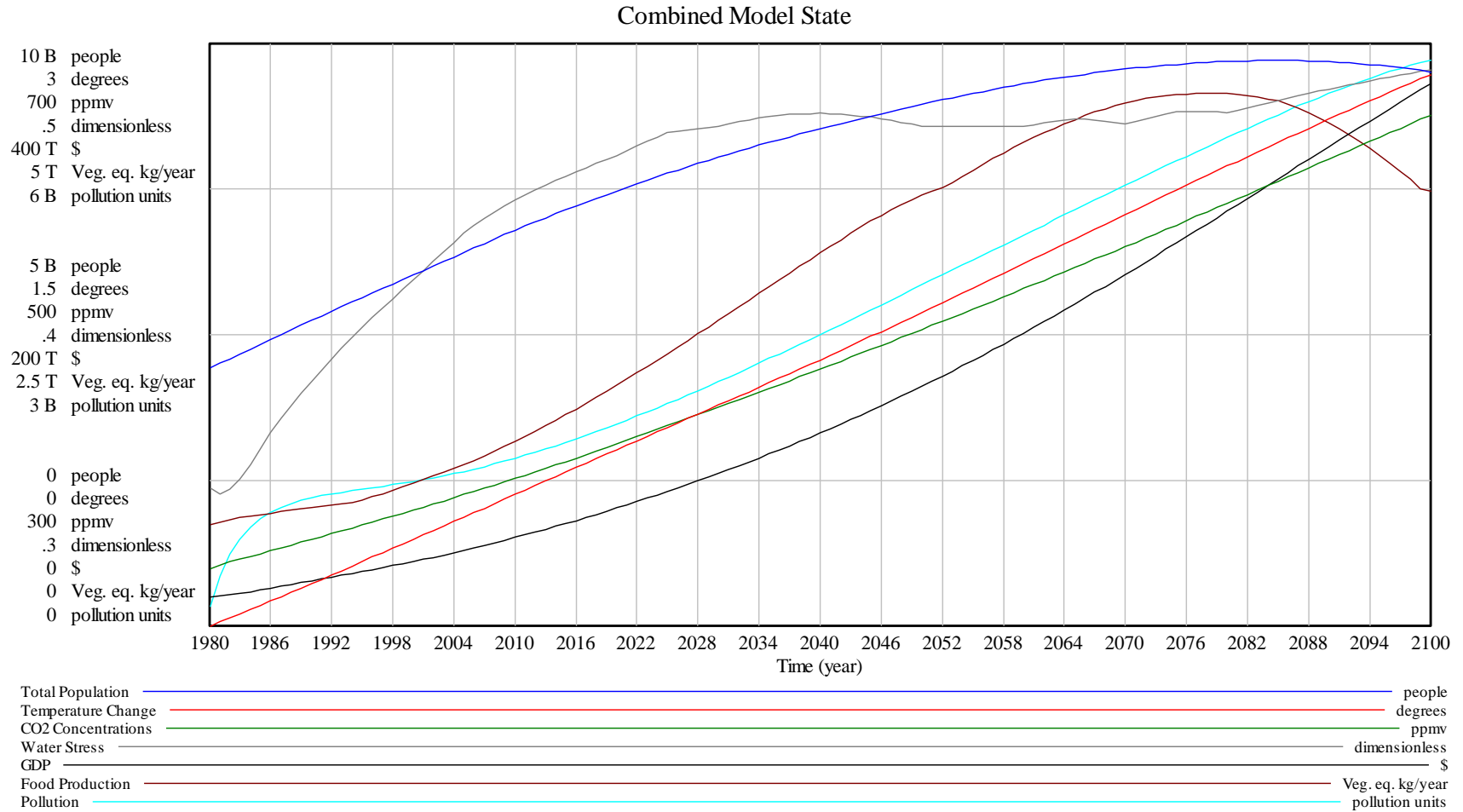


Figure 3.50. ANEMI3 model performance for the period 1980 - 2100.

The 2019 revision of the UN World Population Prospects (UN WPP) report (United Nations 2019c) contains future population scenarios defined by projected variants in fertility, mortality, and migrations rates to the year 2100. When ANEMI3 is compared to the projections, the results are shown to lie between the low and medium projections (Figure 3.51). This is likely due to the fact that negative feedbacks on population growth which are considered endogenously in the ANEMI3 model.

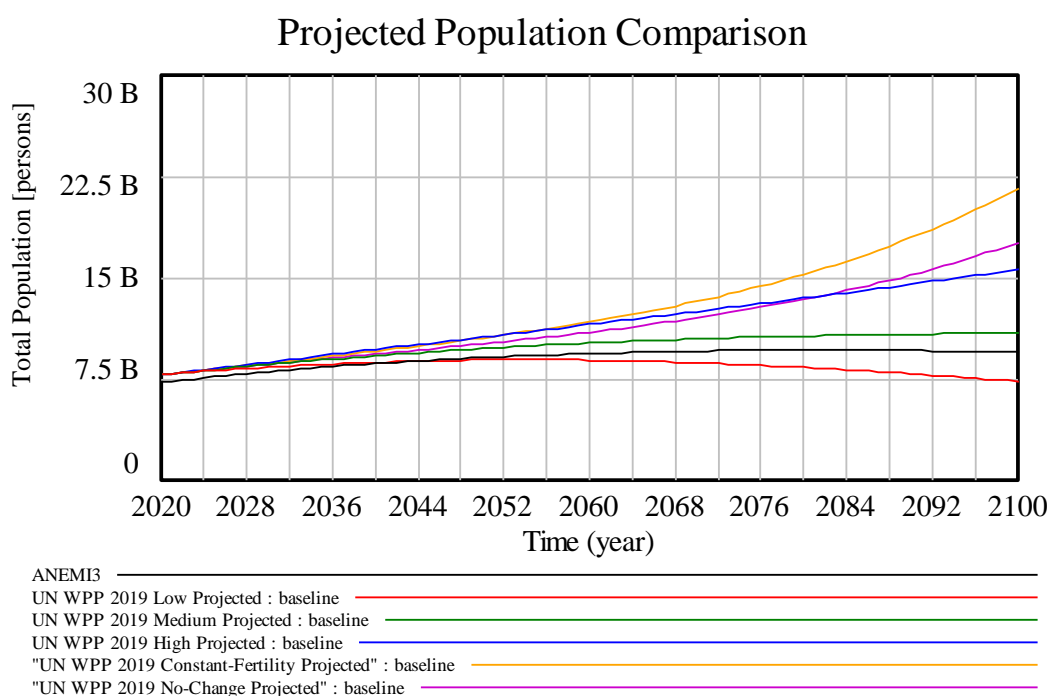


Figure 3.51. ANEMI3 population projections compared to those in United Nations (2019).

The change in global atmospheric temperatures follows an almost linear path, reaching a change of almost 3 degrees by the year 2100. This is due to increasing CO<sub>2</sub> levels, which start at an atmospheric concentration of 339ppmv and rise to 650ppm. This corresponds to an increase of 1.9 times.

The ANEMI3 model was run with the emissions scenarios for the greenhouse gases of carbon dioxide, methane, nitrogen dioxide, and chlorofluorocarbons from the fifth assessment report of the IPCC in order to compare the resulting temperature changes from the different RCP scenarios (Krinner et al. 2013). Each of the RCP scenarios represents a different socioeconomic pathway for greenhouse gas emissions and are defined by the total radiative forcing on the climate system at the end of the century. For example, RCP4.5 represents a socioeconomic pathway for emissions resulting in a total radiative forcing of  $4.5\text{W/m}^2$  by the year 2100. The socioeconomic pathways embedded in each RCP scenario contain projections of population, GDP, energy production, and land use. Comparing the differences in global surface temperatures projected from the ANEMI baseline to those projected from the RCPs allows for a much more general comparison of where the overall socioeconomic pathway of ANEMI stands.

The change in global surface temperatures resulting from running the ANEMI model with the RCP scenarios, is shown in Figure 3.52. The ANEMI3 results are found to be within what is projected with the RCP scenarios, between those of RCP6 ( $2.6^\circ\text{C}$  by 2100) and RCP8.5 ( $4.3^\circ\text{C}$  by 2100) corresponding to a  $2.7^\circ\text{C}$  temperature change by the year 2100. Comparing the  $\text{CO}_2$  concentrations of the RCP scenarios to that of the ANEMI model also shows a similar result, with a very close trajectory to RCP6 (Figure 3.53). This indicates that the overall socioeconomic pathway of the ANEMI baseline run is between one that is medium to high in terms of emissions with some climate change mitigation present, and is similar to that of the AIM integrated assessment model (van Vuuren et al. 2011).

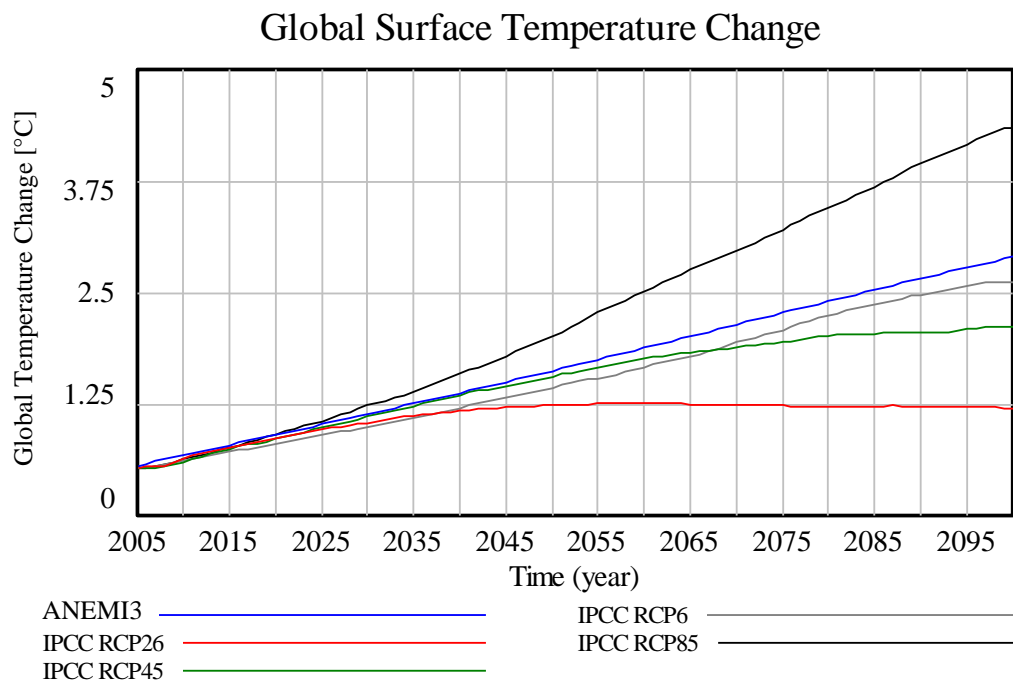


Figure 3.52. Global surface temperature change comparison between ANEMI3 baseline and ANEMI3 running with the RCP scenario GHG emissions.

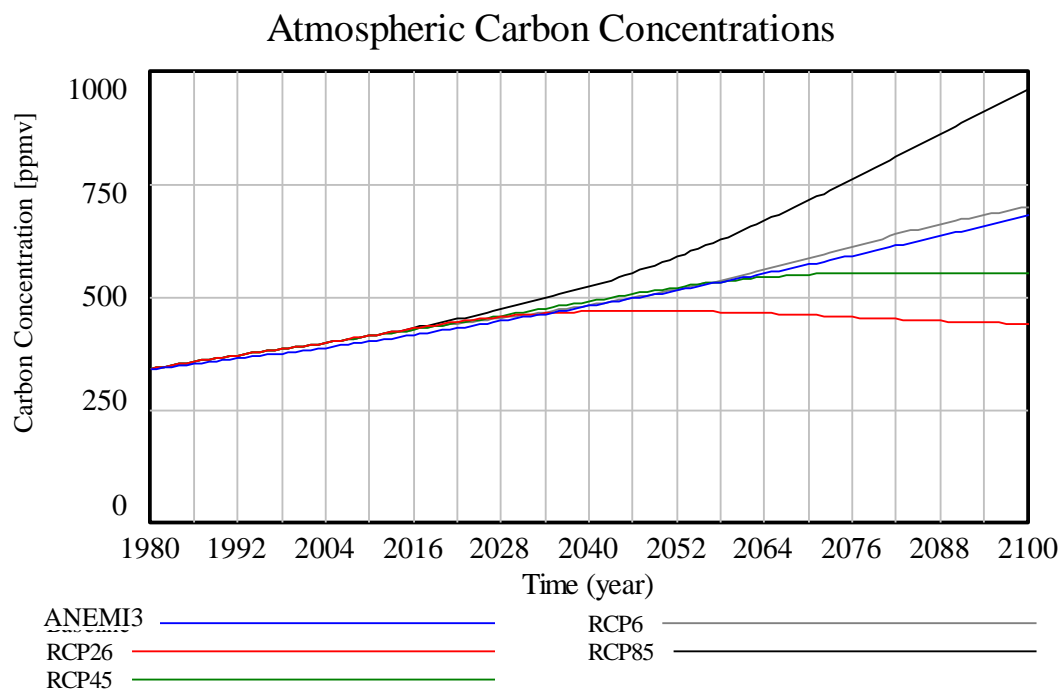


Figure 3.53. Comparison of atmospheric CO<sub>2</sub> concentration between ANEMI3 baseline and ANEMI3 running with the RCP scenario GHG emissions.

Thresholds of water stress have been defined by United Nations (1997). Low, moderate, medium-high, and high levels of water stress corresponds to values of less than 0.1, 0.1 to 0.2, 0.2 to 0.4, and greater than 0.4 respectively, where water stress ( $WTA$ ) is defined as the ratio of surface water withdrawals ( $SWW$ ) to availability ( $ASW$ ),

$$WTA = \frac{SWW}{ASW} \quad (3.100)$$

. In the ANEMI3 model, water stress can be calculated using different formulations. Water pollution and green water dilution effects ( $WTA_{poll}$  and  $WTA_{poll+gw}$ ) can be applied to the WTA ratio in order to gain a more conservative measure of water stress (Davies and Simonovic 2011).

$$WTA_{pollution} = \frac{SWW + URW \cdot WDF}{Total\ Renewable\ Flow} \quad (3.101)$$

$$WTA_{pollution+gw} = \frac{SWW + URW \cdot WDF + GWR}{Total\ Renewable\ Flow} \quad (3.102)$$

$URW$  = Untreated returnable water [ $km^3/y$ ]

$WPF$  = Water pollution factor

$GWR$  = Green water requirement for crops and pasture [ $km^3/y$ ]

In this research, an additional representation is used based on the ratio of total water supply to the amount of available conventional water resources of surface water ( $R_{sw}$ ) and groundwater ( $R_{gw}$ ).

$$WTA_{water\ supply} = \frac{\sum WS_i}{R_{sw} + R_{gw}} \quad (3.103)$$

The total amount of water supply includes both, conventional and alternative water resources, allowing for increased alternative water resources to reduce water stress. The projected water stress values using the formulations mentioned above are shown in Figure 3.54.

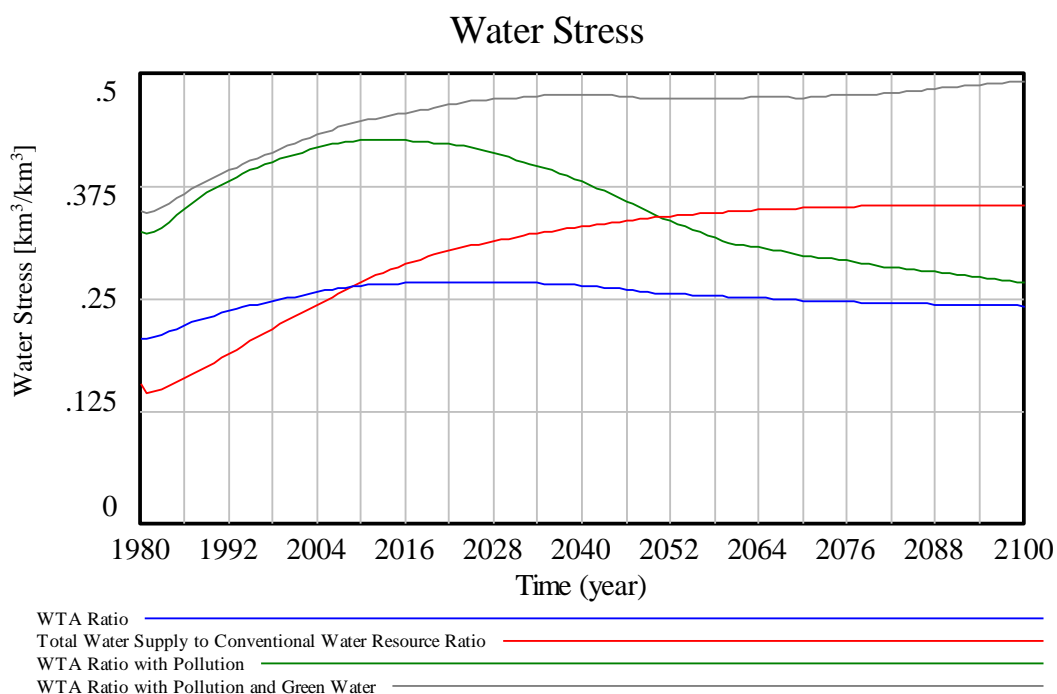


Figure 3.54. ANEMI3 simulated levels of water stress using the withdrawal to availability ratio and alternate formulations.

When the effects of pollution and green water dilution are included, water stress values are much higher. Using only the WTA ratio, water stress values start initially at a value of 0.21 and rise up to 0.24, which is on the low end of the medium-high water stress category. In contrast, when pollution and green water effects are considered, the starting values range between 0.32 to 0.35.

As the simulation progresses, water stress with only pollution effects considered on top of the WTA reaches a peak in the year 2010 and declines afterwards. This is because in this case the pollution effects are represented only through wastewater inputs, which decrease as domestic and industrial water demands decrease in the model due to reduced water intensities with greater global economic output. When water pollution in the form of agricultural runoff or green water is included, water stress values continue to rise to a value of 0.5 by the end of the simulation. This indicates severe levels of water stress. Using the ratio of water supply to available water resource levels as an indicator of water stress result in a starting value of 0.15 which follows S-shaped growth to 0.35. This indicates a shift from low levels of water stress to the high end of the medium-high water stress category.

Despite economic damages from climate change, economic output increases exponentially from 19.4 to 372 trillion 1980 USD (Figure 3.55). When compared with the ANEMI2 model, it is interesting to note that the simulated values follow a similar trajectory. The same initial value of the global capital stock was used between the two models, but the model structure of the economic

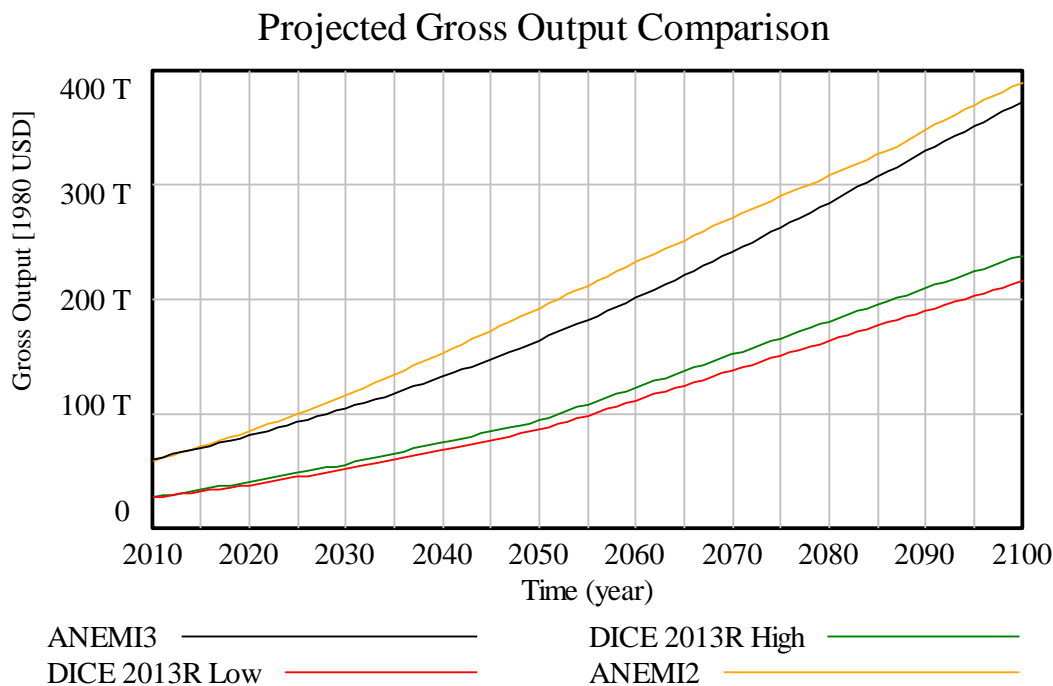


Figure 3.55. Comparison of gross economic output between ANEMI2, ANEMI3, and DICE2013R models.

sectors of ANEMI2 and ANEMI3 are entirely different. As mentioned in Section 3.2.9, the second version of ANEMI uses a computable general equilibrium model to generate economic output and investment in capital stocks, while the ANEMI3 uses the system dynamics simulation approach based on the FREE model of Fiddaman (1997). Although the projections from the DICE2013R (Nordhaus 2013) model show values that are considerably lower than that of ANEMI versions 2 and 3, the general pattern of consistent exponential growth is the same, and the differences likely stem from the choice of initial values. The rates of per capita consumption show a similar pattern as well amongst the models (Figure 3.56).



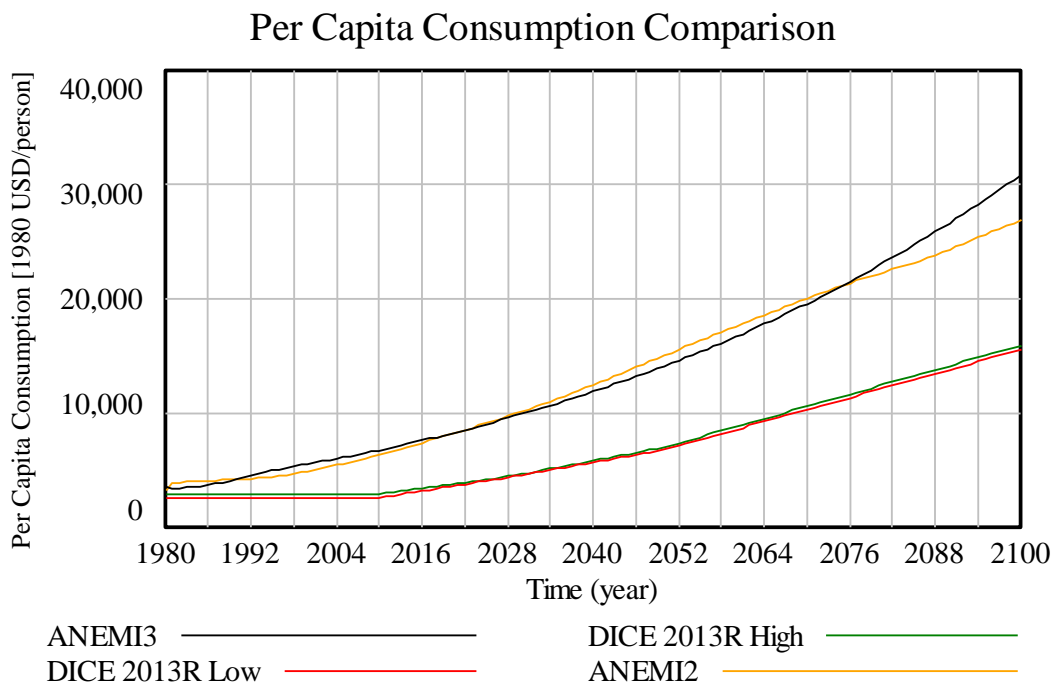


Figure 3.56. Comparison of per capita consumption rates between ANEMI2, ANEMI3, and DICE2013R models.

Simulated water demands were compared with those made by the H08, WaterGAP, and PCR models found in Wada et al. (2016) for both domestic and industrial water demand (Figure 3.57).

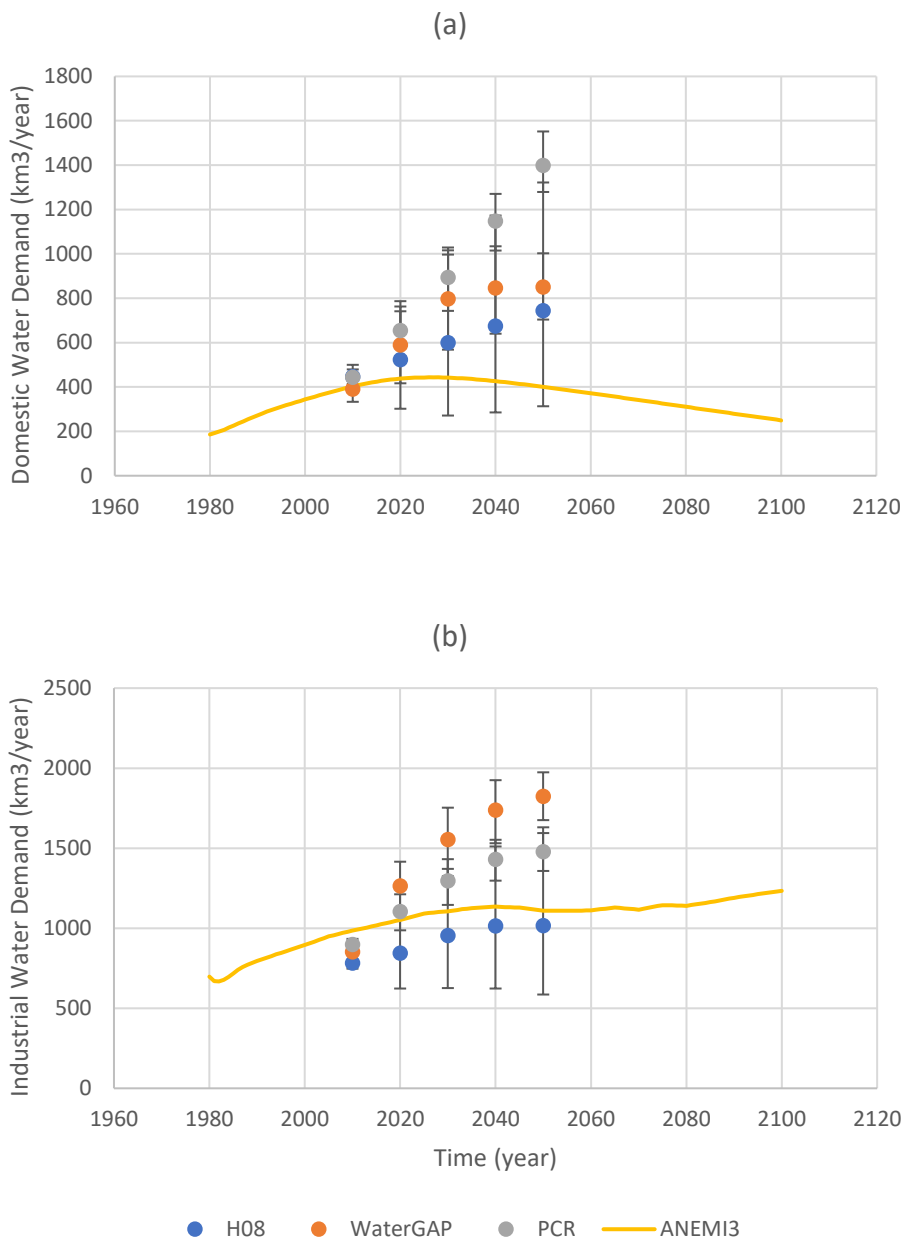


Figure 3.57. Comparison of (a) domestic and (b) industrial water demands from ANEMIS3 simulated values and model projections by Wada et al. (2016). Error bars represent the range in water demands resulting from the use of different shared socioeconomic pathways in each projection made in Wada et al. (2016).

From this comparison it is shown that the domestic water demands fall very close to those from the three other models in the year 2010. After this point, the domestic water demands in the

ANEMI3 are shown to be well below the average values projected by other models, but remains within the range of projections for the H08 model resulting from the use of different exogenous socioeconomic pathways. In the case of industrial water demands, the simulated ANEMI3 values are on the high end of the projections for the year 2010, and are in the mid-range of projections until the year 2050.

Agricultural water demand is driven mainly by irrigation. In this research the projected amount of irrigated land is compared against the exogenous scenarios provided by FAO (2018) (Figure 3.58). The projected values are a close match to the 2010 value at the start of the exogenous scenarios in the FAO (2018) report. The “Business as Usual” scenario depicts a substantial increase in irrigated area to 2025 which slows afterwards until 2050. The “Towards Sustainability” scenario assumes a drastic decrease in irrigated agriculture from 2010 to 2050. The baseline scenario of ANEMI3 projects irrigated agriculture area to be between these two scenarios, and continues increasing from 2050 to 2100. The agricultural water demand resulting from the expansion of irrigated agriculture also includes the effect of technological change in per hectare water withdrawals for irrigation, showing a decrease in agricultural water demand for all scenarios except for “Business as Usual” due to the rapid increase in irrigation area (Figure 3.58b).

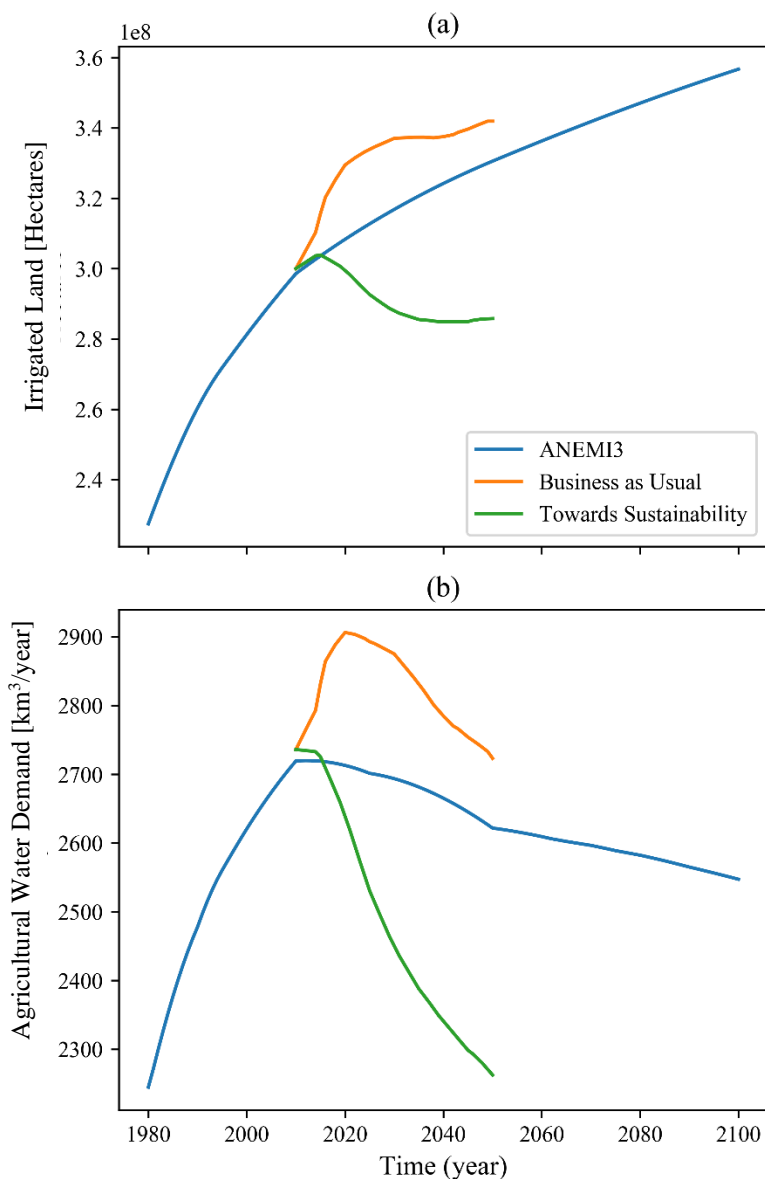


Figure 3.58. Comparison of (a) irrigated land area for agriculture and (b) agricultural water demand between ANEMI3 and irrigation scenarios by FAO (2018).

Simulated water supply rates for the ANEMI3 model and that of Wada and Bierkens (2014) are compared for surface and groundwater supply (Figure 3.59). The trajectories for both surface water and groundwater are similar, however the water supply rates are higher for surface water over the

duration of the simulation in Wada and Bierkens (2014). Groundwater supply rates are similar between the two models, but diverge after the year 2040. This is likely due to increased utilization of alternative water supplies in the form of wastewater reuse and desalination.

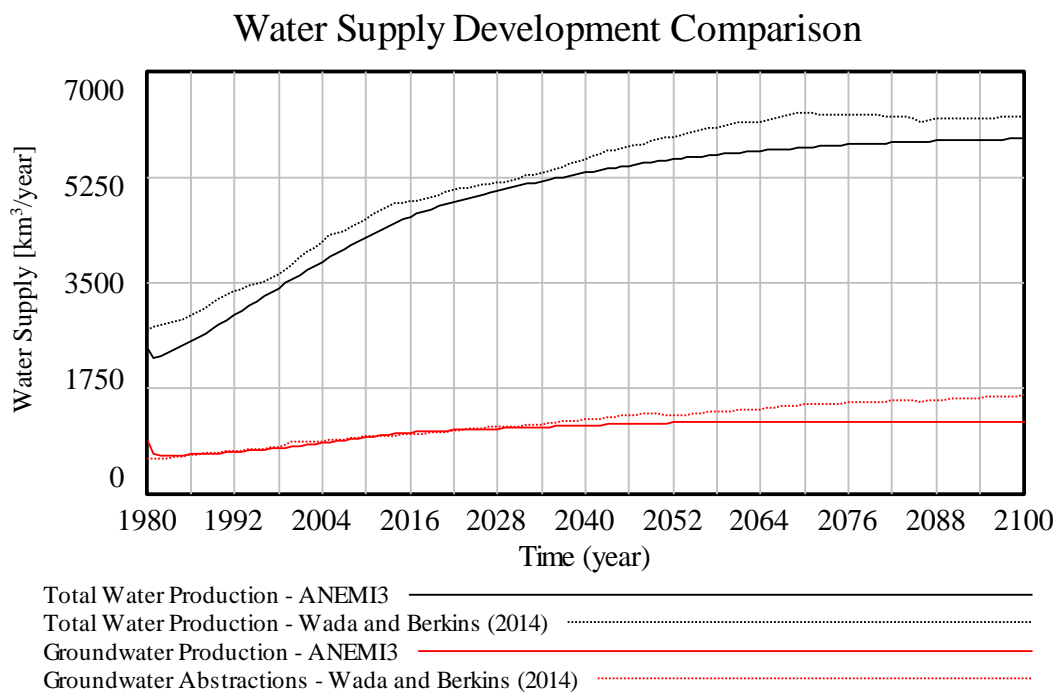


Figure 3.59. Comparison of projected surface and groundwater production rates between ANEMI3 and Wada and Bierkens (2014).

The development of desalination water supplies in the ANEMI3 model are compared to that of Hanasaki et al. (2016) and Fichtner GmbH (2011). From this comparison it is shown that the simulated values by the ANEMI3 fall within the range of the projection after the year 2010 (Figure 3.60). However, because the simulated values are slightly higher than the projections before 2005, the slope in desalination production is lower than the projections. Overall, the development of water supplies is comparable to that of future projections in the available literature.

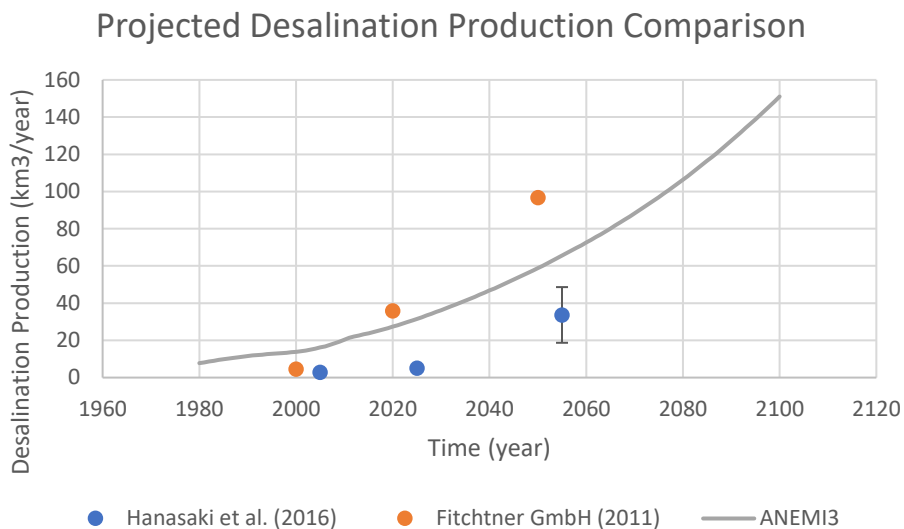


Figure 3.60. Comparison of projected desalinated water production.

Energy production for coal, oil and gas, hydro and nuclear, and renewable energy sources are compared amongst models in Figure 3.61. The ANEMI3 model uses a completely different model structure to represent energy production than in ANEMI2, while the GCAM results are based on energy production rates from the GCAM model for the period of 2005 to 2100 reported in Davies et al. (2013). For the production of energy from coal, The ANEMI version 2 and 3 values along with Ito et al. (2000) all start at similar values in 1980. After this point, all models show a steady increase in coal production over time, with the exception of the ANEMI2 model which has a peak in the year 2042 and 2100 (Figure 3.61a). In the case of energy production from oil and gas, it is the same case as coal regarding initial values. From this point all models show a similar increase until the year 2020 where the ANEMI3 model shows a peak in oil and gas production, and eventually decreases due to the effects of depletion and saturation. This effect is also present in the ANEMI2 model, except the peak is in the year 2055. The GCAM values for both coal as well

as oil and gas are significantly lower than the other models. and there is no peak in production for oil and gas with the GCAM model and Ito et al. (2000).

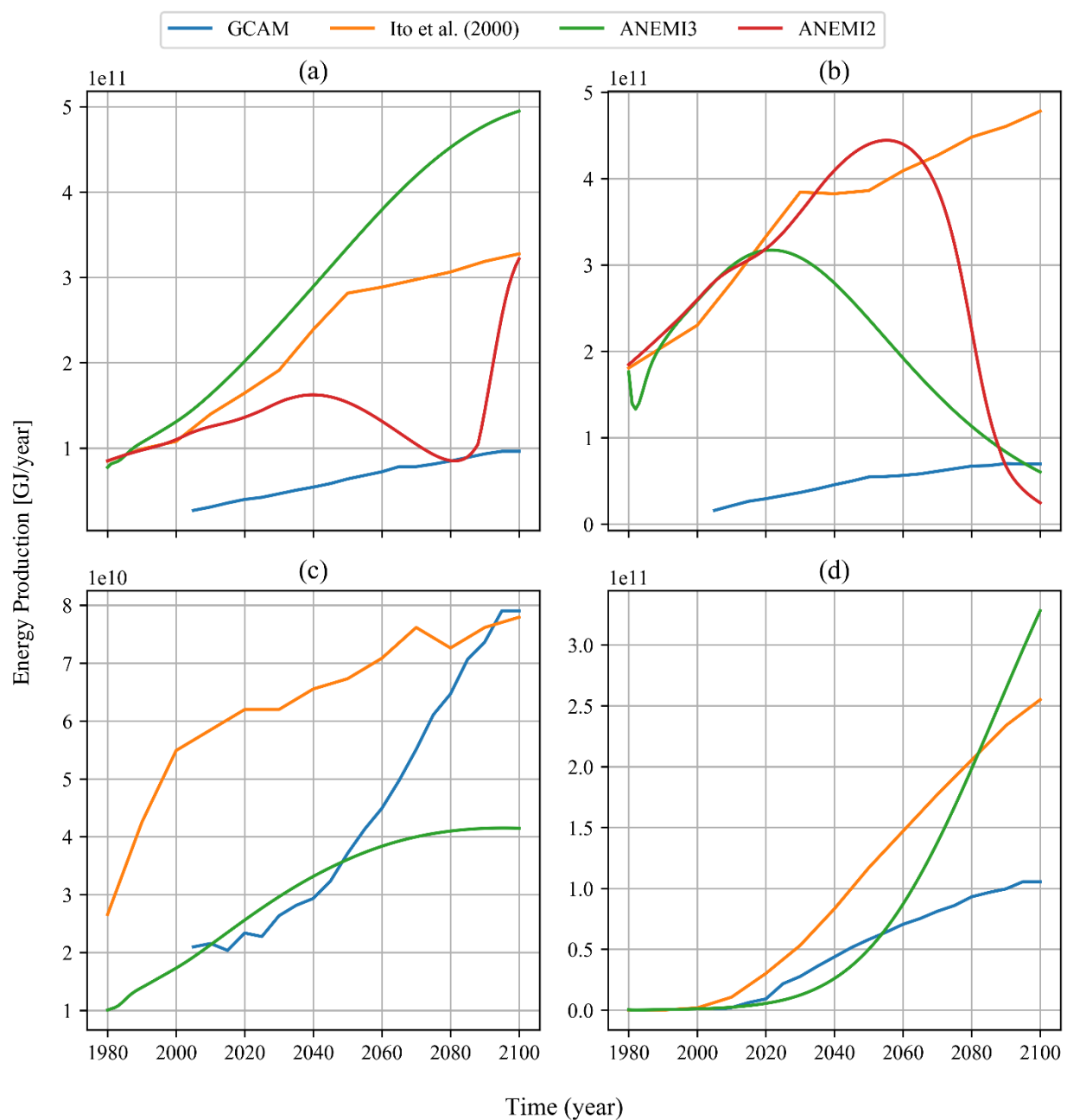


Figure 3.61. Energy production from (a) coal, (b) oil and gas, (c) hydro and nuclear energy, and (d) renewables.

Hydro and nuclear energy production in Figure 3.61c shows a large difference in initial values between ANEMI3 and Ito et. al (2000). However, from 2005 to 2045 the ANEMI3 values are similar to those projected by GCAM. After this point however, hydro and nuclear energy production in the ANEMI model starts to slow down, while the GCAM model shows an increase in production until 2095. Renewable energy production in all models (except for ANEMI2 as this value is not available) shows a similar trend, with the largest amount of increase in ANEMI3 and the smallest in GCAM.

### 3.5.3. Integration Error

Numerical integration of ordinary differential equations (ODEs) can result in errors when compared with analytical solutions. This is dependent on the time step being used, as well as the integration method. This is particularly true for ODEs that are considered stiff, or involve rapidly changing components together with slowly changing ones, whereby the appropriate time step is the one that solves the rapidly changing component to an acceptable degree of accuracy (Chapra 2008).

In the ANEMI3 model, a system of ODEs is being solved, including many that could be considered stiff. Therefore, the time step must be small enough so that integration errors are not artificially being introduced into the results. Roberts et al. (1983b) provide some guidance on the topic of numerical integration error in system dynamics models. As a rule of thumb, it was suggested that for positive feedback loops, a time step should be used that is one fifth to one tenth of the doubling time, while for negative feedback loops a time step should be used that is one third to one fourth



of the halving time. The difference in recommended time steps between the two types of feedback loops is due to the faster rates of change typically exhibited by positive feedback loops.

In order to test integration errors in the ANEMI3 model, the state variables that are used to represent the combined model state in Figure 3.50 are used. These variables are tightly coupled to all other sectors and state variables in the model. For the Earth system represented in ANEMI3, it is impossible to test true integration errors. However, the time step can be made to be small enough so that any changes in the state variables can be considered as errors from this point. It is assumed that the deviations shown from this set of state variables will be a good indicator of the numerical integration error present in the model under different time steps.

The maximum percentage error between the lowest time step used and the remaining time steps for each state variable is shown in Figure 3.62. Here it is shown that the maximum total error is generally decreasing as the time step decreases. The CO<sub>2</sub> concentration shows the highest sensitivity to changes in the time step used. This is because the carbon cycle uses the smallest time constants in the model to represent flow of carbon between biomass, litter, humus, and charcoal stocks. Temperature change shows the next most sensitive values, because they are mostly influenced by the carbon cycle through the atmospheric CO<sub>2</sub> concentrations. In the case of the time step being 1/128 years, as in the baseline scenario, the maximum total error is below 0.8%. Of this value, the largest error corresponds to the CO<sub>2</sub> concentrations which have an error of approximately 0.25%. The time step of 1/64 years was tested too, resulting in numerical instability of the model. This can happen when the time step is larger than the smallest time constant. Overall,

the maximum error in all time steps including the one that is used in the baseline scenario is very small, and thereby confirms the validity of the time step used.

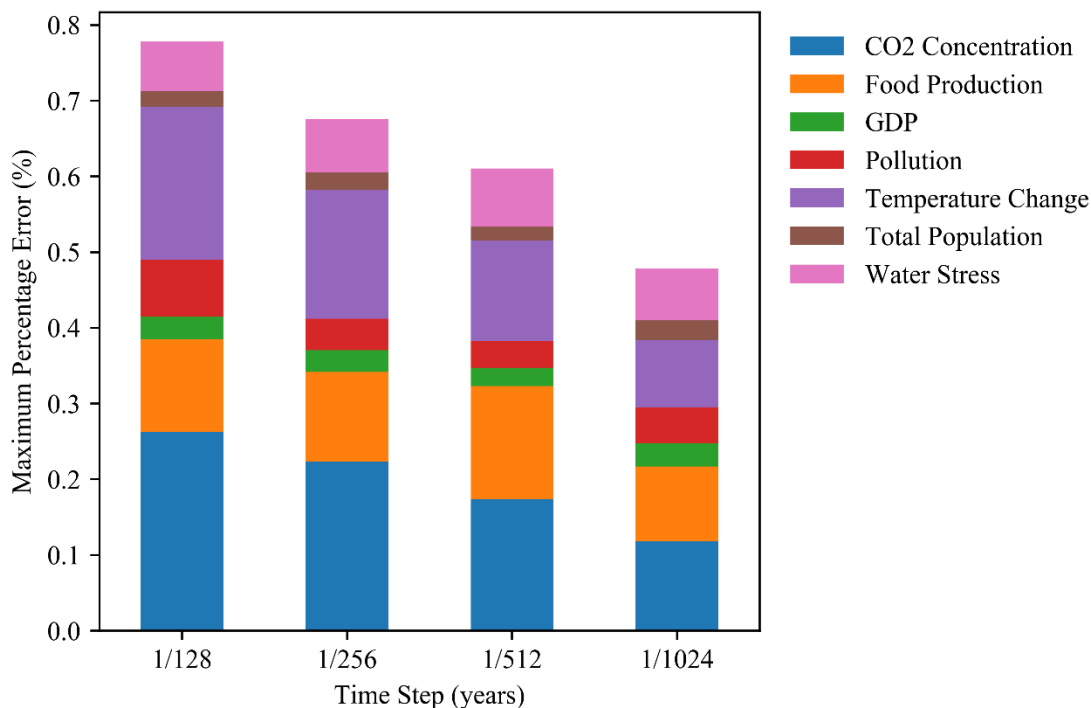


Figure 3.62. Maximum percentage integration error for selected state variables using varying time steps. Error is calculated based on the results provided by a time step that is 1/2048<sup>th</sup> of a year.

### 3.5.4. Sensitivity Analysis and Extreme Conditions

In system dynamics simulation models uncertainty is exhibited in many forms, including the parameters defining model constants, initial values, and the structure of the model itself (Breierova and Choudhari 1996). Often the parameters that are uncertain can be difficult or impossible to measure. When drawing conclusions, it is important to understand the sensitivity in parameter values that are either uncertain, assumed, averaged, or likely fluctuate over time. Sensitivity

analyses can be used to assess various forms of uncertainty in system dynamics models including numerical sensitivity, behaviour mode sensitivity, and policy sensitivity (Sterman 2000).

For this analysis, a set of variables were selected from the model to test the sensitivity of the main state variables. They are shown in Table 3.14. The selected parameters are chosen due to uncertainty in their values or the model structure for which they are used. This will determine whether the alternate types of model behaviour are possible by varying the assumed values of these parameters.

Table 3.14. Parameters used to test the sensitivity of key state variables in the ANEMI3.

<b>State Variable</b>	<b>Parameters</b>	<b>Minimum Change</b>	<b>Maximum Change</b>
Population	Water Stress Effects	-10%	+10%
	GDP Effects	-10%	+10%
	Food Production Effects	-10%	+10%
	Pollution Effects	-10%	+10%
Surface Temperature Change	Climate Feedback Parameter	-10%	+10%
	Base Precipitation Multiplier	-20%	+20%
Water Stress	Stable and Usable Runoff Percentage	-20%	+20%
	Wastewater Pollution Factor	-20%	+20%
	Energy Withdrawal Factors	-10%	+10%
	Specific Water Intake Factor for Agriculture	-10%	+10%
	Standard of Living Factor for Domestic Water Demands	-10%	+10%
Food Production	Cropping Intensity of Net Arable Land	-10%	+10%
	Processing Loss Fraction	-20%	+20%
	Average Life of Land	-20%	+20%
	Delay in Cultivation of Potential Arable Land		

Economic Output	Initial Global Capital Amount	-20%	+20%
Water Supply	Initial Surface Water Supply Capital	-20%	+20%
	Initial Groundwater Supply Capital	-20%	+20%
	Initial Wastewater Reuse Supply Capital	-20%	+20%
	Initial Desalination Supply Capital	-20%	+20%
	Initial Water Producer Prices	-20%	+20%
	Water Supply Construction Delay	-20%	+20%
	Water Elasticity	-10%	+10%
	Water Capital Substitution Elasticity	-10%	+10%
	Water Order Adjustment Coefficient	-10%	+10%
	Attractiveness Width	-10%	+10%
	Water Quality Share Parameter	-10%	+10%
Nutrient Surface Water Concentration	Phosphorus Removal Efficiency from Wastewater	-10%	+10%
	Nitrogen Removal Efficiency from Wastewater	-10%	+10%
	Phosphorus Leaching from Cropland	-20%	+20%
	Nitrogen Leaching from Cropland	-20%	+20%
	Phosphorus Wastewater Concentration	-20%	+20%
	Nitrogen Wastewater Concentration	-20%	+20%
Persistent Pollution	Initial Pollution Assimilation Half-Life	-20%	+20%
	Persistent Pollution Transmission Delay	-20%	+20%
	Technology Development Delay	-20%	+20%
	Industrial Material Toxicity Index	-20%	+20%
	Agricultural Material Toxicity Index	-20%	+20%

Monte Carlo analysis provides an efficient means to test the model sensitivity in this way, by assigning triangular probability distributions to the selected parameters. The highest point of probability in the triangle is assigned to the baseline value of these parameters, where the outer limits are defined by the minimum and maximum percentage changes to the baseline value. The maximum and minimum change assigned to each parameter for the sensitivity analysis is 20%. The

model is then run 200 times using input values sampled from these probability distributions, allowing for the distribution of the model output to be examined.

The sensitivity simulations are first performed separately for each of the state variables shown in Figure 3.63, using the associated input variables only. The results for each of the variables examined are shown as ranges for each confidence level. The 100% confidence level includes the range for a given variable including all outputs for the 200 Monte Carlo simulations. As the confidence level decreases the range of the projected variables becomes smaller. For each of the variables examined, the behaviour modes are the same within the range of the parameters tested. In the case of persistent pollution, the largest range was found, due to the parameters being changed by +/- 20%. Although this variable has a larger range in outputs, the behaviour mode is generally increasing due to the influence of population and economic outputs on persistent pollution generation rates. Pollution effects on population growth appear to be relatively small in that the range in population projection is much smaller than that of persistent pollution.

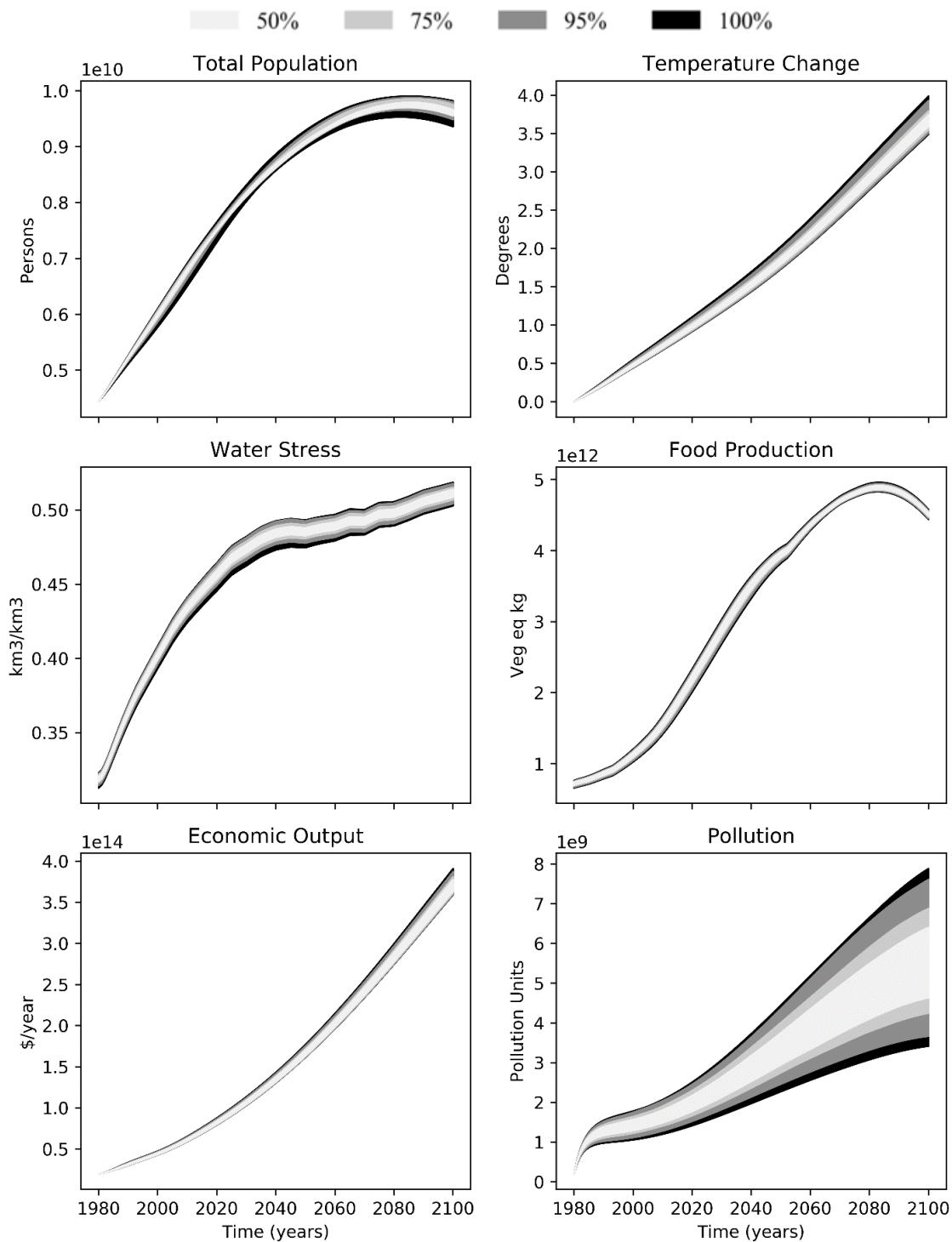


Figure 3.1. Sensitivity of selected state variables using Monte Carlo sensitivity simulation. Shaded areas represent confidence level associated with simulated model variable output.

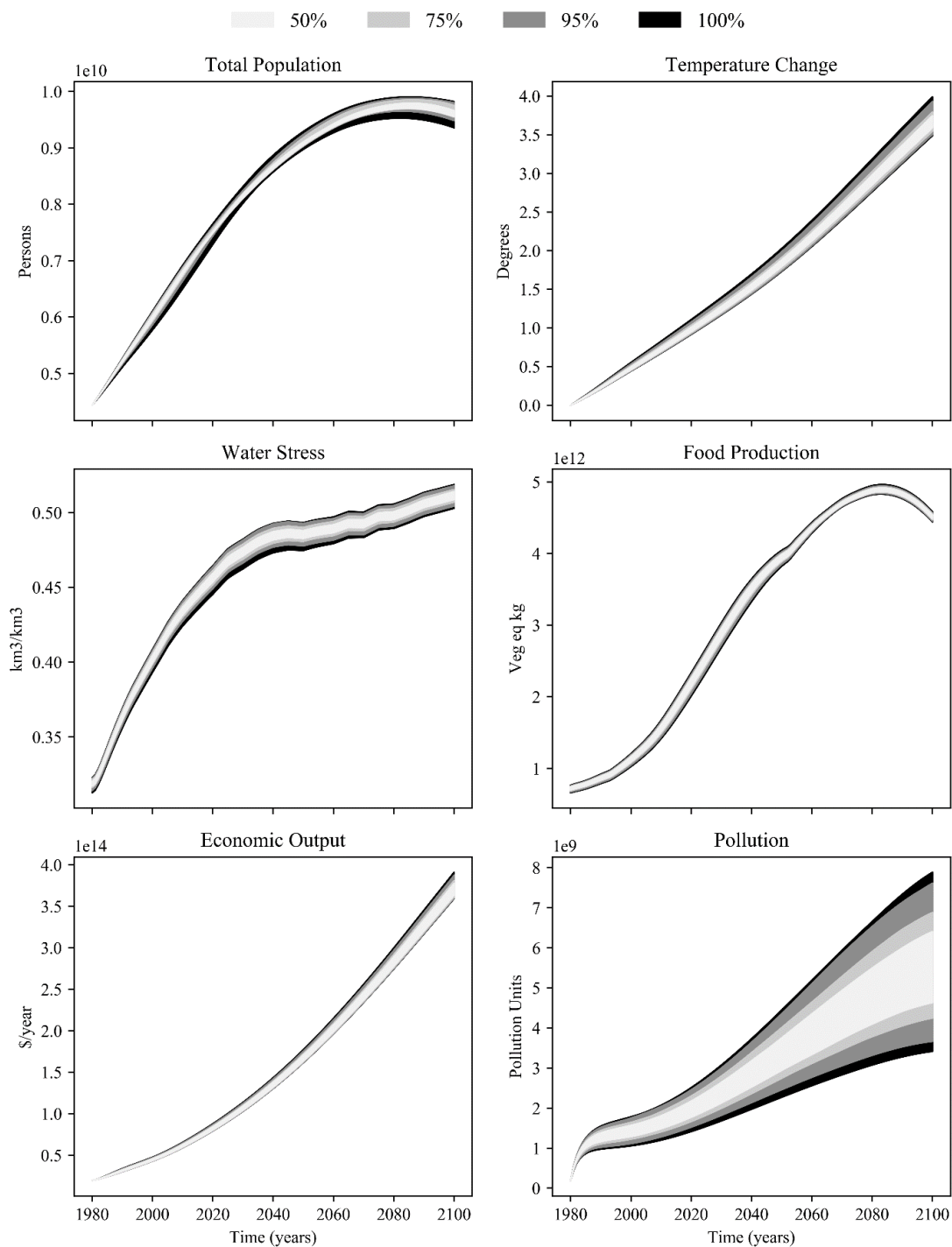


Figure 3.64. Total sensitivity of selected state variables using Monte Carlo sensitivity simulation. Shaded areas represent confidence level associated with simulated model variable output.

Considering all the possible parameter change combinations together, the range in the trajectory of the state variables is larger, however the behaviour of each variable still remains the same (Figure 3.64). The lack of changes in behaviour modes while testing model sensitivity is desirable, because it signifies that the model structure is robust, as well as the projections made when subject to uncertainties such as those used for the input parameters in the Monte Carlo simulation (Sterman 2000). This does not validate the model structure or parameters used in the sense of how well they represent the real world or how accurate future predictions may be. It only provides confidence in the model structure that is used.



## Chapter 4

### 4. Model Experiments

The set of scenarios explored within this Chapter were developed to address the research objectives of analyzing feedbacks between water supply development within the Earth system, assessing the role of conventional and alternative water supplies in adapting to water stress, evaluating potential limits to population growth, exploring the impacts of climate change, and the evaluating the economic impact on water supply development through water quality. Each experiment carried out in this section are related to the research objectives in Table 4.1 below. The baseline ANEMI run or “Baseline” as labelled in the figures presented in this section refers to the model result using the original parameter set without any modifications made. This baseline scenario is used as a point of comparison for the change in output for a given model experiment.

Table 4.1. Links between model experiments and research objectives.

<b>Research Objective</b>	<b>Experiment</b>	<b>Description</b>
<ul style="list-style-type: none"> <li>Examine the impacts of climate change throughout the Earth system</li> </ul>	<ul style="list-style-type: none"> <li>Climate Change Impacts</li> </ul>	<ul style="list-style-type: none"> <li>Use of RCP scenarios in the ANEMI model to illustrate range of climate change effects on food production, available water resources, and economic output</li> </ul>
<ul style="list-style-type: none"> <li>Evaluate potential limits to population growth through the depletion of natural resources (food and water) and the generation of pollution</li> </ul>	<ul style="list-style-type: none"> <li>Population Dynamics and Limits to Growth</li> </ul>	<ul style="list-style-type: none"> <li>Use of UN WPP population scenarios to gauge feedbacks on population due to changes in food supply, water stress, economic growth, and pollution generation through life expectancy</li> </ul>

	<ul style="list-style-type: none"> <li>• Food Production</li> </ul>	<ul style="list-style-type: none"> <li>• Tests the role of technological change, climate change, and FAO irrigation scenarios in meeting prescribed food production increase of the World Resources Institute</li> </ul>
<ul style="list-style-type: none"> <li>• Assess the potential impacts of water quality on the development of water supply</li> </ul>	<ul style="list-style-type: none"> <li>• Water Quality Effects on Water Supply</li> </ul>	<ul style="list-style-type: none"> <li>• Assess the effect of change in water quality on water supply development through reduced wastewater treatment</li> </ul>
<ul style="list-style-type: none"> <li>• Analyze feedbacks between water supply development and the Earth system</li> </ul>	<ul style="list-style-type: none"> <li>• Water Supply Development in the Context of Global Change</li> </ul>	<ul style="list-style-type: none"> <li>• Evaluated the response of the water supply development system to depletion of available water resources by 10%, 25%, and 50%</li> </ul>
<ul style="list-style-type: none"> <li>• Analyze the role of water supply development for conventional and alternative water supply in adapting to water stress</li> </ul>		

The details of each experiment along with the results are provided in the following sections.

#### 4.1. Climate Change Impacts

Climate change from the greenhouse effect is likely to raise the global average temperature by over 2 degrees C by the year 2100 relative to the 1850-1900 period (IPCC 2013). As a result, water in the hydrologic cycle is expected to move faster resulting in more extreme and frequent rainfall and streamflow. As ocean temperature rises more moisture will enter the atmosphere resulting in greater amounts of rainfall on land on average. Therefore, there will be more available surface water in total, but potentially less available water in time and space for human use due to the expected shifts in global rainfall patterns. Increased surface temperatures are also expected to be

linked to more frequent and severe heat waves that have the potential to increase mortality rates in young and elderly demographics in certain areas of the World. In addition, more areas will become feasible for new agriculture (King et al. 2018), potentially allowing for greater food production.

In this section the impacts of climate change on various components of the Earth system are explored. The main driver of climate change in the Earth system is greenhouse gas emissions, which are in turn driven by energy consumption from a growing population. In order to examine the range of global impacts due to climate change in the model, the RCP emissions scenarios (discussed in Section 3.5.2) are used and compared to the ANEMI3 baseline. This will allow for a range of climate change effects from changes in global surface temperature and precipitation to be examined.

Global surface temperature changes resulting from the RCP greenhouse gas emission scenarios are shown below (Figure 4.1). The resulting range of global surface temperature change is between 2 to 4.4 degrees by the year 2100. The temperature change in the RCP2.6 scenario shows an increase in temperature until the year 2060, after which temperatures slightly decrease. The RCP8.5 scenario is increasing almost linearly after the year 2045 until the year 2100. The changes in global surface temperatures are used in the hydrologic cycle of the ANEMI3 model to drive changes in precipitation amounts for rainfall and snowfall, as well as evapotranspiration (Figure 4.2).

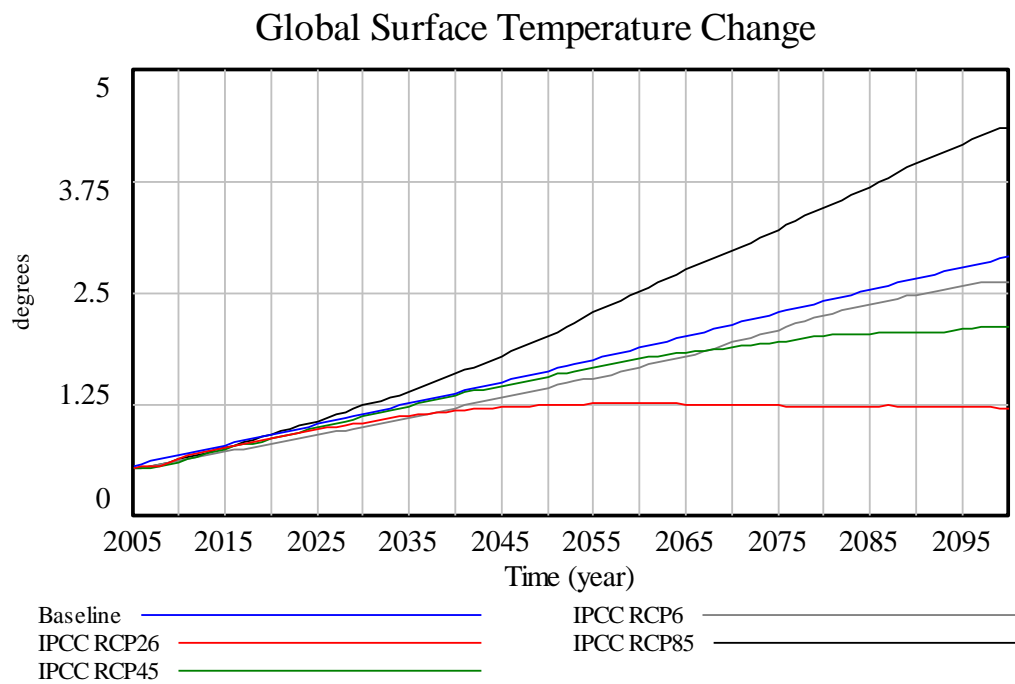


Figure 4.1. Global surface temperature change resulting from the baseline ANEMI3 run and RCP scenario runs.

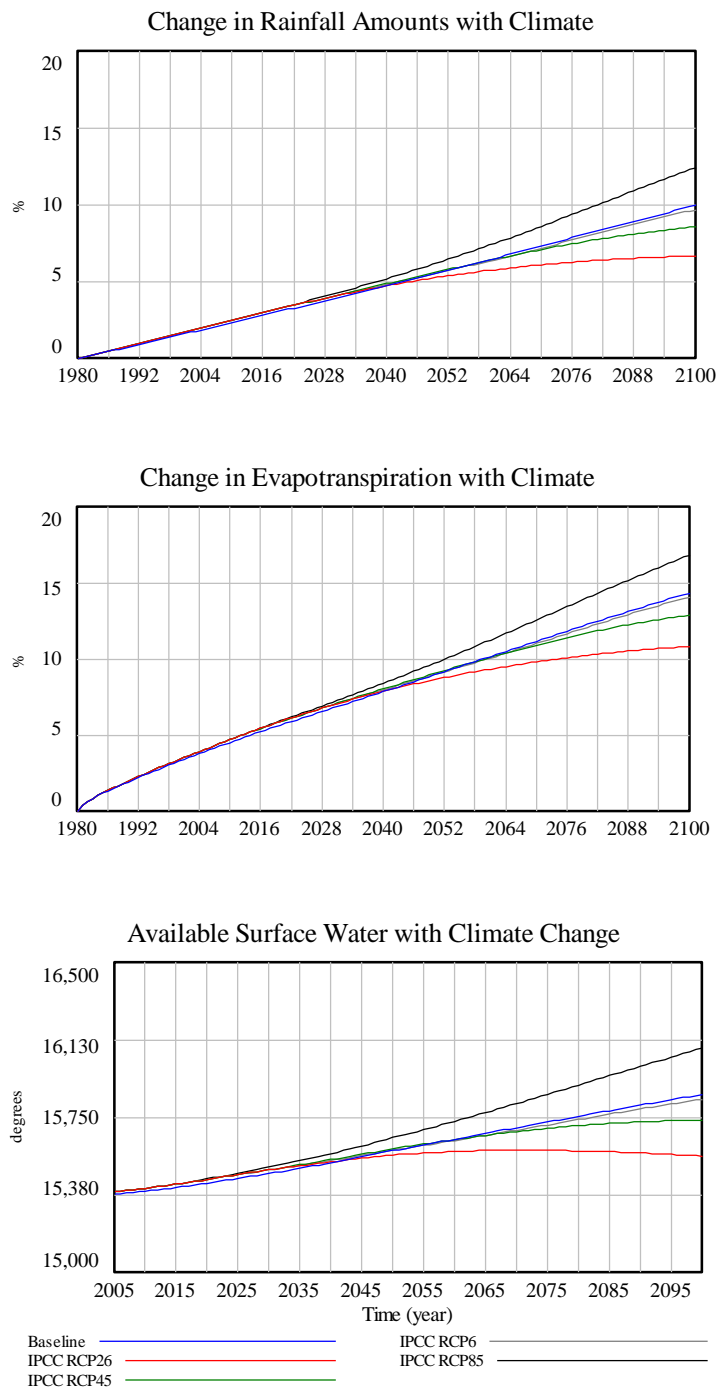


Figure 4.2. Changes of precipitation, evapotranspiration, and available surface water with five climate change scenarios.

Increases in global surface temperatures result in changes in precipitation amounts ranging from 11 to 16.5%, with the largest changes occurring for the RCP8.5 scenario. This is due to reduced amounts of snowfall on the land surface, as well as increase in ocean evaporation and evapotranspiration. Evapotranspiration increases between 7 and 13% as a result of increase in surface temperatures. The combined effect results in more available surface water from increase in streamflow ranging from 15,602 to 16,000 km<sup>3</sup>/year by 2100 up from the initial value of 15,240 km<sup>3</sup>/year. In the case of RCP2.6 the amount of available surface water decreases slightly after the year 2070 when the climate change signal is not as strong, however global surface temperature is still increasing slightly at this point (Figure 4.1). This is due to human consumption having a negative effect on available surface water, although the influence of climate on a global scale has a larger impact on the net result.

The effect of climate change on the net arable land is shown in Figure 4.3a. Overall, all climate change scenarios have a positive effect on net arable land, with an increase ranging from 0.5 to 0.8 billion hectares. This is because of increased arable land through conversion of boreal forests to agriculture as temperature increases (Figure 4.3b), along with the impacts of sea level rise on agricultural land (Figure 4.3c). Although sea level rise removes arable land from the net value as agricultural areas become inundated, the effect of utilizing new potentially arable land as a result of warmer climates in northerly regions is dominating. The land yield rates affect the amount of food that is produced from the net amount of arable land in the model (Figure 4.3d). In all climate change scenarios, land yield is reduced significantly via increase in global surface temperature as a result of heat stress.

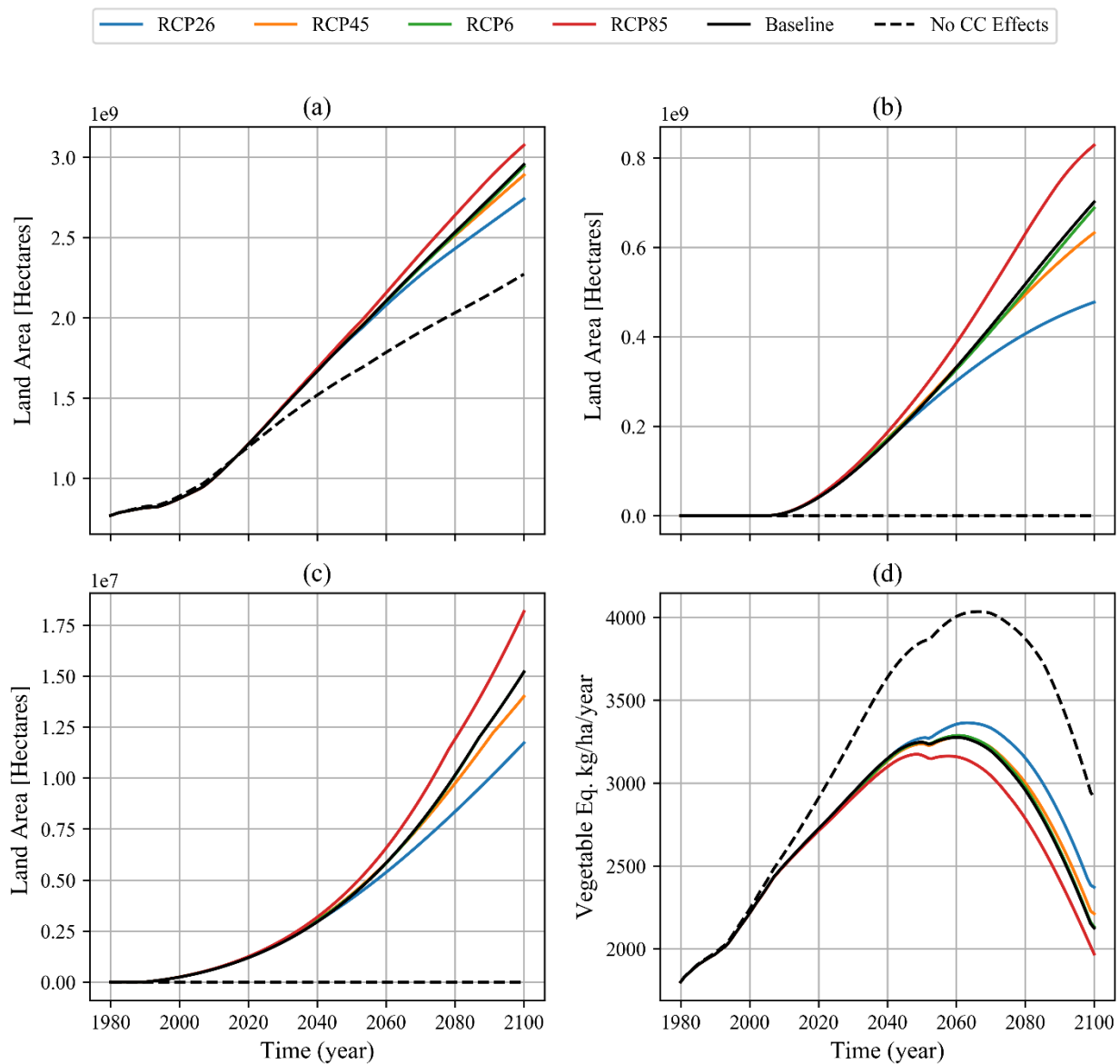


Figure 4.3. Effect of climate change on (a) net arable land and factors affecting food production including (b) increase in arable land through boreal forest conversion, (c) impacted agricultural land by the sea level rise, and (d) land yield.

The net effect of climate change on food production including changes in net arable land from sea level rise and arable land expansion, and land yield is shown in Figure 4.3.

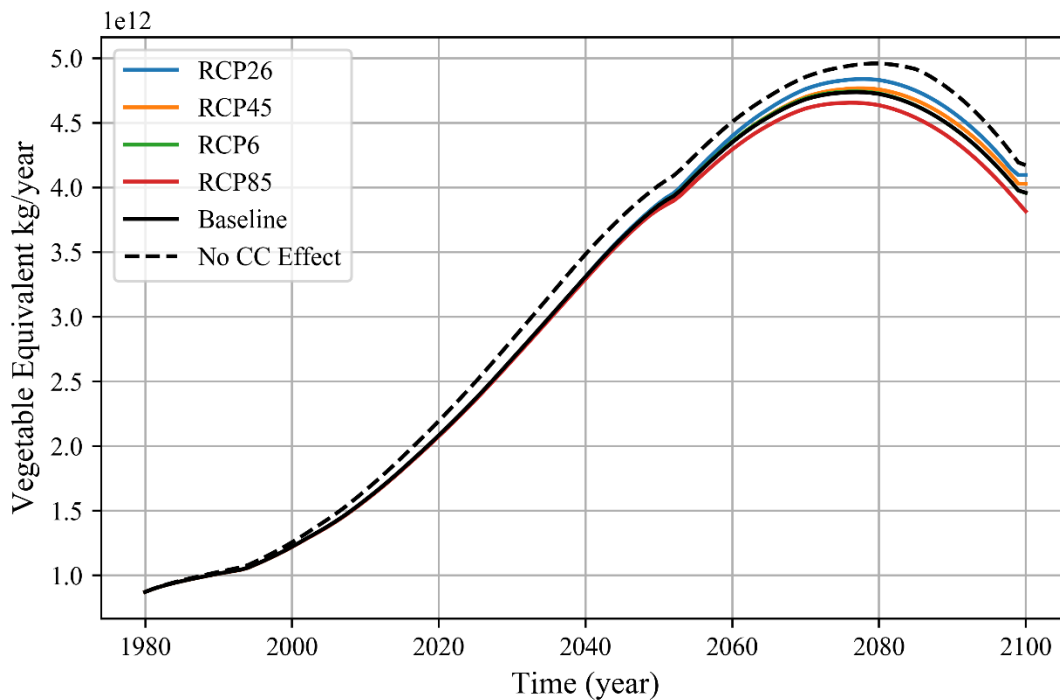


Figure 4.4. Net effect of climate change on food production including the effects of changes in net arable land and land yields.

Considering all the climate change effects included in the ANEMI3 model on food production, the result is a net decrease in food production corresponding to a maximum of 9% when comparing the RCP8.5 scenario to the scenario with no climate change effects applied (Figure 4.4). Climate change effects on land yield and net arable land balance themselves to a degree, but in this case the effects of reduced land yield are slightly stronger. It should be noted that there are uncertainties, spatial variations, and climate change effects that are not considered here. These are discussed further in Section 5. The food production in ANEMI3 overtime shows a behaviour mode of overshoot and decrease in all scenarios. This effect will be further discussed in the food production experiment of Section 4.5.



Economic impact of climate change and its effect on global economic output is represented by the climate damage function in the ANEMI3 model, shown in Figure 4.5.

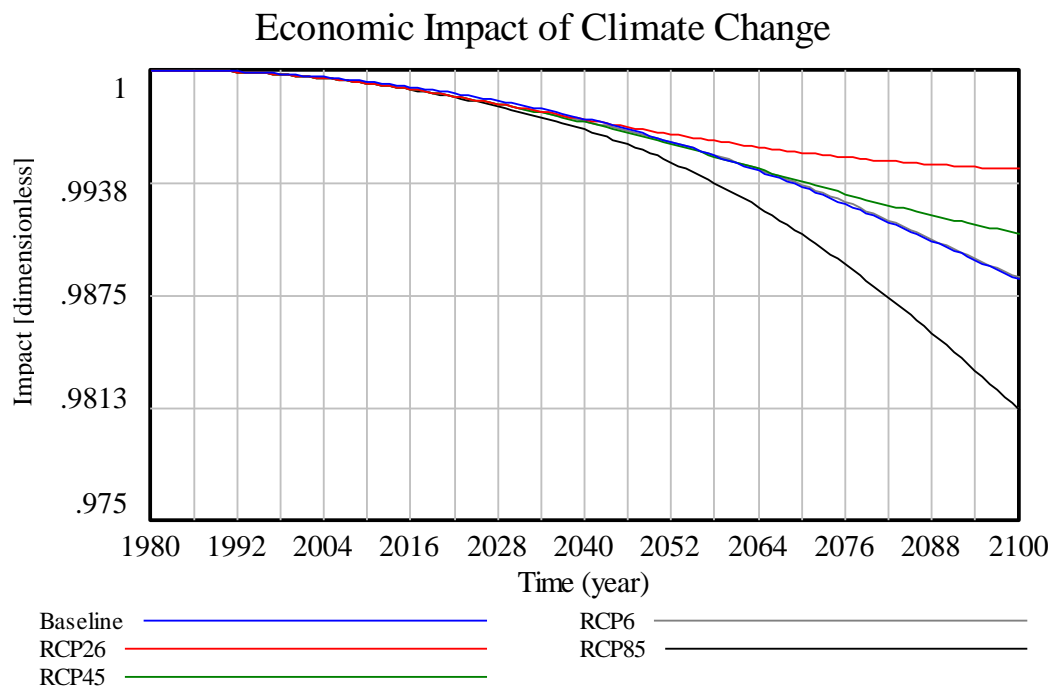


Figure 4.5. Climate damage functions.

The climate damage multiplier for representing the impact on economic output varies from 1 (no climate impact) in 1980 to a range between 0.994 and 0.981 for RCP2.6 and RCP8.5 climate scenarios in 2100, respectively. This represents almost a 2% reduction in global economic output per year, which corresponds to a value of 7.6 trillion 1980 US\$ for the RCP8.5 scenario. Under the RCP2.6 scenario, climate damages appear to level off by the year 2100, however in the case of RCP8.5 the negative slope is increasing. The baseline scenario follows a pathway that is almost identical to RCP6. This is due to the temperature changes being nearly the same between the ANEMI baseline and RCP6 scenarios as discussed in Section 3.5.2.

## 4.2. Population Dynamics and Limits to Growth

Human population growth is one of the most important factors driving global change. It is affecting all systems within the Earth system both physical and socio-economic and is driven by a positive feedback loop. Increase in population could result in food and water scarcity, as well as increase in pollution of air, water and land. All positive feedback loops in human and physical systems are eventually met with limits to growth in the form of negative feedbacks. The purpose of this experiment is to examine these potential limits to growth with respect to the dynamics of the human population.

Within the Earth system there are several limits to population growth in the form of negative feedbacks due to resource constraints, human health, and environmental degradation. Because of long delays that are intrinsic to this system, the effects of these negative feedbacks are not felt immediately. In the climate system, CO<sub>2</sub> persists long after the time of emission (~100 years) and even if an equilibrium is met in terms of resource consumption, climate change will continue to affect human populations in the form of heat waves, flooding, sea level rise, etc. Therefore, there exists the potential for overshoot and decrease behaviour for global population and oscillatory behaviour in attempt to reach an equilibrium as negative feedbacks on population growth become more prevalent.

The goal of this scenario is to evaluate the impact of increased population growth on the Earth system and to identify the key negative feedbacks that could potentially act as limits to population growth. In order to analyze this behaviour, exogenous scenarios for population were simulated in

addition to that of the endogenous baseline scenario of ANEMI3. The exogenous scenarios used to test the effects of changes in population on the global system are taken from the 2019 revision of the UN World Population Prospects (UN WPP) report (United Nations 2019c). These scenarios are defined by projected variants in fertility, mortality, and migrations rates to the year 2100. The negative feedbacks on population for food, water, and pollution in the endogenous ANEMI3 baseline scenario do not affect the population projections of the exogenous scenarios. This allows for the extent of these feedbacks to be explored. Life expectancy rates are given in Figure 4.6.

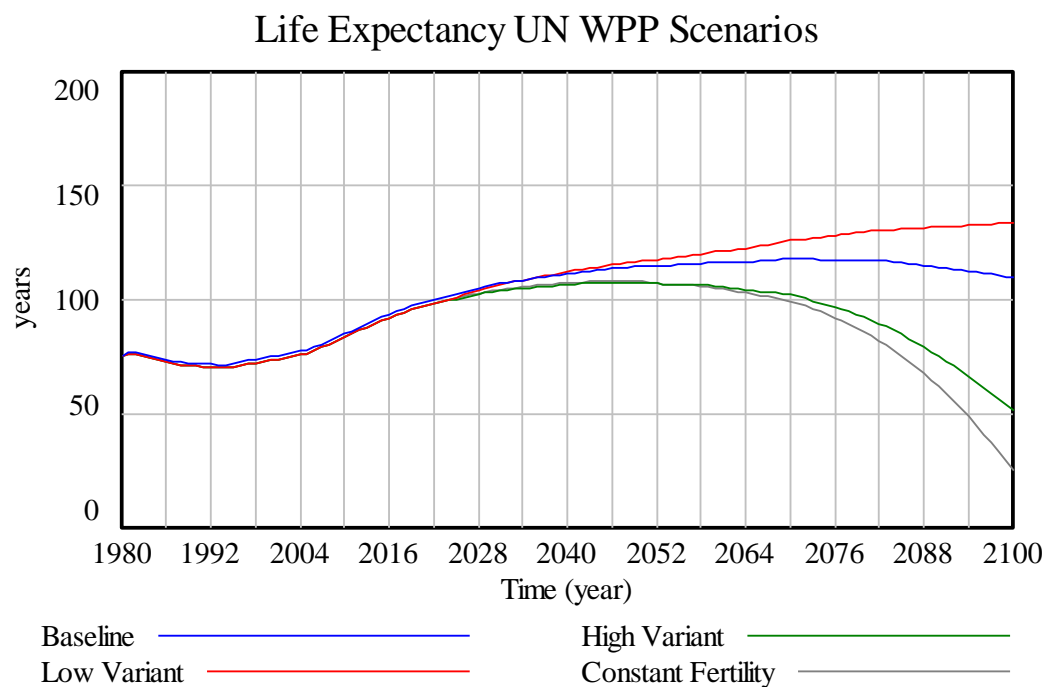


Figure 4.6. Life expectancy values for ANEMI3 baseline and UN WPP scenarios.

It should be noted that the life expectancy values shown are not necessarily meant to be accurate predictions when it comes to absolute values. Life expectancy acts as a multiplier on mortality rates in the population sector and there are other parameters used to obtain realistic population projections in the form of fertility rates for example. The value in viewing the life expectancy

results is in the long-term dynamics experienced by negative feedbacks acting on population growth. With that said, the life expectancy values start at approximately 75 years, and drop slightly before increasing to when the population scenarios diverge. The highest population scenarios (high variant and constant fertility) level off in 2050 and drop rapidly, while the baseline scenario stabilizes, and the low variant population scenario increases to 2100. Decreases in life expectancy result from negative feedbacks relating to pollution and resource constraints such as food and water. Increases come in the form of economic development increasing the quality and extent of health services to the population.

The relative impact of these factors on life expectancy is shown in Figure 4.7 for the baseline and constant fertility scenarios. The constant fertility scenario was selected as it results in the highest population by 2100. In both scenarios, the economic, water stress, food supply, and pollution effects on life expectancy remain almost the same until the year 2050. After the year 2050, the negative feedbacks on life expectancy from food supply, water stress, and pollution intensify for the constant fertility scenario. By incorporating this constant fertility scenario exogenously into the ANEMI3 model, the negative feedback multipliers are not able to act on population and continue to magnify. The economic effect represents a positive feedback loop because population growth would increase labor force and economic output in the economy sector, thereby increasing health service quality and extent, further boosting population. This effect however is not strong enough to compete against the negative feedbacks on population growth.

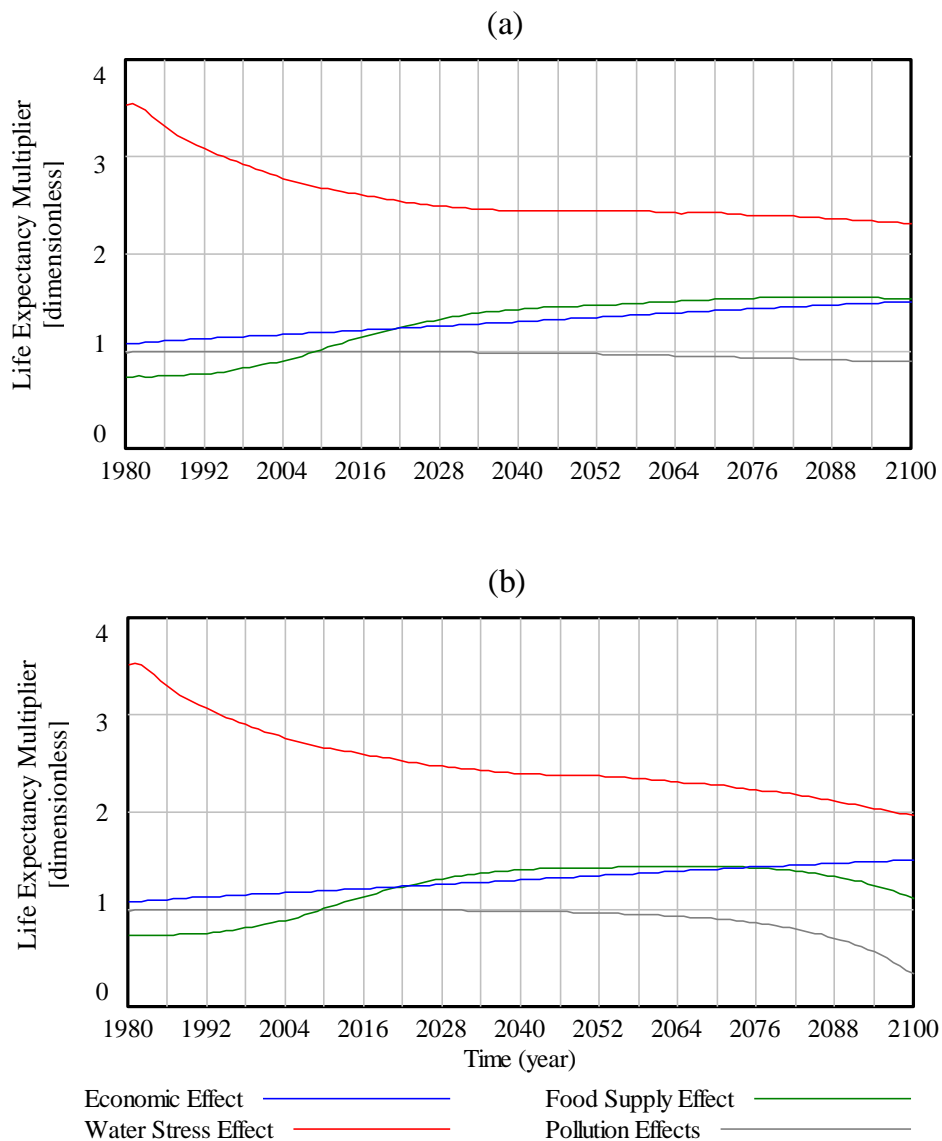


Figure 4.7. Life expectancy multipliers in ANEMI3 for (a) baseline and (b) constant fertility scenarios.

Population growth affects all levels of water demand. In the case of domestic water demand, the effect is more direct in that each individual of the population has a water requirement. In the case of industrial demands, this is primarily based upon global capital growth as energy requirements. Agricultural demand is mostly determined by the amount of irrigated agricultural area present and

not necessarily food production. This is because technological change in the food production sector leads to lower water withdrawals per hectare of agricultural land. The water demand from the population scenarios is shown in Figure 4.8.

Domestic water demand generally peaks around 2020 and then decreases to the year 2100 due to decrease in domestic structural water intensity as a result of global economic growth (Figure 4.8c). After the year 2050 however, water demand increases rapidly in the constant fertility scenario. The timing of this increase corresponds to the sharp increase in population in the constant fertility scenario. The high variant scenario also shows increase in population up to 2100, however the increase does not change the general shape of the global domestic water demand curve. The only other variable used to calculate domestic water demand is the per capita withdrawals based on economic output, and this factor is not strongly affected by population changes. This means that the reason for the difference in domestic water demand for the constant fertility scenario is that it is the only scenario that reaches the point where population growth outpaces technological change.

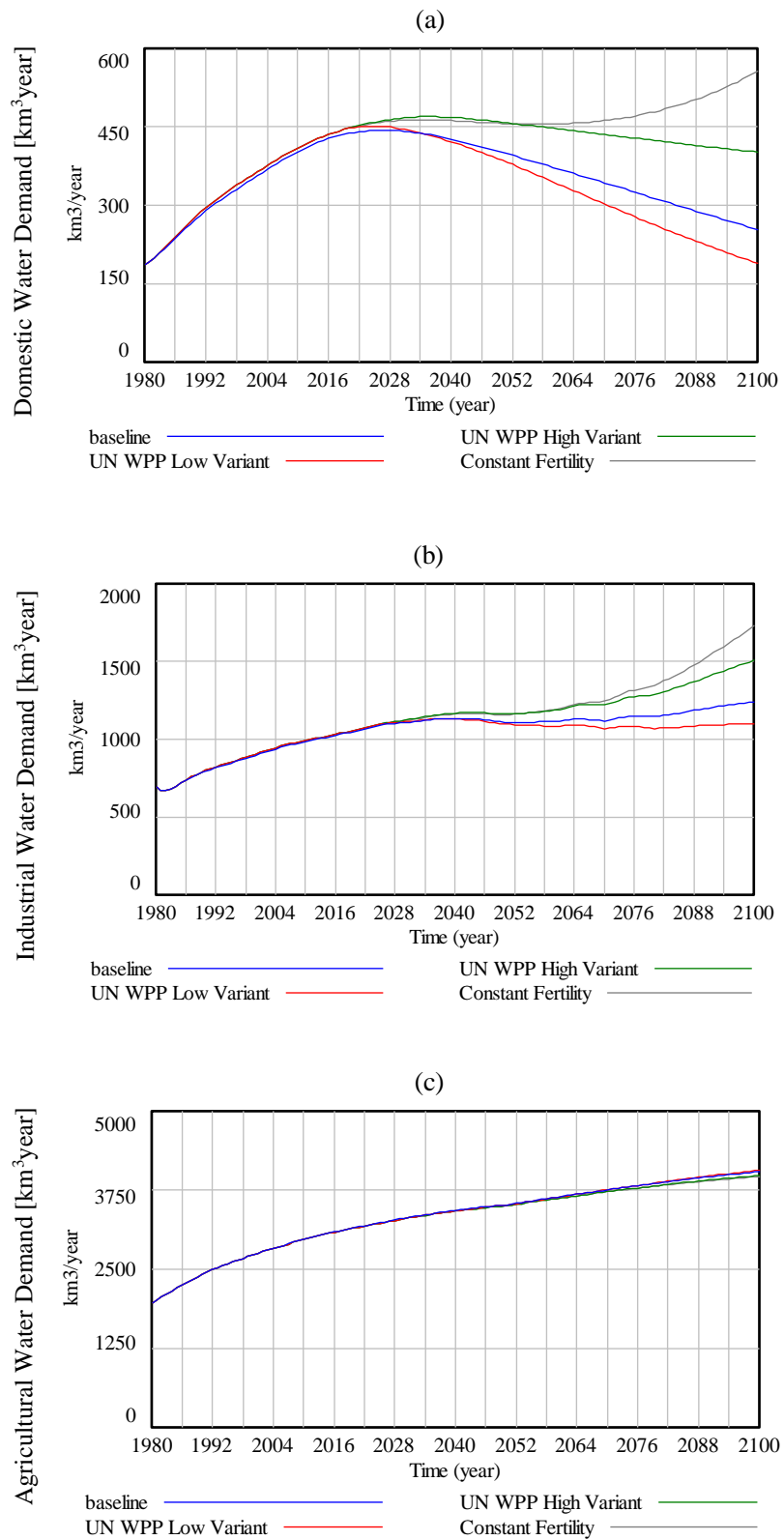


Figure 4.8. Influence of population change on (a) domestic, (b) industrial, and (c) agricultural water demands.

### 4.3. Water Quality Effects on Water Supply

Water quality in ANEMI3 is represented by the changing concentrations of nutrient levels in surface waters. It acts as a multiplier that increases the supply price of surface water resources through hypothesized cost of increased treatment. This hypothesis is supported by the studies mentioned previously (Eikebrokk et al. 2004; Ritson et al. 2014), but the extent of this effect is unknown and has never been looked at on a global scale. In addition to increased nutrients, wastewater inputs also render a portion of water resources unusable for the purpose of water supply as shown in Equation 3.71, thereby contributing directly to water stress. If water quality becomes severely degraded in the future on a global scale, costs to produce water supplies could increase if technology does not progress fast enough to address potential treatment issues. Because of this, it is hypothesized that alternative water supplies may become more attractive and play a larger role in the future. The nutrient inputs to surface water are shown in Figure 4.8.



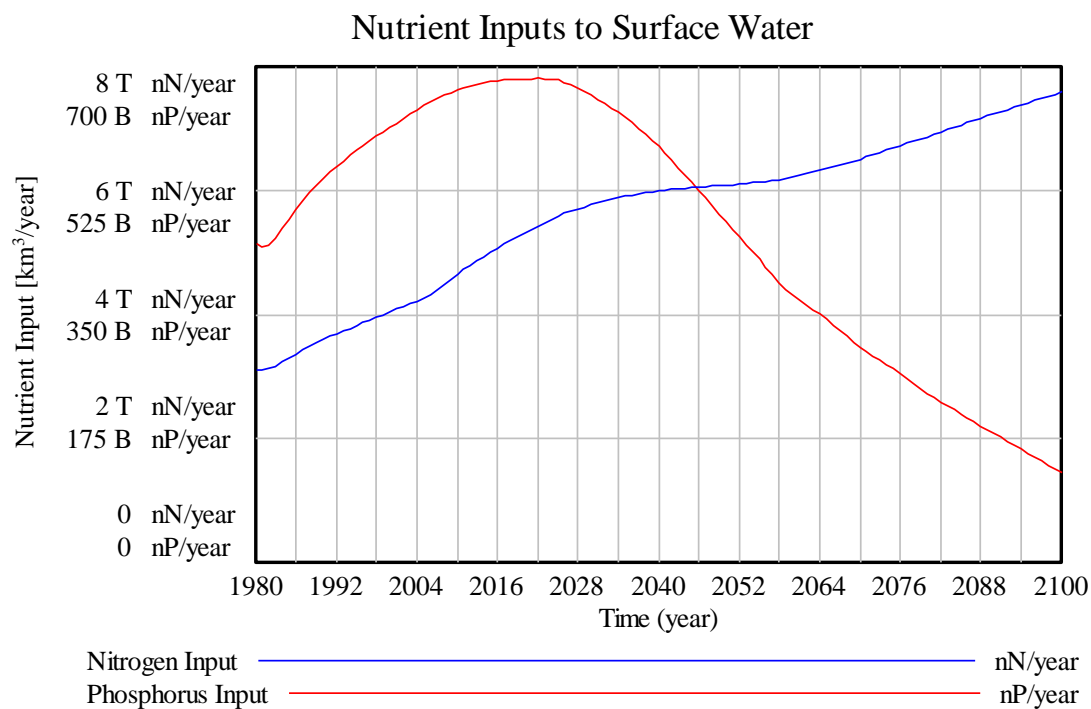


Figure 4.9. Total nitrogen and phosphorus input to surface water under the ANEMI3 baseline scenario. Left axis represent number of moles of nitrogen and phosphorus inputs to surface water per year.

The input of nitrogen to surface waters is increasing throughout the baseline simulation starting at an initial rate of 3.1 trillion moles or 4.3 Mt per year to a rate of 7.6 trillion moles or 10.5 Mt per year (Figure 4.9). Input of phosphorus to surface waters on the other hand, increases from 451 billion moles or 13.5 Mt per year to a peak value of 681 billion moles or 20.4 Mt per year in the year 2025. After this point phosphorus input decreases significantly, down to 126 billion moles per year.

The reason for the difference in the pattern of nitrogen and phosphorus inputs lies in their respective amounts in different sources. For nitrogen, on a global scale, agriculture is the main

anthropogenic supplier of nutrients to surface waters, while domestic and industrial wastewaters are the main supplier of phosphorus. Phosphorus input decreases after the year 2025 due to increasing levels of wastewater treatment on a global scale, which reduces the input significantly. The levels of treated and untreated wastewater are shown in Figure 4.10.. Initially, the amount of untreated wastewater is greater than treated on a global scale in 1980. Under the ANEMI3 baseline scenario, wastewater treatment increases from the initial rate of 160 km<sup>3</sup>/year and surpasses that of the untreated percentages in 2010. After this point, treatment rate increases further to approximately 550km<sup>3</sup>/y.

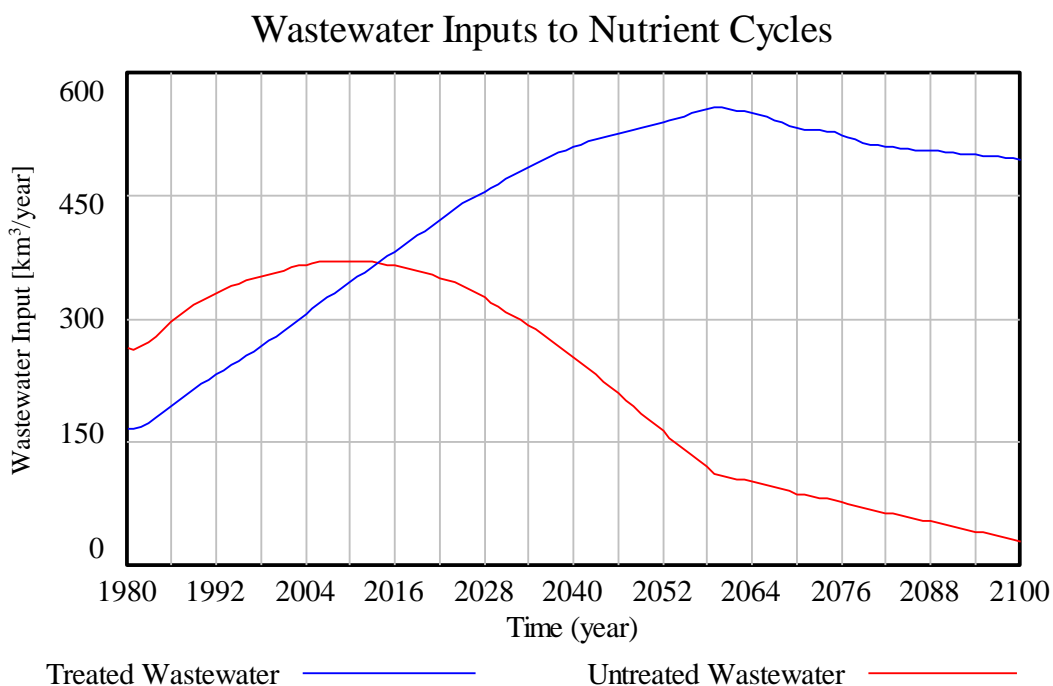


Figure 4.10. Treated and untreated wastewater inputs to the nutrient cycles over time.

Nutrient inputs act as an additional rate that affects the surface water stock in the nutrient cycle model. Combining this with the stock of surface water in the hydrologic cycle model allows for the concentrations of nutrients in surface water on a global scale to be examined, as shown in

Figure 4.11.. The concentration considers changes in hydrologic cycle. The patterns are almost the same because the global amount of streamflow does not change very much due to climate change increase and surface water consumption having a balancing effect in the ANEMI3 baseline scenario.

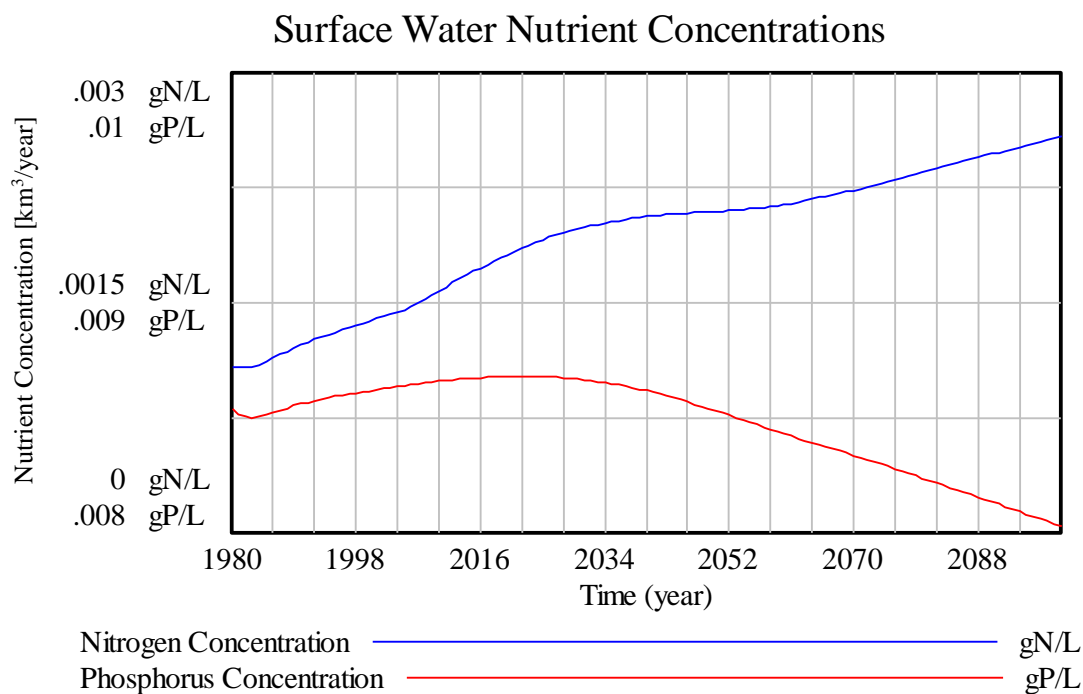


Figure 4.11. Surface water nutrient concentrations of nitrogen and phosphorus.

The impact of surface water quality on water supply development was tested by setting the wastewater treatment level for domestic and industrial wastewater treatment as constant for the duration of the simulation. This corresponds to a global treatment rate of 49 km<sup>3</sup>/y and 118 km<sup>3</sup>/y for domestic and industrial water use, respectively. The resulting surface water nutrient concentrations are shown in Figure 4.12..

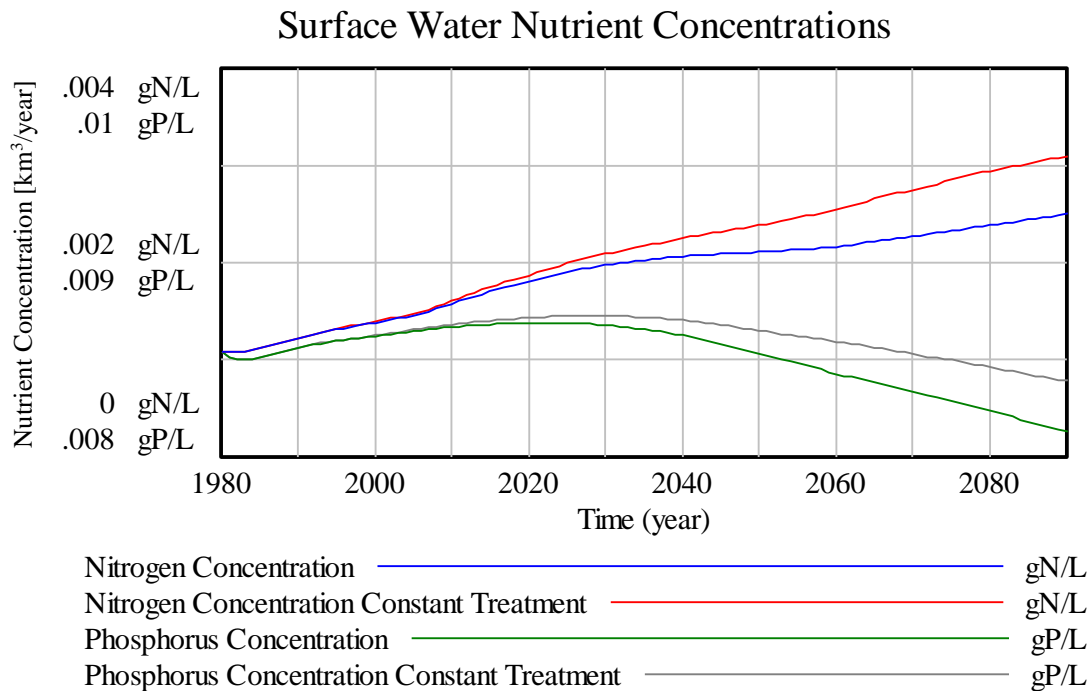


Figure 4.12. Surface water nutrient concentrations under the ANEMI3 baseline and constant wastewater treatment scenarios.

Nutrient concentrations are higher when constant wastewater treatment is implemented, rather than exogenous increase in the ANEMI3 baseline scenario. Nutrient concentrations are used as an indicator for water quality in the production of surface water supplies, whereby higher concentrations act as a multiplier to the surface water production costs. The effect of constant wastewater treatment on water supply development is shown in Figure 4.13. Under this scenario, the establishment of surface water supplies is only slightly affected by the change in surface water quality on a global scale (Figure 4.13a). Under the ANEMI3 baseline parameterization scheme, water quality does not appear to play a significant role in the establishment of surface water supplies, even if wastewater treatment levels are held at constant 1980 values for the entire simulation. Both wastewater reuse and desalination supplies show major increases from 1980 to

the year 2100. Wastewater reuse increases from 10 to 280 km<sup>3</sup>/year, while desalination increases from 10 to 75m<sup>3</sup>/year, although the absolute numbers are small in comparison to conventional water supplies. With reduced wastewater treatment rates there is a major difference in the level of wastewater reuse, as there is less available wastewater resource to be used (Figure 4.13b). Due to scarce wastewater for reuse there is a drop from 274 km<sup>3</sup>/year to 143 km<sup>3</sup>/year by the year 2100.

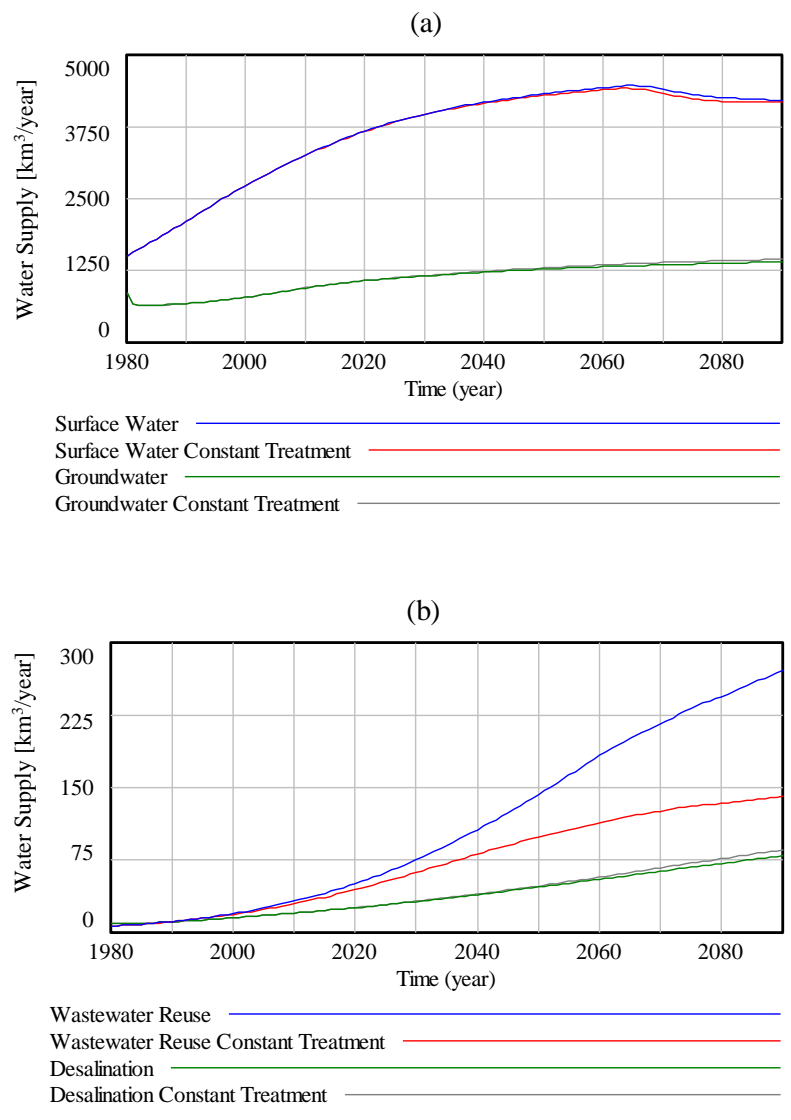


Figure 4.13. Development of water supplies under the baseline and constant wastewater treatment scenarios for (a) conventional water supplies and (b) alternative water supplies.

#### 4.4. Water Supply Development in the Context of Global Change

Growing populations and industrial output will increase the demand for water in the domestic, industrial, and agricultural sectors, thereby increasing the pressure on freshwater resources. It is expected that these resources will become increasingly stressed overtime, such that the ratio of demand to available water resources will increase. In order to overcome water stress, alternative supplies in addition to conventional surface water and groundwater will be needed, such as desalinated water and the wastewater reuse. The ability to analyze the distribution of water supplies through time will provide insight as to when the water resources become stressed, and to what degree alternative water supplies will be needed in the future.

The production of water supplies in the ANEMI3 is driven economically through the investment in capital stocks for each source, representing the current level of infrastructure that is in place to support production. For example, the capital stock for surface water supply represents dams and reservoirs, drinking water treatment facilities, distribution networks, pumping stations etc. By taking an economic approach to the production of water supplies a feedback loop is created between water production and the overall economy. If a significant amount of investment is required in order to produce the level of water supplies required to sustain global populations, then there is less money invested in capital for the production of goods and services. This could lead to a trickle-down effect where reduced economic output increases domestic and industrial structural water intensities in the model, thereby increasing water stress, creating a positive feedback loop.

The development of water supplies for surface water, groundwater, wastewater reuse and desalination under the ANEMI3 baseline scenario are shown in Figure 4.14.

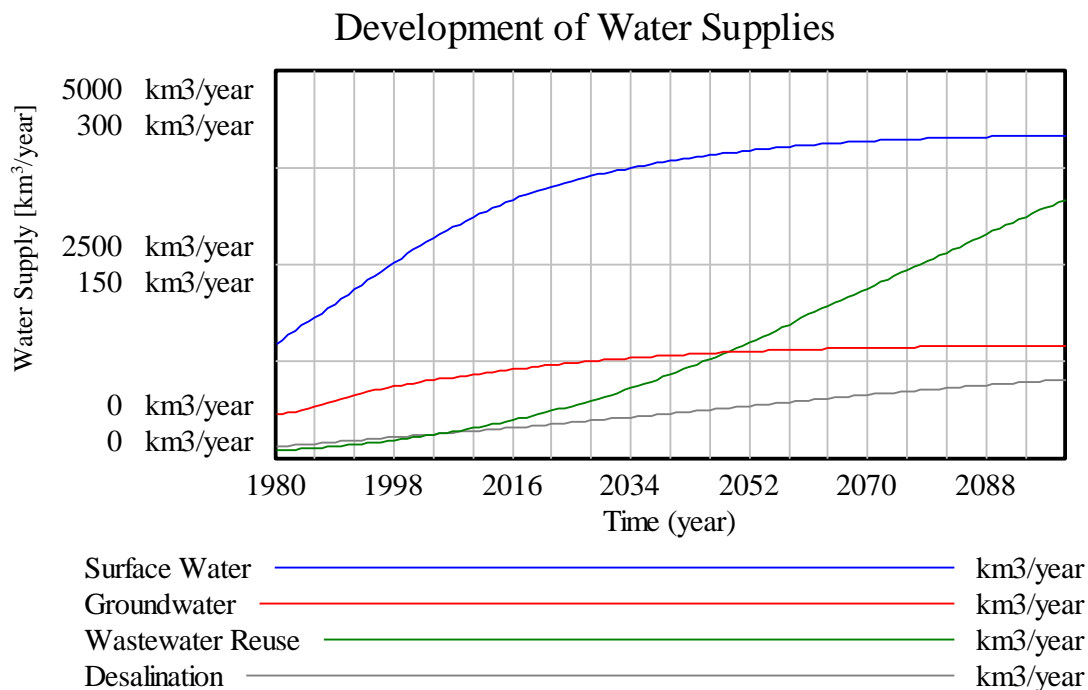


Figure 4.14. Development of water supplies in the ANEMI3 model. The upper scale labels are used for surface water and groundwater supply while the lower labels are for wastewater reuse and desalination.

Surface water supplies on a global scale have made up the largest fraction of water supply along with groundwater resources. This is because they are the least costly to find and extract, and there is much more capital currently invested in these supply types. However, in places where rivers or streams are not present groundwater may be a cheaper option especially if the quality of the surface water is poor. Surface water supplies start at an initial value of 1504 km<sup>3</sup>/year and climb to a maximum of 4422 km<sup>3</sup>/year. Groundwater supplies increase at a much slower rate from 877

km<sup>3</sup>/year to 1439 km<sup>3</sup>/year. Both wastewater reuse and desalination supplies increase at a rate that is much faster than surface and groundwater, however the amounts of which are also much smaller initially, with wastewater reuse and desalination reaching 292 and 87 km<sup>3</sup>/year by the end of the century, respectively.

Surface water supplies are the dominant source of water supply globally for the ANEMI3 baseline run. This is because the supply is relatively inexpensive and abundant, compared to the other water sources on a global scale. However, this is not always the case on a regional level. There are many areas of the world where either surface or groundwater resources are currently depleted or unavailable in time and space, thus prompting the use of alternative water resources, such as desalination and wastewater reuse.

To test the effects of depletion on the global water supply development scheme, available surface and groundwater resources have been reduced by 10%, 25%, and 50% linearly over the duration of the simulation. This effect is shown for conventional water supplies in Figure 4.15. By artificially reducing available groundwater and surface water resources used for the development of supply, the effect of depletion occurs. This acts to increase production costs, causing less surface and groundwater supplies to be developed. The reductions applied for 10%, 25%, and 50% of available surface water resources causes production to drop progressively earlier in the simulation run and by larger amounts. The same can be observed for the depletion effect of groundwater supply development, but to a lesser extent. In the case of alternative water supplies, there is a little change in the global production levels of desalination and wastewater reuse (Figure 4.16).



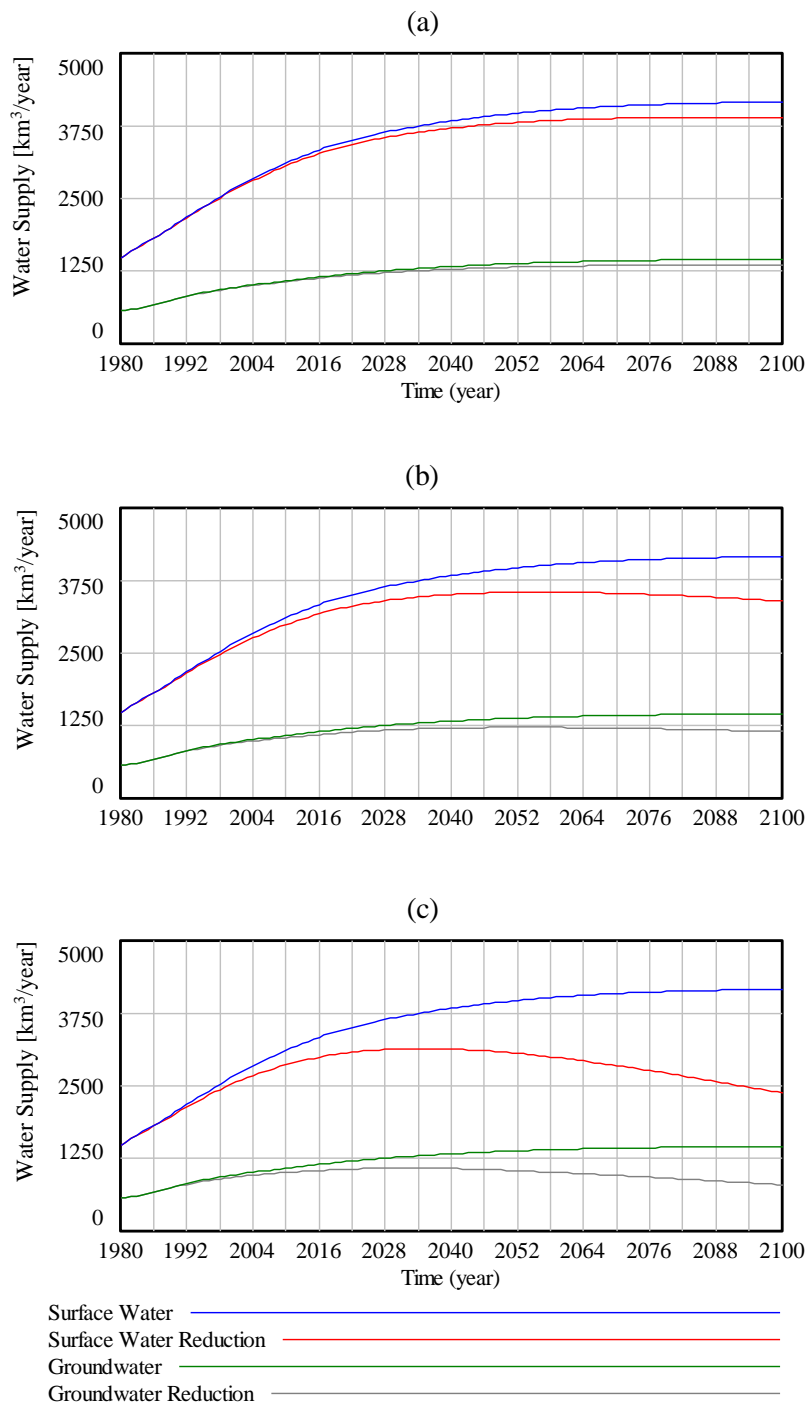


Figure 4.15. Depletion effects on conventional water supplies for (a) 10%, (b) 25%, and (c) 50% reduction in available water resources compared to the ANEMI3 baseline scenario.

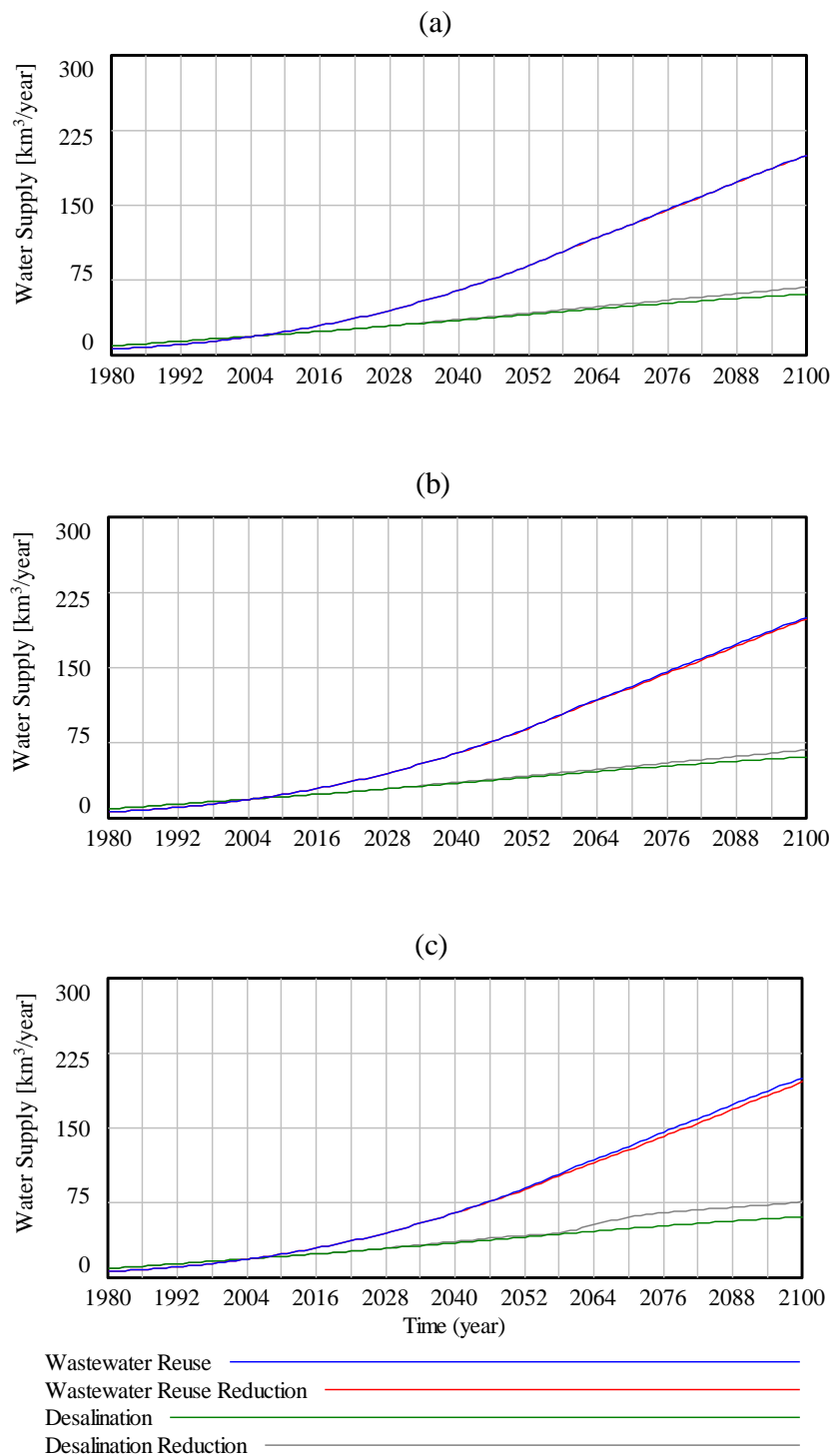


Figure 4.16. Effect of conventional water supply depletion on alternative water supplies for (a) 10%, (b) 25%, and (c) 50% reduction in available water resources compared to the ANEMI3 baseline scenario.

Even when available water resources are reduced 50% by the year 2100, desalination only responds marginally with an increase in desalination supplies of 15 km<sup>3</sup>/year or 25%. This is in contrast to the reduction in surface and groundwater supplies by 1778 and 655 km<sup>3</sup>/year, respectively in the year 2100. As a result, there is a high level of water stress created, because supply in this case cannot keep up with the demand for water. The reason for this can be found by first looking at the producer price variation for the different water supplies. In Figure 4.17, the range of water producer prices is shown for each type of water supply under the conventional water resource depletion scenario.

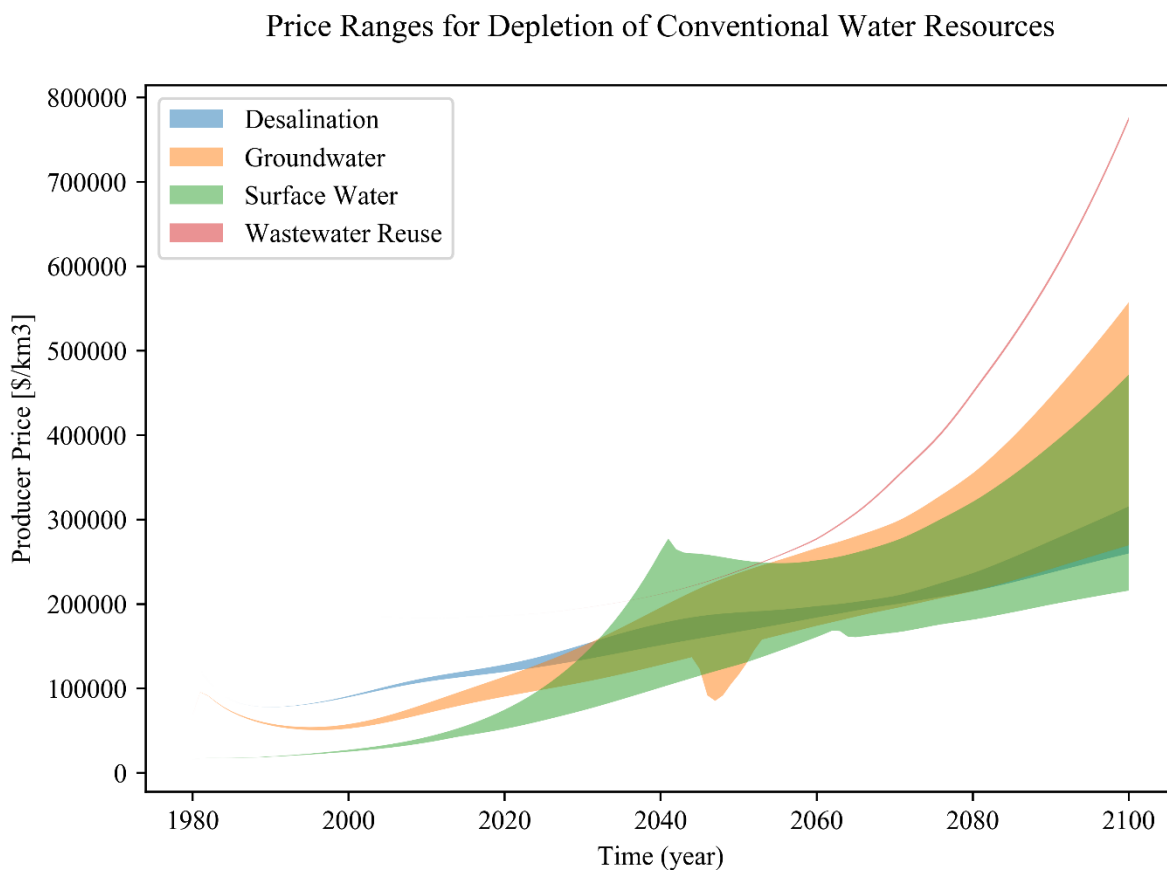


Figure 4.17. Prices ranges shown by shaded areas for depletion scenarios of 10%, 25%, and 50% reduction of available water resources for surface water and groundwater supply.

The lower bound of the shaded areas for the conventional water supplies represents the baseline trajectory of prices with no artificial depletion effects applied, while the upper bound represents the 50% reduction of available water resources for surface water and groundwater. In this case, surface water supply has the lowest production price throughout the entire simulation. However, in the 50% reduction scenario, there is a point between 2030 and 2055 where surface water supply becomes the most expensive. After which, wastewater reuse and groundwater supply become the most expensive, with desalination as the least costly option.

Therefore, in the case of 50% reduction in available conventional water resources, it would be expected that desalination levels will increase to satisfy water demands. In Figure 4.16c it is shown that desalination levels do increase but only marginally. The reason for this is that there is a large discrepancy in the production capacity for alternative water supply and conventional water supply when conventional resources become depleted. As a result, there is not enough time for alternative water supplies, such as desalination and wastewater reuse, to build enough capital through capital investments to fill the gap in water supply.

Depletion effect of water supply is shown by the range in maximum production capacities for each type of water supply across the depletion scenarios (Figure 4.18). Maximum production capacities for each type of water supply are determined by their associated capital stocks which increase as a result of investment and diminish due to depreciation. Maximum production capacity for desalination responds to favorable pricing under the depletion scenarios by increasing

investment rates, however this is not nearly enough to compensate for diminished supplies of conventional water resources.

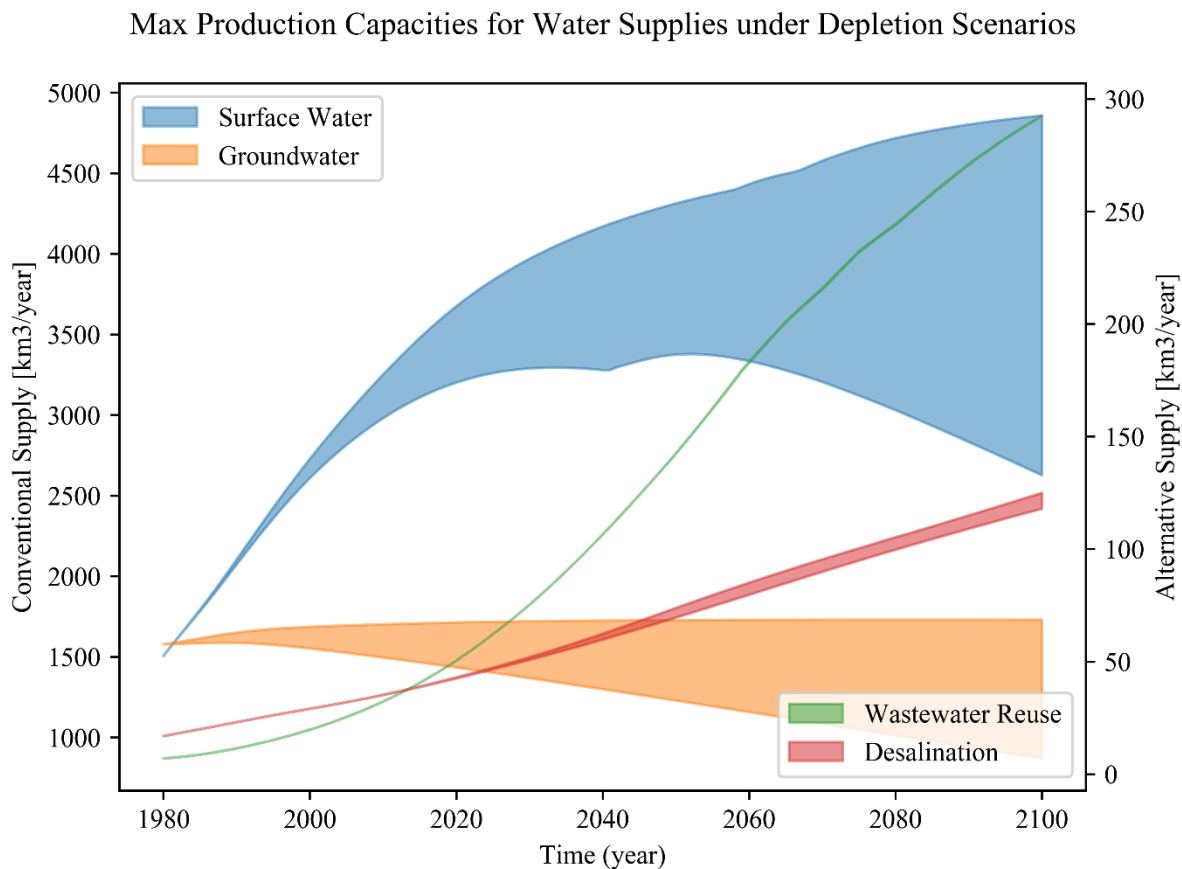


Figure 4.18. Maximum production capacities based on the capital accumulation of water supply under depletion scenarios of conventional water resources.

The net result of the reduction scenarios for conventional water supplies is an increase in water stress due to a discrepancy of supply and demand that cannot be filled fast enough by alternative water supplies (Figure 4.19).

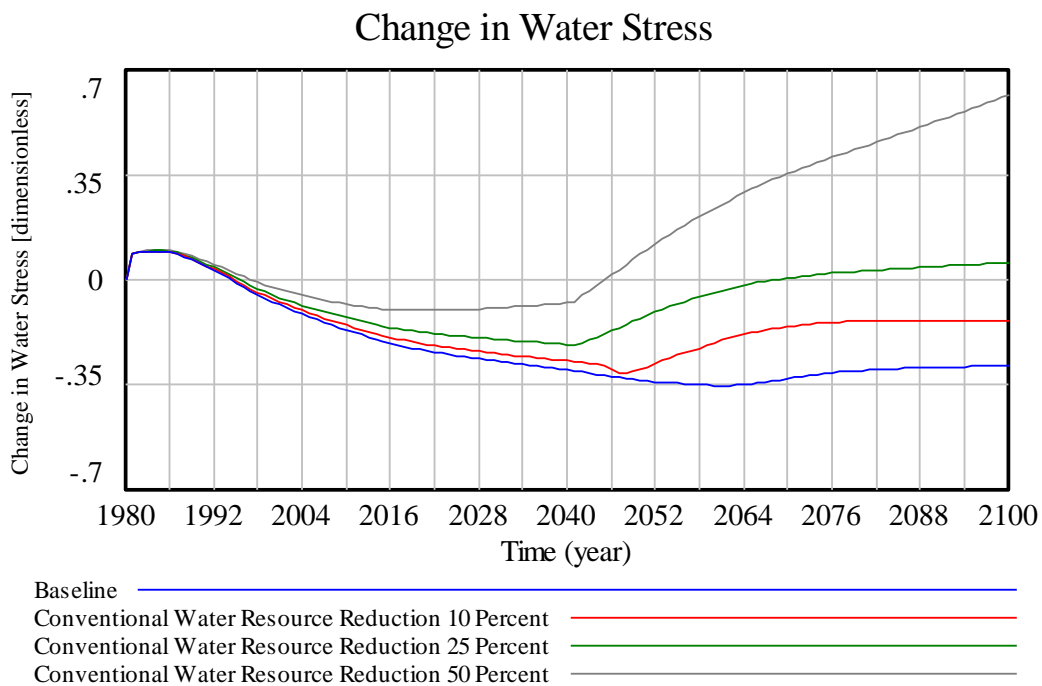


Figure 4.19. Change in water stress values for each depletion scenario.

In the ANEMI3 baseline scenario, water stress values are decreasing due to technological change and investments in water supply capital over time. However, in the 25% and 50% reduction scenarios, water stress is significantly increasing by the year 2100.

## 4.5. Food Production

The production of food supports the growth of population overtime. However, not all people have access to secure source of food. Each year approximately 9 million people die from starvation, and in 2019, 820 million people were suffering from chronic undernourishment (FAO et al. 2019). Hunger rates have dropped by 42% due, in part, to the establishment of the Millennium Development Goal (MDG) to halve the proportion of hungry people by 2015. Following the MDGs, in 2012 the United Nations launched a “Zero Hunger Challenge” to address five of the Sustainable Development Goals (SDGs) which aims to eliminate all forms of malnutrition by the year 2030. In order to achieve this goal, the Zero Hunger Challenge calls for; sustainable food systems from production to consumption, doubling small scale producer income and productivity, eliminating loss or waste of food in all food systems, and provide access to adequate food and healthy diets for all people.

Aiming to eliminate world hunger and malnutrition is an ambitious, but important goal. However, it should be kept in mind that water for irrigated agriculture is becoming increasingly scarce due to depletion of ground and surface water supplies, increased competition from domestic and industrial water users and greater concerns for water quality (Hanjra and Qureshi 2010). Increased food production is also limited by the amount of arable land for agriculture, as saturation effects make additional agricultural lands increasingly less economically feasible. Advances in agricultural technologies can help to increase productivity of existing agricultural lands and reduce water use by increasing irrigation efficiency. However, this only slows the rate of increase in water and land requirements to produce more food (Grübler 2015). Therefore, creative solutions are needed to address the issue of food security for now and in the future.

The World Resources Institute has explored, in a recent report, the issue of feeding the projected population of 10 billion people on Earth by the year 2050 (Searchinger et al. 2019). The report details the amount of food and agricultural land that will be required to solve this problem. Using projections of changes in diets and population growth, it was estimated that food production would need to increase by 56% from the period of 2010-2050.

The goal of this scenario is to test the ability of the impact of the Zero Hunger initiative set out by the United Nations, by using the food production increase scenario of the World Resources Institute on the Earth system in the ANEMI3. Food production under a range of scenarios is explored to gauge the impact of changes in technology, climate, and irrigation. The technological change scenario is used to demonstrate the degree of technological change that is needed to increase land yields and food production in isolation from the effects of climate change and increased irrigation. The climate scenario demonstrates both, positive and negative, climate effects on food production through increased potentially arable land and reduced land yields respectively. The irrigation scenarios from FAO (2018) are used to show the effects of alternative irrigation pathways on food production and associated agricultural water demand. In each scenario, the goal of increasing food production between the years 2010 and 2050 by 56%, is assessed.

In Figure 4.20, the effect of technological change on food production in ANEMI3 is shown by turning on and off these effects on land yield after the year 2010.



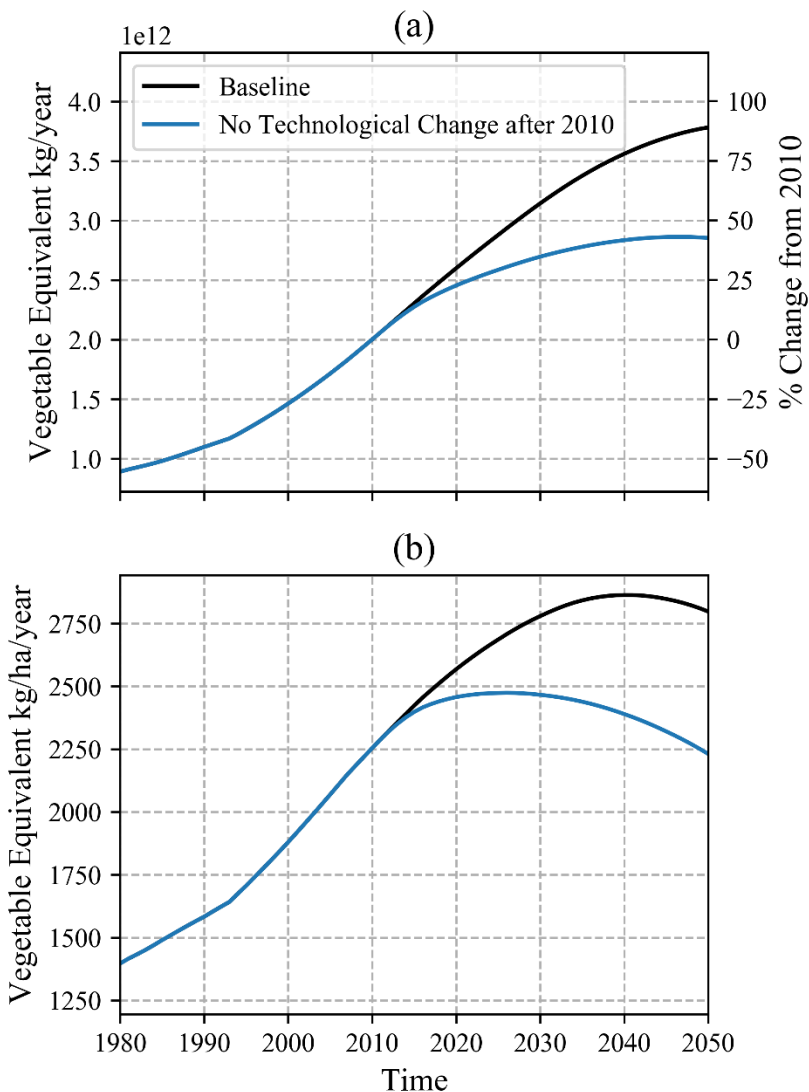


Figure 4.20. Effect of technological change on (a) food production and (b) land yield from 1980 to 2050.

When no additional technological change is applied to land yield after 2010, the rate of food production increases much more slowly, reaching 2.85 trillion vegetable equivalent kg per year by 2050, while in the ANEMI3 baseline scenario this value reaches 3.78 trillion. When these values are converted to percent changes from the baseline 2010 food production rate, the ANEMI3

baseline value shows a 90 percent increase from 2010, while the scenario without technological change reaches a value of 45 percent. The large range in food production values highlights the importance of technological change effects on land yield. In order to reach the target value of 56% increase in food production from 2010, some level of technological change will be needed, all else kept equal.

The effect of climate change on food production was examined in Section 4.1. In this research, each of the climate change factors affecting food production (sea level rise, increased potentially arable land with global temperature change, and reduced land yields) is assessed in isolation with respect to achieving the food production target of Searchinger et al. (2019). The result of which is shown in Figure 4.21. If only the climate change effects on land yield are included, the impact on food production reaches its peak in the year 2082, with a range of approximately 4.5 to 5 trillion vegetable equivalent kg produced annually (Figure 4.21a). This range includes climate change scenarios from the ANEMI3 baseline run, as well as the RCP2.6 and RCP8.5 emission scenarios, and one scenario that omits the effect of climate change on land yield. Without climate change effects the land yield is highest, and under the RCP8.5 scenario, land yield is reduced the most. Climate change impacts on land yield result in a range of 140% to 165% increase in food production relative to 2010, which is well above the target of 56%.

When climate change impacts are isolated for only those related to sea level rise, the effect is relatively minor, and almost indistinguishable in Figure 4.21c. Whether climate effects are included or not, the amount of food produced does not change significantly from the baseline

values. This is because the amount of arable land is much larger than that affected by the sea level rise in the ANEMI3 model.

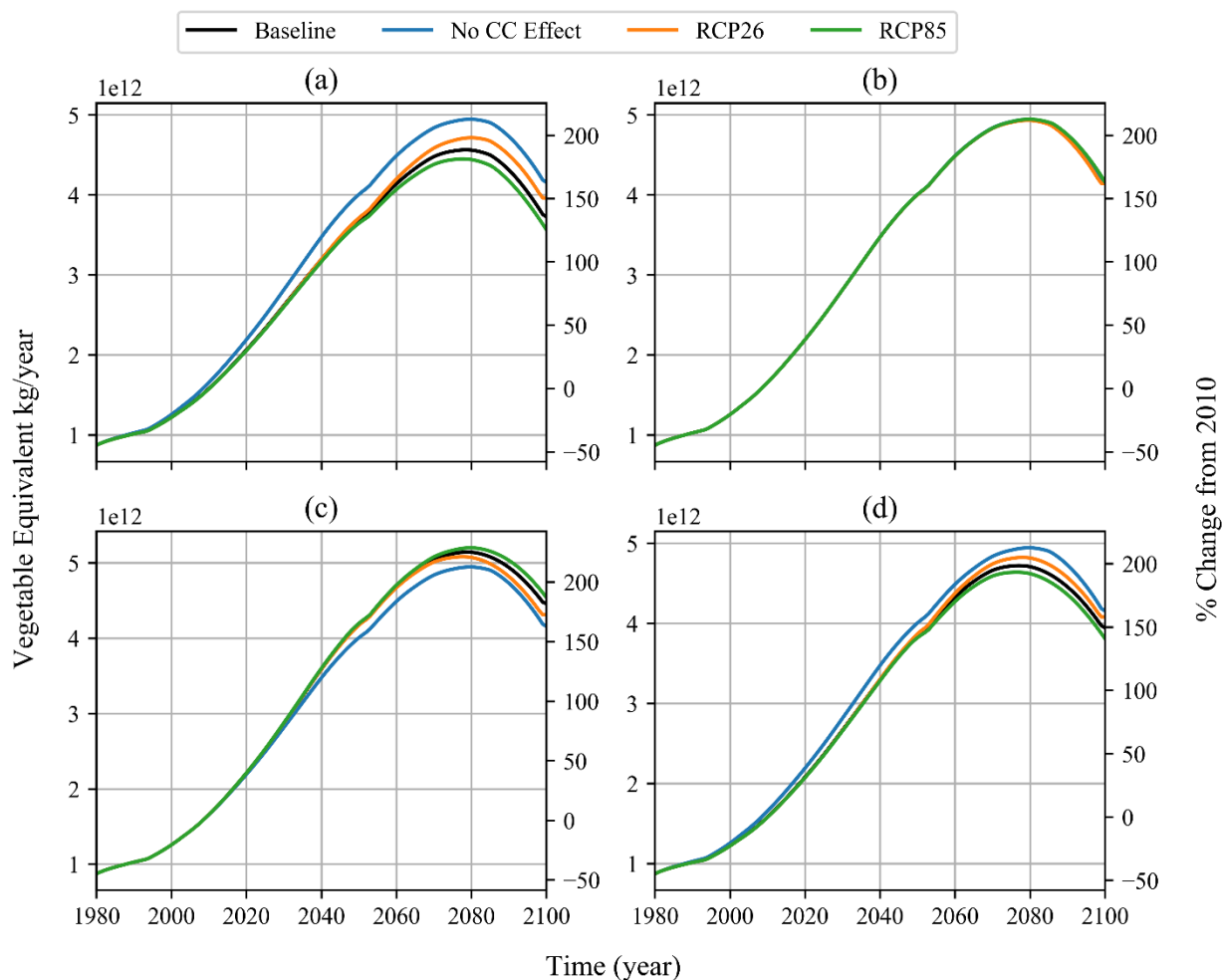


Figure 4.21. Effect of climate change on food production through isolated impacts of (a) land yield (b) sea-level rise, and (c) increase in arable land. Combined effect shown in (d).

When only the effect of climate change on potentially arable land is considered, food production values range from 150% to 170% compared to the baseline 2010 value Figure 4.21c. There is a considerable amount of uncertainty associated with the relationship developed from King et al. (2018) between potentially arable land from boreal regions and global surface temperature change.

However, even in the case of no climate change effect, food production is still well over the 2050 target.

Whether the effects of climate change on food production are considered or not, there is a pattern of overshoot and decrease in the production of food. This behavioural mode was mentioned previously and presented in Figure 2.4e of Section 2.2. Typically, this pattern is exhibited when there are two feedback loops acting together, one positive and one negative, with the presence of a delay. The transition in feedback dominance from positive to negative with the delay, allows the state variable to pass through the equilibrium point followed by a collapse. However, food production is an auxiliary or derived variable and is not a stock or state variable. In Equation 3.27, food production is shown to be a function of land yield and net arable land. Arable land is steadily increasing; however, land yield is shown to decrease after the year 2060 (Figure 4.22a).

The reason for this decrease is due to reductions in land fertility (Figure 4.22b), due to high rates of land fertility degradation (Figure 4.22c). This is due to increasing persistent pollution index from the persistent pollution sector. Additionally, the climate change effect on land yield is shown to have caused a 15% reduction in land yield from the year 1980 to 2100 and continues to drop almost linearly over time. This indicates that the peak and fall of food production in the ANEMI model towards the late 21<sup>st</sup> century is not due to overshoot and decrease behaviour, but rather a decrease in land yield that is occurring at a faster rate than food production can expand through technological changes and the expansion of agricultural lands. This would be a concern if the

population was growing more rapidly, however towards the end of the 21<sup>st</sup> century population growth was shown to slow down and even decrease slightly.

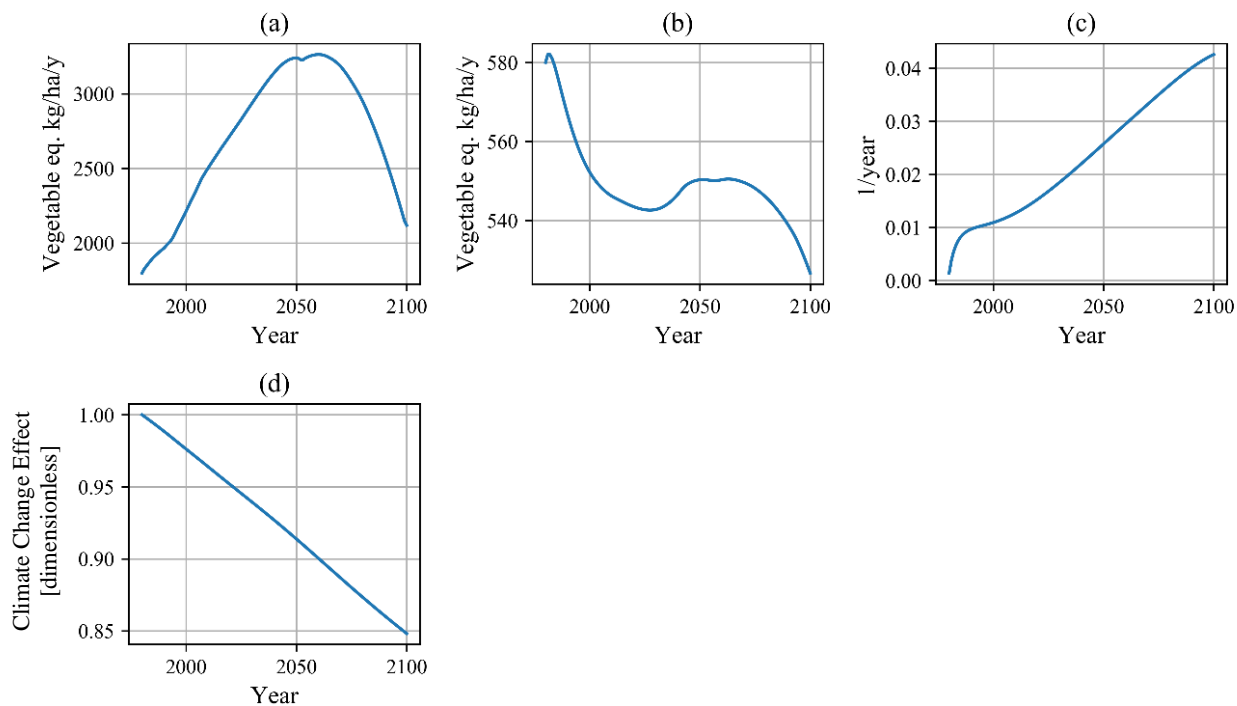


Figure 4.22. Projections of (a) land yield, (b), land fertility, (c) land fertility degradation rate, (d) climate change effect on land yield.

The pathways taken for irrigated agricultural land are based on scenarios taken from FAO (2018) (Figure 4.23). The scenarios from this report incorporate socio-economic, technological and environmental assumptions in order to project future irrigation patterns on a global scale.

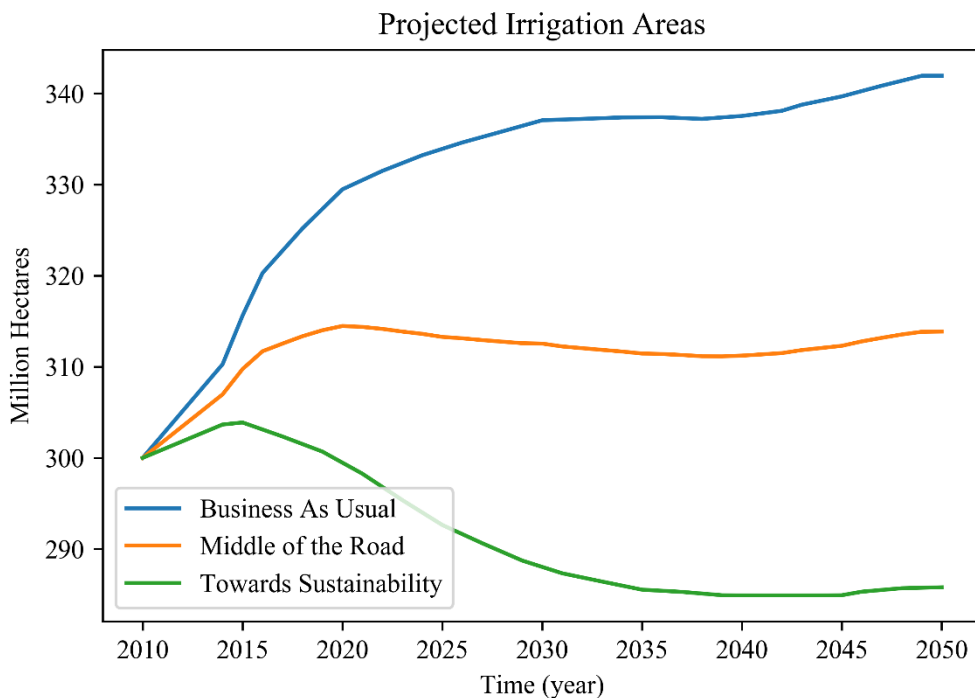


Figure 4.23. Projected irrigation agricultural area from scenarios based on FAO (2018). "Middle of the road" scenario was added which represents the midpoint between "Business as Usual" and "Towards Sustainability" scenarios.

Full summaries of the assumptions used for the development of the "Business as Usual" and "Towards Sustainability" scenarios can be found in FAO (2018). The "Middle of the Road" scenario was included by simply using the midpoint between the other two scenarios. Irrigation in the ANEMI3 model acts to increase agricultural water demand, thereby increasing the potential for water stress. In addition, the ratio of irrigated to rainfed agriculture acts as a multiplier to food production through increased land yield following Döngert (2010). The resulting effects of these scenarios on food production, agricultural water withdrawals, and global water stress are shown below (Figure 4.24).

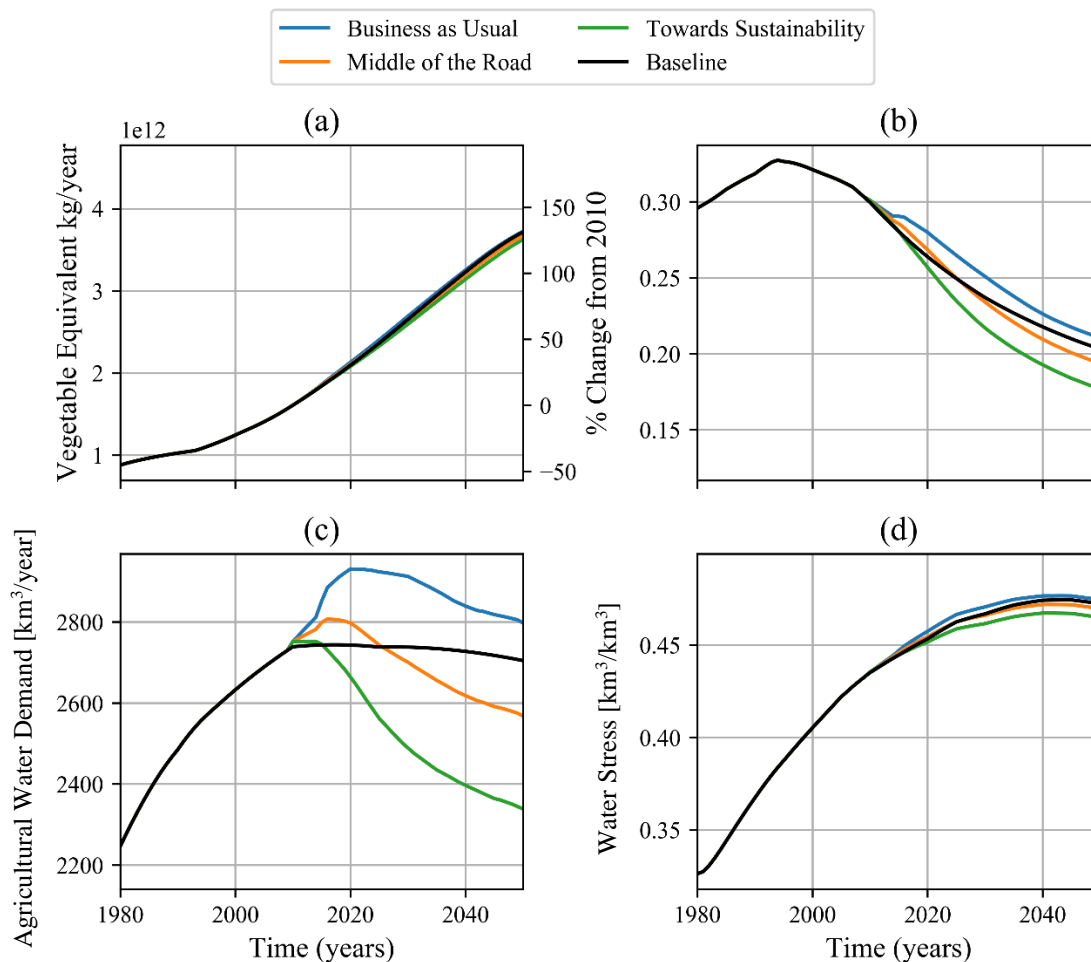


Figure 4.24. Effect of irrigation scenarios on (a) food production, (b) fraction of irrigated agriculture, (c) agricultural water demand, and (d) total water stress.

The irrigation scenarios used here have a small effect on global food production rates (Figure 4.24a). Scenario with the lowest level of food production corresponds to the “Towards Sustainability” FAO scenario with a value of 3.62 vegetable equivalent kg per year. The highest level of food production corresponds to the FAO “Business as Usual” scenario with a value of 3.73 vegetable equivalent kg per year by the year 2050. Although the effect is small, the scenario with higher levels of irrigation results in greater food production due to the increase in land yield.

The reason for the relatively low impact of the irrigation scenarios on food production lies in the much larger increase in total arable land which includes rainfed agriculture. Because of this, the fraction of irrigated agricultural land decreases over time in all irrigation scenarios (Figure 4.24b). There is an initial increase from the ANEMI3 baseline scenario, starting at a value of 0.3 or 30%, which then climbs to 33% in 1995. After this point the percentage of irrigated area decreases to 18% and 21% in the “Towards Sustainability” and “Business as Usual” scenarios.

Higher levels of irrigation in the future lead to increase in water demand for agriculture on a global scale. In the “Business as Usual” irrigation scenario, agricultural water demand increases to 2930 km<sup>3</sup>/year, then slowly decrease to 2800 km<sup>3</sup>/year by 2050 (Figure 4.24c). The “Towards Sustainability” scenario partially aims to reduce water demand from agriculture, and as a result water demand increases slightly then is reduced drastically to 2340 km<sup>3</sup>/year in 2050.

The resulting levels of water stress are shown in Figure 4.24d. Water stress in the ANEMI3 is calculated using the ratio of total water withdrawals (including dilution requirements for agricultural runoff and wastewater inputs) to the total renewable flow of water resources. In the ANEMI3 baseline scenario, water stress value starts at 0.33 and reaches its peak in the year 2040, after which the level of water stress starts to decrease. This is due to reduced withdrawals from the domestic and industrial sectors through increase in water efficiency with increase of global GDP. Food production also slows down as population growth rates begin to decline. Overall, the irrigation scenarios have a relatively minor effect on water stress. The range of water stress values



when it reaches the peak is between 0.46 and 0.48. Both values indicate high levels of water stress regardless of the irrigation scenario that is used.

## Chapter 5

### 5. Summary and Discussion

#### 5.1. Model Performance

Model validation procedures based on those recommended in (Sterman 2000) are carried out in Section 3.5 with the purpose testing the ANEMI3 model ability to simulate realistic values across various sectors. The baseline scenario for ANEMI3 is analyzed by comparing historical and projected datasets to the simulated results. The historical comparisons show that the ANEMI3 model can successfully capture the historical behaviour of the main state variables considered by comparing to published data sources. Exceptions to this include the observed interannual fluctuations in global surface temperature, as well as small fluctuations in the energy production values from coal. The simple structure of the climate and energy sub-sectors is not designed to capture short term fluctuations in climate and detailed market interactions for energy production. The purpose of the ANEMI3 model is to analyze the effects of long-term global changes in the Earth system through the use of feedbacks. The historical comparisons show that the model can accomplish this task.

Comparisons made to other model simulations gives context to where the ANEMI3 model fits in amongst the ranges of future global change projections. The behaviour of the simulated population values is of importance, as the population sector has many feedback relationships with the others. The historical population simulation is shown to successfully reproduce both the magnitude and overall behaviour of the historical observations. When the population is broken down into different

age demographics, each category was shown to reproduce the historical trends, however the 15 to 44 age group was slightly underestimated. Extending the simulation to the year 2100 shows that the ANEMI3 model predicts population on the lower range of the United Nations World Population Prospects scenarios in the 2019 edition of the report, between the “medium” and “low” projections for population growth rate. The reason for this is due to the use of negative feedbacks on population for food production, water stress, pollution effects, and economic factors related to health services.

Historical simulations for global surface temperature change are shown to be comparable to the observed NASA data. However, the interannual fluctuations in surface temperature change are not captured, and the slope of the temperature changes were slightly overestimated. With the simple structure of the ANEMI3 climate sector, it is not possible to capture fluctuations in surface temperature change, as it is only designed to estimate long-term changes in temperature. Simulated future changes in global surface temperature are compared using RCP emission scenarios. The baseline scenario of ANEMI3 is found to be on the higher end of projected surface temperature changes, just above that of the RCP6 scenario. This is due to the anthropogenic emissions that are calculated from the energy production sector. Comparison of the CO<sub>2</sub> emissions that are simulated in ANEMI3 for the RCP scenarios also shows a match with the RCP6 scenario. This scenario corresponds to the outputs of the Asian-Pacific Integrated Model (AIM) and suggests that ANEMI3 may have some similarities in the climate and carbon sectors with this model.

Water demand values were replicated for the historical period as a result of the model validation. Comparing the future values of water demand is a difficult task, as all projections will include socioeconomic assumptions that may differ greatly amongst models. The ANEMI3 model is found to be on the lower end of the domestic water demand when compared to projections compiled by models in the literature, and in the mid range for industrial water demand for the period of 2010 to 2050. Agricultural water demand is shown to follow a path that is between the “Business as Usual” and “Towards Sustainability” scenarios from FAO (2018).

Information on the use of different types of water supply for surface and groundwater resources is limited on the global scale. The water supply development sector is compared to historical and future projected reconstructions made in Wada and Bierkens (2014b). Under the calibrated parameterization scheme, the development of water supplies is able to reproduce the historical values and follow future projected trends for surface and groundwater supplies. Water supply produced through desalination was compared with model projections ranging from the year 2000 to 2050. The simulated values for desalination are shown to be within the range of those projected in the literature.

The new energy-economy sector integrated into ANEMI3 is assessed for its ability to capture global trends in economic output and energy production from coal, oil and gas, hydro and nuclear, and renewable energy sources. The projected values for gross economic output and per capita consumption follow the same general trend as the DICE2013R model (Nordhaus 2013). When these variables are compared with the ANEMI2 model (Akhtar et al. 2013), their trajectories were

very similar despite the major difference between a computable general equilibrium model of ANEMI2 and the feedback-based approach of ANEMI3. Energy production from coal, oil and gas, hydro and nuclear, and renewable energy sources is shown to be between the ANEMI2 model, Ito et al. (2000), and the GCAM model values reported in Davies et al. (2013). Similarities are present between this diverse set of models from the initial values, to the peak in oil production of ANEMI2, and the rapidly increasing production of renewable energy into the 21<sup>st</sup> century. This confirms that the energy production sector behaves in a realistic way and is crucial for the determination of industrial water demand values and CO<sub>2</sub> emissions.

The integration error experiment varies the time from that of 1/1024<sup>th</sup> of a year to 1/128<sup>th</sup> of a year (the current time step). The changes from the lowest time step run are small, ranging from 0.5% to 0.8% in the 1/128<sup>th</sup> year time step. Increasing the time step to 1/64<sup>th</sup> of a year causes the model to become unstable. The time step that is currently being used (1/128<sup>th</sup> of a year) is deemed to be sufficient based on the small differences between that and the smallest time step that is tested in this experiment. Monte Carlo sensitivity analysis results of major state variables in the ANEMI3 model reveal that most of the variables are not overly sensitive to changes in select variables between 10% to 20%, and the behaviour mode of the major state variables remain the same. Based on the model validation experiments the ANEMI3 model is shown to provide realistic estimates of all the variables tested and is robust to parameter changes. The model validation process used in this work builds confidence in the model for the experiments in Section 4.

## 5.2. The Role of Climate in Global Change

The objective of the experiment in Section 4.1, is to assess the climate change impacts through the feedback processes represented within the ANEMI3 model. Climate change plays a central role in the ANEMI3 model and affects all other sectors either directly or indirectly. In Section 1.1 it is shown that the climate sector in ANEMI3 is tied amongst the population and economy sectors for having the highest number of outgoing intersectoral connections in the model. Using greenhouse gas emissions from the Representative Concentration Pathway scenarios, the resulting range of global surface temperatures is used to assess potential impacts of climate change on the hydrologic cycle, food production, and global economy through changes in global average surface temperature and annual precipitation rates. Increased global surface temperatures are shown to affect the hydrologic cycle by increasing evaporative processes including ocean evaporation, evapotranspiration, and evaporation from reservoirs on land. The result of this is increase of atmospheric moisture content and annual rainfall amounts which generate an increase in available water resources in the form of renewable groundwater and runoff on the global scale.

In this iteration of the ANEMI3 model, additional connections are made between the climate and food sectors. The influence of climate change on land yields as a result of potential heat stress is added based on the study of Searchinger et al. (2019). An additional connection is added through the potential increase in arable land from shifting climate zones in boreal forests based on (King et al. 2018). These additions in the ANEMI3 model allow for climate change effects on food production to be analyzed through three different mechanisms simultaneously including sea level

rise, land yield reduction from the heat stress, and increase in arable land from shifting climate zones in northerly boreal forests. It is found that increase in global surface temperature results in an increase of net arable land, despite reductions from sea level rise. Although the amount of land for agriculture increases, the influence of reduced land yield dominates and results in an overall negative effect on food production.

It should be noted that there are several climate change related effects that are not included in this work which could alter these findings. One example is the case of CO<sub>2</sub> fertilization having a positive effect on land yields by supporting crop growth, as well as increase in temperature providing beneficial growing conditions for crops during certain times of the year (Zhao et al. 2017). The impacts of sea level rise may be understated in ANEMI3 as agricultural areas do not necessarily need to be inundated for significant impacts to occur. Currently, low-lying coastal areas are more frequently being submerged in saltwater, causing farmers to find new livelihoods (Chen and Mueller 2018). The impact of change in precipitation amounts for rain-fed agriculture is also not included, as this would require finer spatial and temporal resolution than what is currently possible with the ANEMI3 model. This effect would increase the impact of irrigation on land yields as the majority of the agriculture is currently rainfed.

### 5.3. Considerations for Water Supply Development in the 21<sup>st</sup> Century

The addition of the feedback-driven, economically based water supply development sector in ANEMI3 is the main objective of this thesis. The approach is novel in that global water supply is

able to evolve endogenously and allows for the development of conventional and alternative water supplies, while including effects of water quality on surface water resources. This objective is achieved by incorporating the new energy-economy sector into the ANEMI3 and adding water supply development as a new production sector. The development of water supply infrastructure is assessed from an economic perspective. Capital stocks for each type of water supply grow over time with investment, which is made based on the inverse supply prices and allocated using Wood's algorithm. Endogenous technological change is also incorporated for the desalination and wastewater reuse technologies, as well as the effects of depletion and diminishing water quality of conventional supplies.

The ANEMI3 baseline simulation for the development of water supplies shows that surface water resources are dominating the share of water supply during the entire simulation period from the year 1980 to 2100. This is because surface water resources are by far the least expensive option for water supply in the ANEMI3 baseline scenario. When only the global scale is considered, there is enough stable and renewable surface water resources to satisfy the demand of a growing population by the year 2100. In order to test the impact of depletion of the development of water supplies, available water resources for surface and groundwater supplies are reduced by 10%, 25%, and 50% linearly over the duration of the simulation.

As a result, surface and groundwater production are lower after the year 2050 because of resource depletion, however alternative water supplies in the form of desalination and wastewater reuse are not able to respond fast enough to fill the diminished conventional supplies. In the case of a 50%



reduction in available conventional water resources, desalination becomes the least expensive option after the year 2030. However, capital stocks for desalination cannot increase fast enough during this time to fill the gap in production capacity due to the presence of time delays in establishing new capital. For desalination to play a larger role on the global scale under this scenario, greater investment in desalination infrastructure is necessary before conventional water resources become depleted.

The potential for water quality impacts on the development of surface water supplies is assessed. Nutrient concentrations in surface water resources are calculated using the global cycles of water, nitrogen, and phosphorus. The difference in sources of nitrogen and phosphorus inputs to the nutrient cycles, result in different long-term behaviours in their respective surface water concentrations. For nitrogen, the main source that is represented consists of agricultural runoff, which increases throughout the simulation period, with increased net arable land for food production. Phosphorus inputs on the other hand, are driven mainly through untreated wastewater which increases initially and decreases as treatment rates increase and wastewater volumes drop due to reduced domestic and industrial water demand.

Under the current parameterization scheme, water quality is not shown to be a significant factor for the development of surface water supplies. When wastewater treatment rates are fixed at their initial values, surface water nutrient concentrations increase, but not enough to show large impacts on surface water production. Using increased nutrient concentrations as an indicator for water quality provides a way to represent the impact of different sources of water pollution, but on a

globally aggregated scale these impacts are averaged and likely understated. The reduced wastewater treatment scenario did however influence wastewater reuse. The lower quantity of treated wastewater available for reuse resulted in a greater saturation effect on the development of water supplies from wastewater reuse, thereby reducing its potential to develop as an alternative water resource.

This work presents a new approach to the incorporation of water supply development into the ANEMI model. However the water supply development sector could also be included in other integrated assessment models of global change, and global hydrologic models that are currently attempting to implement these concepts such as those of Wada et al. (2016), Hanasaki et al. (2016), and Turner et al. (2019).

## Chapter 6

### 6. Conclusions and Recommendations

The following sections detail the findings and contributions of this work, along with the limitations and recommendation for future work.

#### 6.1. Findings and Contributions

In the third iteration of the ANEMI model, a tighter coupling between climate and food production was made by incorporating the potential changes in arable land and land yield as a result of increased surface temperatures. A new energy-economy model was included to replace the computable general equilibrium model that existed prior, and a novel global scale water supply development model was created and incorporated within it. The water supply model shares parallels with energy production, and includes the effects of depletion, saturation, and endogenous technological change on the development of surface water, groundwater, wastewater reuse, and desalination supplies. The effect of water quality degradation on surface water supplies was also included, which requires a way to quantitatively represent water quality on a globally aggregated scale. For this, a nutrient cycle sub-system was included in the model for the cycles of nitrogen and phosphorus-based compounds. Nutrient levels in surface water stocks were combined with that of the hydrologic cycle in order to represent nutrient concentrations in surface waters over time, ultimately acting as a multiplier on the supply price of surface water supplies.

The tighter coupling of climate change to food production in the ANEMI3 model allows for climate change impacts on land yield and increased potentially arable land from shifting climate to be represented in addition to sea level rise through inundation of agricultural areas. Assessing the influence of all three factors simultaneously results in most of the climate change impacts on food production to be cancelled out. Food production rates were compared to a recent report by the World Resources Institute, which assesses the issue of feeding the projected population of 10 billion people on Earth by the year 2050 (Searchinger et al. 2019). From this assessment it was estimated food production would need to increase by 56% from the year 2010 to achieve this goal. In this comparison it is found that technological change in land yield rates is the most important factor in producing enough food to sustain our growing population. It was also found that in the late 21<sup>st</sup> century, the influence of the persistent pollution was causing land yield rates to drop due to degradation of land fertility, however in the ANEMI3 model population growth rates are zero or negative by the 21<sup>st</sup> century. If the population were to continue growing beyond this point, the model suggests that issues related to land fertility would likely need to be addressed.

The effects of depletion, saturation, technological change, and water quality on water supply development were not well represented on the global scale due to the aggregated nature of the model masking regional issues that would allow for these effects to occur. Examples of this include the increasing availability of surface water resources a result of climate change due to increased annual precipitation amounts. Climate change is expected to alter the spatial and temporal distributions of water resources from their points of use in many areas around the globe. If represented on a regional or local scale and finer temporal resolution, climate change would likely cause a greater need for further development of alternative water supplies, due to decreased

availability of conventional water resources. The dynamics included in the water supply development sector could be isolated and tested at different spatial scales in order to fully explore them.

The system dynamics simulation approach of the ANEMI3 model is ideal for representing the feedbacks between multiple sub-systems of the Earth system in order to model various aspects of global change. However, in order to better capture the dynamics of global change a finer temporal and spatial scale are needed. In order to do this either all or some of the sub-systems in the ANEMI3 model would need to be disaggregated or replaced with existing disciplinary models that include more spatial components.

## 6.2. Limitations

This work is focussed on representing global scale feedbacks that are driving global change and assessing their importance and influence within the Earth system. However, there are processes occurring at finer spatial scales that have global impacts which cannot be represented (discussed in previous section). Future work should focus on effectively “downscaling” the ANEMI model such some sectors can be broken down into finer spatial and temporal scales. This could allow for additional processes to be represented such as population migration driven by climate change through food and water scarcity, and sea level rise (Piguet 2008; Ionesco et al. 2017; United Nations 2019b) to be represented. Water scarcity may be a driver of population migrations, however the migrations may in turn create water scarcity in other regions creating a feedback loop. This may be an important driver of water supply development in the future.

There are concepts within the ANEMI model that are either understated or misrepresented due to the use of a globally aggregated spatial scale. An example of this is the increased water availability as a result of climate change shown in Section 4.1. This makes it appear as though climate change would result in less water stress, however the accepted notion is that climate change is altering the distribution of water resources in time and space, thereby increasing water stress by shifting water resources from where they are currently being used. Another is in the representation of water quality on a globally aggregated scale. There is no spatial component for wastewater inputs, as well as river flows for calculating nutrient concentrations. Areas with poor water quality will likely have high levels of untreated wastewater which are generally found in lower income countries (WWAP 2017). It is in these regions where studying the effect of water quality of surface water production from an integrated perspective will be the most beneficial.

The dynamics of the water supply development sector incorporated into ANEMI3 model were not well represented on the global scale in the baseline ANEMI scenario. This is because surface water resources were enough to sustain the water demand when the available water resources consider the entire amount on Earth. This was also true for water quality, as it is averaged across the globe as well. However, if the water supply development model is regionalized, or adapted for use in a grid-based model, the effects of resource depletion and water quality effects on surface water supply could be explored in more detail. In doing this, location specific details with regards to water supply development could be considered, such as distribution costs for areas that are further away from coastlines in the case of desalination, or the depth of regional aquifers for groundwater extraction costs.

### 6.3. Future Work

As the Earth system becomes increasingly complex due to global change, there is the potential for changes in the structure of the system to manifest that are not currently captured in the ANEMI model. Because of this, future work may involve identifying relationships in the model that may need to be updated based on recent findings. An example of a more recent change to the Earth system lies in the relationship between economic output and pollution. In the persistent pollution sector of the ANEMI model, functional relationships are used to relate economic output to resource consumption as well as pollution generation rates from both industrial and agricultural activities. In the book titled, “More from Less” (McAfee 2019) evidence is provided for decreasing consumption of resources and pollution per unit of GDP in the United States. Further research can be done to understand the drivers of this change and how it can be represented on a global scale. In the ANEMI model, Reduced pollution rates would delay the impacts of pollution on population mortality rates and food production, thereby allowing for greater population.

Another example of structural changes that may become more important future is the issue of limited phosphorus supply. As food production increases, so too will the demand for fertilizer and phosphorus is a key component. The production of phosphorus from phosphate rock reserves is becoming increasingly unsustainable and could result severely depleted phosphorus levels in the next 100 years (Oelkers and Jones 2008; Chowdhury et al. 2017). Currently, the ANEMI model only includes wastewater inputs to the phosphorus cycle. Future research may incorporate additional anthropogenic effects such as the extraction of phosphorus from phosphate rock reserves. The incorporation of additional feedbacks to food production may be possible due to

limitations on fertilizer application as phosphorus becomes depleted from land-based stocks on a global scale.

In addition to including modified relationships and new structure in the ANEMI model, the representation of existing sectors may also be improved. Many of the disciplinary models that make up ANEMI are simple in their representation. This makes identifying feedback processes that drive global change easier, but also limits the number of feedbacks that can be examined. For example, the land use sector is based on Goudriaan and Ketner (1984) and uses a set of base land use transfer rates to represent land use change from 6 different biomes. The only factor that affect the rates of change are population growth. A new, more physically based model may be used in its place in order for climate change impacts and sea level rise to be incorporated.

Future work can also include the development of additional scenarios to run using the ANEMI3 model for global policy development. An example of this was the assessment of food production considering the World Resources Institute report's recommendation of a 56% increase in food production by 2050. In this case the ANEMI3 model was able to be used to test the implications of such an increase in food production on the Earth system. As world issues continue to evolve there will be more interesting dynamics to consider and include into future versions of the ANEMI model.



## References

- (IGBP) International Geosphere-Biosphere Programme. (2010) *Vision*. <http://www.igbp.net/about/vision.4.1b8ae20512db692f2a6800017590.html>. Accessed 15 Dec 2019.
- Advisian Worley Group. (2019) *The Cost of Desalination*. <https://www.advisian.com/en/global-perspectives/the-cost-of-desalination>. Accessed 15 Oct 2019.
- Akhtar M.K. (2011) *A System Dynamics Based Integrated Assessment Modelling of Global-Regional Climate Change: A Model for Analyzing the Behaviour of the Social-Energy-Economy*. Ph.D. thesis. Department of Civil and Environmental Engineering, University of Western Ontario, London, Ontario, Canada.
- Akhtar M.K., Wibe J., Simonovic S.P., MacGee J. (2013) *Integrated assessment model of society-biosphere-climate-economy-energy system*. *Environmental Modelling and Software*, 49:1–21. doi: 10.1016/j.envsoft.2013.07.006.
- Alcamo J., Döll P., Henrichs T., et al. (2003a) *Development and testing of the WaterGAP 2 global model of water use and availability*. *Hydrological Sciences Journal*, 48:317–337. doi: 10.1623/hysj.48.3.317.45290.
- Alcamo J., Döll P., Henrichs T., et al. (2003b) *Global estimates of water withdrawals and availability under current and future “business-as-usual” conditions*. *Hydrological Sciences Journal*, 48:339–348. doi: 10.1623/hysj.48.3.339.45278.
- Alcamo J., Flörke M., Märker M. (2007) *Future long-term changes in global water resources driven by socio-economic and climatic changes*. *Hydrological Sciences Journal*, 52:247–275. doi: 10.1623/hysj.52.2.247.
- Aulakh R. (2014) *China wakes up to its water crisis*. *The Star*. Retrieved from: [https://www.thestar.com/news/world/2014/05/12/china\\_wakes\\_up\\_to\\_its\\_water\\_crisis.html](https://www.thestar.com/news/world/2014/05/12/china_wakes_up_to_its_water_crisis.html).
- Borucke M., Moore D., Cranston G., et al. (2013) *Accounting for demand and supply of the biosphere’s regenerative capacity: The National Footprint Accounts’ underlying methodology and framework*. *Ecological Indices*, 24:518–533. doi: 10.1016/j.ecolind.2012.08.005.
- Breach P.A. and S.P. Simonovic (2018) *Wastewater Treatment Energy Recovery Potential For Adaptation To Global Change: An Integrated Assessment*. *Environmental Management*, 61:624–636. doi: 10.1007/s00267-018-0997-6.
- Breierova L. and M. Choudhari (1996) *An Introduction to Sensitivity Analysis*. RoadMaps, Article D-4526, Massachusetts Institute of Technology, 40 pages.

- Calvin K., Patel P., Clarke L., et al. (2019) *GCAM v5.1: Representing the linkages between energy, water, land, climate, and economic systems*. Geoscientific Model Development, 12:677–698. doi: 10.5194/gmd-12-677-2019.
- Capellán-Pérez I., González-Eguino M., Arto I., et al. (2014) *New climate scenario framework implementation in the GCAM integrated assessment model*. BC3 Working Paper Series 2014-04. Basque Centre for Climate Change (BC3). Bilbao, Spain.
- Chapra S.C. (2008) *Applied Numerical Methods with MATLAB for Engineers and Scientists*, 3rd edition. McGraw-Hill, New York, NY.
- Chaturvedi V., Hejazi M., Edmonds J., et al. (2013) *Climate mitigation policy implications for global irrigation water demand*. Mitigation and Adaptation Strategies for Global Change, 20:389–407. doi: 10.1007/s11027-013-9497-4.
- Chen J. and V. Mueller (2018) *Climate change is making soils saltier, forcing many farmers to find new livelihoods*. The Conversation. Retrieved from: <http://theconversation.com/climate-change-is-making-soils-saltier-forcing-many-farmers-to-find-new-livelihoods-106048>.
- Chowdhury R.B., Moore G.A., Weatherly A.J. and M. Arora (2017) *Key sustainability challenges for the global phosphorus resource, their implications for global food security, and options for mitigation*. Journal of Cleaner Production, 140:945-963. doi: 10.1016/j.jclepro.2016.07.012.
- Cox P. and N. Nakicenovic (2004) *Assessing and Simulating the Altered Functioning of the Earth System in the Anthropocene*. Earth system analysis for sustainability. MIT Press, pp 293–312.
- Davies E.G. (2007) *Modelling Feedback in the Society-Biosphere-Climate System*. Ph.D thesis. Department of Civil and Environmental Engineering, University of Western Ontario, London, Ontario, Canada.
- Davies E.G.R., Kyle P. and J.A. Edmonds (2013) *An integrated assessment of global and regional water demands for electricity generation to 2095*. Advances in Water Resources, 52:296–313. doi: 10.1016/j.advwatres.2012.11.020.
- Davies E.G.R. and S.P. Simonovic (2010) *ANEMI: a new model for integrated assessment of global change*. Interdisciplinary Environmental Review, 11:127–161. doi: 10.1504/IER.2010.037903.
- Davies E.G.R. and S.P. Simonovic (2011) *Global water resources modeling with an integrated model of the social-economic-environmental system*. Advances in Water Resources, 34:684–700. doi: 10.1016/j.advwatres.2011.02.010.

- Davies J., Macgee J., Wibe J., et al. (2011) *The Impact of Climate Change and Climate by The Impact of Climate Change and Climate Policy on the Canadian Economy*. Economic Policy Research Institute EPRI Working Paper Series, 2011-2, University of Western Ontario, London, Ontario, Canada.
- den Elzen M.G.J., Beusen A.H.W. and J. Rotmans (1997) *An integrated modeling approach to global carbon and nitrogen cycles: Balancing their budgets*. *Global Biogeochemical Cycles*, 11:191–215. doi: 10.1029/96GB03938.
- DIVERSITAS International (2011) *Mission and History*. <https://www.diversitas-international.org/about/mission-and-history/>. Accessed 14 Dec 2019.
- Dowgert M. (2010) *The Impact of Irrigated Agriculture on a Stable Food Supply*. Proceedings of the 22nd Annual Central Plains Irrigation Conference, Kearney, NE., February 24-25.
- Dunford R., Harrison P. and M.D. Rounsevell (2014) *Exploring scenario and model uncertainty in cross-sectoral integrated assessment approaches to climate change impacts*. *Climatic Change*. doi: 10.1007/s10584-014-1211-3.
- Eikebrokk B., Vogt R.D. and H. Liltved (2004) *NOM increase in Northern European source waters: Discussion of possible causes and impacts on coagulation/contact filtration processes*. *Water Science and Technology: Water Supply*, 4:47–54.
- FAO, IFAD, UNICEF, et al. (2019) *The State of Food Security and Nutrition in the World: Safeguarding Against Economic Slowdowns and Downturns*. Rome, FAO. Licence: CC BY-NC-SA 3.0 IGO.
- (FAO) Food and Agricultural Organization of the United Nations (2019a) *Eutrophication of Surface Waters. Fertilizers as Pollutants*. <http://www.fao.org/3/w2598e/w2598e06.htm>. Accessed 15 Oct 2017.
- (FAO) Food and Agricultural Organization of the United Nations(2019b) *FAOSTAT Crop Database*. <http://www.fao.org/faostat/en/#data/QC>. Accessed 10 Dec 2019.
- (FAO) Food and Agriculture Organization of the United Nations (2018) *The future of food and agriculture – Alternative pathways to 2050*. Rome. 224 pp. Licence: CC BY-NC-SA 3.0 IGO.
- Fichtner GmbH (2011) *MENA Regional Water Outlook Part II: Desalination Using Renewable Energy*. Fichtner, Stuttgart, Germany.
- Fiddaman T.S. (2002) *Exploring policy options with a behavioral climate-economy model*. *System Dynamics Review*, 18:243–267. doi: 10.1002/sdr.241.

- Fiddaman T.S. (1997) *Feedback Complexity in Integrated Climate-Economy Models*. Ph.D. thesis. Department of Operations Management and System Dynamics, Massachusetts Institute of Technology, Cambridge, Massachusetts.
- Gao L., Yoshikawa S., Iseri Y., et al. (2017) *An economic assessment of the global potential for seawater desalination to 2050*. *Water (Switzerland)* 9(10). doi: 10.3390/w9100763.
- Goodman M.R. (1989) *Study Notes in System Dynamics*. Productivity Press, Portland, Oregon.
- Goudriaan J. and P. Ketner (1984) *A simulation study for the global carbon cycle, including man's impact on the biosphere*. *Climatic Change* 6(2):167–192. doi: 10.1007/BF00144611.
- Grübler A. (2015) *Technology and global change*. International Institute for Applied Systems Analysis, Laxenburg, Austria, 459 pages.
- Gude V.G. (2017) *Desalination and water reuse to address global water scarcity*. *Reviews in Environmental Science and Biotechnology*, 16:591–609. doi: 10.1007/s11157-017-9449-7.
- Haines A., Harris F., Kasuga F. and C. Machalaba (2017) *Future Earth - Linking research on health and environmental sustainability*. *BMJ (Online)* 357. doi: 10.1136/bmj.j2358.
- Hamilton S.H., Elsawah S., Guillaume J.H., et al. (2015) *Integrated assessment and modelling: Overview and synthesis of salient dimensions*. *Environmental Modelling Software*, 64:215–229. doi: 10.1016/j.envsoft.2014.12.005.
- Hanasaki N., Yoshikawa S., Kakinuma K. and S. Kanae. (2016) *A seawater desalination scheme for global hydrological models*. *Hydrology Earth System Sciences*, 20:4143–4157. doi: 10.5194/hess-20-4143-2016.
- Hanjra M.A. and M.E. Qureshi. (2010) *Global water crisis and future food security in an era of climate change*. *Food Policy*, 35:365–377. doi: 10.1016/j.foodpol.2010.05.006.
- Cisneros, B.E.J., Oki T., Arnell, N.W., et al. (2014) *Freshwater resources*. In: *Climate Change 2014: Impacts, Adaptation, and Vulnerability. Part A: Global and Sectoral Aspects. Contribution of Working Group II to the Fifth Assessment Report of the Intergovernmental Panel on Climate Change*. Cambridge University Press, Cambridge, United Kingdom and New York, NY, USA, pp. 229-269.
- Harvey L.D. and S.H. Schneider (1985) *Transient climate response to external forcing on 100–104 year time scales part I: Experiments with globally averaged, coupled, atmosphere and ocean energy balance models*. *Journal of Geophysical Research*, 90. doi: 10.1029/JD090iD01p02191

- Henze M. and Y. Comeau (2008) *Wastewater Characterization. In: Biological Wastewater Treatment: Principles Modelling and Design*. IWA Publishing, London, UK, pp 33–52.
- (HYDE) Historical Database of the Global Environment (2016) *Land Use Data*. <https://themasites.pbl.nl/tridion/en/themasites/hyde/landusedata/index-2.html>. Accessed 10 Aug 2019.
- Holden P.B. and N.R. Edwards (2010) *Dimensionally reduced emulation of an AOGCM for application to integrated assessment modelling*. *Geophysical Research Letters*, 37:1–5. doi: 10.1029/2010GL045137.
- Hudman F. (1999) *Wastewater treatment and water reuse*. *Water*, 26:22–23. doi: 10.1016/j.coesh.2018.03.005.
- International Group of Funding Agencies for Global Change Research (2011) *The Belmont Challenge: A Global, Environmental Research Mission for Sustainability*. Washington, DC.
- (IHP) International Hydrological Programme (2000) *World Freshwater Resources*. Prepared by I.A. Shiklomanov, International Hydrologic Programme, UNESCO International.
- Ionesco D., Mokhnacheva D. and F. Gemenne (2017) *The Atlas of Environmental Migration*. Routledge Taylor & Francis Group, 357 pages.
- (IPCC) Intergovernmental Panel on Climate Change (2013) *Climate Change 2013: The Physical Science Basis*. Contribution of Working Group I to the Fifth Assessment Report of the Intergovernmental Panel on Climate Change. Cambridge University Press, Cambridge, United Kingdom and New York, NY, USA
- (IPCC) Intergovernmental Panel on Climate Change (2014) *Climate Change 2014: Impacts, Adaptation, and Vulnerability*. Part A: Global and Sectoral Aspects. Contribution of Working Group II to the Fifth Assessment Report of the Intergovernmental Panel on Climate Change. Cambridge University Press, Cambridge, United Kingdom and New York, NY, USA, 1132 pp.
- Ito K., Murota Y., Morita, Y. and H. Mitsuhide (2000) *Ultra-Long Term Global Energy Supply / Demand Models And Simulation*. The Institute of Energy Economics, Japan, 19 pages.
- Janetos A.C. (2008) *Science Challenges and Future Directions: Climate Change Integrated Assessment Research*. U.S. Department of Energy, Workshop on Integrated Assessment, 100 pages.
- Jevrejeva S., Jackson L.P., Grinsted A., et al. (2018) *Flood damage costs under the sea level rise with warming of 1.5°C and 2°C*. *Environmental Research Letters*, 13. doi: 10.1088/1748-9326/aacc76.

- Jin S., Yu W., Jansen H.G.P., Lansing E. (2012) *The Impact of Irrigation on Agricultural Productivity: Evidence from India*. Department of Agriculture, Food, and Resource Economics, Michigan State University, East Lansing, Michigan, 39 pages.
- Jones E., Qadir M., van Vliet M.T.H., et al. (2019) *The state of desalination and brine production: A global outlook*. *Science of the Total Environment*, 657:1343–1356. doi: 10.1016/j.scitotenv.2018.12.076.
- Kahrl F. and D. Roland-Holst (2008) *China's water energy nexus*. *Water Policy* 10:51–65.
- Kauffman D.L.J. (1980) *Systems One: An Introduction to Systems Thinking*, 2nd Edition. The Future Systems Series, Future Systems Inc., TLH Associates, Saint Paul, MN.
- Keyfitz N., Flieger W. (1971) *Population: facts and method of demography*. W.H. Freeman, San Francisco, 613 pages.
- King M., Altdorff D., Li P., et al (2018) *Northward shift of the agricultural climate zone under 21st-century global climate change*. *Scientific Reports*, 8:1–10. doi: 10.1038/s41598-018-26321-8.
- Klohn W., Faurès J., Vallée D., et al. (2003) *Securing food for a growing population*. The World Water Development Report. UNESCO-WWAP.
- Kotir J.H., Smith C., Brown G., et al. (2016) *A system dynamics simulation model for sustainable water resources management and agricultural development in the Volta River Basin, Ghana*. *Science of the Total Environment*, 573:444–457. doi: 10.1016/j.scitotenv.2016.08.081.
- Krinner G., Germany F., Shongwe M., et al. (2013) *Long-term climate change: Projections, commitments and irreversibility*. *Climate Change 2013: The Physical Science Basis*, Working Group I Contribution to the Fifth Assess Report of the Intergovernmental Panel on Climate Change. doi: 10.1017/CBO9781107415324.024.
- Larsen M.A.D. and M. Drews. (2019) *Water use in electricity generation for water-energy nexus analyses: The European case*. *Science of the Total Environment*, 651:2044–2058. doi: 10.1016/j.scitotenv.2018.10.045.
- Lipton M., Litchfield J. and M. Faures (2003) *The Effects of Irrigation on Poverty: A Framework for Analysis*. *Journal of Water Policy*, 5:413–427. doi: 10.2166/wp.2003.0026.
- Liu Y., Hejazi M., Li H., et al. (2017) *A hydrological emulator for global applications*. *Geoscientific Model Development Discussions*. doi: <https://doi.org/10.5194/gmd-2017-113>.
- Mackenzie F.T. (1999) *Global Biogeochemical Cycles and the Physical Climate System*. Global Change Instruction Program, University Corporation for Atmospheric Research, Hawaii.

- Mackenzie F.T., Ver L.M., Sabine C. and M. Lane (1993) *C, N, P, S Global Biogeochemical Cycles and Modeling of Global Change*. Interactions of C, N, P and S Biogeochemical Cycles and Global Change, Springer, Verlag, pp 1–61.
- Masterson W. and C. Hurley (2009) *Chemistry: Principles and Reactions*, 6th Edition. Brooks/Cole Cengage Learning.
- Matsuoka Y., Morita T. and M. Kainuma (2001) *Integrated Assessment Model of Climate Change: The AIM Approach*. Present and Future of Modeling Global Environmental Change: Toward Integrated Modeling, TerraPub, pp 339–361.
- McAfee A. (2019) *More from Less*. Scribner, New York, NY.
- Meadows D., Behrens W., Meadows D., et al. (1974) *Dynamics of Growth in a Finite World*. Wright-Allen Press, Inc., Cambridge, MA.
- Meadows D.H. and R. Jorgen (1992) *Beyond the Limits: Confronting Global Collapse, Envisioning a Sustainable Future*. Chelsea Green Pub., Hartford, VT.
- Meadows D.H., Meadows D.L., Behrens W.W. and J. Randers (1972) *Limits to Growth*. Universe Books, New York.
- Moss R.H., Edmonds J., Hibbard K., et al. (2010) *The next generation of scenarios for climate change research and assessment*. Nature, 463:747–756. doi: 10.1038/nature08823.
- (NASA) National Aeronautics and Space Administration (2019) *Global Temperature*. Global Land-Ocean Temperature Index. <https://climate.nasa.gov/vital-signs/global-temperature/>. Accessed 17 Oct 2019.
- Nordhaus W.D. (1992) *The “DICE” Model: Background and Structure of a Dynamic Integrated Climate-Economy Model of the Economics of Global Warming*. No 1009, Cowles Foundation Discussion Papers, Cowles Foundation for Research in Economics, Yale University.
- Nordhaus W.D. (1994) *Managing the Global Commons: The Economics of Climate Change*. MIT Press, Cambridge, MA.
- Nordhaus W.D. (2013) *DICE 2013R: Introduction and User’s Manual*, 2<sup>nd</sup> Edition. Yale University Press, 102 pages.
- Oelkers E.H. and E. Valsami-Jones (2017) *Phosphate Mineral Reactivity and Global Sustainability*. Elements, 4(2):83-87, doi: 10.2113/gselements.4.2.83.
- Olmstead S.M. (2010) *The economics of water quality*. Review of Environmental Economics and Policy, 4:44–62.

- (PAGES) Past Global Changes (2019) *ESSP Open Science Conference - Global Environmental Change: Regional Challenges*. Past Meeting.  
<http://pastglobalchanges.org/calendar/past/127-pages/1387-essp-open-science-conference-global-environmental-change-regional-challenges>. Accessed 23 Feb 2020.
- Piguat É. (2008) *Migration and climate change*. *Futuribles: Analyse et Prospective*, 341.
- Prescott E.C. (1988) *Robert M. Solow's Neoclassical Growth Model: An Influential Contribution to Economics*. *Scandinavian Journal of Economics*, 90:7–12.
- Price M.F. (1989) *Global change: Defining the ill-defined*. *Environment: Science and Policy for Sustainable Development*, 31:18–44. doi: 10.1080/00139157.1989.9928971.
- Rahmstorf S. (2007) *A Semi-Empirical Approach to Projecting Future Sea-Level Rise*. *Science*, 315:368–370.
- Richardson G.P. (1986) *Problems with causal-loop diagrams*. *System Dynamics Review*, 2:158–170. doi: 10.1002/sdr.4260020207.
- Ritchie H. and M. Roser (2018a) *Renewable Energy*. Our World Data.  
<https://ourworldindata.org/renewable-energy>. Accessed 15 Sep 2019.
- Ritchie H. and M. Roser (2018b) *Energy Production & Changing Energy Sources*. Our World Data. <https://ourworldindata.org/energy-production-and-changing-energy-sources>. Accessed 15 Sep 2019.
- Ritson J.P., Graham N.J.D., Templeton M.R., et al. (2014) *The impact of climate change on the treatability of dissolved organic matter (DOM) in upland water supplies: A UK perspective*. *Science of the Total Environment* 473:714–730. doi: 10.1016/j.scitotenv.2013.12.095.
- Roberts N., Anderson D., Deal R., et al. (1983a) *Introduction to Delays*. *Introduction to Computer Simulation: A System Dynamics Modeling Approach*. Productivity Press, Portland, Oregon, pp 301–333.
- Roberts N., Anderson D., Deal R., et al. (1983b) *Using Simulation to Analyze Simple Positive and Negative Loops*. *Introduction to Computer Simulation: A System Dynamics Modeling Approach*. Productivity Press, Portland, Oregon, pp 261–284.
- Rogers P., Bhatia R. and A. Huber. (1998) *Water as a Social and Economic Good: How to Put the Principle into Practice*. Global Water Partnership Technical Advisory Committee, Stockholm, Sweden, 40 pages.
- Rotmans J. and H. Dowlatabadi. (1998) *Integrated Assessment of Climate Change: Evaluation of Methods and Strategies*. *Human Choices and Climate Change: A State of the Art Report*.



- Rotmans J. and M. van Asselt (1999) *Integrated Assessment Modelling*. Working Paper FNU-102. Research Unit Sustainability and Global Change, Hamburg University and Centre for Marine and Atmospheric Science, Hamburg, Germany, 29 pages.
- Schlösser C.A., Strzepek K., Gao X., et al. (2014) *The Future of Global Water Stress: An Integrated Assessment*. MIT Joint Program on the Science and Policy of Global Change, 254, 33 pages.
- Scholes R.J., Reyers B., Biggs R., et al. (2013) *Multi-scale and cross-scale assessments of social-ecological systems and their ecosystem services*. *Current Opinions on Environmental Sustainability* 5:16–25. doi: 10.1016/j.cosust.2013.01.004.
- Schuster-Wallace C.J., Grover V.I., Adeel Z., et al. (2008) *Safe Water as the Key to Global Health*. UNU-INWEH, Tokyo.
- Schwartz J., Levin R., Goldstein R. (2000) *Drinking water turbidity and gastrointestinal illness in the elderly of Philadelphia*. *Journal of Epidemiology and Community Health*, 54:45–51. doi: 10.1136/jech.54.1.45.
- Searchinger T., Waite R., Hanson C., Ranganathan J. (2019) *Creating a Sustainable Food Future: A Menu of Solutions to Feed Nearly 10 Billion People by 2050*. World Resources Institute, 558 pages.
- Shiklomanov I. (2000) *Appraisal and Assessment of World Water Resources*. *Water International*, 25:11–32. doi: 10.1080/02508060008686794.
- Simonovic S.P. (2002a) *World water dynamics: global modeling of water resources*. *Journal of Environmental Management*, 66:249–267. doi: 10.1006/jema.2002.0585.
- Simonovic S.P. (2002b) *Global water dynamics: issues for the 21st century*. *Water Science and Technology*, 45:53–64.
- Simonovic S.P. (2012) *Managing water resources: Methods and tools for a systems approach*. UNESCO, Paris and Earthscan James & James, London.
- Sokolov A.P., Schlösser C.A., Dutkiewicz S., et al. (2005) *The MIT Integrated Global System Model (IGSM) Version 2: Model Description and Baseline Evaluation*. Report No. 124, Joint Program on the Science and Policy of Global Change, Cambridge, MA, 46 pages.
- Sood A. and V. Smakhtin (2014) *Global hydrological models: a review*. *Hydrological Sciences Journal*, 60:549–565. doi: 10.1080/02626667.2014.950580.
- Steffan W., Sanderson A., Tyson P., et al. (2004) *Global Change and the Earth System: A Planet Under Pressure*. Springer, Berlin, Heidelberg, New York, Hong Kong, London, Milan, Paris, Tokyo.

- Stehfest E., van Vuuren D., Kram T., and L. Bouwman (2014) *Overview of IMAGE 3.0. Integrated Assessment of Global Environmental Change with IMAGE 3.0: Model description and policy applications*. PBL Netherlands Environmental Assessment Agency, pp 32–54.
- Sterman J.D. (1980) *The Use of Aggregate Production Functions in Disequilibrium Models of Energy-Economy Interactions*. Working Paper D-3234, System Dynamics Group, MIT, Cambridge, MA, 02139.
- Sterman J.D. (2000) *Business Dynamics: Systems Thinking and Modeling for a Complex World*. Irwin McGraw-Hill, Boston, MA.
- Storn R. and K. Price (1995) *Differential Evolution - A simple and efficient adaptive scheme for global optimization over continuous spaces*. International Computer Science Institute, Berkeley, CA, 15 pages.
- Strzepek K., Schlosser A., Gueneau A., et al. (2013) *Modeling water resource systems within the framework of the MIT integrated global system model: IGSM-WRS*. Journal of Advances in Modeling Earth Systems, 5:638–653. doi: 10.1002/jame.20044.
- Thissen W. and C. De Mol (1978) *The agricultural and persistent pollution subsystems in world*. IEEE Transactions on Systems, Man and Cybernetics, 8:159–172. doi: 10.1109/TSMC.1978.4309927.
- Thomas W.L. (1956) *Man's Role in Changing the Face of the Earth*. The University of Chicago, Chicago, Illinois.
- Tol R.S.J. and P. Vellinga (1998) *The European forum on integrated environmental assessment*. Environmental Modeling and Assessment, 3:181–191. doi: 10.1023/A:1019023124912.
- Turner S.W.D., Hejazi M., Yonkofski C., et al. (2019) *Influence of Groundwater Extraction Costs and Resource Depletion Limits on Simulated Global Nonrenewable Water Withdrawals Over the Twenty-First Century*. Earth's Future, 7:123–135. doi: 10.1029/2018EF001105.
- (UIA) Union of International Associations (2020) *UIA Open Yearbook. International Human Dimension Programme on Global Environmental Change (IHDP)*. <https://uia.org/s/or/en/1100051966>. Accessed 20 Dec 2019.
- United Nations (2019a) *World Population Prospects 2019: Highlights*. Department of Economics and Social Affairs, Population Division, 46 pages.
- United Nations (2019b) *Migration and the climate crisis: the UN's search for solutions*. UN-News. Retrieved from: <https://news.un.org/en/story/2019/07/1043551>.

- United Nations (2019c) *World Population Prospects 2019: Methodology of the United Nations Population Estimates and Projections*. Department of Economic and Social Affairs, Population Division.
- United Nations (1997) *Comprehensive Assessment of the Freshwater Resources of the World. Urban Water: Towards Sustainability*. Stockholm Environment Institute, Stockholm, Sweden.
- (US-EPA) United States Environmental Protection Agency (2010) *The National Rivers and Streams Assessment 2008/2009*.
- van Vuuren D.P., Edmonds J., Kainuma M., et al. (2011) *The representative concentration pathways: An overview*. *Climatic Change*, 109:5–31. doi: 10.1007/s10584-011-0148-z.
- Virtanen P., Gommers R., Travis E.O., et al. (2019) *Scipy 1.0-Fundamental Algorithms for Scientific Computing in Python*. *Nature Methods*, 17:261-272/
- Vörösmarty C.J., McIntyre P.B., Gessner M.O., et al. (2010) *Global threats to human water security and river biodiversity*. *Nature*, 467:555–561. doi: 10.1038/nature09549.
- Wada Y. and M.F.P. Bierkens (2014) *Sustainability of global water use: past reconstruction and future projections*. *Environmental Research Letters*, 9. doi: 10.1088/1748-9326/9/10/104003.
- Wada Y., Flörke M., Hanasaki N., et al. (2016) *Modeling global water use for the 21st century: The Water Futures and Solutions (WFaS) initiative and its approaches*. *Geoscientific Model Development*, 9:175–222. doi: 10.5194/gmd-9-175-2016.
- Wada Y., Wissler D. and M.F.P. Bierkens (2014) *Global modeling of withdrawal, allocation and consumptive use of surface water and groundwater resources*. *Earth System Dynamics*, 5:15–40. doi: 10.5194/esd-5-15-2014.
- Wang J., Li Y., Huang J., et al. (2017) *Growing water scarcity, food security and government responses in China*. *Global Food Security*, 14:9–17. doi: 10.1016/j.gfs.2017.01.003.
- Wood A. and B. Wollenberg (1996) *Power Generation, Operation and Control*, 2nd Edition. Wiley, New York.
- (WCRP) World Climate Research Programme (2020) *About WCRP*. <https://www.wcrp-climate.org/about-wcrp/wcrp-overview>. Accessed 19 Dec 2019.
- World Commission on Environment and Development (1987) *Our Common Future*. Oxford University Press, Oxford.
- World Nuclear Association (2018) *Nuclear Power in the World Today*. <https://www.world-nuclear.org/information-library/current-and-future-generation/nuclear-power-in-the-world-today.aspx>. Accessed 10 Dec 2019.

- (WWAP) United Nations World Water Assessment Programme (2017) *Wastewater: The Untapped Resource*. UNESCO, Paris.
- Yuan Z., Yan D., Yang Z., et al. (2016) *Impacts of climate change on winter wheat water requirement in Haihe River Basin*. *Mitigation and Adaptation Strategies of Global Change*, 21:677–697. doi: 10.1007/s11027-014-9612-1.
- Zabel F., Putzenlechner B. and W. Mauser. (2014) *Global agricultural land resources - A high resolution suitability evaluation and its perspectives until 2100 under climate change conditions*. *PLOS ONE*, 9(12): e114980. doi: 10.1371/journal.pone.0107522.
- Zhao C., Liu B., Piao S., et al. (2017) *Temperature increase reduces global yields of major crops in four independent estimates*. *Proceedings of the National Academy of Sciences of the United States of America*, 114:9326–9331. doi: 10.1073/pnas.1701762114.
- Ziolkowska J.R. (2014) *Is Desalination Affordable?—Regional Cost and Price Analysis*. *Water Resources Management*, 29:1385–1397. doi: 10.1007/s11269-014-0901-y.

## Appendices

### Appendix A. List of Intersectoral Feedback Loops

The following list is an output from Vensim using the “Loops” tool on the causal loop diagram shown in Figure 3.1.

Loop Number 1 of length 2

- Nutrient Cycles
  - Water Supply Development
  - Hydrologic Cycle

Loop Number 2 of length 2

- Nutrient Cycles
  - Water Supply Development
  - Food Production

Loop Number 3 of length 3

- Nutrient Cycles
  - Water Supply Development
  - Population
  - Water Demand

Loop Number 4 of length 3

- Nutrient Cycles
  - Water Supply Development
  - Energy Economy
  - Food Production

Loop Number 5 of length 3

- Nutrient Cycles
  - Water Supply Development
  - Energy Economy
  - Water Demand

Loop Number 6 of length 4

- Nutrient Cycles

Water Supply Development

Population

Land Use

Water Demand

Loop Number 7 of length 4

Nutrient Cycles

Water Supply Development

Energy Economy

Persistent Pollution

Food Production

Loop Number 8 of length 4

Nutrient Cycles

Water Supply Development

Population

Energy Economy

Food Production

Loop Number 9 of length 4

Nutrient Cycles

Water Supply Development

Hydrologic Cycle

Population

Water Demand

Loop Number 10 of length 4

Nutrient Cycles

Water Supply Development

Population

Land Use

Food Production

Loop Number 11 of length 4

Nutrient Cycles

Water Supply Development

Population

Energy Economy

Water Demand

Loop Number 12 of length 4

Nutrient Cycles

Water Supply Development

Food Production

Population

Water Demand

Loop Number 13 of length 4

Nutrient Cycles

Water Supply Development

Population

Persistent Pollution

Food Production

Loop Number 14 of length 5

Nutrient Cycles

Water Supply Development

Energy Economy

Carbon

Population

Water Demand

Loop Number 15 of length 5

Nutrient Cycles

Water Supply Development

Hydrologic Cycle

Population

Energy Economy

Food Production

Loop Number 16 of length 5

Nutrient Cycles

Water Supply Development

Energy Economy

Food Production

Population

Water Demand

Loop Number 17 of length 5

Nutrient Cycles

Water Supply Development

Food Production

Population

Land Use

Water Demand

Loop Number 18 of length 5

Nutrient Cycles

Water Supply Development

Hydrologic Cycle

Population

Energy Economy

Water Demand

Loop Number 19 of length 5

Nutrient Cycles

Water Supply Development

Population

Land Use

Persistent Pollution

Food Production

Loop Number 20 of length 5

Nutrient Cycles

Water Supply Development

Hydrologic Cycle

Population

Persistent Pollution

Food Production

Loop Number 21 of length 5

Nutrient Cycles

Water Supply Development

Hydrologic Cycle



Population  
Land Use  
Water Demand

Loop Number 22 of length 5

Nutrient Cycles  
Water Supply Development  
Energy Economy  
Carbon  
Climate  
Food Production

Loop Number 23 of length 5

Nutrient Cycles  
Water Supply Development  
Energy Economy  
Carbon  
Climate  
Hydrologic Cycle

Loop Number 24 of length 5

Nutrient Cycles  
Water Supply Development  
Population  
Energy Economy  
Persistent Pollution  
Food Production

Loop Number 25 of length 5

Nutrient Cycles  
Water Supply Development  
Energy Economy  
Persistent Pollution  
Population  
Water Demand

Loop Number 26 of length 5

Nutrient Cycles

Water Supply Development

Food Production

Population

Energy Economy

Water Demand

Loop Number 27 of length 5

Nutrient Cycles

Water Supply Development

Hydrologic Cycle

Population

Land Use

Food Production

Loop Number 28 of length 6

Nutrient Cycles

Water Supply Development

Hydrologic Cycle

Population

Land Use

Persistent Pollution

Food Production

Loop Number 29 of length 6

Nutrient Cycles

Water Supply Development

Population

Land Use

Carbon

Climate

Food Production

Loop Number 30 of length 6

Nutrient Cycles

Water Supply Development

Energy Economy

Persistent Pollution

Food Production

Population

Water Demand

Loop Number 31 of length 6

Nutrient Cycles

Water Supply Development

Hydrologic Cycle

Population

Energy Economy

Persistent Pollution

Food Production

Loop Number 32 of length 6

Nutrient Cycles

Water Supply Development

Energy Economy

Carbon

Climate

Land Use

Food Production

Loop Number 33 of length 6

Nutrient Cycles

Water Supply Development

Population

Land Use

Carbon

Climate

Hydrologic Cycle

Loop Number 34 of length 6

Nutrient Cycles

Water Supply Development

Energy Economy

Food Production

Population

Land Use

Water Demand

Loop Number 35 of length 6

Nutrient Cycles

Water Supply Development

Energy Economy

Carbon

Population

Land Use

Water Demand

Loop Number 36 of length 6

Nutrient Cycles

Water Supply Development

Energy Economy

Persistent Pollution

Population

Land Use

Water Demand

Loop Number 37 of length 6

Nutrient Cycles

Water Supply Development

Energy Economy

Carbon

Climate

Land Use

Water Demand

Loop Number 38 of length 6

Nutrient Cycles

Water Supply Development

Population

Energy Economy

Carbon

Climate

Food Production

Loop Number 39 of length 6

## Nutrient Cycles

Water Supply Development

Energy Economy

Carbon

Population

Persistent Pollution

Food Production

## Loop Number 40 of length 6

## Nutrient Cycles

Water Supply Development

Energy Economy

Carbon

Population

Land Use

Food Production

## Loop Number 41 of length 6

## Nutrient Cycles

Water Supply Development

Population

Energy Economy

Carbon

Climate

Hydrologic Cycle

## Loop Number 42 of length 6

## Nutrient Cycles

Water Supply Development

Energy Economy

Carbon

Climate

Population

Water Demand

## Loop Number 43 of length 6

## Nutrient Cycles

Water Supply Development

Energy Economy  
Persistent Pollution  
Population  
Land Use  
Food Production

Loop Number 44 of length 7

Nutrient Cycles  
Water Supply Development  
Population  
Energy Economy  
Carbon  
Climate  
Land Use  
Water Demand

Loop Number 45 of length 7

Nutrient Cycles  
Water Supply Development  
Energy Economy  
Persistent Pollution  
Food Production  
Population  
Land Use  
Water Demand

Loop Number 46 of length 7

Nutrient Cycles  
Water Supply Development  
Hydrologic Cycle  
Population  
Land Use  
Carbon  
Climate  
Food Production

Loop Number 47 of length 7

## Nutrient Cycles

Water Supply Development

Energy Economy

Carbon

Climate

Population

Land Use

Water Demand

## Loop Number 48 of length 7

## Nutrient Cycles

Water Supply Development

Energy Economy

Carbon

Climate

Population

Land Use

Food Production

## Loop Number 49 of length 7

## Nutrient Cycles

Water Supply Development

Energy Economy

Carbon

Climate

Food Production

Population

Water Demand

## Loop Number 50 of length 7

## Nutrient Cycles

Water Supply Development

Population

Land Use

Carbon

Climate

Energy Economy

Food Production

Loop Number 51 of length 7

Nutrient Cycles

Water Supply Development

Energy Economy

Carbon

Climate

Land Use

Persistent Pollution

Food Production

Loop Number 52 of length 7

Nutrient Cycles

Water Supply Development

Food Production

Population

Energy Economy

Carbon

Climate

Hydrologic Cycle

Loop Number 53 of length 7

Nutrient Cycles

Water Supply Development

Population

Land Use

Carbon

Climate

Energy Economy

Water Demand

Loop Number 54 of length 7

Nutrient Cycles

Water Supply Development

Hydrologic Cycle

Population

Energy Economy

Carbon



Climate

Food Production

Loop Number 55 of length 7

Nutrient Cycles

Water Supply Development

Population

Energy Economy

Carbon

Climate

Land Use

Food Production

Loop Number 56 of length 7

Nutrient Cycles

Water Supply Development

Energy Economy

Carbon

Population

Land Use

Persistent Pollution

Food Production

Loop Number 57 of length 7

Nutrient Cycles

Water Supply Development

Food Production

Population

Land Use

Carbon

Climate

Hydrologic Cycle

Loop Number 58 of length 7

Nutrient Cycles

Water Supply Development

Energy Economy

Carbon

Climate

Hydrologic Cycle

Population

Water Demand

Loop Number 59 of length 7

Nutrient Cycles

Water Supply Development

Energy Economy

Carbon

Climate

Population

Persistent Pollution

Food Production

Loop Number 60 of length 8

Nutrient Cycles

Water Supply Development

Population

Energy Economy

Carbon

Climate

Land Use

Persistent Pollution

Food Production

Loop Number 61 of length 8

Nutrient Cycles

Water Supply Development

Energy Economy

Food Production

Population

Land Use

Carbon

Climate

Hydrologic Cycle

Loop Number 62 of length 8

Nutrient Cycles

Water Supply Development

Population

Land Use

Carbon

Climate

Energy Economy

Persistent Pollution

Food Production

Loop Number 63 of length 8

Nutrient Cycles

Water Supply Development

Energy Economy

Persistent Pollution

Population

Land Use

Carbon

Climate

Hydrologic Cycle

Loop Number 64 of length 8

Nutrient Cycles

Water Supply Development

Energy Economy

Carbon

Climate

Land Use

Food Production

Population

Water Demand

Loop Number 65 of length 8

Nutrient Cycles

Water Supply Development

Hydrologic Cycle

Population

Land Use

Carbon

Climate

Energy Economy

Water Demand

Loop Number 66 of length 8

Nutrient Cycles

Water Supply Development

Energy Economy

Carbon

Climate

Population

Land Use

Persistent Pollution

Food Production

Loop Number 67 of length 8

Nutrient Cycles

Water Supply Development

Food Production

Population

Energy Economy

Carbon

Climate

Land Use

Water Demand

Loop Number 68 of length 8

Nutrient Cycles

Water Supply Development

Hydrologic Cycle

Population

Land Use

Carbon

Climate

Energy Economy

Food Production

Loop Number 69 of length 8

## Nutrient Cycles

Water Supply Development

Energy Economy

Persistent Pollution

Population

Land Use

Carbon

Climate

Food Production

## Loop Number 70 of length 8

## Nutrient Cycles

Water Supply Development

Food Production

Population

Land Use

Carbon

Climate

Energy Economy

Water Demand

## Loop Number 71 of length 8

## Nutrient Cycles

Water Supply Development

Hydrologic Cycle

Population

Energy Economy

Carbon

Climate

Land Use

Water Demand

## Loop Number 72 of length 8

## Nutrient Cycles

Water Supply Development

Hydrologic Cycle

Population

Energy Economy

Carbon  
Climate  
Land Use  
Food Production

Loop Number 73 of length 8

Nutrient Cycles  
Water Supply Development  
Energy Economy  
Carbon  
Climate  
Hydrologic Cycle  
Population  
Land Use  
Food Production

Loop Number 74 of length 8

Nutrient Cycles  
Water Supply Development  
Energy Economy  
Carbon  
Climate  
Hydrologic Cycle  
Population  
Land Use  
Water Demand

Loop Number 75 of length 8

Nutrient Cycles  
Water Supply Development  
Energy Economy  
Carbon  
Climate  
Hydrologic Cycle  
Population  
Persistent Pollution  
Food Production

Loop Number 76 of length 8

Nutrient Cycles

Water Supply Development

Energy Economy

Carbon

Climate

Land Use

Persistent Pollution

Population

Water Demand

Loop Number 77 of length 8

Nutrient Cycles

Water Supply Development

Energy Economy

Carbon

Climate

Food Production

Population

Land Use

Water Demand

Loop Number 78 of length 9

Nutrient Cycles

Water Supply Development

Hydrologic Cycle

Population

Land Use

Carbon

Climate

Energy Economy

Persistent Pollution

Food Production

Loop Number 79 of length 9

Nutrient Cycles

Water Supply Development

Hydrologic Cycle

Population  
Energy Economy  
Carbon  
Climate  
Land Use  
Persistent Pollution  
Food Production

Loop Number 80 of length 9

Nutrient Cycles  
Water Supply Development  
Energy Economy  
Carbon  
Climate  
Land Use  
Persistent Pollution  
Food Production  
Population  
Water Demand

Loop Number 81 of length 9

Nutrient Cycles  
Water Supply Development  
Energy Economy  
Carbon  
Climate  
Hydrologic Cycle  
Population  
Land Use  
Persistent Pollution  
Food Production

Loop Number 82 of length 9

Nutrient Cycles  
Water Supply Development  
Energy Economy  
Persistent Pollution  
Food Production



Population

Land Use

Carbon

Climate

Hydrologic Cycle

## Appendix B. Parameters for the Nutrient Cycles

Table B.6.1. Initial values and residence times of carbon, nitrogen, and phosphorus stocks in their respective cycles from Mackenzie et al. (1993).

Reservoir (No.)	CARBON		NITROGEN		PHOSPHORUS	
	Mass, moles	RT, years	Mass, moles	RT, years	Mass, moles	RT, years
Land Biota (1)	$4.98 \times 10^{16}$	9.5	$7.14 \times 10^{14}$	9	$9.69 \times 10^{13}$	9.5
Humus (2)	$2.05 \times 10^{16}$	4	$2.43 \times 10^{15}$	30	$4.01 \times 10^{14}$	39
Inorganic Soil (3)	$5.98 \times 10^{16}$	1,300	$1.23 \times 10^{14}$	1.4	$1.15 \times 10^{15}$	1,770
Coastal Waters (4)	$6.00 \times 10^{15}$	2.3	$1.08 \times 10^{14}$	1.1	$4.50 \times 10^{12}$	0.75
Coastal Biota (5)	$4.21 \times 10^{13}$	0.07	$6.35 \times 10^{12}$	0.07	$3.76 \times 10^{11}$	0.07
Coastal Sediments (6)	$2.07 \times 10^{17}$	5,400	$2.28 \times 10^{15}$	370	$9.20 \times 10^{15}$	11,000
Surface Ocean (7)	$3.54 \times 10^{17}$	22	$2.05 \times 10^{14}$	0.41	$2.65 \times 10^{14}$	8.8
Ocean Biota (8)	$2.21 \times 10^{14}$	0.07	$3.36 \times 10^{13}$	0.07	$1.97 \times 10^{12}$	0.07
Deep Ocean (9)	$2.75 \times 10^{18}$	1,200	$5.11 \times 10^{16}$	1,500	$2.97 \times 10^{15}$	1,100
Atmosphere (10)	$6.15 \times 10^{16}$	3.6	$2.80 \times 10^{20}$	11,400,000		

Table B.6.2. Rate constants used to describe flow in the cycles of carbon, nitrogen, and phosphorus from Mackenzie et al. (1993).

$k_{ij}$	CARBON		NITROGEN		PHOSPHORUS	
	Flux, moles/year	k, /year	Flux, moles/year	k, /year	Flux, moles/year	k, /year
k 101	$5.25 \times 10^{15}$	$8.54 \times 10^{-2}$	$9.60 \times 10^{12}$	$3.43 \times 10^{-8}$		
k 103	$3.40 \times 10^{13}$	$5.53 \times 10^{-4}$	$6.90 \times 10^{12}$	$2.46 \times 10^{-8}$		
k 104	$1.51 \times 10^{15}$	$2.45 \times 10^{-2}$	$5.07 \times 10^{11}$	$1.81 \times 10^{-9}$		
k 105			$2.37 \times 10^{12}$	$2.56 \times 10^2$		
k 107	$1.03 \times 10^{16}$	$1.68 \times 10^{-1}$	$4.59 \times 10^{12}$	$1.64 \times 10^{-8}$		
k 108			$6.30 \times 10^{11}$	$1.29 \times 10^2$		
k 12	$5.25 \times 10^{15}$	$1.05 \times 10^{-1}$	$8.33 \times 10^{13}$	$1.17 \times 10^{-1}$	$1.02 \times 10^{13}$	$1.05 \times 10^{-1}$
k 23			$8.15 \times 10^{13}$	$3.35 \times 10^{-2}$		
k 210	$5.22 \times 10^{15}$	$2.54 \times 10^{-1}$				
k 31			$7.37 \times 10^{13}$	$5.99 \times 10^{-1}$		
k 310			$1.42 \times 10^{13}$	$1.15 \times 10^{-1}$		
k 45	$6.00 \times 10^{14}$	$1.00 \times 10^{-1}$	$9.07 \times 10^{13}$	$8.40 \times 10^{-1}$	$5.37 \times 10^{12}$	$1.19 \times 10^0$
k 47	$5.00 \times 10^{14}$	$8.33 \times 10^{-2}$	$7.50 \times 10^{12}$	$6.94 \times 10^{-2}$	$6.40 \times 10^{11}$	$1.42 \times 10^{-1}$
k 410	$1.51 \times 10^{15}$	$2.51 \times 10^{-1}$	$1.10 \times 10^{12}$	$1.02 \times 10^{-2}$		
k 54	$5.76 \times 10^{14}$	$1.37 \times 10^1$	$8.69 \times 10^{13}$	$1.37 \times 10^1$	$5.15 \times 10^{12}$	$1.37 \times 10^1$
k 56	$2.40 \times 10^{13}$	$5.70 \times 10^{-1}$	$6.14 \times 10^{12}$	$9.67 \times 10^{-1}$	$2.20 \times 10^{11}$	$5.85 \times 10^{-1}$
k 64	$3.10 \times 10^{13}$	$1.50 \times 10^{-4}$	$4.39 \times 10^{12}$	$1.93 \times 10^{-3}$	$5.10 \times 10^{11}$	$5.54 \times 10^{-5}$
k 610			$3.33 \times 10^{12}$	$1.46 \times 10^{-3}$		
k 74	$4.29 \times 10^{14}$	$1.21 \times 10^{-3}$	$6.44 \times 10^{12}$	$3.14 \times 10^{-2}$	$3.20 \times 10^{11}$	$1.21 \times 10^{-3}$
k 78	$3.15 \times 10^{15}$	$8.90 \times 10^{-3}$	$4.80 \times 10^{14}$	$2.34 \times 10^0$	$2.82 \times 10^{13}$	$1.06 \times 10^{-1}$
k 79	$2.16 \times 10^{15}$	$6.10 \times 10^{-3}$	$1.14 \times 10^{13}$	$5.57 \times 10^{-2}$	$1.59 \times 10^{12}$	$6.00 \times 10^{-3}$
k 710	$1.04 \times 10^{16}$	$2.94 \times 10^{-2}$	$5.80 \times 10^{12}$	$2.83 \times 10^{-2}$		
k 87	$3.02 \times 10^{15}$	$1.37 \times 10^1$	$4.57 \times 10^{14}$	$1.36 \times 10^1$	$2.71 \times 10^{13}$	$1.37 \times 10^1$
k 89	$1.26 \times 10^{14}$	$5.71 \times 10^{-1}$	$2.33 \times 10^{13}$	$6.93 \times 10^{-1}$	$1.13 \times 10^{12}$	$5.72 \times 10^{-1}$
k 97	$2.28 \times 10^{15}$	$8.29 \times 10^{-4}$	$3.42 \times 10^{13}$	$6.69 \times 10^{-4}$	$2.40 \times 10^{12}$	$8.08 \times 10^{-4}$
k 910			$2.10 \times 10^{11}$	$4.11 \times 10^{-6}$		
k 2R	$3.30 \times 10^{13}$	$1.61 \times 10^{-3}$	$2.21 \times 10^{12}$	$9.09 \times 10^{-4}$	$1.02 \times 10^{13}$	$2.54 \times 10^{-2}$
k 3R	$4.70 \times 10^{13}$	$7.86 \times 10^{-4}$	$8.20 \times 10^{11}$	$6.67 \times 10^{-3}$	$6.50 \times 10^{11}$	$5.65 \times 10^{-4}$
k R1					$1.02 \times 10^{13}$	
k R4	$6.60 \times 10^{13}$		$1.03 \times 10^{12}$		$3.00 \times 10^{10}$	
k R6	$1.40 \times 10^{13}$		$2.00 \times 10^{12}$		$6.20 \times 10^{11}$	
F 6out	$7.00 \times 10^{12}$		$4.20 \times 10^{11}$		$3.30 \times 10^{11}$	
F 9out	$6.00 \times 10^{12}$		$2.70 \times 10^{11}$		$3.20 \times 10^{11}$	
F out2			$3.90 \times 10^{11}$			
F out3	$1.30 \times 10^{13}$		$3.00 \times 10^{11}$		$6.50 \times 10^{11}$	

## Appendix C. Differential evolution algorithm for parameter estimation of ANEMI3

The differential evolution algorithm of Storn and Price (1995) was used for parameter estimation of the ANEMI3 model baseline run. This evolutionary algorithm was selected because of its ability to find the global optimum of high-dimensional objective functions without the need for the function derivative to be specified.

Differential Evolution (DE) is a brute-force stochastic algorithm that falls within the family of Evolutionary Algorithms (EA). Within the set of EAs there exists a common set of principles that are used to reach a solution to global optimization problems that are otherwise difficult to obtain from traditional non-linear solvers in certain circumstances. Solutions tend to evolve from an initial population of feasible solutions based on their level of fitness in achieving the goal of the optimization. Each individual of the population is defined by a set of genes, representing the elements of a feasible solution vector. As the evolution process proceeds, individuals' genes are mutated and combined to reach a new generation whose overall level of fitness is increased. Individuals of the population either make it to the next generation or are discarded based on their level of fitness with respect to the objective function. It is this evolutionary principle of “survival of the fittest” that EAs use to progressively improve their set of feasible solutions.

The DE algorithm steps are discussed here while the interested reader is referred to Storn and Price (1995) for details of the original DE algorithm (rand/1/bin).

1. DE starts with an objective function  $F(X)$  where  $X$  represents a set of  $N$  decision variables.
2. Each gene of the  $N$  trial vectors are initialized randomly between a specified set of bounds for which the optimal solution of  $F(X)$  is to be found
3. The evolution process is composed of three steps, mutation (i), crossover (ii), and selection (iii).
  - i. Mutation combines the genes of two randomly selected members of the population with another randomly selected unique member. This is done by taking the difference between the first two randomly selected individuals, applying a mutation factor  $F$ , and adding the result to the third, which defines the mutation vector. One mutation vector is generated for each individual or target vector of the population.
  - ii. Crossover transfers genes from the mutated vector to the target vector. For each gene of both the mutated and target vectors a random number,  $r \sim U(0, 1)$  is compared to a predefined crossover probability constant,  $CR$ . If  $r < CR$  the mutated gene replaces the target gene, while if  $r > CR$  the target gene is kept. To ensure that at least one mutated gene is transferred to the new individual, a randomly generated number  $rn \sim U(0, N)$  is compared to the index  $i \in [0, N]$  of each gene. If  $i = rn$  then the mutated gene is transferred regardless of the value of  $r$ . The resulting vector is termed the trial vector.
  - iii. Finally, the fitness of the trial vector is compared to the target vector using the by inputting them into the objective function. The vector with the best objective function value is kept in the population for the next generation.

As the evolution proceeds, termination is reached when the maximum number of iterations is met, or a tolerance level is satisfied. At this point the fittest individual in the population at the final generation is retained as the final solution that optimizes the objective function.

This algorithm was incorporated into the parameter estimation process of the Vensim model by using the VenPy automation software described in Appendix A. The differential evolution algorithm was implemented using the Scipy software package (Virtanen et al. 2019). The Python code used to run the differential algorithm with the ANEMI3 model is provided below.

```
import venpy as vp
import time
from scipy.optimize import differential_evolution as de

# Parameters were loaded from another .cin file
parameters = {}
Nfeval = 1

def func(x):
    global Nfeval
    print(f"Running parameter estimation simulation number {Nfeval}")
    Nfeval += 1

    # Load the compiled Vensim model
    model = vp.load('ANEMI3.vpm')

    # Set the model parameters
    for xi, p in zip(x, parameters):
        model[p] = xi

    # Run the model and return high number in the case of errors
    try:
        model.run('total_parameter_estimation_run')
    except:
        print("Error running simulation")
        return 1e10
    time.sleep(0.2)
    try:
        # Obtain total error of parameter estimation objective function
        # defined in Vensim
        error = model.result(names=['Total Error'])
        if len(error) == 121:
```

```
        total_error = error.values.sum()
        print(f"Current error is: {total_error}")
        return total_error
    else:
        print(f"Simulation did not finish. Total length is {len(error)}")
        return 1e10

except IOError:
    print("Could not obtain error for this run")
    return 1e10

# Return the value of the objective function
return error

# Run objective function with bounds for parameter values
result = de(func, list(parameters.values()), disp=True, polish=False)

print("Done.")
```

## Appendix D. VenPy code used for automation of ANEMI3 model runs

The code presented in this appendix creates an interface between Vensim and the Python programming language in order to automate the process of running model scenarios in ANEMI3. It works by accessing the Vensim DLL which is packaged Vensim and contains a set of subroutines written in the C programming language. The Python interface handles inputs and output processing for ease of use and provides a way to incorporate user defined python functions into Vensim models. The VenPy software package is MIT licenced and open source. The VenPy project is hosted at <https://github.com/pbreach/venpy> and is also included below.

```

"""
Created on Mon Oct 12 22:50:41 2015

@author: Patrick Breach
@email: <pbreach@uwo.ca>
"""
import ctypes
from ctypes import util
import platform
import re
from itertools import product

import numpy as np
import pandas as pd

def load(model, dll='vend1132.dll'):
    """Load compiled Vensim model using the Vensim DLL.

    Parameters
    -----
    model : str
        compiled (.vpm) Vensim model filepath
    dll : str, default 'vend1132.dll'
        name of installed Vensim dll file

    Returns
    -----
    VenPy model object
    """

```



```

return VenPy(model, dll)

class VenPy(object):

    def __init__(self, model, dll):
        #Get bitness and OS
        bit, opsys = platform.architecture()

        #Filter numbers out of string
        nums = lambda X: "".join(x for x in X if str.isdigit(x))

        #Assert same bitness of Python and Vensim
        assert nums(dll) == nums(bit), \
            "%s version of Python will not work with %s" % (bit, dll)

        #Get path to Vensim dll
        path = util.find_library(dll)

        #Make sure OS is Windows
        if "Windows" not in opsys:
            raise OSError("Not supported for %s" % opsys)
        #Test if path was obtained for Vensim dll
        elif not path:
            raise IOError("Could not find Vensim DLL '%s'" % dll)

        #Load Vensim dll
        try:
            self.dll = ctypes.windll.LoadLibrary(path)
        except Exception as e:
            print(e)
            print("'%s' could not be loaded using the path '%s'" % (dll,
path))

        #Load compiled vensim model
        self.cmd("SPECIAL>LOADMODEL|%s" % model)

        #Get all variable names from model based on type
        types = {1: 'level', 2: 'aux', 3: 'data', 4: 'init', 5: 'constant',
                6: 'lookup', 7: 'group', 8: 'sub_range', 9: 'constraint',
                10: 'test_input', 11: 'time_base', 12: 'game',
                13: 'sub_constant'}

        self.vtype = {}

        for num, var in types.items():
            maxn = self.dll.vensim_get_varnames(b'*', num, None, 0)
            names = (ctypes.c_char * maxn)()
            self.dll.vensim_get_varnames(b'*', num, names, maxn)
            names = _c_char_to_list(names)

            for n in names:

```

```

        if n:
            self.vtype[n] = var

#Set empty components dictionary
self.components = {}
#Set runname as none when no simulation has taken place
self.runname = None

def __getitem__(self, key):

    #Test for subscript type of string
    if self._is_subbed(key):
        #Get subscript element information
        var, elements, combos = self._get_sub_info(key)

        if all(len(e)==1 for e in elements):
            return self._getval(key)

        else:
            #Get shape of resulting array
            shape = [len(e) for e in elements]
            #Get values of subscript combinations
            values = [self._getval(c) for c in combos]

            return np.array(values).reshape(shape).squeeze()

    else:
        return self._getval(key)

def __setitem__(self, key, val):

    if isinstance(val, (int, float)):
        #Setting single int or float
        self._setval(key, val)

    elif hasattr(val, "__call__"):
        #Store callable as model component called when run
        self.components[key] = val

    elif (type(val)==np.ndarray or type(val)==list) and
self._is_subbed(key):
        #Get subscript element information
        var, elements, combos = self._get_sub_info(key)

        if all(len(e)==1 for e in elements):
            TypeError("Array or list cannot be set to fully subscripted "
\
            "variable %s" % key)

        else:
            #Convert values to strings and flatten out array

```

```

        values = np.array(val).flatten().astype(str)
        #Make sure correct number of elements are being set
        assert len(values) == len(combos), "Array has %s elements, "
\
        "while '%s' has %s elements" % (len(values), key,
len(combos))
        #Set subscript combinations
        for c, v in zip(combos, values):
            self._setval(c, v)

    else:
        message = "Unsupported type '%s' passed to __setitem__ for Venim"
\
        "variable '%s'." % (type(val), key)
        raise TypeError(message)

def run(self, runname='Run', interval=1):
    """
    Run the loaded Vensim model.

    Parameters
    -----
    runname : str, default 'Run'
        Label for model results. Use a different name for distinguishing
        output between multiple runs.
    interval : int, default 1
        The number of time steps defining the interval for which the
        control of the simulation is returned to the user defined
functions
        (if any). Communication occurs at the beginning of each interval.
    """
    #Do not display any messages from Vensim
    self.dll.vensim_be_quiet(1)
    #Set simulation name before running
    self.runname = runname
    self.cmd("SIMULATE>RUNNAME|%s" % runname)

    #Run entire simulation if no components are set
    if not self.components:
        self.cmd("MENU>RUN|O")
    else:
        #Run simulation step by step
        initial = self.__getitem__("INITIAL TIME")
        final = self.__getitem__("FINAL TIME")
        dt = self.__getitem__("TIME STEP")

        if (initial - final) % interval:
            msg = "total time steps are not evenly divisible by
interval."
            raise ValueError(msg)
        elif interval < dt:

```

```

        raise ValueError("Interval should be greater than time
step.")

#Start the simulation
self.cmd("MENU>GAME|O")
self.cmd("GAME>GAMEINTERVAL|%s" % interval)

step = interval if interval else dt

#Run user defined function(s) at every step
for t in np.arange(initial, final, step):
    self._run_udfs()
    self.cmd("GAME>GAMEON")

self.cmd("GAME>ENDGAME")

def cmd(self, cmd):
    """Send a command using the Vensim DLL.

    Parameters
    -----
    cmd : str
        Valid string command for Vensim DLL
    """
    success = self.dll.vensim_command(_prepstr(cmd))
    if not success:
        raise Exception("Vensim command '%s' was not successful." % cmd)

def result(self, names=None, vtype=None):
    """Get last model run results loaded into python. Specific variables
    can be retrieved using the `names` attribute, or all variables of a
    specific type can be returned using the `vtype` attribute.

    All variables of type 'level', 'aux', and 'game' are returned by
    default.

    Parameters
    -----
    names : str or sequence, default None
        Variable names for which the data will be retrieved. By default,
        all model levels and auxiliaries are returned. If an iterable is
        passed, a subset of these will be returned.
    vtype : str, default None
        Return result for variable names of specific types(s). Valid
types
        that can be specified are 'level', 'aux', and/or 'game'.

    Returns
    -----
    result : dict

```

```

model      Python dictionary will be returned where the keys are Vensim
each      names and values are lists corresponding to model output for
          timestep.
          """
          #Make sure results are generated before retrieved
assert self.runname, "Run before results can be obtained."
          #Make sure both kwargs are not set simultaneously
assert not (names and vtype), "Only one of either 'names' or 'vtype'"
          " can be set."
          valid = set(['level', 'aux', 'game'])
if names:
            #Make sure all names specified are in the model
            assert all(n in self.vtype.keys() for n in names), "One or more "
            "names are not defined in Vensim."
            #Ensure specified names are of the appropriate type
            types = set([self.vtype[n] for n in names])
            assert valid >= types, "One or more names are not of type " \
            "'level', 'aux', or 'game'."
            varnames = names
elif vtype:
            #Make sure vtype is valid
            assert vtype in valid, "'vtype' must be 'level', 'aux', or
'game'."
            varnames = [n for n,v in self.vtype.items() if v == vtype]
else:
            varnames = [n for n,v in self.vtype.items() if v in valid]
if not varnames:
            raise Exception("No variables of specified type(s).")
          allvars = []
for v in varnames:
            if self._is_subbed(v):
                allvars += [v + s for s in self._get_sub_elements([v])[0]]
            else:
                allvars.append(v)
          result = {}
for v in allvars:
            maxn = self.dll.vensim_get_data(_prepstr(self.runname),
            _prepstr(v),
            b'Time', None, None, 0)

```

```

vval = (ctypes.c_float * maxn)()
tval = (ctypes.c_float * maxn)()

success = self.dll.vensim_get_data(_prepstr(self.runname),
                                   _prepstr(v),
                                   b'Time', vval, tval, maxn)

if not success:
    raise IOError("Could not retrieve data for '%s' \
                  " corresponding to run '%s'" % (v, self.runname))

result[v] = np.array(vval)

return pd.DataFrame(result, index=np.array(tval))

def _run_udfs(self):
    for key in self.components:
        #Ensure only gaming type variables can be set during sim
        if self._is_subbed(key):
            name, _ = self._get_subs(key)
        else:
            name = key

        assert self.vtype[name] == 'game', \
            "%s must be of 'Gaming' type to set during sim." % key
        #Set vensim variable using component function output
        val = self.components[key]()
        self.__setitem__(key, val)

def _getval(self, key):
    #Define ctypes single precision floating point number
    result = ctypes.c_float()
    #Store value based on key lookup in result
    success = self.dll.vensim_get_val(_prepstr(key),
    ctypes.byref(result))

    if not success:
        raise KeyError("Unable to query value for '%s'." % key)
    elif result.value == -1.298074214633707e33:
        vtype = self.vtype[key]
        raise KeyError("Cannot get '%s' outside simulation." % vtype)

    return result.value

def _setval(self, key, val):
    #Set the value of a Vensim variable
    cmd = "SIMULATE>SETVAL|%s=%s" % (key, val)
    self.cmd(cmd)

```

```

def _get_sub_info(self, key):
    var, subs = self._get_subs(key)
    elements = self._get_sub_elements(subs)
    combos = [var + "[%s]" % ','.join(c) for c in product(*elements)]
    return var, elements, combos

def _get_sub_elements(self, subs):
    elements = []
    for s in subs:
        if self.vtype[s] != 'sub_constant':
            maxn = self.dll.vensim_get_varattrib(_prepstr(s), 9, None, 0)
            res = (ctypes.c_char * maxn)()
            self.dll.vensim_get_varattrib(_prepstr(s), 9, res, maxn)
            elements.append(_c_char_to_list(res))
        else:
            elements.append([s])
    return elements

def _is_subbed(self, key):
    maxn = self.dll.vensim_get_varattrib(_prepstr(key), 9, None, 0)
    return False if maxn == 2 else True

def _get_subs(self, key):
    names = [str.strip(i) for i in re.findall(r'[^\\[\\^\\]|^,]+', key)]
    return names[0], names[1:]

def _c_char_to_list(res):
    names = []
    for r in list(res)[-2:]:
        if isinstance(r, str):
            names.append(r)
        else:
            names.append(r.decode('utf-8'))
    names = ''.join(names).split('\x00')

    return names

def _prepstr(in_str):
    return in_str if isinstance(in_str, bytes) else in_str.encode('utf-8')

```

## Appendix E. Model Code

The entire model code is provided in the “anemi” GitHub repository located at <https://github.com/FIDS-UWO/anemi> as a Vensim model file titled “ANEMI3.mdl”. This is a text file which can be viewed by opening with any text editor. Included are all constants, lookup tables, equations, and comments for the ANEMI3 model. This file can be opened using the Vensim software in order to view the model structure. A free Vensim PLE licence can be obtained from <https://vensim.com>, which can be used to view the stock and flow diagram that makes up the model structure. Due to the advanced features used in the ANEMI model, a Vensim DSS license is required to run the model.



## Curriculum Vitae

**Name:** Patrick Alan Breach

**Post-secondary Education and Degrees:** Western University  
London, Ontario, Canada  
2010-2014 B.E.Sc in Civil and Environmental Engineering

**Honours and Awards:** Province of Ontario Graduate Scholarship  
2014-2015

**Related Work Experience:** Teaching Assistant  
The University of Western Ontario  
2014-2019

### Publications:

Mandal, S., Arunkumar, R., Breach, P.A. and S.P. Simonovic. (2019). Reservoir Operations under Changing Climate Condition. *Journal of Water Resources Planning and Management*, 145(5), doi:10.1061/(ASCE)WR.1943-5452.0001061.

Breach, P. and S.P. Simonovic. (2018). Wastewater Treatment Energy Recovery Potential for Adaptation to Global Change: An Integrated Assessment. *Environmental Management*, 61(4), 624-636, doi:10.1007/s00267-018-0997-6.

Sohom Mandal, Patrick A. Breach, Abhishek Gaur and Slobodan P. Simonovic (2017). Tools for Downscaling Climate Variables: A Technical Manual. Water Resources Research Report no. 097, Facility for Intelligent Decision Support, Department of Civil and Environmental Engineering, London, Ontario, Canada, 95 pages. ISBN: (print) 978-0-7714-3135-7; (online) 978-0-7714-3136-4.

Breach, P.A., Simonovic, S.P. and Z. Yang. (2016). Global Climate Model Selection for Analysis of Uncertainty in Climate Change Impact Assessments of Hydro-Climatic Extremes. *American Journal of Climate Change*, 5(4), 505-525, doi: 10.4236/ajcc.2016.54036.

Mandal, S., Breach, P.A. and S.P. Simonovic. (2016). Uncertainty in Precipitation Projection under Changing Climate Conditions: A Regional Case Study. *American Journal of Climate Change*, 5(1), 116-132, doi:10.4236/ajcc.2016.51012.

Yuan Z., Yan, D.H., Yang, Z., Yin, J., Breach, P.A. and D. Wang. (2014). Impacts of climate change on winter wheat water requirement in Haihe River Basin. *Mitigation and Adaptation Strategies for Global Change*, 21, 677-697, doi:10.1007/s11027-014-9612-1.